Copyright Warning & Restrictions

The copyright law of the United States (Title 17, United States Code) governs the making of photocopies or other reproductions of copyrighted material.

Under certain conditions specified in the law, libraries and archives are authorized to furnish a photocopy or other reproduction. One of these specified conditions is that the photocopy or reproduction is not to be "used for any purpose other than private study, scholarship, or research." If a, user makes a request for, or later uses, a photocopy or reproduction for purposes in excess of "fair use" that user may be liable for copyright infringement,

This institution reserves the right to refuse to accept a copying order if, in its judgment, fulfillment of the order would involve violation of copyright law.

Please Note: The author retains the copyright while the New Jersey Institute of Technology reserves the right to distribute this thesis or dissertation

Printing note: If you do not wish to print this page, then select "Pages from: first page # to: last page #" on the print dialog screen

ABSTRACT

COMBUSTION OF METHYL CHLORIDE, MONOMETHYL AMINE, AND THEIR MIXTURES IN A TWO STAGE TURBULENT FLOW REACTOR

by
Fuhe Mao

The feasibility of converting fuel-bound chlorine and nitrogen into HCl and N_2 with reduced pollutant emissions of CO, NO, and unburned hydrocarbons was investigated in a two-stage turbulent flow reactor. The study consists of four segments: completion and validation of the experimental facility, experimental and modeling studies of methyl chloride (CH_3Cl) combustion, similar studies on monomethyl amine (CH_3NH_2), and finally studies on simultaneous CH_3Cl and CH_3NH_2 combustion.

Validation of the experimental facility was made by combustion of ethylene (C_2H_4) and air under both fuel-lean and fuel-rich conditions. Premixed C_2H_4 and air, fed into the first stage, served as the primary fuel and oxidant for all experiments. Additional air or steam was injected into the second stage as required. Perfect stirred and plug flow sequential reactor (PSR+PFR) behavior was demonstrated by good agreement between the experimental data and the modeling predictions.

An experimental and modeling study of methyl chloride combustion and the effects of steam injection on combustion emissions was performed. Reactor temperatures, O_2, CO, CO_2, and light hydrocarbon concentrations were measured in both fuel-lean and fuel-rich cases. Experimental data showed that CH_3Cl inhibits the CO burnout and increases the yield of incomplete products of combustion (PICs). Model predictions agree well with the experimental observations. Analysis of the modeling results indicates that reaction $OH + HCl \Leftrightarrow Cl + H_2O$ is a major OH consumption channel, which inhibits the

CO burnout reaction OH + CO $\Leftrightarrow$ CO_2 + H. Results of experiments and modeling show that steam injection into the second stage can effectively enhance CO burnout and reduce PIC emissions.

Monomethyl amine, serving as a source of fuel-bound nitrogen, has been burned in air with fuel ethylene. Experiments showed that NO formation from the first stage dramatically decreased as the fuel equivalence ratio (ϕ) in this stage was increased from ϕ=0.86 to 1.45. While the first stage was operated fuel-rich, air was injected into the second stage to achieve overall fuel-lean combustion. Under such air staging conditions a minimum NO emission from the second stage was observed and the corresponding optimal fuel equivalence ratio (ϕ_m=1.28 to 1.38) in the first stage was determined to be a function of the feed CH_3NH_2 concentration. Data indicated that the NO emission was reduced by more than 60% with air staging combustion as compared to the fuel-lean only case at the same ϕ. A detailed elementary reaction mechanism has been used together with the PSR+PFR reactor simulation to model the experimental data. Rate-of-production (ROP) analyses based on the successful modeling have illuminated the key pathways to NO formation and destruction.

The simultaneous combustion of monomethyl amine and methyl chloride was studied using the two-stage reactor. Interactions of the chlorine- and nitrogen-containing species during combustion were observed from the experiments. Under staged conditions, the interactions resulted in lower NO emissions as the methyl chloride loading in the feed was increased. A proposed interaction mechanism has been satisfactorily used to predict the experimental observations.

COMBUSTION OF METHYL CHLORIDE, MONOMETHYL AMINE, AND THEIR MIXTURES IN A TWO STAGE TURBULENT FLOW REACTOR

by
Fuhe Mao

A Dissertation
Submitted to the Faculty of
New Jersey Institute of Technology
in Partial Fulfillment of the Requirements for the Degree of
Doctor of Philosophy

Department of Chemical Engineering,
Chemistry, and Environmental Science

January 1995

APPROVAL PAGE

COMBUSTION OF METHYL CHLORIDE, MONOMETHYL AMINE, AND THEIR MIXTURES IN A TWO STAGE TURBULENT FLOW REACTOR

Fuhe Mao

Dr. Robert B. Barat, Dissertation Advisor — Date
Assistant Professor of Chemical Engineering, NJIT

Dr. Joseph W. Bozzelli, Committee Member — Date
Distinguished Professor of Chemistry, NJIT

Dr. Richard S. Magee, Committee Member — Date
Professor of Chemical Engineering and Mechanical Engineering, NJIT
Director of The Hazardous Substances Management Center

Dr. Henry Shaw, Committee Member — Date
Professor of Chemical Engineering, NJIT

Dr. Javad Tavakoli, Committee Member — Date
Associate Professor of Chemical Engineering, Lafayette College

BIOGRAPHICAL SKETCH

Author: Fuhe Mao

Degree: Doctor of Philosophy in Chemical Engineering

Date: January 1995

Undergraduate and Graduate Education:

- Doctor of Philosophy in Chemical Engineering
  New Jersey Institute of Technology, NJ, 1995
- Master of Science in Chemical Engineering
  Beijing Institute of Chemical Technology, Beijing, 1984
- Bachelor of Science in Chemical Engineering
  Beijing Institute of Chemical Technology, Beijing, 1982

Major: Chemical Engineering

Presentations and Publications

Mao, F., Kretkowski, D., and Barat R. B., "A Two Zone Turbulent Flow Reactor for Study of Staged Combustion of Hazardous Wastes", Paper Presented at *The Eastern States Section Meeting of the Comb. Inst.*, Princeton, NJ(1993). *Comb. Sci. & Tech.*, in press.

Mao, F. and Barat, R. B., "Experimental and Modeling Studies of Staged Combustion Using A Reactor Engineering Approach", Submitted to *Chem. Eng. Comm.* (1994)

Mao, F. and Barat, R. B., "Minimization of NO During Staged Combustion of CH_3NH_2", Submitted to *Comb. & Flame* (1994)

Mao, F. and Barat, R. B., "Staged Combustion of Cl- and N-containing Hydrocarbons in a Two Zone Turbulent Flow Reactor", Paper Presented at *The International ACS Meeting*, San Diego, CA(1994)

Mao, F. and Barat, R. B., "Combustion Inhibition by Methyl Chloride and the Effects of Steam Injection", Submitted to *Comb. Sci. & Tech.* (1994)

Mao, F., and Zheng, C., "The Reaction Kinetics and Transport Processes in V_2O_5 Catalyst during SO_2 oxidation", *Sulfuric Acid Industry* (Chinese), No. 5, p72(1985)

This thesis is dedicated to
Rena and David

ACKNOWLEDGMENT

I would like to express my most sincere appreciation to my thesis advisor, Professor Robert B. Barat for his guidance and support throughout this study. His enthusiasm and encouragement have contributed greatly to the accomplishment of this research. I would like to thank Professor Joseph W. Bozzelli for his significant suggestions on the reaction mechanisms and rate constants. What I have learned from his class has been very helpful for my combustion research. Many thanks to Professor Richard S. Magee, Professor Henry Shaw, and Professor Javad Tavakoli for their significant comments and suggestions on the research progress report.

I would like to thank Doug Kretkowski for his very good work on building the HCl scrubber and operating the Beckman analyzer. Many thanks to senior technician Benedict W. Barat for his professional work on construction and maintenance of the experimental facility.

Finally, I would like to thank to my parent, their deep and great grace is my constant source of inspiration. To my wife, Rena, I would like to let her know how much I love her for being my support always.

I wish to thank the Hazardous Substance Management Research Center, The National Science Foundation, and the Exxon Education Foundation for their financial support of this research.

TABLE OF CONTENTS

TABLE OF CONTENTS
(Continued)

TABLE OF CONTENTS
(Continued)

TABLE OF CONTENTS
(Continued)

LIST OF TABLES

LIST OF TABLES
(Continued)

LIST OF FIGURES

LIST OF FIGURES
(Continued)

Figure **Page**

LIST OF FIGURES
(Continued)

Figure **Page**

LIST OF FIGURES
(Continued)

Figure **Page**

LIST OF FIGURES
(Continued)

Figure **Page**

LIST OF FIGURES
(Continued)

Figure **Page**

CHAPTER 1

INTRODUCTION

1.1 Background

Chlorocarbons (CHCs), such as carbon tetrachloride, polyvinyl chloride (PVC), and pesticides are important environmental concerns. Although the total production of chlorofluorocarbons worldwide has decreased in the 1990s, the production and use of chlorinated organic chemicals in industrial and manufacturing processes still occurs on a large scale. Pollutant emissions from chlorinated compounds use are increasing. For examples, in the U.S. the emissions of methyl chloroform, which is extensively used as a cleaning solvent, were in excess of 300,000 metric tons per year according to EPA estimates (U.S. EPA 1993). Atmospheric concentrations of methyl chloroform have been growing by about 5 percent annually (Intergovernmental Panel on Climate Change 1993). Because these hazardous substances have high global warming potentials, toxicity, and long lifetimes, management and safe disposal of chlorine-containing wastes are of great significance to the environment.

Pyrolysis and incineration of chlorocarbons or chlorine-containing wastes can attain high destruction efficiencies if the combustion devices are operated at optimal conditions. Chlorinated compounds are also well recognized as inhibiting combustion processes while promoting the emissions of soot and products of incomplete combustion (PICs), such as methane and acetylene. The methane from the effluent gas is a potent greenhouse gas considering its high heat absorption capacity; for example, one molecule of methane can have 20 times the effect on the climate as one molecule of carbon dioxide (Wuebbles and Edmonds 1991). Acetylene is a seed for higher molecular weight growth and soot formation during the combustion process (Senser, Cundy, and Morse 1987;

Karra, Gutman, and Senkan 1988). When the chlorocarbons are present in combustion, the burnout of carbon monoxide to carbon dioxide is limited, and the waste destruction efficiency is decreased due to the combustion inhibition (Fisher et al. 1990; Ho, Barat, and Bozzelli 1992).

The mechanism of chlorocarbon inhibition of hydrocarbon combustion has been widely studied by a few researchers (Bose and Senkan 1983; Chang and Senkan 1985; Ritter and Bozzelli 1990; Barat 1990; Ho 1993). There is a growing need for investigation and demonstration of the means to overcome the inhibition and decrease the pollutant gas emissions.

Nitrogen oxides (NO and NO_2 together referred to as NO_X) emissions produced from fossil fuel combustion is another major environmental concern. In the atmosphere, NO_X have been increased steadily over the last twenty years. Figure 1.1 (All figures are listed in App. A) shows the increasing trends of NO_X emissions in North America and worldwide, which indicates that more than 70% of combustion-generated NO_X is produced in the North America. Present levels of NO_X emissions already pose a significant threat to human health and the environment due to the unusual chemical properties of NO_X. Nitrogen oxides are not only directly harmful to the human body, but also can contribute to the formation of green house gases, to destruction of ozone in the stratosphere, and to production of urban smog by photochemical reactions. They can also be converted into nitric acid rain.

The main direct source of nitrogen oxides emissions is fossil fuel combustion. More than 60 percent of the NO_X emissions from fossil fuel combustion is released from stationary sources, such as power plant furnaces and industrial boilers. The remaining NO_X comes from automobiles, aircraft, and other motor vehicles (Bowman 1992). One reason for higher NO_X emission from stationery sources is that high level nitrogen-containing fuels, such as coal and heavy oil, are used in generating stations and utility

boilers. Studies (Martin and Dederick 1977; Miller et al. 1985) indicate that conversion of the fuel-bound nitrogen to NO_X in combustion can be up to 70 percent under certain operating conditions. When combustion is performed in oxygen-rich (fuel-lean) environments, the conversion can increase to much higher levels. From the point of view of low NO_X emission, excess air in combustion devices is not good. Even when there is no nitrogen contained in the fuel, the nitrogen oxides are still produced during combustion because the typically high temperature favors the oxidation fixation of nitrogen from the air. The nitrogen oxides formed this way are commonly known as thermal NO_X which is very sensitive to the combustion temperature.

Many technologies have been studied and developed to control combustion-generated nitrogen oxides, which has been previously summarized by the EPA (U. S. EPA 1980) and recently by Bowman (1992). These technologies include fuel denitrogenation, pulverized coal low-NO_X burner, fuel reburning, catalytic NO_X reduction, and staged combustion. Staged combustion is applicable to a wide range of fuels and energy facilities including large-scale power plant furnaces and small-scale industrial boilers. When the combustor is operated with an optimal first stage fuel equivalence ratio, the NO_X emission can be significantly reduced to a minimum level.

The minimum NO_X has been reported by experimental data from previous studies on staged combustion of nitrogen compounds, such as HCN and NH_3 (Martin and Dederick 1977; Toshimi, Toshharo, and Mitsunibo 1979; Song et al. 1981). These studies have shown minimum NO emission in the second stage, but with different values of the optimal first stage fuel equivalence ratio corresponding to the minimum NO_X. However, the reasons for the variation in these values, and the subsequent influence on the minimum NO_X emissions, were not explained. While the staged combustion for NO_X control has been used in industrial boilers and coal burners, its application to incineration of hazardous chemical wastes has not been investigated.

Although the modern waste incinerator can attain high destruction efficiencies under well controlled steady state conditions, there still is resistance to build an incinerator in many communities. The most important concern about the incinerator is emissions of gaseous pollutants, such as CO, NO_x, products of incomplete combustion, and other combustion-generated hazardous materials. It has been shown that increased PICs and undesirable byproducts can be emitted to the atmosphere during incineration of chlorinated compounds with excess air (Senkan 1986; Chuang and Bozzelli 1986). Under fuel-lean conditions, NO_x emissions can be high from combustion of nitrogen-containing fuels (Gerhold, Fenimore, and Dederick 1978) because the oxygen-rich environment favors NO_x formation. Therefore, it is necessary to investigate and understand the incineration processes of chlorocarbons and fuel-bound nitrogen with hydrocarbon fuels to increase destruction efficiencies and minimize undesirable emissions.

In case of the simultaneous incineration of chlorinated compounds and nitrogen-containing compounds, for example, using nitrogen-containing fuel for burning chlorine-containing chemical hazardous wastes, it is very possible that the interactions between the chlorine species and the nitrogen species could occur in the high temperature incineration environment. Under very low pressure (10^{-3} to 10^{-5} torr) and room temperature, chemiluminescence studies of N atom reactions (Jeoung, Choo, and Benson 1991) have shown that the nitrogen atom and CN radical can react with $CHCl_2$, $CHCl_3$, NCl, and CNCl to form various intermediates and products, such as HCN, HCl, and N_2. Investigation of the interaction of chlorine-containing and nitrogen-containing species at high temperature is of practical importance for the incineration process because there is the possibility of co-combustion of these compounds in the industrial incinerator. Information obtained from the interaction studies will help to clarify the effects of nitrogen species on the chlorocarbon-induced inhibition and the influence of chlorinated species on the NO_x emissions.

1.2 Objectives

The main goal of this research has been to obtain a better understanding of incineration processes of chlorocarbons and nitrogen-containing chemical wastes in a two-stage combustor. The feasibility of minimizing nitrogen oxides emissions and overcoming the chlorocarbon inhibition by staged combustion and steam injection has been investigated. The information obtained from this study can guide hazardous waste incinerator design and operation. The specific objectives of this dissertation have been to:

1. Complete the two-stage reactor and the analytical system, and validate the facility using known combustion reaction mechanisms.
2. Investigate the chlorocarbon-induced inhibition of hydrocarbon combustion, especially through measurement of CO conversion and unburned hydrocarbon emission levels.
3. Examine and demonstrate the effects of steam injection on overcoming this inhibition.
4. Investigate the classical NO_X minimum behavior during staged combustion of fuel-bound nitrogen (Gibbs, Pereira, and Beer 1977; Martin and Dederick 1977; Toshimi, Toshharo, and Mitsunibo 1979; Song et al. 1981), and the effects of fuel equivalence ratio and the combustion temperature on the NO_X emission.
5. Investigate the influence of feed fuel-nitrogen concentration on the optimal first stage equivalence ratio and corresponding NO_X emission.
6. Burn fuel-bound chlorine and fuel-bound nitrogen simultaneously in the two-stage combustor and determine the interaction of two simulated wastes.
7. Study literature reaction mechanisms for methyl chloride combustion, and the NO_X formation chemistry during combustion of monomethyl amine, making modifications

based on fundamental thermochemical kinetics where needed to generate better agreement with experimental observations.

8. Model these combustion processes and compare the calculated results with the experimental data to make interpretations on the observations by using a reactor model and the reaction mechanisms.

9. Identify the important reaction pathways responsible for the production and destruction of key species via the rate-of-production analysis based on the modeling results.

1.3 Research Approach

This study used a two-stage turbulent flow reactor as the combustor which can be considered as a perfectly stirred reactor followed by a plug flow reactor. This type of reactor can simulate many practical combustion systems such as liquid feed waste incinerators and low-NO_X burners.

Methyl chloride was used as a model waste chlorocarbon in this study due to its relative ease of use, and since its oxidation and pyrolysis mechanism are available in the literature (Ho and Bozzelli 1992; Ho 1993). To study nitrogen oxide formation from fuel-bound nitrogen, monomethyl amine was selected. This nitrogen-containing compound is less toxic and less corrosive to the seal materials in the feed line; also it is easy to withdraw as gas from the cylinder.

The experiments were performed as follows: First, the reactor was validated as a PSR+PFR sequence based on ethylene / air combustion. Second, methyl chloride and monomethyl amine were burned in the two-stage combustor separately with specific feed and injection conditions. Third, both of the model wastes compounds were combusted simultaneously. The important data obtained from the experiments are temperature profiles in the reactor, the effects of chlorocarbon loading on CO, CO_2, and PICs

emission, the effects of steam injection on the CO burnout and PICs reduction, the effects of fuel equivalence ratio and combustion temperature on the NO_X production, the effect of air injection on minimized NO_X, and the influence of methyl chloride on the NO_X production during fuel-bound nitrogen combustion.

Modeling with detailed reaction mechanisms has been utilized to predict the experimental observations. Rate of production analysis based on acceptable model calculations has been applied to determine the destruction and production pathways of the species of interest.

CHAPTER 2

LITERATURE SURVEY

2.1 Chlorocarbons Combustion

2.1.1 Pyrolysis and Oxidation of Chlorocarbons

The early studies of chlorinated hydrocarbons (CHCs) pyrolysis and oxidation were performed at low temperature (T < 700 C) under flameless conditions (Barton and Howlett 1951; Goodal and Howlett 1954; Hoare et al. 1959). A large number of breakdown products, including carbon monoxide and chlorinated compounds, were detected in the pyrolysis gas. Results from these studies supplied available data to the later work of flame combustion of CHCs.

Gas-phase reactions of chloroform and 1,1,2-trichloroethane with hydrogen have been studied by Chuang and Bozzelli (1986) in a tubular flow reactor with 550-1100 °C temperature range. The major stable species such as HCl, CH_4, and carbon solids were observed in the experiments when the temperature was above 850 °C. Low concentrations of chlorinated byproducts, chloromethane and vinyl chloride, were also observed in the pyrolysis gas. The results showed that higher temperatures were required for further decomposition of these byproducts. The authors also found that nearly quantitative removal of chlorine as HCl can be reached with an H_2 rich environment due to fact that the H_2 is thermodynamically favorable to form HCl and supplies more available destruction energy to the system.

Using the tubular flow reactor operated between 835 to 1275 K at one atmosphere, Ritter and Bozzelli (1990) investigated thermal reactions of chloro and dichlorobenzene in H_2 and H_2/O_2 mixtures. Their experimental data showed that complete conversion of chlorobenzene in hydrogen required temperature above 1100 K, while the equivalent conversion can be obtained at 893 K when small quantities of oxygen was added to the reaction mixtures. In addition to the major products of benzene and HCl, CH_4 and C_2H_6 also were observed in low concentration levels. The results from detailed kinetic mechanisms indicated that displacement of the chlorine by H radical was responsible for conversion of the chlorobenzene. O_2 can initiate the chain mechanism by reaction $H_2 + O_2 \Leftrightarrow HO_2 + H$ which explains the low required temperature for conversion when oxygen is present.

An experimental and modeling study of CH_3Cl and CH_2Cl_2 pyrolysis and oxidation in a tubular flow reactor was conducted by Ho (1993). Experimental species profiles as functions of temperature and residence time were presented. In this work, the thermodynamic properties for related species were calculated by using the techniques of group additivity (Benson 1976) and the THERM computer code (Ritter and Bozzelli 1991). Many of reaction kinetic parameters were estimated according to the QRRK theory (Dean, A. M. 1985). The detailed reaction mechanism included 67 species and 265 reactions. The mechanism constructed by the author successfully predicted his experimental data. Sensitivity analysis results from this research indicated that the reaction $OH + HCl = H_2O + Cl$ is a major channel to OH loss which is a key factor in inhibition of the CO burnout to CO_2 via the reaction $CO + OH = CO_2 + H$. This conclusion was further demonstrated by the observation of increasing of CO / CO_2 ratios with CH_3Cl loading in a recent flat flame study (Wang, Jalvy, and Barat 1993).

Combustion of trichloroethene has been studied by Bose and Senken (1983) using a premixed flat flame at 1 atm. The reaction path they proposed is that C_2HCl_3 undergoes

fast decomposition by oxidative reactions to produce CO, HCl, and Cl_2 in the first flame zone, then the HCl and Cl_2 inhibited, slow CO burnout reaction finally leads to the establishment of the second flame zone. A number of chlorinated intermediates were noted in the first zone and they decomposed relatively fast compared to the slow oxidation of CO. A global and semi-detailed reaction kinetic model was present in the work to explain the flame observations.

Karra and Senkan (1987) performed comparative studies of CH_3Cl / CH_4 and CH_4 flames using a flat flame burner. The experiments showed that the CH_3Cl rapidly decomposes in the flame zone and the concentrations of CO, C_2H_4, and C_2H_2 are clearly higher in the CH_3Cl / CH_4 flame than that in the CH_4 flame. Basing on the observations and the reaction mechanism analysis, the authors also noted that methyl chloride in the flame promotes soot formation because the increased concentrations of C_2H_3 and C_2H_2 enhance the rate of surface growth.

2.1.2 Incineration of Chlorocarbons

Although incineration has been a principal method for destruction of hazardous chlorinated substances, there are many concerns of its destruction efficiency and pollutant emissions. Incineration of chlorinated wastes in an oxygen-rich environment (e. g. with excess air) does not guarantee the removal of the chlorine as the most thermodynamically stable and desirable product HCl. For example, molecular chlorine Cl_2, phosgene CCl_2O, hexachlorobenzene C_6Cl_6, and other chlorinated byproducts were observed in an oxygen-rich C_2HCl_3 flame (Senkan 1986).

An experimental study (Lyon 1990) demonstrated the existence of a second threshold during incineration of methyl chloride under fuel-lean conditions. Operating a incinerator below the threshold may limit the destruction efficiency of the toxic organic.

The author found that when the molar concentration of methyl chloride in the feed was lower than 100 ppm, the fraction of undecomposed CH_3Cl remaining in the effluent gas was as high as 30 percent. Otherwise, when the feed concentration exceeded this threshold, the CH_3Cl quickly decomposed to a 97 percent conversion level at 1200 K with 0.52 second residence time. The study also showed that adding CO into the incinerator can greatly increase the toxic organic oxidation rate.

Incinerator performance at off-design operating conditions has been investigated by Fisher et al. (1990) and Koshland et al. (1992) using a tubular flow reactor. The experimental simulation of an incinerator operated at failure conditions involved injecting a small quantity of chlorocarbons (CH_3Cl, C_2H_5Cl, or 1,1,1-$C_2H_3Cl_3$) into a simulated post-flame zone. They observed that the breakdown of these injected chlorocarbons is sensitive to the injection temperature. For the highest temperature cases (injection location T = 1253 K), destruction of these injected chlorocarbons was rapid, and observed product species were HCl, CO, H_2O, and CO_2. For cooler injection temperatures (injection location T = 932 to 1012 K), both chlorinated and non-chlorinated byproducts, such as C_2H_3Cl, C_2H_2, and C_2H_4, in the exhaust gas were observed.

The incineration processes of methyl chloride used as a model hazardous waste and propane used as auxiliary fuel were examined in a fluidized bed combustor (Bloomer and D. L. Miller 1992). In this study, the inlet air temperature, fuel equivalence ratio, and the methyl chloride loading level were varied to study their effects on combustion temperature and emissions. The experimental results showed that the bed temperatures decreased at higher Cl / H ratios and the emissions of CO, C_2H_2, C_2H_4, CH_2Cl_2, and CCl_4 increased as the feed CH_3Cl loading increased. A very interesting phenomena observed from this work is that the prompt nitrogen oxides emitted from the bed increased when the chlorine loading increased in the feed, even though the bed temperature (1050 K) was lower than that in no CH_3Cl loading case.

2.1.3 Chlorocarbon Inhibition of Combustion

The phenomena of hydrocarbon combustion inhibition by chlorocarbons has been studied by many researchers using many kinds of combustion devices, such as flat flame burners, turbulent flow reactors, well stirred reactors, and fluidized bed reactors. Chelliah et al. (Chelliah, Yu, Hahn, and Law 1992) have made experimental and modeling studies to examine the effects of CH_3Cl content and fuel equivalence ratio on the premixed and nonpremixed CH_4 flame burning velocities. The results indicated that the burning velocities in both premixed and nonpremixed flame decreased with increased feed CH_3Cl content. The maximum burning velocity was observed at feed fuel equivalence ratio = 1.1. The study of fluidized bed combustion of C_3H_8 loaded with methyl chloride (Bloomer and D. L. Miller 1992) indicated that CH_3Cl in the feed delayed the ignition times and caused a decrease in destruction efficiency.

Garner et al.(Garner, Long, Graham, and Badakshan 1957) examined the flame inhibition characteristics by using chlorinated compounds, such as HCl, CH_3Cl, and CH_2Cl_2, and water as additives in the CH_4 fuel. The experiments was conducted using a brass nozzle burner. They found that the flame velocities decreased when the additive concentrations was increased in the feed. The data also showed that the inhibition effects of these additives on the flame velocity was enhanced in the order of CH_2Cl_2 > CH_3Cl > HCl > H_2O. In this study, the maximum mole percent of these additives in the feed was 1%. Much heavier chlorocarbon loading of CH_2Cl_2 in a CH_4-air flame were studied by Senser et al. (Senser, Cundy, and Morse 1987). The flame was burned at constant fuel equivalence ratio of ϕ = 0.8 and with increased chlorocarbon loading from Cl / H = 0.06 to 0.72. Gas samples from the flame were analyzed by gas chromatography. Peak concentrations of product species, such as C_2H_2, C_2H_4, C_2H_6, C_2H_3Cl, C_2HCl_3, and C_2Cl_4 were clearly increased with the heavier loading of chlorocarbon in the feed. Measurements showed that the temperature in the flame zone decreased, while the

temperature in the post-flame zone increased, as the feed CH_2Cl_2 concentration was increased.

Barat (1990) studied the combustion characteristics and the influences of chlorocarbons in a well stirred reactor. Enhanced flame instability and localized blowout in the C_2H_4 / air / CH_3Cl combustion was observed in his study. Brouwer et al. (Brouwer, Longwell, Sarofim, Barat, and Bozzelli 1992) also investigated the effects of methyl chloride on the well-stirred combustion behavior and emissions. The experimental temperature was held constant at T = 1600 K. Under fuel-lean (ϕ = 0.75) conditions, CH_3Cl could be added up to a ratio of Cl / C = 0.5 without increasing the incidence of localized blowout of combustion. However, under fuel-rich (ϕ = 1.25) conditions, sudden blowout was observed when Cl / C ratio exceeded 0.25. Also they observed that the emissions of CO, O2, and unburned hydrocarbons increased with the higher feed ratio of Cl / C.

The detailed mechanism of combustion inhibition by chlorocarbons has been proposed in several studies (Westbrook 1982; Chang and Senkan 1985; Senser et al. 1987; Barat 1990; Ho 1990; Ho, Barat, and Bozzelli 1992). During combustion, Cl produced from chlorocarbons attacks the hydrogen atom from the fuel compounds in a fast abstraction reaction

$$Cl + RH = HCl + R \qquad (R2.1)$$

where RH stands for the fuel hydrocarbon and R represents the hydrocarbon radical. HCl produced from the above reactions then reacts with H atoms

$$HCl + H = H_2 + Cl \qquad (R2.2)$$

The reaction R2.2 offers a lower activation energy path (E_a = 3500 cal/mol, Westbrook 1982) for H radical consumption and then limits the following important chain branching reaction

$$H + O_2 = OH + O \qquad \text{(R2.3)}$$

The decreased rate of reaction R2.3 (E_a = 16790 cal/mol, Baulch et al. 1976) also limits the production of the very active radicals OH and O. Further inhibition is induced by consumption of OH radical in the reaction

$$HCl + OH = H_2O + Cl \qquad \text{(R2.4)}$$

Thus, the decreased concentration of OH radical inhibits the CO burnout reaction of

$$CO + OH = CO_2 + H \qquad \text{(R2.5)}$$

The overall effects on the combustion resulting from the inhibitions include longer ignition time, slower flame velocity, lower chlorocarbons destruction efficiency, and higher PICs emissions.

The studies on techniques to overcome this inhibition has rarely been reported. Ho (1990) suggested injection of H_2O (steam) as a means to enhance the OH radical supply via the reactions

$$H_2O + O = OH + OH \qquad (R2.6)$$

and

$$H_2O + Cl = HCl + OH \qquad (R2.7)$$

However, the experimental confirmation of this hypothesis is needed.

2.2 Nitrogen Oxide Formation and Reduction

2.2.1 NO Chemistry

The primary nitrogen oxide produced from most combustion sources is NO. The NO formation mechanisms in fossil fuel / air combustion processes have been studied by several researchers. There are three sources of NO formation during combustion: (1) *thermal* NO, (2) *prompt* NO, and (3) *fuel bound nitrogen* NO. A brief overview of thermal NO and prompt NO will be presented in this section, and a more detailed survey on the fuel-bound nitrogen NO will be described in the next section.

Thermal NO

The thermal NO mechanism, also called the "Zeldovich mechanism", consists of following three reactions:

$$O + N_2 = N + NO \qquad (R2.8)$$

$$N + O_2 = O + NO \qquad (R2.9)$$

$$N + OH = H + NO \qquad (R2.10)$$

The original formulation and verification of the thermal NO mechanism is attributed to the Zeldovich study of gaseous explosions in a combustion bomb (Zeldovich 1946). These

reactions occur at very high temperature (T > 1800 K) due to the high endothermicity (ΔH = 76 kcal/mol) of R2.8. Also this reaction is the rate-limiting step in the thermal NO formation mechanism. A global rate equation of NO formation was reported (Westengerg 1971) as

$$d[NO] / dt = 1.5E7\ [T]^{0.5}\ Exp[-69460 / T]\ [O_2]_{eq}\ [N_2]_{eq} \qquad (E2.1)$$

where $[O_2]_{eq}$ and $[N_2]_{eq}$ indicate the concentrations at equilibrium state of reaction.

The rate parameters for reaction R2.8 have been estimated and measured over a wide temperature range. Duff et al. (Duff and Davidson 1959) calculated theoretically the rate constant of R2.8 using Glick data (Glick, Klein, and Squire 1957), and indicated that the rate constant should be increased by approximately 35 percent at high temperature (T = 3000 K). Baulch et al. (Baulch, Drysdale, and Horne 1969) published their recommendation for the rate constants according to the experimental data obtained by Clyne et al. (Clyne and Thrush 1961). A critical evaluation of these kinetic parameters for thermal NO reactions has been given by Hanson and Salimian (1984).

To decouple the thermal NO from other NO sources in hydrocarbon combustion, a traditional approximation is to calculate the thermal NO production rate using equilibrium concentration values of O_2, N_2, O, and OH. The error introduced by this approximation has been evaluated by Miller and Bowman (1989) by comparing the NO formation rate at equilibrium with the rate calculated from a detailed kinetic model (the prompt NO reactions were deleted from the mechanism). They found that the NO concentration calculated from kinetics is much higher than the NO obtained from equilibrium calculations at T = 1800 K.

Prompt NO

Experimentally measured nitrogen oxide formation rates near the flame zone of hydrocarbon combustion is higher than that produced from direct oxidation of atmospheric nitrogen calculated by the thermal NO mechanism discussed above. This faster NO formation phenomena was first observed and defined as "prompt NO" by Fenimore (1971). He compared the NO formation rates in the flames of methane, ethylene, and propane with those in the hydrogen and carbon monoxide flames. He found that the growth of nitrogen oxide in the hydrocarbon flames is higher than that in the non-hydrocarbon flames. This nitrogen oxide growth rate is relatively weakly temperature dependent, and could not be described by the thermal NO mechanism. The author suggested that the hydrocarbon species did play important roles in the quick formation of nitrogen-containing intermediates via reactions

$$CH + N_2 = HCN + N \qquad (R2.11)$$

$$C_2 + N_2 = CN + CN \qquad (R2.12)$$

The N atom can react with non-equilibrium OH radical to form NO by reaction N + OH = NO, and the intermediates HCN and CN might convert into NO in further reactions.

In addition to CH and C_2, other hydrocarbon fragments, such as CH_2 and C, also can attack molecular nitrogen and contribute to formation of nitrogen oxide in the prompt mechanism by the following reactions (Blauwens, Smets, and Peeters 1977; Matsui and Nomaguchi 1978; Matsui and Yuuki 1985)

$$CH_2 + N_2 = HCN + NH \qquad (R2.13)$$

$$CH_2 + N_2 = CH_2N + N \qquad \text{(R2.14)}$$

$$C + N_2 = CN + N \qquad \text{(R2.15)}$$

Experimental results of Blauwens et al. (1977) suggest that the reactions R2.11 and R2.13 are the major channel to NO formation in the prompt mechanism.

Many studies have been made to determine the rate constant of reaction R2.11. The reported activation energy of R2.11 varies in a wide range of 11000 cal / mole to 20400 cal /mole, and the responding rate constants at T = 2000 K are from 8×10^9 to 4×10^{10} cm^3 / mol-sec. Some reported kinetic data on the reaction $CH + N_2 = HCN + N$ are listed in Table 2.1

Table 2.1 Kinetic Parameters for Reaction $CH + N_2 = HCN + N$

($k = A\,[T]^n\,Exp[-E / R / T]$ cm^3 / mol-sec)

A	n	E (cal / mole)	Sources
1.44E10	0	0	Morly 1976
8.0E11	0	11000	Blauwens et al. 1977
4.0E11	0	13600	Matsui et al. 1978
1.0E12	0	19200	Roth et al. 1984
1.2E12	0	13600	Matsui et al. 1985
4.2E12	0	20400	Dean et al. 1988
3.0E11	0	13600	Miller et al. 1989

It can be seen from the Table 2.1 that there is a significant variation among the kinetic parameters. A more direct determination of the rate constant was performed by Dean et al. (Dean, Davidson, and Hanson 1988) using a shock tube reactor in the temperature range 2700 K to 3700 K. The rate constant parameters from this study are also listed in the Table 2.1.

2.2.2 NO Formed from Fuel-Bound Nitrogen

The nitrogen oxide formed from combustion of fuel-bound nitrogen is termed fuel NO. The most common form of fuel nitrogen is organically bound nitrogen present in liquid and solid fuels such as heavy oils and coal. The bonds between nitrogen and carbon or other hydrocarbon atoms break more easily than the molecular nitrogen bond (N-N, 226 kcal / mole). For examples, the C-N bond energy is 179 kcal / mole and the N-H bond energy is only 80 kcal / mole.

Most of the NO emission from combustion is fuel NO. Compared to the tens of ppm NO emission levels from thermal NO and prompt NO (Fenimore 1971), the NO emitted from the industrial utility boilers which burn nitrogen-containing fuels might be 200 to 1000 ppm if the boilers are operated at fuel-rich conditions (Wood 1994).

The yield of nitrogen oxide from small additions of nitrogen compounds was measured in a premixed ethylene flame by Fenimore (1972). The flame temperatures were 1860 K to 2250 K, and the fuel equivalence ratios were 0.9 to 2.0. The added nitrogen compounds were pyridine, methacrylonitrile, methyl amine, and ammonia. From the experimental data reported by the author, the fuel NO formation rate was more dependent on fuel stoichiometry than flame temperature. The author found that with any addition of these nitrogen compounds, the observed yield of total NO satisfied a global rate equation

$$[NO] = f(T, \phi, [N]) \qquad (E2.2)$$

where [NO] = total NO formed from the flame; [N] = fuel bound nitrogen concentration in the feed; T = flame temperature; and ϕ = feed fuel equivalence ratio. There was no detailed mechanism reported in this paper, but the author suggested that in the NO formation process, there were fuel nitrogen intermediates, represented by *I*, which either go to NO or N_2 depending on following reactions

$$I + R \rightarrow NO \qquad (R2.16)$$

$$I + NO \rightarrow N_2 \qquad (R2.17)$$

where R is a nitrogen free species which caused the eventual oxidation of *I* to NO.

Shock tube and modeling studies of monomethylamine (CH_3NH_2) oxidation and decomposition in O_2 and Ar was performed by Higashihara et al. (Higashihara, Gardiner Jr., and Hwang 1987) and Hwang et al. (Hwang, Higashihara, Shin, and Gardiner Jr. 1990). The oxidation of CH_3NH_2 was investigated at temperatures from 1260K to 1600 K by IR laser kinetic absorption spectroscopy. The decomposition of CH_3NH_2 was described by 26 elementary reactions. Major products from the decomposition are NH_2 and HCN. The suggested important reactions to produce the NH_2 are

$$CH_3NH_2 = CH_3 + NH_2 \qquad (R2.18)$$

$$CH_2NH_2 + H = CH_3 + NH_2 \qquad (R2.19)$$

$$CH_2NH + H_2 = CH_3 + NH_2 \qquad (R2.20)$$

and the suggested reactions to produce HCN are

$$CH_2NH + M = HCN + H_2 + M \qquad (R2.21)$$

$$CHNH + M = HCN + H + M \qquad (R2.22)$$

$$CHNH + H = HCN + H_2 \qquad (R2.23)$$

Most of the kinetic parameters in the above reactions were adjusted to fit the experimental data. A 141 reaction mechanism which included the CH_2NH_2 oxidation, CO, H_2, C_1, and C_2 combustion, thermal NO, and prompt NO chemistry was constructed by the authors to predict the NO concentration. The absorption profiles measured in this study and the NO and NH profiles taken from other studies of NH_3 and HCN flames (Salimian, Hanson, and Kruger 1984; Szekely, Hanson, and Bowman 1985) have been compared to this model calculation results.

A recent survey and study on the mechanism and modeling of nitrogen chemistry in combustion was published by Miller and Bowman (1989). A 234 reaction mechanism was reported in the article. This mechanism considered thermal and prompt NO formation, fuel nitrogen (NH_3 and HCN) conversion to NO, and NO removal processes. The calculation results of this mechanism have been compared to the literature experimental data from HCN and NH_3 flames (Miller, Branch et. al 1985; Bian et al. 1986). Fuel nitrogen conversion data from a well-stirred reactor (Sun et al. 1987) was also modeled by this mechanism. The calculation results showed that the mechanism underpredicted the NO at fuel-lean conditions and NH_3 at fuel-rich conditions.

Sensitivity and rate-of-production analyses have been applied in Miller and Bowman (1989) model calculations to determine which reactions and reaction kinetic parameters are of greatest importance in the NO formation and reduction processes. The

analysis results have shown that, in the HCN flame, the most sensitive reactions to NO formation are

$$N + OH = NO + H \qquad (R2.10)$$

$$HCN + O = NCO + H \qquad (R2.24)$$

In the NH_3 flame, the most sensitive reactions to NO formation are R2.10 and

$$NH + OH = HNO + H \qquad (R2.25)$$

In both of the flames, the analysis indicated that the reaction

$$N + NO = N_2 + O \qquad (R2.26)$$

is the most important to removal of NO as N_2.

From these studies mentioned above, we can clearly see that the formation mechanism of fuel NO has completely different characteristics from the thermal or prompt mechanism. In addition to that the fuel NO emission levels are much higher than the thermal NO and the prompt NO (fuel NO is usually higher than 1000 ppm and the thermal or prompt NO is only at tens ppm levels), the fuel NO is much more sensitive to the fuel equivalence ratio and the fuel nitrogen content in the feed than to the combustion temperature. These suggested NO mechanisms also indicate that O and OH radicals play very important rules in the NO formation process.

2.2.3 NO Control and Reduction

At the present time, the most promising methods for controlling and reducing NO_X emissions can be divided into three category according to the combustion procedure: before combustion, during combustion, and post-combustion.

Before Combustion

To reducing the NO_X emissions from fuel nitrogen in combustion, one available approach is to remove the nitrogen contained in the fuels before the fuel enters the combustion chamber. This technology is called "denitrogenation". Fuel-bound nitrogen can be removed from natural fuels and synthetic fuels by mixing hydrogen gas and these fuels in a catalytic bed. By heating the gaseous mixture and the bed, the fuel-bound nitrogen will combine with hydrogen gas to produce ammonia and clean fuel (U.S. EPA 1980).

During Combustion

The methods used for reducing NO_X emissions during combustion involve combustion process modifications. There are two approaches currently applied in industrial combustion devices. They are low-temperature combustion and staged combustion.

Low-temperature combustion is only effective for reducing thermal NO_X, but not fuel NO_X. One way to reduce the combustion temperature is to recirculate the flue gas to the combustion chamber. Data published (Wood 1994) showed that 10 to 20 percent flue gas recirculation can provide more than 70 percent thermal NO decrease. Another way to reduce combustion temperature is to inject steam into the primary combustion zone. An experimental study was performed in a laminar opposed flow diffusion flame by Blevins et al. (Blevins and Roby 1992). They found that at least 60 percent of NO formed in hydrocarbon and CO/H_2 flames can be reduced by steam injection. The data measured in this study also indicate that NO could not be further suppressed when steam injection is over a high level limit. For practical application, steam injection has not been used in any

combustion devices other than gas turbines because the absorption of energy by steam decrease the combustion efficiency (Wood 1994).

Staged combustion includes air staging and fuel staging. In air staging, the total combustion air is split into two streams. One enters the first stage while the remainder enters the second stage of the combustor. The primary combustion zone operates fuel-rich and the secondary burnout zone operates fuel-lean. Generally the condition is overall fuel-lean. On the contrary, fuel staging feeds the fuel separately into the two-stages, making the first stage combustion fuel-lean and the second stage combustion fuel-rich. Both of the staging techniques have been investigated in the laboratory, but only the air staging method has been successfully used in low-NO_x burners and other practical combustion processes to control NO_x emissions (Bowman 1992; Wood 1994).

Kolb et al. (Kolb, Jansohn, and Leuckel 1988) investigated fuel staging of natural gas combustion with dopant ammonia. They operated the first stage fuel-lean (ϕ_1 = 0.91) and injected fuel into second stage to make this stage operate with ϕ_2 = 1.05 to 1.25. A minimum NO concentration was measured at ϕ_2 = 1.15. But the author did not report the CO emission from the second fuel-rich zone. Generally speaking, CO emission from fuel rich combustion is higher than 1000 ppm which exceeds air emission regulations.

Air staging combustion has the advantages of suppressing NO_x in the first stage (oxygen lean) and burning out CO in the second zone (oxygen rich). This NO_x reduction technique has been widely studied in the laboratory and used in industrial combustion processes. Gibbs et al. (Gibbs, Pereira, and Beer 1977) observed more than 30 percent NO reduction by injecting 25 percent of the total air into the second combustion zone, but no minimum NO was measured in this experiments. The minimum NO emission from air staged combustion was observed in the studies of Martin and Dederick (1977) and Toshimi et al. (Toshimi, Toshharo, and Mitsunibo 1979). They found that with the first stage operated fuel-rich at ϕ_1 = 1.2 to 1.4 and the second stage operated at slightly fuel

lean by secondary air injection, a minimum NO level was observed at the outlet. Both studies used ammonia as the fuel nitrogen in the feed. Also using NH_3 and by injecting air, Song and Blair (1981) showed that the optimal first stage fuel equivalence ratio corresponding to a minimum NO is from $\phi_1 = 1.7$ to 1.9.

Representative reductions of NO_x emissions by air staged combustion are 50 to 70 percent as compared to all fuel-lean combustion in practice. Data reported by Bowman (1992) indicated that in small-scale coal-fired fluidized bed combustors, up to 50 percent NO reduction and 130 ppm NO emission (at 3 percent O_2) was achieved. In a large scale heavy oil boiler, the NO emission has been reduced to 90 to 130 ppm (at 3 percent O_2) by air staged combustion.

Post-Combustion

Reduction of NO_x at *post-combustion* involves controlling NO_x formation in the burnout zone and reducing the formed NO_x in the flue gas. During selective catalytic reduction (SCR), a gas mixture of ammonia with air is fed with the cooled flue gas into a catalytic reactor. The NO is removed by the catalyzed reaction $NH_3 + NO = N_2 + H_2O$. The lower operating temperature (250 to 400 °C) in this step limits thermal NO formation. Another method used for control of NO in the post-combustion flue gas is selective non-catalytic reduction (SNCR). In this method, ammonia- or urea-based reagents are directly injected into to the combustion flue gases. The efficiency of this process depends on the flue gas temperature, the mixing of the additives and the gas, the residence time , and other operating conditions. Among these factors, the temperature operating window is very sensitive for NO reduction. For example, deviations from the optimal temperature window (950°C) during the selective non-catalytic NO reduction process can results in a very low NO reduction efficiency.

2.2.4 Effects of Other Chemical Compounds on NO

The effects of other chemical species such as chlorine- and sulfur-containing compounds on NO formation during combustion have been reported by a few researchers. An enhancement of NO formation has been observed by Bloomer and D. L. Miller (1992) when methyl chloride was added into a propane / air combustion system. The authors considered that the "hot spots" existing in the fluidized combustion bed enhances the thermal NO formation.

As fuel sulfur was introduced into the fuel nitrogen flame, the interaction of sulfur species and nitrogen species also can alter the NO formation rate. Wendt and Ekmann (1975), in CH_4 / air flames, found that high levels of fuel-S (2.5 percent SO_2 or H_2S) inhibited the formation of NO. In contrast to these results, another study (Tseregounis and Smith 1983) showed that NO formation was enhanced when sulfur dioxide (SO_2) was present in the C_2H_2 and H_2 flames seeded with C_2N_2.

2.3 Combustion Studies in Two-stage Reactors

Studying combustion processes in a two-stage laboratory reactor has practical implications for industry because many combustion systems employed two-stage combustion devices (Breen 1977; Sarofim and Flagen 1976). The early study of fuel NO emissions by Martin and Dederick (1977) was carried out in a two-stage combustor. The first stage of the combustor consisted of a cylindrical stainless-steel cup mounted vertically on a 0.75 inch feed mixture pipe. A 2 inch diameter quartz tube was fitted to the cup as the second stage. Secondary air was injected through four symmetrical radial jets on the bottom of the quartz tube. Gerhold et al. (Gerhold, Fenimore, and Dederick 1978) investigated nitrogen oxide formation in pyridine doped-oil combustion using a nearly adiabatic two-stage reactor. The first stage consisted of an air atomized fuel nozzle in a plenum chamber. This

was followed by a 8.1 cm I. D., 61 cm long quartz tube as the second stage. Samples were taken from both of the stages by water-cooled (20 C water) stainless steel probes. Data showed that NH_3 and HCN formed in the primary stage converted into NO in the secondary stage. In both of the studies, sufficient reductions of NO were achieved with air staged combustion.

An experimental investigation of the formation of polycyclic aromatic hydrocarbons (PAH) and soot was performed in a two-stage turbulent flow reactor (Lam 1988). This reactor consisted of a jet-stirred primary zone and a linear flow secondary zone. In this study, the secondary zone was considered to be a plug-flow reactor due to the high gas velocity inside the tube (Reynolds number = 4×10^5). The performance of the primary zone has been studied, and the measured results from the study (Barat 1990) suggested that the jet stirred combustor can be taken as a perfectly stirred reactor at high temperature conditions.

CHAPTER 3

EXPERIMENTAL METHODS

3.1 Schematic of Experimental Flowsheet

The schematic of the experimental apparatus is shown in Figure 3.1. The flowsheet can be divided into three parts: feed and mixing system, staged combustion system, and analytical system.

The primary fuel used in this experiment is ethylene (C_2H_4) which is supplied by Spectra Gases Company. The purity grade of the ethylene is UHP. The purity specifications are listed in Table 3.1.

Table 3.1 Ethylene Purity Specifications

Typical Contaminants	vppm
Acetylene	5
Carbon Dioxide	5
Carbon Monoxide	5
Ethane	5
Hydrogen	2
Methane	20
Nitrogen	20
Oxygen	10
Propane	5
Water	5

Two ethylene cylinders are connected in parallel to the feed line through a two-stage regulator which decreases the ethylene pressure from 1200 psig (cylinder) to 80 psig at the inlet of the ethylene flowmeter. In order to prevent regulator freeze-up from Joule-Thomson cooling, the ethylene fluid at the cylinder conditions is preheated through a stainless steel coil bathed in hot water before the regulator. The temperature in the water bath is controlled at 70 to 90 °C depending on the pressure in the cylinder. After preheating, the ethylene gas temperature measured at the regulator outlet is typically 20 ° C which is desirable for the feed temperature.

High pressure air (120 psig) from an in-house compressor is used as the oxidant. A knock-out filter is mounted on the combustion air line before the flowmeter to remove any oil particles and saturated moisture from the air. Low pressure house air (60 psig) is used for combustion ignition and the analytical instruments. The analytical instrument air was dried by flowing through an activated charcoal / molecular sieve packed column.

Methyl chloride (CH_3Cl) and monomethyl amine (CH_3NH_2) were used as model chlorine- and nitrogen-containing hazardous wastes. Both are stored as liquids in cylinders which were supplied by Matheson Gases Inc.. The monomethyl amine vapor is withdrawn from the cylinder by a gooseneck tube equipped above the liquid surface in the cylinder. The methyl chloride is also withdrawn as a vapor.

Nitrogen gas (stored as refrigerated liquid in a tank) is used for diluting the fuel-rich feed and controlling the reactor temperature. Addition of nitrogen gas does not change the feed fuel equivalence ratio, but dose change the feed and product concentrations. Therefor it is considered during modeling and result analyses.

The flow rates of each feed gas are measured by calibrated rotor flowmeters. The flow rates read from the flowmeter are corrected as needed for gas specific gravity, metering pressures, and metering temperature. Considering the gas mixture as ideal gas, the actual flow rates are obtained from the equations

$$K = \sqrt{\left(\frac{P_a}{P_c}\right)\left(\frac{T_c}{T_a}\right)\left(\frac{W_c}{W_a}\right)} \qquad \text{(E3.1)}$$

$$V_a = KV_c \qquad \text{(E3.2)}$$

where K = correction factor; P_a = actual metering pressure (psia); P_c = calibration pressure marked on the meter (psia); T_c = calibration temperature marked on the meter (K); T_a = actual metering temperature (K); W_c = gas molecular weight for which meter was calibrated; W_a = molecular weight of gas being metered; V_c = volumetric flow rate from meter reading (STP units); and V_a = actual volumetric flow rate (STP units).

After metering, the ethylene, primary air, methyl chloride, monomethyl amine, and dilution nitrogen as needed are mixed and enter the first stage of the reactor. Secondary air or steam are injected into the second stage. These injection material rates also are measured by rotor flowmeters.

3.2 Two-stage Reactor

A one atmosphere absolute pressure, two-stage turbulent flow reactor was used in this experiment. The first stage of the reactor is a jet-stirred toroidal combustion chamber pictured in Figure 3.2. The chamber is constructed from a castable high temperature alumina cement. Thirty two jets are positioned on the outer torus wall 20 degrees off radius. Figure 3.3 shows the jet ring and the jet positions on the ring. Pre-mixed fuel, air, and / or dilution nitrogen are introduced into the chamber through these jets at sub-sonic speed producing a swirling, highly turbulent, and intensely back-mixed combustion zone in the first stage. The fluid mixing and chemical reaction interactions in this zone have been described by Nenniger (Nenniger 1983) and Barat (Barat 1990). The first stage volume is

250 cm^3. The typical residence time in this zone ranges from 5 to 7 milliseconds. Typical axial bulk gas velocity is in the range of 40 to 50 meter / second resulting in Reynolds numbers on the order of 5×10^5.

The combustion gases exit the first stage, proceed over a flow straightener, and then enter the second stage of the reactor. The secondary stage is constructed from a pre-cast alumina tube, 30 centimeters in length and 5 centimeters in inner diameter. Typical gas velocities in the tube are 20 to 30 (with air injection) meter / second, yielding Reynolds numbers on the order of 3×10^5. The residence time in the second stage is about 15 milliseconds without secondary air injection and about 10 milliseconds with air injection.

To reduce heat losses from the reactor, both stages are insulated with heat insulation materials and enclosed in stainless steel jackets. To consume unburned species in the exhaust gas, large volume of air is injected into the section after the second stage. Cooling water is sprayed into the hot flue gas before venting. A schematic of the two-stage reactor including the injector, thermocouples, sample probes, and the afterburner section is shown in Figure 3.4.

A ceramic tube injector is inserted into the zone between the two-stages to inject air or steam into the second stage. The 1/4 inch outer diameter tube is closed at the injection end, with four small radial holes of 1/16 inch diameter located 5 millimeters from the closed end. Inside the ceramic tube is a 1/8 inch outer diameter stainless steel tube with an open end as outlet. Steam is flowed through the inside tube and air is flowed through the annulus. Figure 3.5 shows the injector design. The injection air flow rate is measured by a rotor flowmeter, and injected at room temperature. The injection steam is produced, after water metering, in an external electrically heat-traced stainless steel U tube. The temperature of the steam was controlled above 100 °C by an OMEGA temperature controller.

The temperature in the first stage is measured by an uncoated type R (Pt / Pt + 13% Rh) micro-thermocouple inserted into the torus from the bottom of the reactor, approximately 6 millimeter from the inside wall. Three identical thermocouples are radially inserted into the second stage to measure the temperature profile in this zone. The positions of the three thermocouples along the second stage length are at 6.5, 10.5, and 14.5 inches from the first stage exit. The thermocouple tips extend in past the inside reactor wall 6 millimeters.

All four temperatures measured at different points in the reactor are monitored by digital thermometers. The temperatures of the first stage and the middle of the second stage are displayed on an analog temperature recorder. It took about one and half hour to see the straight lines on the recorder, that is, the combustion needed that time from the ignition to reach its steady-state. Sample temperature output curves from the recorder are shown in Figure 3.6, indicating the temperature transient from start-up to steady state.

3.3 Analytical System

3.3.1 Sampling

Gas samples from each stage are drawn by a metal-bellows pump through two water-cooled stainless steel probes. The outer diameter of the probes is 6.3 millimeters with a central core inner diameter of 1 millimeter. A cross section view of the probe is shown in Figure 3.7. The overall length of the first stage probe is 11.5 inches, and the length of the second stage probe is 24 inches. The first stage probe extends 6 millimeters into the torus, and is fixed in position. The second stage probe is movable along the second stage length, which allows the sample to be taken at different residence times.

The coolant used in the probes is an approximately equal volume ethylene glycol and water mixture available from a closed loop in-house supply. The coolant, usually supplied at 17 °C, is preheated to 40 to 50 °C by passing it through a heat removal coil attached to the exterior of the exhaust section. The temperature of the coolant is controlled by adjusting the coolant flow rate, which is monitored by a flow switch/alarm system. The warmed coolant, while still sufficiently cool for maintenance of probe integrity and combustion gas sample quenching, keeps the gas sample temperature above the HCl acid dew point. Heat tracing is applied to the gas sample lines up to the HCl scrubber. Before the gas sample enters the analytical instruments, it is cooled in a low temperature bath to condense any water vapor. Droplets formed after the bath are removed in a knockout filter.

3.3.2 Light Hydrocarbon Analyses

The light hydrocarbons present in the gas sample include methane (CH_4), ethylene (C_2H_4), acetylene (C_2H_2), and ethane (C_2H_6). These are analyzed by a Hewlett-Packard Model 5890 gas chromatograph. The gas sample flows through either of two sample loops at fixed temperature and pressure (average of loop inlet and outlet). Each loop is connected to a heated Valco six port gas sample valve. Upon sample injection, the loops are flushed by carrier gas into packed columns. A schematic of the sample flowing, separation, and detecting system in the GC is shown in Figure 3.8.

The gas chromatograph is equipped with two 1/8 inch outer diameter stainless steel packed columns. A 1.0 meter long column packed with AT-1000 separates the light hydrocarbons. Another 1.2 meter long column packed with Carbosphere separates carbon monoxide, carbon dioxide, and C_1-C_2 hydrocarbons. Nitrogen is the carrier gas in the AT-1000 column, and helium is the carrier gas in the Carbosphere column. Species separated in the AT-1000 column are determined by a flame ionization detector (FID).

The CO, CO_2, and C_1-C_2 hydrocarbons are analyzed by a thermal conductivity detector (TCD). The appropriate Scotty standard gas mixtures are used to calibrate the gas chromatograph. The separated species peaks are recorded and integrated by a Hewlett-Packard integrator.

The GC temperature program for the FID column starts at 35 °C for 1 minute, increasing to 45 °C for 1 minute after a 5 °C / minute ramp. The retention times for each species from the FID column are listed in Table 3.2 , with sample output peaks shown in Figure 3.9.

Table 3.2 Retention Times of Compounds Detected by FID

Compounds	Formula	Time (min.)
Methane	CH_4	1.35
Acetylene	C_2H_2	1.92
Ethylene	C_2H_4	2.24
Ethane	C_2H_6	2.68

The temperature program for the TCD column starts at 90 °C for 2 minute, increasing to 200 °C for 10 minute after a 15 °C / minute ramp. The retention times for each species from the TCD column are listed in Table 3.3, with sample output peaks shown in Figure 3.10. The length of sample lines from the sample probes to the chromatograph is about 2 meters. Before injection of sample into the GC column, the sample lines were flushed for about 3 minutes to washout any residual compounds from the last sample gas.

3.3.3 Beckman Stack Gas Analyzer

The Beckman Stack Gas Analyzer, which is shown in Figure 3.11, can continuously monitor emission levels in the combustion gas. In this experiment, compounds contained in the gas samples, such as carbon dioxide, carbon monoxide, oxygen, and nitrogen oxides were determined by this analyzer. The analyzer is routinely calibrated using a standard gas mixture during the experimental runs.

Table 3.3 Retention Times of Compounds Detected by TCD

Compounds	Formula	Time (min.)
Air		1.66
Carbon monoxide	CO	2.70
Methane	CH_4	5.39
Carbon dioxide	CO_2	8.17
Acetylene	C_2H_2	11.10
Ethylene	C_2H_4	12.99
Ethane	C_2H_6	15.06

NO_x Analysis

Levels of NO_x are determined by the Beckman Model 951A NO_x analyzer using a chemiluminescent detection method. The principle of the detection is based on the nitric oxide (NO) reaction with ozone (O_3) to produce nitrogen dioxide (NO_2) and oxygen. Some of the nitrogen dioxide thus produced is initially in an electronically-excited state (NO_2*). The NO_2* reverts immediately to the ground state, with emission of photons. The reactions involved are:

$$NO + O_3 = NO_2^* + O_2 \qquad (R3.1)$$

$$NO_2^* = NO + h\nu \qquad (R3.2)$$

where h = Planck's constant and ν = frequency, Hz.

As NO (contained in the sample) and O_3 (produced by a ozone generator in the analyzer) get mixing in a small reaction chamber, the chemiluminsent reaction produces light emission that is directly proportional to the concentration of NO contained in the sample. This emission is measured by a photomultipiler tube and converted into an electric signal.

The NO_2 determination is identical to the NO determination except that, prior to entry into the small reaction chamber, the sample is passed through a converter where the NO_2 component is converted into NO by reaction

$$2NO_2 = 2NO + O_2 \qquad (R3.3)$$

In this way, the total NO in the converted sample is determined, and the NO_2 concentration is obtained by subtracting the NO determined in the original sample from the sum. The NO_2 could not be determined during most experiments in this work and in other studies (Miyauchi et al. 1981; Blevins and Roby 1992). The possible reason is that certain species exist in the flame front which cause the catalyst in the NO_2 to NO converter to reduce both NO_2 and NO back to N_2 (Drake 1985), and in the post-flame zone the NO_2 will be converted rapidly back to NO (Miller and Bowman 1989) through a possible reaction channel of $NO_2 + H = NO + OH$.

O_2 Analysis

Oxygen is determined by the Beckman Model 755 O_2 analyzer using a paramagnetic method based on the capability of the oxygen molecule to become a temporary magnet when placed in a magnetic field. Measurement is accomplished by a torque force balance system. The force produced in this system is proportional to the sample oxygen content. Variables that will influence the measurement precision are sample gas pressure and operating temperature. Therefore, it is necessary to calibrate the instrument at the same pressure as the actual sample, and to warm up and maintain the analyzer temperature as required at 60 °C.

CO and CO_2 Analyses

Although the gas chromatograph discussed above has the capability of determining CO and CO_2 composition in gas samples, it is not used for routine analysis of these species due to its time consumption (CO_2 retention time is 8.2 minute). Beckman Model 864/865 analyzers are used to determine the CO and CO_2 based on their fast responses and continuous monitoring capabilities.

In the 864/865 analyzers, non-dispersive infrared radiation produced from two separate energy sources pass through two cells: one cell containing a non-absorbing reference gas (hydrogen), the other cell containing the continuous flowing sample. A portion of infrared radiation is absorbed by the component of interest in the sample and the absorbed portion is proportional to the component concentration in the sample. The detector converts the difference in energy between the two cells to a capacitance change. This capacitance change, equivalent to the component concentration, is amplified and indicated on a meter.

Before injection samples to the Beckman board, the instruments on the board were warm up for at least one hour. Calibrations were performed using on-line standard gases in advance of each experimental run.

3.3.4 HCl Scrubber and HCl Measurement

When methyl chloride was present in the combustion system, the gas samples from the probes first pass through a counter-current water scrubber to absorb gaseous HCl from the flow into the water. The scrubbing column is a one meter long, five centimeters diameter plastic tube packed with small pieces of polyethylene tubing (6.3 millimeter outer diameter × 10 millimeters average length) simulating Rashing rings. The scrubber is oversized to affect complete HCl recovery from the sample gas.

The aqueous HCl is continuously analyzed by means of a reference / chloride ion specific electrode pair. This pair is calibrated by standard HCl solutions using titration. The scrubber and electrodes system were constructed in-house. The measurement system are shown in Figure 3.12.

3.4 Measurement Limitation and uncertainty

The maximum detection sensitivity for the Hewlett-Packard GC/FID used for the light hydrocarbon analyses is in a mole fraction range of about 5×10^{-6} to 10×10^{-6} (5 to 10 ppm). Reproducibilities for the GC injections of the standard samples and the experimental samples of fuel-rich combustion were usually better than +/-5 %. Species concentrations near the FID detection limit were reproducible to about +/-30 %. The specifications of standard gas used for calibration of the GC are of +/-2 % accuracy. For both of the CO and CO_2 concentrations determined by the Beckman analyzers, the instrument precision is 2 % of full-scale. The reading errors on these meters are estimated to be about 1 %.

Absorption efficiency of the HCl scrubber was better than 95 % according to analysis of the residual-HCl-absorbed solution after the scrubber. The detectable limit of the reference/chloride ion specific electrode system is on the order of 1×10^{-4} moles / liter HCl in the aqueous solution. The pH meter response is such that a tenfold change in HCl concentration resulted in a potential change of 70 mV in the higher HCl range, while a 400 mV potential change would result from the same HCl change in very diluted solution, which could cause higher uncertainty of HCl measurement in the lower concentration range.

The sensitivity of the NO_x chemiluminescent detector is 1 ppm on the 100 ppm range which was set for fuel-bound nitrogen free combustion cases, and it is 10 ppm on the 1000 ppm range which was set for the CH_3NH_2 combustion cases. The instrument precision is 2 %. Meter reading error is about 1%. The analyzer was routinely calibrated using a cylinder of NO/NO_2 standard gas of +/-2 % accuracy.

Carbon balances and chlorine balances were made in the related runs to indicate the overall measurement uncertainty. In the later chapters, error bars will be shown on the data in representative figures to describe these data limitations.

CHAPTER 4

MODELING METHODS

4.1 Reactor Model

Jet Stirred First Stage

The jet stirred toroidal primary zone of the two-stage combustor can be simulated as a Perfectly Stirred Reactor (PSR) under most combustion conditions (Lam 1988; Barat 1990; Vaughn 1991; Barat 1992). Departure from PSR behavior generally occurs at elevated mass flow rates which make the temperature drop and push the first stage toward extinction (Barat 1990). This departure from PSR behavior as blowout is approached seems to be less pronounced under fuel-rich conditions (Brouwer 1992). For all of the experiments performed in this study, PSR behavior were maintained since only moderate feed flow rates (7.5 to 8.7 grams / second) are used in both fuel-lean and rich conditions. In addition, high temperature in the first stage is maintained (T > 1730 K).

At steady state, the total mass flow rate, G, at the reactor inlet is equal to that at the reactor outlet. Based on the perfectly stirred first stage behavior, the governing species balance equation in the PSR can be written as

$$G(Y_k - Y_{k0}) = \omega_k W_k V \qquad \text{(E4.1)}$$

where Y_k is the mass fraction of species k, Y_{k0} is the mass fraction of k in the feed, ω_k is the net molar rate of production by reactions which involve the species k, W_k is the

molecular weight of species k, and V is the volume of first stage. There are K species balance equations for the total number of K species.

Linear Flow Second Stage

The linear turbulent flow secondary zone of the reactor can be simulated as a Plug Flow Reactor (PFR) with high axial flow velocity. The axial dispersion of components was not considered and the PFR model was used for this same type reactor in MIT (Lam 1988). The gas velocities in the second stage tube under the experimental conditions in this study are 20 to 30 meters /second, which results in a high Reynold number ($3 * 10^5$) and a large axial Peclet number ($P_e > 5$). These results suggest the axial dispersion of species is not important and the plug flow reactor performance is valid for the second stage.

At steady state, the governing species balance equations (for K species) in the PFR are given by a set of ordinary differential equations

$$\frac{dY_k}{dt} = \frac{\omega_k W_k}{\rho} \qquad \text{(E4.2)}$$

where t is residence time and ρ is mass density of the combustion gas. The residence time is related to the second stage reactor volume, V, and the total feed mass flow rate, G, by equation

$$t = \frac{\rho V}{G} \qquad \text{(E4.3)}$$

where the mass density ρ is calculated from the ideal gas equation of state,

$$\rho = \frac{P\,\overline{W}}{R\,T} \qquad \text{(E4.4)}$$

where P is the pressure (one atmosphere), T is the absolute temperature, R is the universal gas constant, and $\overline{W}$ is the mean molecular weight of the combustion gas mixture.

Material Injection

Materials (air / steam) injected into the second stage inlet are assumed to rapidly mix with the first stage outlet flow in a small transition section. This step is modeled with a non-reactive mixing module. The species balance and energy balance equations in this model are written as

$$(GY_k)_{PSR} + (GY_k)_{inj} = (GY_k)_{PFR\ inlet} \qquad \text{(E4.5)}$$

$$\sum(GY_k h_k)_{PSR} + \sum(GY_k h_k)_{inj} = (hG)_{PFR\ inlet} \qquad \text{(E4.6)}$$

where G is the mass flow rate, Y_k is the mass fraction of species k, h_k is the enthalpy of species k, and h is the mean enthalpy of the gas mixture. The subscripts stand for locations in the reactor. The injected air flow rate was measured by two rotameters and injected into the reactor at room temperature. The injected steam was produced by a house-made small steam generator, and it is injected at around 100 °C. The steam flow rate was determined by measuring the water flow rate.

Temperature Interpolation

Energy conservation equations in both of the PSR and PFR are decoupled from the species mass balance equations by using measured PSR temperature and PFR temperature profiles as input parameters in the modeling. Therefore, only the mass balance equations for each species need to be solved in most of the modeling cases. The measured PSR temperature is directly input into the reactor model. The temperatures measured at the different lengths of the PFR are smoothly interpolated as a second order polynomial

$$T = T_{psr} + B \times t + C \times t^2 \qquad \text{(E4.7)}$$

where T_{psr} is the PSR temperature, t is PFR residence time, B and C are regression coefficients. The equation of E4.7 is input to the model to describe the axial temperature distribution in the second stage.

For special purpose of reactor heat loss estimation, the model is run in an adiabatic mode to calculate the adiabatic reactor temperature. This can then be compared with the measured values to determine the heat losses.

A configuration of the two-stage reactor, including the injection mixer, for computer simulation is illustrated in Figure 4.1. The PSR + PFR reactor simulation program is an original application driver code which accesses the general-purpose FORTRAN chemical kinetics code package, CHEMKIN (Kee and Miller 1986). This package provides a means to describe symbolically the reaction mechanism (input by user with forward reaction rate constants) and a means to describe computationally an arbitrary system of governing equations. The PSR code (Glarborg et al. 1986) and the LSODE (Hindmarsh 1983) ordinary differential equation solver were used to solve the governing equations. The feed compositions and flow rate, the measured temperatures in both stages,

either the PSR volume or residence time, the reactor pressures (one atmosphere), and the injection temperature, compositions, and the flow rate were used as input to the modeling. The computer code and input cards are given in Appendixes B and C.

4.2 Reaction Mechanism

The net chemical production rate of species k, ω_k, in the equations E4.1 and E4.2 are determined by CHEMKIN subroutines as functions of the species concentrations and combustion temperature with the aid of the user input reaction mechanism and measured temperature. The rate of each reaction which involves that species is calculated according to the law of mass action and the forward rate coefficient k_f. The coefficients are expressed by the modified Arrhenious form

$$k_f = AT^n \exp(\frac{-E_A}{RT}) \qquad \text{(R4.8)}$$

where the pre-exponential factor A, the temperature exponent n, and the activation energy are required input to the CHEMKIN package for each reaction included in the mechanism. The reverse rate constant k_r is related to the forward rate constant k_f through the reaction equilibrium constant K as

$$k_r = \frac{k_f}{K} \qquad \text{(E4.9)}$$

The equilibrium constant K is calculated by CHEMKIN based upon the temperature and species thermodynamic properties. The CHEMKIN user supplies a thermodynamic database consisting of standard $H°_f$ (298 K), S° (298 K) and heat capacities as function of temperature.

The reaction mechanisms used for the modeling are primarily drawn from literature. For the C_2H_4/air/N_2 and C_2H_4/CH_3Cl/air/N_2 combustion system in this work, the mechanisms are taken from Ho and Bozzelli (1993). For the combustion of C_2H_4/CH_3NH_2/air/N_2, most of the CH_3NH_2 oxidation reactions are taken from Hwang and Gardiner (1990) with some new reactions added. The NO formation chemistry is extracted from Miller and Bowman (1989), and the C1/C2 hydrocarbon combustion mechanism from (Ho 1993) are used in this study. In the modeling of C_2H_4/CH_3Cl/CH_3NH_2/air/N_2 combustion, the overall mechanism is constructed from four subsets: C_1/C_2 and chlorocarbon combustion mechanism (Ho 1993), NO chemistry (Miller and Bowman 1989), CH_3NH_2 pyrolysis and oxidation reactions (Hwang et al. 1990), and a group of reactions which involved the interaction between chlorine-containing and nitrogen-containing species.

To make the mechanism more consistent with the experimental conditions (bath gas, pressure, and temperature range) used in this study, modifications for selected reactions were made in each combustion mechanism. For these reactions, such as unimolecular dissociations, radical-radical combinations, and radical-unsaturate additions, the Quantum Rice-Ramsberger-Kassel (QRRK) method (Dean 1985) was used to estimate the kinetic parameters in the experimental pressure and temperature range of this study. Specific modifications on the literature mechanisms will be discussed in following appropriate chapters. The modified mechanisms are shown in Appendix D and the thermodynamic properties of species involved in these reaction mechanisms are listed in Appendix E.

4.3 Rate-of-Production Analysis

It is often interesting to determine how each reaction is important to the production or destruction of a key species. The two-stage reactor simulator, PSR + PFR driver program, includes options to request net Rate-Of-Production (ROP) information obtained from calls to selected CHEMKIN subroutines. The net generation and destruction rates for selected species are calculated, including breakdowns of these net rates into the rates of each contributing reaction. The net molar rate of production by reaction ω_k of species k is calculated by

$$\omega_k = \sum_{i=1}^{I} \gamma_{ki} \xi_i \qquad \text{(E4.10)}$$

where I is the total number of elementary reactions in the mechanism, γ_{ki} are the stoichiometric coefficients of species k in reaction i, and ξ_i is the rate of progress for the reaction i. The contribution percentage, called normalized rate-of-production C_{ki}, to the ROP of species k from reaction i is calculated from

$$C_{ki}(\%) = 100 \times \frac{\gamma_{ki} \xi_i}{\sum_{i=1}^{I} \gamma_{ki} \xi_i} \qquad \text{(E4.11)}$$

From C_{ki} one can recognized how reaction i contributes to the formation or consumption of species k. Contributions below a preset lower limit are not reported (a typical lower limit is 1 %). The information obtained from the ROP analysis is extremely useful in

identifying production and destruction pathways for important species, and in constructing the chemical pathways for reactant consumption, intermediate, and product formation. The ROP calculations are warranted if a good fit of the model predictions to experimental data is achieved. In the following chapters, the ROP analysis are used for the experimental data interpretation based on reasonable model prediction.

CHAPTER 5

COMBUSTOR CHARACTERIZATION AND VALIDATION

For the purposes of system testing and validation, a series of runs with ethylene and air under various feed conditions were made in the two-stage combustor. These runs included straight fuel-lean and fuel-rich combustion runs and air injection into the second stage for the both cases. Species concentrations and reactor temperature were measured in all runs and detailed modeling with known reaction mechanisms was performed for representative fuel-lean and fuel-rich cases. The measurements and comparisons between the data and model prediction served to validate the system.

The feed condition is characterized by the fuel equivalence ratio, which is defined as the actual fuel to air ratio divided by the stoichiometric fuel to air ratio. The fuel equivalence ratio usually is given by a symbol ϕ and its general calculation equation is

$$\phi = \frac{(\text{Fuel} \ / \ \text{Air})_{\text{actual}}}{(\text{Fuel} \ / \ \text{Air})_{\text{stoich.}}} \qquad \text{(E5.1)}$$

where Fuel and Air stand for volumetric or mole flow rates of fuel and air in the feed mixture. For fuel-rich feed, there is more fuel than the stoichiometric amount and $\phi > 1$. For fuel-lean systems, excess air (oxygen) is present in the combustion and $\phi < 1$. At stoichiometric condition, $\phi = 1$.

The stoichiometric condition is determined based on the assumption of complete combustion to the most thermodynamically stable products. For example, for combustion

of ethylene, methyl chloride, and monomethyl amine, the assumed global stoichiometries are:

$$C_2H_4 + 3O_2 = 2H_2O + 2CO_2 \qquad \text{(R5.1)}$$

$$CH_3Cl + 1.5O_2 = H_2O + CO_2 + HCl \qquad \text{(R5.2)}$$

$$CH_3NH_2 + 2.25O_2 = 2.5H_2O + CO_2 + 0.5N_2 \qquad \text{(R5.3)}$$

Utilizing E5.1, R5.1, R5.2, and R5.3, one can easily obtain equivalence ratio equations for each specific combustion case. For ethylene combustion,

$$\phi = \left(\frac{3}{0.21}\right)\left(\frac{\text{Eethylene}}{\text{Air}}\right)_{\text{actual}} \qquad \text{(E5.2)}$$

for methyl chloride combustion,

$$\phi = \left(\frac{1.5}{0.21}\right)\left(\frac{\text{Methyl Chloride}}{\text{Air}}\right)_{\text{actual}} \qquad \text{(E5.3)}$$

and for monomethyl amine combustion,

$$\phi = \left(\frac{2.25}{0.21}\right)\left(\frac{\text{Monomethylamine}}{\text{Air}}\right)_{\text{actual}} \qquad \text{(E5.4)}$$

where the compound name in each equation stands for volumetric or mole flow rates of these species.

When two or three of these fuels is simultaneously present in the combustion feed, the equivalence ratio can be calculated by

$$\phi = \frac{\left(\frac{\text{Ethylene} + \text{Methyl Chloride} + \text{Monomethylamine}}{\text{Air}}\right)_{\text{actual}}}{\left(\frac{\text{Ethylene} + \text{Methyl Chloride} + \text{Monomethylamine}}{\frac{3}{0.21}\text{Ethylene} + \frac{1.5}{0.21}\text{Methyl Chloride} + \frac{2.25}{0.21}\text{Monomethylamine}}\right)_{\text{stoich.}}} \qquad \text{(E5.5)}$$

When dilution nitrogen exists in the feed, it does change the feed compositions, but does not influence the equivalence ratio because ϕ is independent of feed composition and total flow rate.

5.1 Combustion of C_2H_4 under Fuel-lean Conditions

An isothermal condition in the first stage is essential for considering this zone as a Perfectly stirred Reactor (PSR). During fuel-lean combustion of ethylene at $\phi = 0.53$ and a residence time 7.5 milliseconds, temperatures in the first stage were measured by moving the thermocouple across the torus diameter perpendicular to its axial plane. The feed conditions for this run are shown in Table 5.1 and the measured temperature profile is plotted in Figure 5.1.

The normal position of the thermocouple bead is located approximately at 25 % of the torus diameter. As shown in Figure 5.1, the first stage is effectively isothermal to within +/- 20 K from the value at the routine measurement location.

Temperature measurement errors due to heat radiation from the thermocouple bead to lower temperature surroundings usually occurs in open, wall-less flame. In this two-stage reactor, high turbulent flow and a small temperature gradient (hot reactor walls) ensure that radiation corrections to the measured temperatures are not needed.

Table 5.1 Feed Conditions of Fuel-lean Case 1

Feed	Flow Rate (scfm)
C_2H_4	0.41
Air	11.0
Diluent N_2	0
Equivalence Ratio	0.53

For testing the air injection effects on the reactor performance, a simple fuel-lean case (ϕ = 0.59) was examined with and without second stage air injection. The overall equivalence ratio ($\phi_{overall}$) considering injected air was 0.56. The feed and injection conditions are shown in Table 5.2. Temperatures, CO, and CO_2 concentrations in each stage were measured. The concentrations are shown in Figure 5.2 and temperatures are in Figure 5.3. As indicated by Figure 5.2, CO is almost burnt out in the first stage by excess air and thus CO_2 stays constant along the second stage. With air injection, Figure 5.3

shows second stage temperature is lower due to dilution. The second stage temperature decreases in both cases are caused by heat losses in this zone, which actually is advantageous in the point of view of low thermal NO.

Table 5.2 Feed Conditions of Fuel-lean Case 2

Feed	Flow Rate (scfm)
C_2H_4	0.52
Air	12.5
Diluent N_2	0
Injected Air	0.83
Equivalence Ratio	0.59
Overall Equivalence Ratio	0.56

Another fuel-lean test run was executed at ϕ = 0.61. This experiment was simulated with the PSR+PFR model using a known reaction mechanism (Ho 1993) for C_1/C_2 hydrocarbon combustion. Two calculation modes were used in modeling of this case: adiabatic reactor and fixed temperature (i.e. measured) reactor. With the adiabatic simulation mode, energy balance and species balance equations were solved simultaneously and the adiabatic temperature was calculated. By comparing the calculated temperature with the measured temperature, reactor heat losses were estimated by following equation:

$$\frac{Q_{losses}}{Q_{input}} = \frac{G_{feed} C_p (T_{adiabatic} - T_{measured})}{G_{fuel}(-\Delta H_{rxn})} \qquad \text{(E5.6)}$$

where Q_{losses} = heat loss from reactor, Q_{input} = heat input to reactor by fuel, G = flow rate (mole / second), C_p = mean heat capacity of the combustion gas (kJ / mole / C), ΔH_{rxn} = heat formation (kJ / mole), and T = reactor temperature (C)

The estimations show that heat losses from the first stage is less than 10 percent and it is less than 15 percent in the second stage (average PFR temperature was used). With the temperature given calculation mode, measured PSR temperature and PFR temperature profile were used as input to the model. The modeling results and experimental data are presented in Table 5.3. The good agreement between data and model suggests that the first stage is indeed behaving as a PSR.

5.2 Combustion of C_2H_4 under Fuel-rich Conditions

Effort was expanded in the characterization and validation of the system for fuel-rich combustion of ethylene with air. Under fuel-lean conditions, the large amount of nitrogen carried by the combustion air serves as a natural diluent and heat sink. Under fuel-rich conditions, however, such a heat sink is not available due to the considerably lower amount of feed air. Therefore, all fuel-rich runs require dilution nitrogen in the feed for temperature control.

A vertical thermocouple trace, taken for a first stage C_2H_4/Air/N_2 feed of ϕ = 1.30 and a residence time of 5.1 milliseconds, is shown in Figure 5.4. As shown in the fuel-lean case, the measured temperature profile shows that the torus is also effectively isothermal in the fuel-rich case.

Table 5.3 Feed Conditions and Results of Fuel-lean Case 3

Feed	Flow Rate (scfm)
C_2H_4	0.49
Air	11.41
Diluent N_2	0
Equivalence Ratio	0.61
First Stage Temperature (K)	1733

First Stage Compositions (mole fraction)

	(measured)	(model)
CO	0.0041	0.0039
CO_2	0.079	0.085
O_2	0.085	0.086
CH_4	0	0
C_2H_2	0	0.000027
C_2H_4	0	0.000039
C_2H_6	0	0

Data measured from combustion of ethylene and air with dilution nitrogen (ϕ = 1.32) have been predicted using the same reactor model as mentioned in the fuel-lean case. For the purpose of thermal NO formation prediction in the fuel-rich case, NO chemistry taken from the literature (Miller and Bowman 1989) was add to the C_1/C_2 hydrocarbon combustion mechanism (Ho 1993) which has been used in the fuel-lean case modeling (More discussion of the NO mechanism used in this model will be given in Chapter 7). Feed conditions for this case and comparisons of model predictions with experimental measurements are listed in Table 5.4.

The model results in the table 5.4 were obtained by using measured temperature as input to the model. The calculated adiabatic temperature in the first stage from the model is 1836 K. Using equation E5.6, heat losses from the first stage in the fuel-rich case are estimated to be about 4.5 percent.

As a further test of secondary air injection, a fuel-rich (ϕ = 1.52) run was performed in the first stage as a base case, with small flows of air injected into the second stage for enhancing burnout. Table 5.5 shows the feed conditions. The overall reactor fuel equivalence ratio with air injection still is fuel-rich ($\phi_{overall}$ = 1.43). . The measured temperature profiles for both base and injection cases are shown in Figure 5.5. Due to the additional burnout occurring in the second stage, the temperature profile with air injection is higher than that measured in the case without air injection, though heat losses still result in a falling trend.

Species concentrations for the above case are presented in Figures 5.6, 5.7, and 5.8. As might be expected, the additional burnout due to air injection into the second stage results in lower levels of CO and C_2H_2 with increased CO_2. In general, the relative fit of the model prediction to the experimental observation is acceptable, especially considering that all data are plotted on a linear scale. Both of the concentrations shown on these figures have been corrected to account for the injection air dilution.

Table 5.4 Feed Conditions and Data of Fuel-rich Case 2

Feed	Flow Rate (scfm)
C_2H_4	1.1
Air	11.94
Diluent N_2	5.91
Equivalence Ratio	1.32
First Stage Temperature (K)	1756

First Stage Compositions (mole fraction)

	(measured)	(model)
CO	0.055	0.058
CO_2	0.051	0.057
O_2	0.002	0.0016
CH_4	8.4E-4	1.6E-4
C_2H_2	1.8E-3	1.4E-3
C_2H_4	2.8E-3	1.5E-4
C_2H_6	2.7E-5	1.6E-6
NO	31 (ppm)	12 (ppm)

Carbon atom balances for three typical runs including the fuel-lean, fuel-rich, and fuel-rich with air injection were made and used as an indicator of measurement accuracy. These balances were obtained directly from measured concentrations of C-containing species. They are plotted as functions of residence time and shown in Figure 5.9. According to the C-balances, it is estimated that the measurement accuracy of C-containing species is around +/- 5 % which is reflected by the error bars shown on the data of Figure 5.6.

Table 5.5 Feed Conditions of Fuel-rich Case 3

Feed	Flow Rate (scfm)
C_2H_4	1.07
Air	10.08
Diluent N_2	3.93
Injected Air	1.03
Equivalence Ratio	1.52
Overall Equivalence Ratio	1.38

5.3 Summary

A two zone turbulent flow reactor has been constructed and validated for use in staged combustion studies. Measured temperature profiles shown that the first stage is effectively isothermal in both fuel-lean and fuel-rich cases. Modeling with a PSR + PFR reactor simulation and detailed reaction mechanism predicted well the observed data in

both the first and second stage. These results represent an important validation of the experimental facility. Chapter 6, 7, and 8 will discuss the research on the specific topics of methyl chloride, monomethyl amine combustion, and co-combustion of these chlorine- and nitrogen-containing simulated hazardous wastes.

CHAPTER 6

COMBUSTION OF METHYL CHLORIDE

6.1 Introduction

Incineration is an effective method for disposal of hazardous chemical wastes, such as chlorine-containing species. Under well controled operating conditions, the chlorine compound destruction efficiency can be high (Fisher et al., 1990). But incomplete combustion in the incinerator can lead to low destruction efficiency and high level pollutant emissions, such as unburned hydrocarbons, CO, high molecular weight compounds, and products of incomplete combustion (PICs). Chlorine-containing compounds are well recognized hydrocarbon combustion inhibitors which limit CO burnout and promote the formation of PICs.

Previous studies of chlorocarbon combustion (Westbrook 1982; Chuang and Bozzelli 1986; Kara and Senkan 1987; Ritter and Bozzelli 1990; Barat 1990; Brouwer 1992; and Ho 1993) have provided better understanding of the reaction pathways and the chlorine inhibition phenomenon, but few have suggested means to overcome the inhibition and reduce PIC emissions. Reaction mechanism analysis based on the fundamental thermodynamic kinetics and modeling by Ho et al. (1992) hypothesized that injection of steam into the chlorocarbon combustion system is a possible way to enhance CO burnout.

In this current experimental and modeling study, the two stage turbulent flow reactor was used to simulate a nozzle-fed liquid industrial incinerator consuming chlorocarbons. The combustion inhibition by methyl chloride and the effects of steam injection as a means to overcome the inhibition have been investigated. Detailed

experimental results and modeling predictions are reported. The model predictions, based on a detailed $CH_3Cl/C_2H_4/Air/N_2$ mechanism, agree well with the experimental observations. Rate of production and reaction pathway analyses provide further understanding of the chlorocarbon combustion process.

6.2 Experimental Cases and Data

Base cases

Two baseline cases are ethylene / air combustion without methyl chloride loading in the feed. The first base case is fuel-lean at $\phi = 0.6$. In this case, measured temperature in the PSR is 1731 K. The measured temperature profile as a function of total reactor residence time is shown in Figure 6.1. Species concentrations were measured in the PSR and at the PFR outlet (residence time = 15 milliseconds). The feed conditions and measurements in this base case are listed in Table 6.1

The light hydrocarbons are effectively burnt out in this fuel-lean combustion and their concentrations in the sample are lower than the method detection limit (5 to 10 ppm). The NO formation measured in the first stage is 11 ppm and grows to 15 ppm at the outlet of the second stage, even though the PFR temperature is lower than that in the PSR. This NO growth with the increased residence time is consistent with the NO observations in a flame study by Blauwnes et al. (1977).

The second base case is fuel-rich at $\phi = 1.3$. Diluent nitrogen was added to the fuel-rich feed to control the PSR temperature at 1737 K. The measured temperature profile along the reactor length is shown in Figure 6.2. Feed conditions and measured species concentrations include light hydrocarbons and NO for this fuel-rich base case are listed in Table 6.2.

Table 6.1 Feed Conditions and Results of Base Case 1 (fuel-lean)

Feed	Flow rate (scfm)
C_2H_4	0.616
Air	14.67
Diluent N_2	0
CH_3Cl/C_2H_4 (molar ratio)	0
Equivalence Ratio	0.6

Measured Species Concentrations (mole fraction)

	PSR	PFR(outlet)
CO	0.0036	0
CO_2	0.076	0.080
O_2	0.094	0.092
CH_4	/	/
C_2H_2	/	/
C_2H_4	/	/
C_2H_6	/	/
NO	11 (ppm)	15 (ppm)

Table 6.2 Feed Conditions and Data of Base Case 2 (fuel-rich)

Feed	Flow rate (scfm)
C_2H_4	0.893
Air	9.81
Diluent N_2	5.48
CH_3Cl/C_2H_4 (molar ratio)	0
Equivalence Ratio	1.30

Measured Species Concentrations (mole fraction)

	PSR	PFR(outlet)
CO	0.058	0.054
CO_2	0.054	0.057
O_2	0.002	0.0
CH_4	1.85E-4	6E-7
C_2H_2	3.33E-4	1E-6
C_2H_4	2.80E-4	0
C_2H_6	3.2E-5	0
NO	36 (ppm)	46 (ppm)

CH_3Cl Loaded Cases

Methyl chloride were added to the combustion feed to examine its effect on the combustion process and emission levels. The feed molar ratios of CH_3Cl / C_2H_4 were set at 0.1, 0.2, 0.3, and 0.4. As the methyl chloride loading in the feed increased, the concentration of primary fuel, ethylene, in the feed was reduced to keep the fuel equivalence ratios constant at the baseline values (ϕ = 0.6 and 1.3). In the fuel-rich cases, the diluent nitrogen was added and its flow rate was maintained constant as methyl chloride loading changed. In this way, the reactor temperature changes due to methyl chloride addition were examined. The feed conditions at four methyl chloride loading levels are shown in Table 6.3 for the fuel-lean case and in Table 6.4 for the fuel-rich case.

When running with methyl chloride, the sample gas was continuously pulled through the DI-water scrubbing packed tower. The scrubbed aqueous HCl was analyzed by means of a referenced chloride ion electrode. The HCl mole fractions in the sample gas were obtained by solving the HCl mass balance equation and the measured aqueous HCl concentration, sample gas flow rate, and the DI-water flow rate.

The measured HCl concentrations in the gas samples from the PFR outlet are shown in Figure 6.3. for both ϕ = 0.6 and ϕ = 1.3 cases. Chlorine balances which were obtained from measured HCl concentrations are shown in Figure 6.4. It can be seen from the chlorine balance that the measured chlorine levels in HCl at the lower CH_3Cl loading case is lower than the feed and modeling values. The possible reason for this is that it is difficult to get better HCl measurement at lower concentration. The average measurement error for HCl are estimated to be about 15% based on the chlorine balance and flowmeter reading uncertainty. Error bars have been put on the data in Figure 6.3 to reflect the HCl measurement errors.

Scrubbed sample gas was then directed to an on-line gas chromatograph and an

Table 6.3 Feed Conditions in Methyl Chloride Loaded Cases ($\phi = 0.6$)

	Flow Rate (scfm)			
Feed	case 1	case 2	case 3	case 4
C_2H_4	0.586	0.558	0.533	0.510
Air	14.64	14.62	14.60	14.58
CH_3Cl	0.059	0.112	0.160	0.204
Dil. N_2	0	0	0	0
Total	15.29	15.29	15.29	15.29
CH_3Cl/C_2H_4	0.1	0.2	0.3	0.4

Table 6.4 Feed Conditions in Methyl Chloride Loaded Cases ($\phi = 1.3$)

	Flow Rate (scfm)			
Feed	case 1	case 2	case 3	case 4
C_2H_4	0.847	0.805	0.768	0.734
Air	9.771	9.736	9.704	9.675
CH_3Cl	0.085	0.161	0.230	0.293
Dil. N_2	5.480	5.480	5.480	5.480
Total	16.18	16.18	16.18	16.18
CH_3Cl/C_2H_4	0.1	0.2	0.3	0.4

on-line industrial stack gas analyzer to determine the concentrations of light hydrocarbons, O_2, CO, CO_2, and NO. For both fuel-lean and fuel-rich runs the measured concentrations of CO and CO_2, in term of the molar ratio of CO/CO_2, as a function of CH_3Cl/C_2H_4, are shown in Figures 6.5 to 6.8. The measured concentrations for other species are shown in Figures 6.9 to 6.12.

Steam Injection Cases

Steam, at one atmosphere and 100 °C, was injected into the zone between the first and second stages under two conditions: CH_3Cl/C_2H_4=0.2, ϕ = 1.3 and CH_3Cl/C_2H_4 = 0.2, ϕ = 1.35. At the first condition, one steam injection level of 0.3 grams/second was investigated. For the second condition, increased steam injection levels were examined with steam flow rates at 0.17, 0.38, and 0.60 grams / second. The corresponding mass ratios of steam to the feed were 0.018, 0.041 and 0.065. In both of these conditions, the measured species concentrations are corrected to account for the steam dilution effect. Steam was not injected for fuel-lean case because all the CO and light hydrocarbons have been burnt out at the reactor outlet with excess oxygen and added PFR residence time.

The results obtained from the first run at ϕ = 1.3, CH_3Cl / C_2H_4 = 0.2 with and without steam injection are reported in Table 6.5. It is noted from this table that the ratio of CO / CO_2 at the reactor outlet has been decreased from 1.14 to 0.89 by injecting steam into the second stage. At the same time, the unburned light hydrocarbons in the combustion also decreased with the steam injection.

Temperatures measured under the second condition are plotted as functions of residence time for different steam injection flow rates in Figure 6.13 to compare them with that in the steam = 0 case. It can be seen from these curves, that the steam injection does not cause any effective change in the second stage temperature profiles.

Table 6.5 Comparison of Results: Steam Injection=0 and 0.3 g/s

Feed	Flow rate (scfm)
Air	9.74
C_2H4	0.81
CH_3Cl	0.16
Diluent N_2	5.2
CH_3Cl / C_2H_4	0.2
Total Flow rate (grams/second)	8.98
Equivalence Ratio	1.3

Measured Concentrations at Outlet of PFR (mole fraction):

Species	Steam = 0	Steam = 0.3 g/s
CO	0.063	0.055
CO_2	0.055	0.062
CO/CO_2	1.14	0.89
CH_4	7.0E-6	5.8E-6
C_2H_2	1.8E-5	7.6E-6
C_2H_4	3.2E-6	0
Measured Temperatures (K)		
PSR	1710	1706
PFR	1573	1564

The effects of the steam injections on the CO, CO_2, unburned hydrocarbons, and NO concentrations at the PFR outlet are shown in Figures 6.14 to 6.16. These data show that the CO and hydrocarbon burnout have been enhanced as the steam was injected, and that the NO stays unchanged due to the constant temperature at PFR outlet which is also indicated on the Figure 6.16.

6.3 Mechanism and Modeling

A C_1/C_2 chlorocarbon mechanism taken from Ho (1993) was used in modeling the methyl chloride combustion. This mechanism has been successfully used to predict the experimental data of CH_2Cl_2 and CH_3Cl oxidation in a tubular flow reactor (Ho 1993) over a temperature range of 873 K to 1273 K, as well as generate reasonable fits to flame data of various researchers. In the current experiments of methyl chloride combustion, temperature in the combustor ranged from 1600 K to 1760 K. In order to be more consist with this temperature range, the kinetic parameters of some important reactions in the mechanism have been modified using the QRRK method (Dean 1985). The reactions and their modified kinetic parameters are shown in Table 6.6.

The parameters shown in this table are used in forward rate constants of the form: $k = AT^n e^{\left(\frac{-E_a}{RT}\right)}$ in which the units are cal, moles, cm^3, second, and K. The input parameters for the QRRK calculations are listed in Appendix F. The modified mechanism is incorporated into the PSR+PFR reactor simulations using the CHEMKIN package (Kee and Miller 1986) to accomplish the modeling. The measured temperature profiles, with a smooth interpolation, have all been used as input to the model.

All the calculated species concentration profiles from the modeling have been displayed in the appropriate figures containing the experimental data for the purpose of

comparison. Rate-of-production obtained from the model predictions will be used for interpretation of the data.

Table 6.6 Modified Kinetic Parameters in CH_3Cl Mechanism

Reaction	A	n	E_a
$CH_2Cl+H=CH_3+Cl$	5.2E14	-0.42	830
$CH_2Cl+H=CH_2+HCl$	1.4E12	0	35050
$CH_3Cl=CH_2Cl+H$	7.4E08	1.15	2140
$CH_2Cl+OH=CH_2OH+Cl$	2.1E10	0.82	5980
$CH_2Cl+OH=CH_2O+HCl$	3.4E18	-1.5	3370
$C_2H_6=CH_3+CH_3$	1.2E29	-4.2	16590
$CH_3+CH_3=H+C_2H_5$	4.0E18	-1.62	16080
$CH_3+CH_3=H_2+C_2H_4$	5.6E35	-7.1	20050
$C_2H_4+H=C_2H_5$	3.2E47	-10.1	20100

6.4 Summary of Experimental Observations and Model Predictions

6.4.1 Temperature Profiles

Measured temperature profiles as functions of residence time at different chlorine loading levels are shown in Figure 6.1 (ϕ = 0.6) and Figure 6.2 (ϕ = 1.3) compared with those in the base cases. In the fuel-lean cases (ϕ = 0.6), the PSR temperature drops continuously from 1731 K of the base case to 1714 K with the feed CH_3Cl / C_2H_4 = 0.4, while the PFR outlet temperature increases slightly as the CH_3Cl loading increased. This

phenomena of lower temperature in the first zone, and then higher temperature in the second zone with the increased chlorine loading have been observed in previous studies (Wang et al. 1993; Senser et al. 1987). The study on fuel-lean flame by Senser et al. (1987) showed that the temperature dropped about 30 °C in the flame zone (analogous to the first stage) and increased about 60 °C in the post-flame zone (analogous to the second stage) when the feed ratio of Cl / H changed from 0.06 to 0.72. In the current fuel-rich cases (ϕ = 1.3), with the feed methyl chloride loading increased from CH_3Cl / C_2H_4 = 0 to 0.4, the PSR temperatures dropped from 1737 K to 1663 K. The temperature kept decreasing with a smaller gradient along the PFR until the reactor outlet.

When steam was injected into the second stage, the injection does not appreciably change the temperatures in both PSR and PFR as shown in Figure 6.13. If no additional burnout occurred in the second stage with the injection, the PFR temperature profile would drop because the steam was injected at much lower temperature than the reactor temperature. Therefore, heat production by the enhanced burnout has roughly balanced the heat absorbed by the much cooler saturated steam.

6.4.2 CO Burnout Inhibition and Increase of PICs

The increased loading of methyl chloride into a fuel-lean combustion system resulted in increased concentrations of CO and decreased levels of CO_2 in the PSR. This is described by the molar ratio of CO / CO_2 as a function of methyl chloride loading in Figure 6.5. At PFR outlet, as a result of added residence time (relative to PSR) and the excess oxygen (i.e. fuel-lean), the CO falls to below detectable limits (5 to 10 ppm). The CO_2 is nearly constant with chlorine loading increase, as shown in Figure 6.6.

In the fuel-rich feed condition, the effects of chloride loading on the CO and CO_2 concentrations have also been observed in both stages. Figure 6.7 shows that the ratio of

CO / CO_2 increases more steeply with the feed ratio of CH_3Cl / C_2H_4 in the PSR than that in the PFR as shown in Figure 6.8. The model results presented in these figures agree well with the experimental data. All the results illustrate the inhibitory effect of methyl chloride on the CO burnout to CO_2.

The concentration of O_2 remained constant (see Figure 6.9) with feed CH_3Cl loading for the ϕ = 0.6 case. This is not unexpected since O_2 is in excess for fuel-lean conditions. However, for the fuel-rich run (ϕ = 1.3, see Figure 6.10), where O_2 is the limiting reagent whose consumption is also a good indicator of combustion efficiency (Brouwer et al. 1992), the O_2 levels in the PSR steadily increase with the CH_3Cl loading. The result is consistent with that obtained by Brouwer et al. (1992) for fuel-rich chlorocarbon combustion. In the second stage, the plug flow nature of the reactor resulted in the effectively complete consumption of the unreacted O_2.

At ϕ = 1.3, the concentrations of unburned hydrocarbons which can be considered as PICs, such as CH_4, C_2H_2, and C_2H_4, increased with CH_3Cl loading as shown in Figure 6.11 for the first stage. Even though the model over-predicted the C_2H_2 and C_2H_4 and under-predicted the CH_4, the prediction trends agree quite well with the experimental data. Comparing to the measured concentrations in the base case (CH_3Cl / C_2H_4 = 0), the concentration of C_2H_2 increased by a factor of three, while the concentration of CH_4 more than doubled when the loading was increased to CH_3Cl / C_2H_4 = 0.4. These results are also consistent with those observed by Brouwer et al. (1992).

6.4.3 Effects of CH_3Cl on Thermal NO

For NO formation during the CH_3Cl combustion, two trends are observed from the experiments and are shown in Figure 6.12. First, the measured NO emission from fuel-rich combustion (ϕ = 1.3) is higher than that from fuel-lean (ϕ = 0.6) combustion. Second, in

both of the cases, NO decreased when the CH_3Cl loading in the feed was increased. It should be noted that no fuel-bound nitrogen was present for these runs. Therefore, NO generated here must result from thermal and / or prompt mechanisms.

The temperature profiles shown in Figure 6.1 (ϕ = 0.6) and Figure 6.2 (ϕ = 1.3) are almost in the same range, which indicates the thermal effect on the NO formation in these two cases is small. Modeling results of these experiments show that the radical concentrations of CH, CH_2, and C in fuel-rich combustion (ϕ = 1.3) are much as 100 to 1000 times higher as in the fuel-lean (ϕ = 0.6) case. Therefore, these higher hydrocarbon radical concentrations largely contribute to prompt NO in the fuel-rich case according to the prompt NO mechanism discussed in section 2.2.1. Possible explanations for the interesting effect of chlorine loading on NO will be discussed in Chapter 8.

6.4.4 Effect of Steam Injection

Table 6.5 shows the measurements of CO, CO_2, and unburned light hydrocarbons in the second stage with and without steam injection. With a steam injection flow rate of 0.3 grams/second (3.2% of total rate), the data indicate that the ratio of CO/CO_2 decreased more than 15%. Use of the CO/CO_2 ratio factors out concentration dilution effects by the injected steam.

Keeping feed conditions (ϕ = 1.35 and CH_3Cl / C_2H_4=0.2) constant, increasing steam injection from 0 to 0.6 grams/second results in continuous decreases of CO, CO/CO_2 ratio, and unburned light hydrocarbon concentrations as seen in Figures 6.14 and 6.15. Except for the high model prediction of CH_4, though with the same decreasing trend, the agreement between calculations and observations is reasonable. All the absolute concentrations shown on the charts have been corrected upward to the no steam injection condition to offset pure dilution. The results of experiments and modeling indicated that

steam injection is causing enhanced CO and hydrocarbon burnout. As shown in Figure 6.13, the lack of any appreciable change in the PFR temperature profiles during steam injection is consistent with this enhanced burnout result (i.e. increased conversion of CO and subsequent heat generation overcomes the sensible heat loss due to the relatively cold injection). The NO at PFR outlet remains unchanged with the steam injection which is shown in Figure 6.16. In an extended experiment of C_2H_4 combustion without CH_3Cl loading, the steam enhanced CO burnout has also been observed as shown in Figure 6.17.

6.5 Rate-of-Production Analysis and Discussion

In this section, the principles of CO burnout inhibition, PIC increases, and the effects of steam injection, which have been observed in the experiments and predicted by the model, are discussed based on ROP analysis results.

Several recent studies (Ho et al. 1992; Brouwer et al. 1992; Ho 1993) have hypothesized that chlorocarbon-induced inhibition of hydrocarbon combustion is largely due to the competition for OH radicals by the relatively fast reaction

$$OH + HCl = H_2O + Cl \qquad \text{(R6.1)}$$

$$\Delta H = -16.1 \text{ kcal/mole}$$

and the parallel relatively slow CO burnout reaction

$$OH + CO = CO_2 + H \qquad \text{(R6.2)}$$

$$\Delta H = -24.9 \text{ kcal/mole}$$

ROP analysis performed at the PSR outlet by this study shows that the OH consumption rate of R6.1 dramatically increased, while the rate of R6.2 decreased, with increasing CH_3Cl loading as seen in Figure 6.18. The model predicted OH radical concentration as a function of feed CH_3Cl / C_2H_4 ratio are shown in Figure 6.19, which clearly indicates that the concentration of this most active radical decreases with the chlorine loading. The chlorine effects on the PSR temperatures are also described in these figures.

The ROP calculations also indicate that the reaction R6.2 is a dominant CO burnout channel. In excess of 92% CO conversion to CO_2 occurs through this channel when no methyl chloride added. As the methyl chloride loading increase to CH_3Cl / C_2H_4 = 0.4, the percentage of CO burnout by this channel drops to 80%. Although the CO burnout rate by the channel $CO + HO_2 = CO_2 + OH$ slightly increases, the net CO production rate still increases, which is shown by Figure 6.20. The inhibition of reaction R6.2 and its exothermicity is consistent with the observations of higher CO / CO_2 ratio and lower temperature profile as methyl chloride loading was increased under fuel-rich condition.

The observed increases in light hydrocarbon concentrations with higher chlorine loading can be largely attributed to a reduction in the rate of OH radical abstraction reactions. For example, the reaction

$$C_2H_2 + OH = CH_2CO + H \qquad \text{(R6.3)}$$

$$\Delta H = -23.82 \text{ kcal/mole}$$

is a major pathway of C_2H_2 destruction, but its destruction rate was decreased by about 25 % as feed methyl chloride loading reached CH_3Cl / C_2H_4 = 0.4. On the other hand,

the net production rate of C_2H_2 is increased about 10 %, which is described in Figure 6.21. At the same time, another important reaction

$$OH + H_2 = H_2O + H \qquad \text{(R6.4)}$$

$$\Delta H = -15.0 \text{ kcal/mole}$$

is also inhibited due to the decreased OH concentration. This reaction is the most important source of H radicals which are needed for the radical branching step

$$H + O_2 = OH + O \qquad \text{(R6.5)}$$

$$\Delta H = 17 \text{ kcal/mole}$$

The inhibition, already induced a reduction of OH radicals as shown in Figure 6.19, is illustrated in the reduced O_2 utilization as shown in Figure 6.10.

While the chlorocarbon reduces some key radical such as OH, it has been shown by the ROP that Cl become a major radical substituting for OH in performing many abstractions. For example, Cl consumes HO_2 in the chain termination step

$$Cl + HO_2 = HCl + O_2 \qquad \text{(R6.6)}$$

$$\Delta H = -54.8 \text{ kcal/mole}$$

This reaction can further inhibit CO burnout since HO_2 is also a source of OH.

The above analysis implies that an enhancement of the OH supply might overcome the inhibition induced by CH_3Cl. Steam represents a possible source via shifts in reactions R6.1 and R6.4 to left. However, any enhancement of the exothermic CO burnout by reaction R6.2 will necessarily be partially offset by the endothermicity of OH formation via R6.1 and R6.4 reversal. In addition, injection of saturated steam at 100 °C will cool the combusting flow, thereby acting to slow down everything. Hence, the utility of steam injection was limited in the experiments.

The ROP analyses were also performed along the PFR for the steam injection = 0 and steam injection = 0.37 grams/second cases. Compared to no steam injection, the net production rate of OH with steam injection is dramatically increased near the injection zone and remains higher to the PFR outlet as shown in Figure 6.22. The corresponding increase in OH radical concentration with steam injection are described in Figure 6.23. The ROP analysis shows that reactions R6.1 and R6.4 is primarily responsible for the fast OH production rate and higher OH level upon steam injection. The higher OH radical concentration significantly speeds up the CO burnout rate in the second stage of the combustor as indicated by Figure 6.24. These ROP analysis results are all consistent with the experimental observations. It should be noted that temperature interference in the ROP analysis is small because the reactor temperature profiles, which were input to the model, are not significantly effected by the steam injection rates.

6.6 Conclusions

An experimental and modeling study of hydrocarbon combustion inhibition by methyl chloride, and the effects of steam injection in a two stage, turbulent flow reactor was presented. In the experiments, premixed C_2H_4, air, and diluent nitrogen with or without CH_3Cl were fed to the first stage of the reactor. Steam was injected into the second stage. The feed fuel equivalence ratio was kept constant at ϕ=0.6 or 1.3 The methyl chloride

loading in the feed was changed from CH_3Cl / C_2H_4=0.0 to 0.4. Reactor temperatures and CO, CO_2, O_2, NO, and light hydrocarbon concentrations were measured at both stages of the reactor.

Experiments showed that the presence of CH_3Cl inhibits the CO burnout and increases the yield of incomplete products of combustion (PICs). Detailed reaction model predictions agree well with the experimental observations. Rate of production analysis indicated that reaction OH + HCl = Cl + H_2O is a major channel of OH consumption. The resulting depletion of OH radicals inhibits the CO burnout reaction OH + CO = CO_2 + H. The analysis suggested that injection of steam into the second stage of the reactor might enhance the OH supply and CO burnout. The experimental results with steam injection confirmed this hypothesis, demonstrating a significant reduction of CO and PICs.

CHAPTER 7

STAGED COMBUSTION OF MONOMETHYL AMINE

7.1 Introduction

Air staged combustion for NO reduction has been studied by several researchers. In a fluidized bed coal combustor, Gibbs et al. (1977) investigated the effect of air staging on fuel NO formation. They observed a 33% NO reduction by injecting 25% of the total combustion air into the second stage, but no minimum NO was reported. Minimum NO levels were observed during NH_3-doped CH_4 combustion by Martin et al., (1977) and NH_3-doped C_3H_8 combustion by Toshimi et al., (1979). The first stage equivalence ratios corresponding to these minimum NO levels (ϕ_m) ranged from $\phi_m = 1.2$ to $\phi_m = 1.4$. During later NH_3-doped CH_4 combustion, Song et al. (1981) reported ϕ_m from 1.7 to 1.9. These studies show that air staged combustion is effective for reduction of NO. However, reasons for the significant variation in ϕ_m values, and the subsequent influence on the minimum NO, were not investigated.

While staged combustion for NO emission control has been used in industrial utility boilers and coal combustors (Bowman 1992; Wood 1994), to our knowledge, its application to the incineration of hazardous wastes has been limited. Linak et al. (1991) examined the effects of air staging and fuel staging on NO emission in the co-firing of nitrogen-containing wastes. Their results showed that the fuel staging did not yield significant NO reduction compared to the air staging.

In this study, a two stage small pilot scale turbulent flow combustor burning ethylene in air is used to simulate a hazardous waste incinerator. Monomethyl amine (CH_3NH_2) was used as a model waste dopant containing fuel-bound nitrogen. The effects

of operating conditions, such as first stage fuel equivalence ratio (ϕ), feed CH_3NH_2 concentration, and combustion temperature were examined at specified combustion residence times. Concentrations of NO, CO, CO_2 and unburned hydrocarbon from both the first and second stages were measured. Modeling with detailed hydrocarbon mechanisms and NO chemistry was performed to predict the experimental data. Rate of production calculation results based on the modeling for interesting species were analyzed and the major reaction pathways for important species were identified.

7.2 Experimental Cases

The feed mixture consisted of C_2H_4, CH_3NH_2, air, and N_2 used as a diluent for reactor temperature control in the first zone. The CH_3NH_2 was loaded into the feed at four levels: molar ratio of CH_3NH_2 / C_2H_4 = 0.015, 0.028, 0.058, and 0.09. The first stage ϕ was varied from fuel-lean (ϕ = 0.86) to fuel rich (ϕ = 1.49) at each constant CH_3NH_2 / C_2H_4 ratio.

In the experiments, the fuel-lean case of ϕ = 0.86 at each CH_3NH_2 loading level was used as the baseline case. When the combustion was performed under these baseline cases, there was no air injection into the second stage. Feed conditions for the base cases are listed in Table 7.1.

When the combustion was performed at fuel-rich conditions in the first stage, secondary air was injected into the second zone to make the overall system the same fuel-lean condition as the base cases. In this way, the NO emitted from the overall fuel-lean combustion, measured at the second stage outlet, was compared to the baseline case in order to see the air staging effects on the NO reduction. Also, by the measurements of NO at the first stage, the effect of equivalence ratio, that is, the oxygen availability in the feed, on the NO was examined.

Table 7.1 Base Cases for CH_3NH_2 Combustion

	Flow rate (scfm)			
Feed (ϕ=0.86)	case 1	case 2	case 3	case 4
C_2H_4	0.610	0.611	0.602	0.612
Air	10.29	10.39	10.39	10.67
CH_3NH_2	0.009	0.017	0.035	0.055
Dil. N_2	3.03	4.05	4.40	4.95
CH_3NH_2/C_2H_4	0.015	0.028	0.058	0.090

Secondary air was injected at room temperature through a ceramic tube injector. This air was radially injected at the base of the second stage immediately following a small flow straightener located in the short transition region between the two stages. The flow rate of injected air, A_{inj}, was calculated according to the first stage equivalence ratio, ϕ_1, and the desired overall fuel-lean equivalence ratio, $\phi_{overall}$, by the following equation:

$$A_{inj} = \left(\frac{\phi_1}{\phi_{overall}} - 1 \right) A_1 \qquad \text{(E7.1)}$$

where, A_1 is the volumetric air flow rate to the first stage. The richest ϕ_1 in this study was 1.49, and the corresponding maximum ratio of the secondary air to the primary air was 0.72. The feed conditions for these runs at different CH_3NH_2 loading levels are listed in Tables 7.2 to 7.5.

Table 7.2 Feed Conditions for Staged Combustion at CH_3NH_2/C_2H_4= 0.015 ($\phi_{overall}$ = 0.86)

	Flow rate (scfm)			
Feed	case 1	case 2	case 3	case 4
C_2H_4	0.850	0.940	0.960	0.984
Air	10.08	9.82	9.70	9.70
CH_3NH_2	0.013	0.014	0.014	0.015
Dil. N_2	5.78	4.53	4.11	3.80
Inj. Air	4.20	5.5	6.02	6.6
ϕ_1	1.22	1.38	1.43	1.47

Table 7.3 Feed Conditions for Staged Combustion at CH_3NH_2/C_2H_4= 0.028 ($\phi_{overall}$ = 0.86)

	Flow rate (scfm)			
Feed	case 1	case 2	case 3	case 4
C_2H_4	0.692	0.843	0.908	0.971
Air	10.00	10.15	10.09	10.02
CH_3NH_2	0.018	0.023	0.025	0.027
Dil. N_2	6.5	6.2	4.75	4.00
Inj. Air	1.76	4.18	5.34	6.48
ϕ_1	1.01	1.21	1.31	1.41

Table 7.4 Feed Conditions for Staged Combustion at CH_3NH_2/C_2H_4= 0.058 ($\phi_{overall}$ = 0.86)

	Flow rate (scfm)			
Feed	case 1	case 2	case 3	case 4
C_2H_4	0.703	0.833	0.896	0.959
Air	10.28	10.15	10.08	10.02
CH_3NH_2	0.041	0.048	0.052	0.056
Dil. N_2	6.5	5.2	3.8	3.23
Inj. Air	1.92	4.25	5.51	6.64
ϕ_1	1.02	1.22	1.33	1.43

Table 7.5 Feed Conditions for Staged Combustion at CH_3NH_2/C_2H_4= 0.090 ($\phi_{overall}$ = 0.86)

	Flow rate (scfm)			
Feed	case 1	case 2	case 3	case 4
C_2H_4	0.812	0.877	0.941	1.004
Air	10.46	10.39	10.33	10.26
CH_3NH_2	0.074	0.079	0.085	0.090
Dil. N_2	5.7	4.67	3.82	3.34
Inj. Air	3.69	4.89	6.08	6.24
ϕ_1	1.18	1.29	1.39	1.49

All injected air rates listed in these tables are calculated from equation E7.1 at the desired overall fuel equivalence ratio, $\phi_{overall} = 0.86$. With air injection to the second stage, and in an effort to see real chemical effects on the combustion emissions, the measured mole fractions for species k, indicated by x_k^*, were corrected upward to account for the injected air dilution effect. The corrected mole fractions x_k of the species k, which will be used for comparison to those obtained from base cases, were obtained by the equation

$$x_k = \frac{V_{feed} + A_{inj.}}{V_{feed}} x_k^* \qquad \text{(E7.2)}$$

where, V_{feed} is the total volumetric feed flow rate to the first stage.

In both the base and the staged combustion cases, the first stage temperature was kept constant at 1759 +/- 2 K. The temperature in the second stage changed depending on the ϕ_1 and the amount of injected air. Second stage temperatures were not controlled.

The temperature effect on the NO emission was examined under other fuel-lean (ϕ = 0.65) and fuel-rich (ϕ = 1.41) cases in the first stage. Temperature was changed by the means of adjusting the dilution nitrogen flow rate in a range which did not appreciably affect the reactor residence time. Measured NO mole fractions, x_{NO}^*, in the first stage for these cases has been corrected upward to account for the dilution nitrogen effect by the equation

$$x_{NO} = \frac{V_{feed} + N2_{dil}}{V_{feed}} x_{NO}^* \qquad \text{(E7.3)}$$

where $N2_{dil}$ is the volumetric flow rate of dilution nitrogen and x_{NO} is the corrected NO mole fraction from which the temperature effects can be examined.

7.3 Modeling

As discussed in Chapter 4, the two stage reactor was simulated as a Perfect Stirred Reactor (PSR) + Plug Flow Reactor (PFR). The governing equations for species balances in both of the stages are described by equations 4.1 and 4.2. The mixing process in the air injection zone was described by a non-reactive perfect mixing model to calculate the composition and temperature of the mixture. This has been incorporated into the PSR+PFR driver program.

The measured temperatures in both the PSR and PFR stages , the reactor pressure (one atmosphere), the feed compositions, and the air injection flow rate and temperature are used as input data to the modeling. The temperatures measured in the PFR were smoothly fitted to a function of residence time with the form of $T = A + B\tau + C\tau^2$ (K), where τ stand for the PFR residence time (second).

For both reactive stages of the model, the ω_k values in E4.1 and E4.2 are determined as functions of species concentration and combustion temperature with the aid of detailed elementary reaction mechanism. For this work, the reaction mechanisms are drawn primarily from the literature, though modifications were made to several reactions to better reflect the conditions of this study.

The mechanisms consisted of three subsets: C_1/C_2 hydrocarbon reactions, NO chemistry, and CH_3NH_2 pyrolysis and oxidation. The C_1/C_2 hydrocarbon reaction subset was taken from a mechanism reported by Ho. et al. (1993). This set has been used successfully to predict the author data and the experimental data in this work which was described in Chapter 5. The NO chemistry was primarily extracted from the mechanism of

Miller and Bowman (1989), and some kinetic parameters of the important reactions were modified according the suggested values in a updated nitrogen chemistry (Bozzelli 1994). This subset includes the reactions for thermal NO, prompt NO, and the NO production from NH_3 and HCN fuel nitrogen.

Most of the CH_3NH_2 oxidation reactions are taken from a mechanism initially developed by Hwang et al. (1990). In this prior work, the kinetic parameters for some of the CH_3NH_2 oxidation reactions were adjusted to fit their shock tube data and the literature data. For the current study, kinetic parameters for selected important reactions obtained from sensitivity analysis have been modified using the QRRK method (1985) and other references. Also some new reactions described the radical abstractions of the CH_3NH_2 and CH_2NH (Bozzelli and dean 1994) were added into this subset. The input parameter for the QRRK calculations are listed in Appendix F and the modified kinetic parameters are shown in Table 7.6.

Table 7.6 Modified Kinetic Parameters in CH_3NH_2 Oxidation Mechanism

($k=AT^n\exp(-E_a/R/T)$, Units: cal, moles, second, cm3, and K)

REACTIONS	A	n	E_a	$\Delta H(298K)$	source
$CH_3 + NH_2 = CH_3NH_2$	2.7E+54	-12.1	22700	-85830	a
$CH_3 + NH_2 = CH_2NH_2 + H$	3.8E+15	-0.64	14530	79810	a
$CH_3 + NH_2 = CH_2NH + H_2$	6.2E+27	-4.73	13000	-58520	a
$CH_3 + NH_2 = CH_3NH + H$	4.4E+13	-0.31	16637	15000	a
$CH_3NH = CH_2NH + H$	1.3E+42	-9.2	41337	31000	b
$H_2CNH + O = CH_2O + NH$	1.7E06	2.1	0.0	-23850	b
$CH_3NH_2 + CH_3 = CH_2NH_2 + CH_4$	5.0E+13	0.0	19500	-11020	c
$CH_3NH_2 + NH_2 = CH_2NH_2 + NH_3$	1.1E+12	0.0	9900	-14700	c
$CH_3NH_2 + H = CH_2NH_2 + H_2$	7.2E+08	1.0	4908	-10390	b
$CH_2NH_2 = CH_2NH + H$	1.2E+12	0.0	41000	37000	d
$CH_2NH = CHNH + H$	2.4E+15	-0.53	3500	96430	a
$CHNH + H = HCN + H_2$	5.5E+27	-4.43	6970	10510	a
$CH_2NH + H = CHNH + H_2$	1.5E+14	0.0	10169	-7776	c
$CHNH = HCN + H$	6.9E+12	0.0	21000	18290	d
$NH_3 + OH = NH_2 + H_2O$	5.0E+07	1.6	954	-10650	b
$NH_2 + OH = NH + H_2O$	4.0E+06	2.0	997	-27400	b
$CH_3NH_2 + OH = CH_2NH_2 + H_2O$	1.9E+12	0.0	1790	25410	c
$CH_2NH_2 + OH = CH_2NH + H_2O$	2.4E+13	0.0	0.0	-81520	c
$CH_2NH + O = CHNH + OH$	4.0E+14	0.0	19000	-5926	c
$CH_2NH + OH = CHNH + H_2O$	3.0E+13	0.0	3000	-22800	c

Table 7.6 (Continued)

a. Kinetic parameters were calculated from CHEMACT (NJIT computer code written by E.R. Ritter and J. W. Bozzelli, 1993)

b. Reactions and kinetic parameters taken from Bozzelli and Dean (1994) mechanism

c. Kinetic parameters were taken from NIST data base and reference reactions

d. Kinetic parameters were estimated from similar β scission reactions

7.4 Results Overview

The experimental and modeling results are presented in four sections. In the first two sections, the results obtained from the first stage are reported. They describe the effects of combustion temperature and fuel equivalence ratio on the NO concentrations. The third section shows the results measured and calculated for the second stage with air injection. The minimum NO emissions reached by staged combustion and the corresponding first stage ϕ_m are also presented in this section. The relationship between ϕ_m and feed CH_3NH_2 loading is shown in the final section.

7.4.1 Effect of Temperature on NO

The two cases examined for temperature effect are: $\phi = 0.65$, $CH_3NH_2 / C_2H_4 = 0.028$ and $\phi = 1.41$, $CH_3NH_2 / C_2H_4 = 0.058$. The first stage temperature was changed from 1550 K to 1800 K. For these runs, the NO concentration was only measured in the first stage.

Figure 7.1 shows the measured and calculated NO concentrations in the fuel-lean case, which indicates the NO increase with the combustion temperature. At the PSR T = 1557 K, measured NO is 700 ppm. When the PSR temperature was increased to 1793 K

without any dilution nitrogen in the feed, the NO increased to 1020 ppm. The modeling results, though under predicted, agree fairly well with the experimental data.

For the fuel-rich case, the lowest temperature operated in the PSR was 1718 K due to a limitation on the dilution nitrogen flow meter. Figure 7.2 shows that, at T = 1718 K, the measured PSR NO was 250 ppm. When the temperature was increased to 1820 K, the NO level increased to 450 ppm. The model results in this case show a slower NO increase with temperature compared to the measurements.

From these results, two facts are noted: First, the temperature effect on NO formation during CH_3NH_2 combustion is significant. Second, even with much higher temperatures and higher CH_3NH_2 loading, the NO emitted from fuel-rich combustion is much lower than that in the fuel-lean case.

7.4.2 Effects of Equivalence Ratio on NO

A series of runs were made to investigate the feed ϕ and air staging effects on NO. The base cases for these runs were performed under first stage ϕ = 0.86 conditions. As the feed ϕ was changed from fuel-lean to fuel-rich, the temperature in the first stage was kept constant at 1759 K with the introduction of dilution nitrogen into the feed. The measured PSR temperatures in these runs are shown in Figure 7.3.

For a given CH_3NH_2 loading, Figure 7.4 shows a dramatic decrease in first stage NO concentration as the feed ϕ was increased. Figures 7.5 to 7.7 show similar, though higher, NO profiles at higher CH_3NH_2 loadings. The model predictions presented in these figures show good agreement with the data.

While the NO formation is suppressed in the first stage by reduced oxygen availability at higher ϕ values, CO burnout is reduced as shown in Figure 7.8. The higher ϕ values in the first stage also result in increased concentrations of unburned hydrocarbons

such as CH_4, C_2H_2, and C_2H_4. This is especially well illustrated for C_2H_2, as indicated in Figure 7.9.

To consume the CO and hydrocarbons generated in the fuel-rich combustion, secondary air was applied to bring the overall system ϕ back to the 0.86 level. The air was injected at a rate determined by Equation 7.1. The reduced levels of CO and C_2H_2 are evident in Figures 7.8 and 7.9. Modeling results in both stages agree very well with the data measured in these runs.

7.4.3 Minimized NO Emission from Staged Combustion

Measured temperature profiles in the second stage at four different CH_3NH_2 loadings cases are shown in Figures 7.10 to 7.13. Heat losses are present in this stage, as evidenced by the declining temperature profile for the ϕ = 0.86 base case where there was no air injection. For higher first stage ϕ cases where air injection was applied, however, these heat losses are increasingly balanced by the heat generated due to second stage combustion of CO and hydrocarbons. At the exit of the second stage in these runs, no unburned hydrocarbons were detected, and the CO level was reduced to 0 - 0.4 % as shown in the bottom of Figure 7.8. The advantages of the heat losses are twofold: first, reactor material safety limits are not exceeded, and second, thermal NO formation is not enhanced.

The experimental and modeling results on NO emissions at the second stage outlet as functions of the first stage ϕ (after air injection to the second stage, $\phi_{overall}$ = 0.86) are shown in Figures 7.14 to 7.17 at increasing CH_3NH_2. All the NO concentrations shown in the figures have been corrected for dilution by Equation 7.2. Five important observations can be made from these figures:

1. The classical minima in NO concentration characteristic to air-staged combustion are observed. Compared to the $\phi = 0.86$ base case, these minima represent an average 65 % drop in NO exit concentration.

2. These minimum NO emission levels are still somewhat higher than those which could be achieved at higher first stage ϕ values and without air injection, as evidenced in Figures 7.4 through 7.7. But it should be noted that, without air injection, CO and unburned hydrocarbons are emitted at much higher concentration levels as shown by the upper curves in the Figures 7.8 and 7.9 respectively.

3. The absolute NO concentration at the minimum rises as the feed CH_3NH_2 / C_2H_4 ratio is increased.

4. There is a definite trend to lower first stage ϕ values required to achieve the minimum NO as the fuel-bound nitrogen loading in the feed is increased.

5. These measured NO concentrations, including the NO minima, are well modeled, though the model consistently predicts a minimum which is slightly shifted by approximately 0.1 to lower first stage ϕ values.

7.4.4 Optimal First stage Equivalence Ratio

The optimum first stage ϕ_m, corresponding to an NO minimum at the PFR exit, from these experiments located in a range of 1.26 to 1.38. The lower value is consistent with the value of 1.2 reported by Martin et al. (1977), but quite different from the value of 1.7, obtained by Song et al. (1981). Closer scrutiny of these literature results indicates that Martin et al. used a higher fuel nitrogen concentration in their feed (1500 ppm NH_3), than Song et al. used (600 ppm NH_3). These data suggest a dependence of optimum first stage ϕ_m on fuel nitrogen concentration in the feed. This hypothesis is supported by our experimental observations and model calculations as shown in Figures 7.14 through 7.17.

Figure 7.18 illustrates that ϕ_m decreases with the increasing feed fuel nitrogen content. It is also important to note that at higher feed CH_3NH_2 loading conditions, for example, CH_3NH_2 / C_2H_4 = 0.058 and 0.09, small deviations in ϕ_m will result in significant increases in the NO emission (see Figures 7.16 and 7.17). The variation in ϕ_m with the feed CH_3NH_2 loading is remarkably well modeled.

7.5 NO Production and Destruction Pathways

Since experimental data are generally well predicted by the model, reaction pathway analyses can be performed. These are based on model rate-of-production (ROP) calculations which indicate the direct production and destruction reactions affecting a particular species of interest. Such ROP calculations have been used to discuss the CH_3Cl combustion results in Chapter 6.

Principle pathways to NO formation in the fuel-lean and fuel-rich combustion of CH_3NH_2 are shown in Figure 7.19 The arrow thicknesses approximately indicate the relative rates of the reactions. For both of the fuel-lean and fuel-rich conditions, NH_i (i = 1,2,3), HCN and NCO are very important intermediates for NO formation. These intermediates are primarily produced by the following reactions

$$CH_3NH_2 = CH_3 + NH_2 \qquad \text{(R7.1)}$$

$$CH_3NH_2 + H = CH_3 + NH_3 \qquad \text{(R7.2)}$$

$$NH_2 + H = H_2 + NH \qquad \text{(R7.3)}$$

$$NH_2 + OH = H_2O + NH \qquad \text{(R7.4)}$$

$$CHNH = H + HCN \qquad \text{(R7.5)}$$

$$HCN + O = H + NCO \qquad \text{(R7.6)}$$

$$NH_3 + OH = H_2O + NH_2 \qquad (R7.7)$$

Production pathways of these intermediates from the pyrolysis and oxidation of CH_3NH_2 are common to both fuel-lean and fuel-rich cases. Differences in pathways depending on lean vs. rich conditions become apparent at the point of further reactions of the radicals NH and NCO as shown in the Figure 7.19.

In the fuel-lean cases, more than 70 % of the NO is produced through HNO, which is generated from NH by the reaction

$$NH + OH = H + HNO \qquad (R7.8)$$

Since OH radical is present in the fuel-lean combustion at high concentrations, more than 72 % of NH are consumed through the channel of R7.8. In the fuel-rich case, however, the high H atom concentration and low OH and O concentrations result in up to 75 % of NH conversion into N by the reaction

$$NH + H = H_2 + N \qquad (R7.9)$$

The N atom then becomes an important bridge to NO.

The net production rates of NO under the two conditions are quite different. Figure 7.20 shows the individual production and consumption rates and the net rate of NO in the PSR for a representative case of CH_3NH_2 / C_2H_4 = 0.058 feed molar ratio. The net NO formation rate in the fuel-lean condition is about three times the rate under the fuel-rich condition. Though quite fast, the reactions

$$NO + HO_2 = NO_2 + OH \qquad (R7.10)$$

$$NO_2 + H = NO + OH \qquad (R7.11)$$

operate at nearly equal rate (see Figure 7.20), with little impact on the net NO formation under fuel-lean condition. On the contrary, the reactions

$$HNO + OH = H_2O + NO \qquad (R7.12)$$

$$HNO = H + NO \qquad (R7.13)$$

are the most important steps in formation of NO under fuel-lean conditions. As mentioned above, most of the HNO is produced by R7.8.

Radical OH plays a very important role in these NO formation reactions. Under fuel-lean conditions, model calculations indicate that OH and O concentrations are much higher than those under fuel-rich conditions as shown in Figure 7.21. The high levels of OH and O are a key reason for high NO production in the fuel-lean case, which is illustrated in the pathway diagram of Figure 7.19.

In the fuel-rich cases, high H atom concentration contributes to high N atom levels via reaction R7.9. The N atoms are subsequently responsible for most of the net NO production through the reactions

$$N + O_2 = NO + O \qquad (R7.14)$$

$$N + OH = NO + H \qquad (R7.15)$$

These two channels produced about 80 % of the NO under fuel-rich conditions, the remaining 20 % was produced by R7.13. However, lower O and OH concentrations, resulting from limited O_2 availability in the system under fuel-rich case, help to limit the NO formation. It is interesting to note that under the fuel-rich condition, NO is converted by N atom via the reaction

$$N + NO = N_2 + O \qquad (R7.16)$$

to produce N_2, and the conversion rate is about 6 times faster than that in fuel-lean case (see Figure 7.20). In fact, this step is a major NO consumer which allows NO back to nitrogen, and largely contributes to NO reduction during the staged combustion of fuel-bound nitrogen.

7.6 Discussion

Minimum NO

The major N-containing (fixed nitrogen) stable species in the CH_3NH_2 combustion is HCN, NH_3, and NO. Reaction pathway analyses show that the conversion of fuel-bound nitrogen to HCN and NH_3 occurs mostly in the first stage (see Figure 7.19). Calculated HCN, NH_3, and NO concentrations as functions of the first stage ϕ are shown in Figure 7.22. It can be seen from this diagram that a minimum total [N] can be obtained by combining the decreased NO and the increased HCN and NH_3 concentration profiles. The minimized total [N] presented in the first stage forms a foundation of minimum NO in the second stage at the same ϕ_m.

Based on the ROP calculations, Figure 7.23 describes the NO formation pathways in the second stage during the additional combustion induced by air injection. The HCN from the fuel-rich first stage converts partly into NO and partly into N_2 through the intermediate NCO. On the other hand, the NH_3 formed from the parent nitrogen molecular (CH_3NH) in the first satge totally converts into NO through intermediate HNO in the second stage. As shown by Figures 7.4 to 7.7, the NO level would continue to drop as the first stage ϕ is raised. However, HCN and NH_3 continue to increase, thus shifting the potential for more NO into the second stage. Therefore, the existence of an minimum NO from staged combustion derives from a unique minimum total fixed nitrogen in the first stage.

Optimal ϕ Shift

A discussion of the effect of fuel-bound nitrogen feed loading on the optimal first stage ϕ_m (Figure 7.18) requires a closer examination of the potential minimum NO diagram such as in Figure 7.22. The value of ϕ_m depends on the shapes of the NO, HCN, and NH_3 concentration profiles, and these species profiles are determined by their consumption and production rates. For a typical ϕ value, these rates most depend on the fuel-bound nitrogen concentration in the feed since the first stage temperature and residence time were kept constant.

For example, at the optimal first stage ϕ_m, modeling predicts higher concentrations of HCN, NH_3, and N atoms with increased feed CH_3NH_2 loading as shown in Table 7.7. The higher concentrations of NH_3 and HCN result from their increased production rates as shown in Figure 7.24. On the other hand, the higher N concentrations will increase the rate of the reaction R7.16 which is also indicated in Figure 7.24, thus causing NO to decrease more steeply with the first stage ϕ as feed nitrogen increased. In other words, with more CH_3NH_2 loading in the feed, NO decreases more steeply, and HCN and NH_3

increase more quickly, results in a minimum total fixed nitrogen occurs at lower value of the first stage ϕ_m as shown in Figure 7.22.

Table 7.7 Calculated HCN, NH_3, and N Concentrations in PSR

CH3NH2/C2H4	HCN	NH3	N
0.015	1.6E-4	3.5E-5	1.9E-6
0.028	2.1E-4	5.1E-5	2.3E-6
0.058	2.8E-4	8.8E-5	2.9E-6
0.09	3.4E-4	1.1E-4	3.3E-6

7.7 Summary

Monomethyl amine, serving as a source of fuel-bound nitrogen, has been burned in air with primary fuel C_2H_4 in a two stage turbulent flow reactor. The NO formation from the first stage dramatically decreased as the ϕ was increased. For fuel-rich feeds, air was injected into the second stage to achieve an overall fuel-lean system ($\phi_{overall}$ = 0.86). Fuel-rich ϕ_m values were identified which yielded minimum NO emissions from the second stage. These values are a function of the CH_3NH_2 concentration in the feed. Compared to the all fuel-lean combustion in the base cases, the NO emission was reduced an average 63% by staged combustion.

An elementary reaction mechanism, drawn from the literature, but with selected modifications applied to better represent the experimental conditions in this work, has been used with a two zone reactor model to simulate the experimental data. Rate-of-

production analyses based on the successful modeling have illuminated the key pathways to NO formation and destruction.

The NO formation from CH_3NH_2 combustion under fuel-rich and fuel-lean conditions follows the same pathways from the parent compound CH_3NH_2 through to the intermediates HCN, NH_3, and NCO. The NO formed from HCN, NH_3, and NCO occurred via different channels depending on the first stage ϕ. In either fuel-lean or fuel-rich cases, radicals O and OH are the most important species for NO formation. Limitation of O_2 availability in the system, that is, decreasing the concentration of O and OH radicals, is the key factor in NO reduction.

CHAPTER 8

CO-COMBUSTION OF CH_3Cl AND CH_3NH_2

8.1 Background

The formation of NO from fuel nitrogen such as CH_3NH_2 has been studied by several researchers (Fenimore 1972; Hwang et al.1990; Peck et al. 1991) and in this work. The conversion pathways of fuel-bound nitrogen into NO have been described by the following sequence: First, the nitrogen-containing compound was oxidized and dissociated into intermediates NH_i (i = 1,2, and 3), NCO, and HCN. Second, these intermediates reacted with active radicals, such as O, H, and OH, to form HNO and N. Third, the HNO and N converted into NO by reacting with OH and O_2. For example, the sequence of NO formation from CH_3NH_2-doped C_2H_4 combustion has been shown in Figure 7.19.

There are several strategies for controlling NO emissions from fuel-bound nitrogen combustion. It includes catalytic NO reduction, thermal De-NO_x, and staged combustion (Bowman 1992). As an effective and economic means for NO reduction, staged combustion has been investigated by several researchers (Martin et al. 1977; Toshimi et al. 1979; Song et al. 1981; Linak et al. 1992) and applied in practical combustion devices. This author has investigated the operating conditions, such as fuel equivalence ratio, temperature, and secondary air injection effects on NO emissions, and the results have been described in Chapter 8.

When chlorocarbon is present, it inhibits the combustion by limiting CO burnout and prompting PIC formation. The inhibition mechanism for CO burnout and PIC increases has been described by previous studies (Ho 1993; Chang et al 1985) and in this

work (see Chapter 7). The HCl produced in the combustion consumes OH through the reaction

$$HCl + OH = H_2O + Cl \qquad (R8.1)$$

The reduced OH concentration inhibits the CO burnout reaction

$$CO + OH = CO_2 + H \qquad (R8.2)$$

and limits hydrocarbon destruction, such as the C_2H_2 consumption reaction

$$C_2H_2 + OH = CH_2CO + H \qquad (R8.3)$$

Experimental results from Brouwer et al., (1992) and this study show that CH_3Cl loading in the C_2H_4 / air feed results in higher CO and unburned hydrocarbon levels. The modeling results in this study also indicated that the OH consumption rate in R8.1 was doubled compared to that in R8.2 when the feed ratio of CH_3Cl / C_2H_4 was raised to 0.4.

While the NO chemistry and chlorocarbon combustion have been studied separately, there are very few studies on the interaction of N-containing and Cl-containing species occurring during co-combustion of fuel-bound chlorine and nitrogen. Jeoung et al. (1990) studied the reactions between N atom and chlorine-containing species, but their experiments were performed at very low pressure and room temperature which did not reflect the current combustion environment. It is vital to investigate and understand the

interaction process at high temperature for the purpose of NO and CO control in practical combustion devices; for example, in the case of using N-contained fuel burning Cl-contained hazardous wastes in an incinerator.

This study was performed under atmospheric pressure and high temperature (1700 to 1800 K) to simulate the combustion conditions in a hazardous waste incinerator. CH_3NH_2-doped C_2H_4 was used as N-containing fuel and CH_3Cl was used as Cl-containing waste. The experimental and modeling results reported below show that the NO emission from the co-combustion was reduced more than 15% compared to the CH_3NH_2 only combustion when CH_3Cl was added into the feed to a ratio of CH_3Cl / C_2H_4 = 0.4.

8.2 Experimental Cases

The experiments were conducted in a two stage turbulent flow reactor which has been used for separate CH_3Cl and CH_3NH_2 combustion as discussed in the earlier chapters. The primary fuel used in the combustion was C_2H_4 and the oxidant was air. When the feed in the first stage was fuel-rich, the air is split into two parts. The primary air was introduced into the first stage and the secondary air was injected into the second stage to make the overall system fuel-lean. Additional nitrogen was added into the fuel-rich feed to control the temperature in the first stage. The concentrations of NO, CO, CO_2, and O_2 were measured in both of the stages.

Two series of experiments were performed. The first series of runs were performed under varied first stage fuel equivalence ratios, ϕ_1, from 0.85 to 1.45. The CH_3NH_2 loading in the feed was kept constant at CH_3NH_2 / C_2H_4 = 0.018 (molar ratio). For each run of the first series, two cases were examined: feed molar ratio of CH_3Cl / C_2H_4 = 0 and 0.2. Feed conditions for four typical runs under fuel-lean and fuel-rich

conditions are listed in Table 8.1 From these first series runs, minimized NO by air staging, the effect of CH_3Cl loading on the minimum NO, and the corresponding optimal ϕ_m were investigated.

Table 8.1 Representative Feed Conditions for First Series of Runs

Feed (scfm)	$\phi_1 = 0.85$		$\phi_1 = 1.30$	
	R_{Cl}=0	R_{Cl}=0.2	R_{Cl}=0	R_{Cl}=0.2
Air	10.82	10.77	9.81	9.73
C_2H_4	0.625	0.57	0.88	0.795
CH_3NH_2	0.011	0.01	0.016	0.014
CH_3Cl	0	0.115	0	0.159
Dil. N_2	4.84	4.84	5.42	4.70
Inj. Air	0	0	5.19	5.15
R_N	0.018	0.018	0.018	0.018

$R_{Cl} = CH_3Cl/C_2H_4$

$R_N = CH_3NH_2/C_2H_4$

The second series of runs were performed under constant first stage ϕ_1 (corresponding to the ϕ_m for the minimized NO emission in the second stage which was observed from the first series of runs), constant feed mole fraction of CH_3NH_2 (0.001), and varied methyl chloride loading conditions. It should be noted that to keep the feed mole fraction of CH_3NH_2 constant, the feed molar ratio of CH_3NH_2 / C_2H_4 had to be increased as the CH_3Cl loading was increased. Feed conditions for these cases are listed in Table 8.2.

Table 8.2 Representative Feed Conditions for Second Series of Runs

Feed (scfm)	$\phi_1 = 1.30$			
	R_{Cl}=0.1	R_{Cl}=0.2	R_{Cl}=0.3	R_{Cl}=0.4
Air	9.77	9.73	9.70	9.67
C_2H_4	0.835	0.794	0.757	0.724
CH_3NH_2	0.016	0.016	0.016	0.016
CH_3Cl	0.084	0.159	0.227	0.289
Dil. N_2	4.6	4.5	4.5	4.4
Inj. Air	5.17	5.15	5.14	5.12
R_N	0.019	0.020	0.021	0.022
X_N (%)	0.104	0.104	0.104	0.104

$R_{Cl} = CH_3Cl/C_2H_4$

$R_N = CH_3NH_2/C_2H_4$

X_N = mole percent of CH_3NH_2 in feed.

Sample gas were drawn from both the first and second stage and analyzed. With air injection to the second stage, the measured compositions for species k at the outlet of reactor were corrected upward to account for the secondary air dilution effect. The corrected mole fractions of the species k were obtained from Equation E.7.2. The pressure in the reactor was one atmosphere. Temperatures in both of the stages were measured for all of the runs, from which the chlorine loading effects on the combustion temperature and its consequential effects on NO were indentified. These measured temperatures were used as input in the computer modeling.

8.3 Experimental Data and Observations

8.3.1 First Series of Runs at Constant CH_2Cl/C_2H_4

For the first series runs, the measured temperatures in the first stage and at the second stage outlet are measured and shown in Figure 8.1. These temperatures were measured in both the methyl chloride loading (CH_3Cl/C_2H_4 = 0.2) and no methyl chloride loading cases. The first stage temperatures were kept constant at 1750 K. The temperature at the second stage outlet increased with the first stage ϕ_1 due to injected air induced additional combustion.

The concentration of NO measured at the second stage outlet as a function of first stage ϕ_1 was shown in Figures 8.2 and 8.3. The data shown in these figures have been corrected for air dilution according to equation E7.2. The curves in Figure 8.2 correspond to the CH_3Cl / C_2H_4 = 0.0 case, and the curves in Figure 8.3 correspond to the CH_3Cl / C_2H_4 = 0.2 case. In both of the cases, the CH_3NH_2 addition in the feed was kept constant at CH_3NH_2 / C_2H_4 = 0.018 (molar ratio). Three important observations are noted:

1. The presence of CH_3Cl in the staged combustion of CH_3NH_2 does not affect the existence of a minimum NO emission behavior which had been observed in the CH_3NH_2 only combustion.

2. The optimal first stage equivalence ratio (ϕ_m) corresponding to the second stage minimum NO occurs at approximately same value (ϕ_1=1.3) in both the CH_3Cl / C_2H_4 = 0.0 and CH_3Cl / C_2H_4 = 0.2 cases.

3. The minimum NO emission level significantly decreased when CH_3Cl was added to the system. Compared to the observed 486 ppm of NO emission at CH_3Cl /

C_2H_4 = 0 case, the minimum NO is reduced to 405 ppm for the CH_3Cl / C_2H_4 = 0.2 case, that is, more than a 15 % NO reduction is achieved.

8.3.2 Second Series of Runs at Constant ϕ_1

Extended experiments were performed to examine the effect of higher CH_3Cl loading levels. These experiments were performed at a constant ϕ_1 = 1.3 (corresponding to the ϕ_m for minimum NO obtained from the first series runs), constant feed mole fraction of CH_3NH_2, and with air injection ($\phi_{overall}$ = 0.85). NO concentrations measured in the first stage are shown in Figure 8.4, and the NO levels measured at the second stage outlet are shown in Figure 8.5. From these data, we can see that NO emissions from both the first and second stages decreases with the feed CH_3Cl loading. Figure 8.5 shows that, at the outlet of second stage, the NO emission level has been reduced from 600 ppm (CH_3Cl / C_2H_4 = 0) to 460 ppm (CH_3Cl / C_2H_4 = 0.4).

The measured temperature profiles along the reactor length are shown in Figure 8.6. These profiles do not show significant changes with increased feed CH_3Cl loading. This observation suggests that the NO reduction results from the chemical interaction of CH_3Cl and CH_3NH_2 without interference from different temperature..

The species concentrations for CO, CO_2, and O_2 measured in both of the stages are shown in Figures 8.7 and 8.8. Figure 8.7 indicates that, in the first stage, the combustion inhibition induced by methyl chloride resulted in increasing ratios of CO / CO2 and increasing O_2 concentration, which are consistent with the observations in the combustion of CH_3Cl reported in Chapter 6. Figure 8.8 shows that in the second stage almost all CO has been consumed into CO_2 by injected air, and the oxygen concentration remained constant at a higher level, which is reasonable because excess oxygen exists in this second zone ($\phi_{overall}$ = 0.85) after air injection.

8.4 Interaction Reactions and Modeling

The two stage reactor used in this co-combustion of CH_3Cl and CH_3NH_2 study was simulated as a Perfect Stirred Reactor (PSR) + Plug Flow Reactor (PFR) sequence as described in Chapter 4. The energy balance equations in the reactor model were uncoupled from the species balance equations E4.1 and E4.2 by using the measured PSR temperature and the PFR temperature profile as input to the model. The reactor simulation was performed through the original CHEMKIN application driver code. As done in the previous chapters, the feed composition , temperature, and flow rate, the reactor pressure (one atmosphere), and the injected air flow rate and temperature are used as input in the modeling.

The reaction mechanism used in this modeling was constructed from the following subsets: C_1/C_2/Chlorocarbon mechanism from Ho et al. (1993), NO chemistry including the thermal NO, prompt NO, and fuel-bound nitrogen NO from Miller et al. (1989), and the CH_3NH_2 oxidation mechanism from Hwang et al. (1990). Quantum RRK calculation (Dean 1985) for selected important reactions have been made. The modified parameters and corresponding reactions have already been listed in Tables 6.6 and 7.6.

Another 26 reactions were added to the mechanism to describe the interaction of chlorine and nitrogen species. These are listed in Table 8.3 below. These reactions include abstraction reactions from nitrogen-containing species by radicals Cl, N, OH, and H; and combination reactions of Cl with N, NO, CN, NH_2, and NH_3. Stabilized intermediates produced from these combination reactions, such as NCl, CNCl, NOCl, NH_2Cl and NHCl, are reacted with active radicals, such as OH, H, N, and Cl, and finally converted into N_2, Cl_2, HCl, H_2, and H_2O. Some kinetic parameters for these reactions were obtained from the NIST kinetic database (1992). The parameters which are not available in literature were calculated by the QRRK method (Dean 1985) and referenced to similar reactions. The input data for QRRK calculations are listed in Appendix F.

Table 8.3. Interaction Reactions of Cl- and N-containing Species

($k=AT^n\exp(-E_a/R/T)$; Units: cal, mole, second, cm^3, and K)

Reaction	A	n	E_a	ΔH(298K)	Source
$CH_3NH_2 + Cl = CH_2NH_2 + HCl$	5.4E13	0	1000	-9200	a
$CH_3NH_2 + Cl = CH_3NH + HCl$	5.0E13	0	3000	-2140	a
$NH_3 + Cl = NH_2 + HCl$	5.8E12	0	7800	5570	a
$HCN + Cl = HCl + CN$	1.0E14	0	23000	20820	a
$Cl + NH_2 = NH_2Cl$	2.9E22	-3.7	1850	-68000	b
$Cl + NH_2 = NH + HCl$	3.3E14	-0.12	101	-11180	b
$Cl + NH_2 = NHCl + H$	3.7E16	-0.73	40830	34700	b
$Cl + NH = NHCl$	4.3E13	-1.86	370	-57120	b
$Cl + NH = N + HCl$	1.6E14	-0.01	10	-23150	b
$Cl + NH = NCl + H$	4.2E09	0.6	4090	2990	b
$NH_2Cl + OH = H_2O + NHCl$	2.1E13	0	2500	-16400	a
$NHCl + OH = H_2O + NCl$	1.5E13	0	1200	-59100	a
$NHCl + H = H_2 + NCl$	2.0E13	0	1500	-44100	a
$NHCl + N = N_2 + HCl$	3.0E13	0	0	-192000	a
$NH_2Cl + Cl = HCl + NHCl$	2.5E13	0	2700	-200	a
$NH_2Cl + H = H_2 + NHCl$	3.9E12	0	5000	-1400	a
$N + Cl + M = NCl + M$	8.5E17	0	0	-76860	a
$N + Cl_2 = NCl + Cl$	3.5E12	0	5800	-19060	c
$NCl + NCl = N_2 + Cl_2$	5.8E13	0	0	-130000	a
$NCl + N = N_2 + Cl$	7.6E14	0	0	-149000	a
$CN + Cl + M = CNCl + M$	4.0E16	0	0	-99920	a

Table 8.3 (Continued)

$CN + Cl_2 = CNCl + Cl$	3.6E12	0	0	-42000	c
$CNCl + N = N_2 + CCl$	1.0E13	0	0	-42750	a
$Cl + NO + M = NOCl + M$	1.7E17	-1.39	340	-38000	c
$NOCl + H = HCl + NO$	4.6E13	0	910	-64870	c
$NOCl + Cl = Cl_2 + NO$	4.0E13	0	-350	-19670	c

a. Kinetic parameters are taken from similar reactions

b. Kinetic parameters are calculated by CHEMACT (NJIT computer code written by E. R. Ritter and J. W. Bozzelli)

c. Kinetic parameters are taken from the NIST kinetic database (version 4.0,1992)

Modeling results compare very well with the experimental measurements. It can be seen from these comparisons that the model has satisfactorily predicted the NO decreasing trend as shown by the experiments. The predicted drop in NO with chlorine loading is especially satisfying considering the complexity of the two heteroatoms involved in the hydrocarbon combustion.

8.5 Discussion

Important results obtained from the modeling are rate-of-production (ROP). The ROP not only indicates the production and consumption rates for particular species of interest, but also list the important reactions which contribute to the production and destruction. With the ROP analysis, one can identify the formation and destruction pathways.

The ROP calculations in the PSR for both the chlorine loading and no-chlorine loading cases indicate that more than 90% of NO formed in the combustion under both of the cases is from the following seven reactions:

$$CO_2 + N = NO + CO \qquad (R8.4)$$

$$NO_2 + H = NO + OH \qquad (R8.5)$$

$$HNO = NO + H \qquad (R8.6)$$

$$HNO + OH = NO + H_2O \qquad (R8.7)$$

$$HNO + H = H_2 + NO \qquad (R8.8)$$

$$N + O_2 = NO + O \qquad (R8.9)$$

$$N + OH = NO + H \qquad (R8.10)$$

The importance of each of these reactions are indicated in Figure 8.9. The shadowed bars express the NO production rates in the case of CH_3Cl / C_2H_4 = 0.2, and the blank bars express the rates in the case of CH_3Cl / C_2H_4 = 0. The last two bars in this figure shows the net NO production rates. It can be seen from this figure that, with methyl chloride in the feed, the NO production rate in each reaction (R8.4 to R8.10) is lower than that for the CH_3Cl / C_2H_4 = 0 case. Reaction R8.10 (reaction No. 7 in Figure 8.9), the most important channel for the NO production in the no-chlorine case, shows a very large drop in the NO formation rate under the CH_3Cl loading condition. The net production rate of NO is decreased more than 15 %, which is consistent with the experimental data.

The factors which can significantly affect the NO formation rates are the active radical concentrations, especially the OH and N concentrations. ROP spectra for OH

consumption rates obtained from the modeling of the CH_3Cl/C_2H_4 = 0 and 0.2 cases are shown in Figure 8.10. It can be found that with CH_3Cl loading, OH consumption rates are lower for the reactions

$$OH + C_2H_4 = C_2H_3 + H_2O \qquad (R8.11)$$

$$OH + C_2H_2 = CH_2CO + H \qquad (R8.12)$$

$$OH + CO = CO_2 + H \qquad (R8.13)$$

and much lower for the reaction

$$OH + H_2 = H_2O + H \qquad (R8.14)$$

In contrast to this, the OH consumption rate by reaction

$$OH + HCl = Cl + H_2O \qquad (R8.15)$$

is dramatically increased. This suggests a strong competition for OH radicals and results in a lower OH concentration level in the chlorine loading case as shown in Table 8.4.

The consumption of N radicals is of great interest because the N atom either can convert into N_2 or form NO. From the ROP analysis, the five most important reactions for N consumption and their rates are shown in Figure 8.11. The results in this figure indicate that, with chlorine loaded in the feed, N consumption rates in three major NO formation channels

$$N + CO_2 = NO + CO \qquad (R8.16)$$

$$N + O_2 = NO + O \qquad (R8.17)$$

$$N + OH = NO + H \qquad (R8.18)$$

were all decreased compared to the $CH_3Cl/C_2H_4 = 0$ case, which contributes to the NO reduction. In addition, the ROP spectra shows that, when chlorine is present, N radicals are consumed by combining with Cl radicals to produce intermediate NCl by the reaction

$$N + Cl + M = NCl + M \qquad (R8.19)$$

The NCl then is attacked by N to form N_2 via reaction

$$N + NCl = N_2 + Cl \qquad (R8.20)$$

This N consumption pathway not only decreases the N concentration and thus limits the NO formation rate of R8.18 together with the lower OH levels, it also provides a means to convert N into N_2 by R8.20.

8.6 Implications for NO Reduction

The study of simultaneous staged combustion of CH_3NH_2 and CH_3Cl indicates that the CH_3Cl presence did not affect the minimum NO operating behavior, though it did induce a further reduction of the NO emission. The modified mechanism has described the

interaction between nitrogen- and chlorine-containing species and has modeled the experimental data well. Rate-of-production calculations based on the modeling show that in the co-combustion, consumption of OH radicals by HCl via the reaction OH + HCl = H_2O + Cl and consumption of N radicals by Cl via the reaction N + Cl + M = NCl + M are two important steps to slow the rate of reaction N + OH = NO + H, which ultimately leads to the NO reduction. While the presence of chlorine does have a favorable affect on NO, the inhibitory effects on CO burnout and O_2 utilization still occurs. It remains to see if injection along with the air injection into the second stage will be beneficial.

Table 8.4 Calculated OH Concentration (ppm)

Residence Time (millisecond)	CH_3Cl/C_2H_4=0 OH	CH_3Cl/C_2H_4=0.2 OH
5.6 (PSR)	250	170
Air inj. point	190	130
6.6	970	870
7.6	670	590
8.6	530	470

CHAPTER 9

FINAL CONCLUSIONS AND RECOMMENDATIONS

9.1 Conclusions

From our experimental observations and model predictions of the C_2H_4/air/N_2, C_2H_4/air/CH_3Cl/N_2, C_2H_4/air/CH_3NH_2/N_2, and C_2H_4/air/CH_3Cl/CH_3NH_2/N_2 combustion systems in a two stage turbulent flow reactor, the following conclusions are obtained:

(1) The two stage combustion reactor has been characterized as a PSR+PFR sequence. The facility has been used successfully for studies of chlorocarbon (CH_3Cl) and fuel-bound nitrogen (CH_3NH_2) incineration. The operating conditions, such as model waste loading level, fuel equivalence ratio, combustion temperature, and staged air/steam injections have been investigated to find the effects of these factors on the combustion emissions.

(2) At a fuel-lean condition (ϕ = 0.65), the combustion inhibition of CH_3Cl was observed in the first stage. At a fuel-rich condition (ϕ = 1.3), the inhibition occurred in both the first and second stages. The emissions of CO and PICs (CH_4, C_2H_2, C_2H_4) increased, and the CO_2 decreased, as the feed CH_3Cl loading was increased from CH_3Cl/C_2H_4 = 0 to 0.4.

(3) Steam injection into the second stage effectively enhanced the CO burnout and decreased the PICs emissions from combustion of C_2H_4/air/N_2 and C_2H_4/CH_3Cl/air/N_2 under fuel-rich conditions (ϕ = 1.3 and ϕ = 1.35).

(4) Modeling with a detailed reaction mechanism (measured temperature used as input) satisfactorily predicted the observed concentration profiles of light hydrocarbons and O_2, and the ratio of CO/CO_2 in the CH_3Cl combustion. Rate-of-production analysis (ROP) based on the modeling indicated that reaction

$$OH + HCl = H_2O + Cl \qquad (R9.1)$$

is a major channel of OH consumption. The decreased OH concentration level in the combustion limited the CO and C_2H_2 burnout rates of the reactions

$$CO + OH = CO_2 + H \qquad (R9.2)$$

$$C_2H_2 + OH = CH_2CO + H \qquad (R9.3)$$

With steam injection, the ROP analysis shows that the net production rate of OH is dramatically increased. Reaction R9.1 and reaction

$$H_2 + OH = H_2O + H \qquad (R9.4)$$

are primarily responsible for the higher level of OH due to reaction equilibrium shifting to the left upon steam injection. The higher OH radical concentration speeds up the burnout rates of R9.2 and R9.3.

(5) The NO emission from the combustion of $C_2H_4/CH_3NH_2/air/N_2$ is quite high under fuel-lean conditions (ϕ = 0.86). At a constant temperature (T = 1759 K), the NO

can be dramatically decreased by operating the system under fuel-rich conditions. However, at the same time, the CO emission and unburned hydrocarbons increased with the higher equivalence ratio.

(6) With fuel-rich combustion in the first stage and air injected into the second stage to make the overall system fuel-lean ($\phi_{overall} = 0.86$), not only is all CO consumed, but also NO formation at the reactor exit can be reduced to a minimum level with a correct first stage ϕ. Compared to the fuel-lean only ($\phi = 0.86$) case, more than a 60% reduction of NO has been reached by air-staging combustion.

(7) Modeling results from the two zone reactor simulation combined with a modified NO mechanism agrees well with the experimental data from the CH_3NH_2 combustion. ROP calculations show that HCN and NH_i (i = 1, 2, 3) are the key intermediates in the fuel NO formation process, while O and OH are the most important radicals for NO production. Limited oxygen availability in the fuel-rich system, that is, decreasing the concentrations of O and OH radicals, is the key factor to NO reduction.

(8) The optimum first stage fuel equivalence ratio (ϕ_m) corresponding to the second stage minimum NO depended on the fuel-bound nitrogen loading level in the feed. With higher feed CH_3NH_2 loading, increased N atom concentration enhanced the rate of $N + NO = N_2 + O$, which allows for ϕ_m to shift to lower values. The resulting higher O and OH levels can consume the increased HCN and NH_3 to form either NO or N_2 in the second stage. It was noted that at heavier CH_3NH_2 loading cases small deviations in the ϕ_m will result in significant increases in NO emissions.

(9) The co-combustion of CH_3Cl and CH_3NH_2 in C_2H_4 with air showed that the presence of CH_3Cl does not affect the ϕ_m location of minimum NO which was observed in the staged combustion of CH_3NH_2. However, the absolute NO concentration from the combustion was decreased as CH_3Cl was loaded in the feed. Model calculations using a large reaction mechanism including chlorocarbon combustion, NO chemistry, and

CH_3NH_2 oxidation predicted the minimum NO decreasing with chlorine loading. ROP analysis indicates that consumption of OH radical by HCl via reaction OH + HCl = H_2O + Cl and consumption of N atom by Cl via reaction N + Cl + M = NCl + M are two important steps in reducing NO yield by the reaction N + OH = NO + H.

9.2 Recommendations

According to the capability of using the two stage reactor for studies of hazardous waste incineration, a few recommendations in specific areas are offered for future work.

For the chlorocarbon combustion, a higher chlorine/hydrogen (Cl/H) loading level in the feed should be used to see more clearly the effect on the combustion temperature, CO burnout, and higher molecular weight PIC production. The higher Cl/H loading can be realized by using heavier chlorinated hydrocarbons such as CH_2Cl_2 and $CHCl_3$.

It will be useful to use different form of fuel-bound nitrogen in the fuel NO reduction, study for further identification of the NO formation and reduction pathways. Also the effect of fuel-bound nitrogen molecular structures on the minimum NO and optimal ϕ_m values can be investigated by this way.

To get a better understanding of the interaction of chlorocarbon and fuel-bound nitrogen in the combustion, more detailed identification of product species and determination of their concentrations are recommended. Also, the combined effect of air staging and steam injection should be examined. In particular, it will be essential to make sure if is there any product which is worse than NO formed in the CH_3Cl/CH_3NH_2 co-combustion system.

APPENDIX A

FIGURES

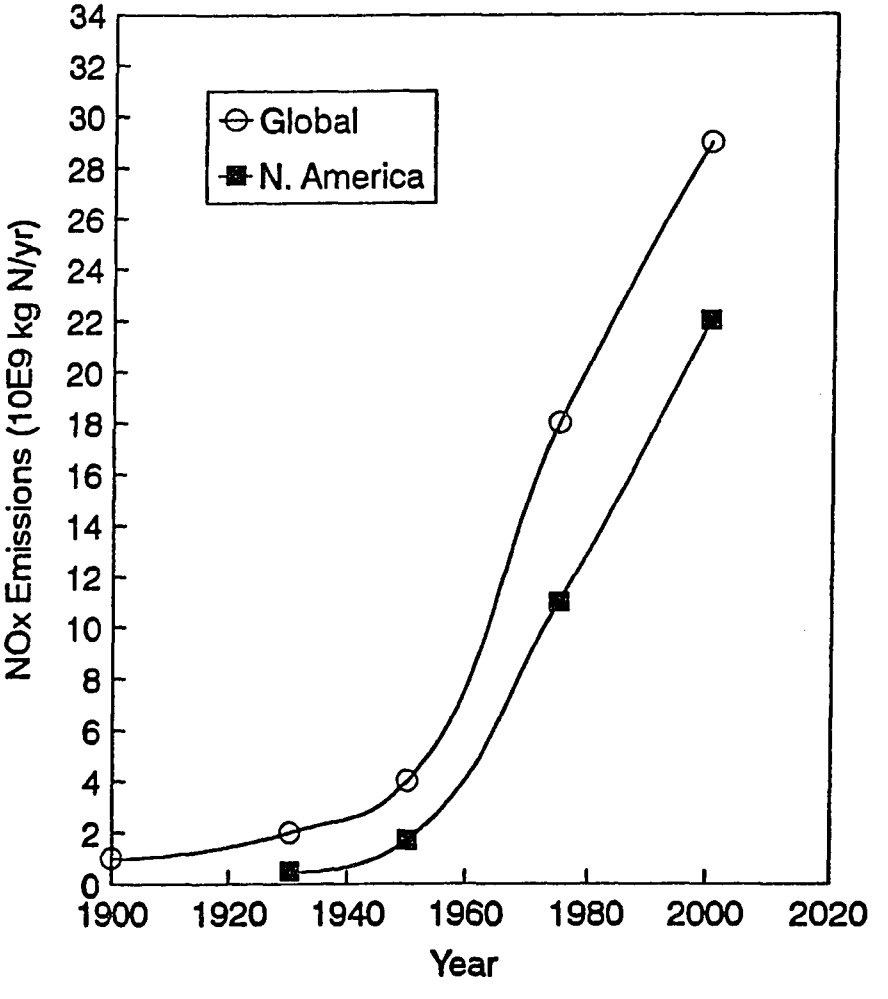

Figure 1.1 Annual increases of combustion-generated NOx in North America and worldwide (data taken from Bowman 1992)

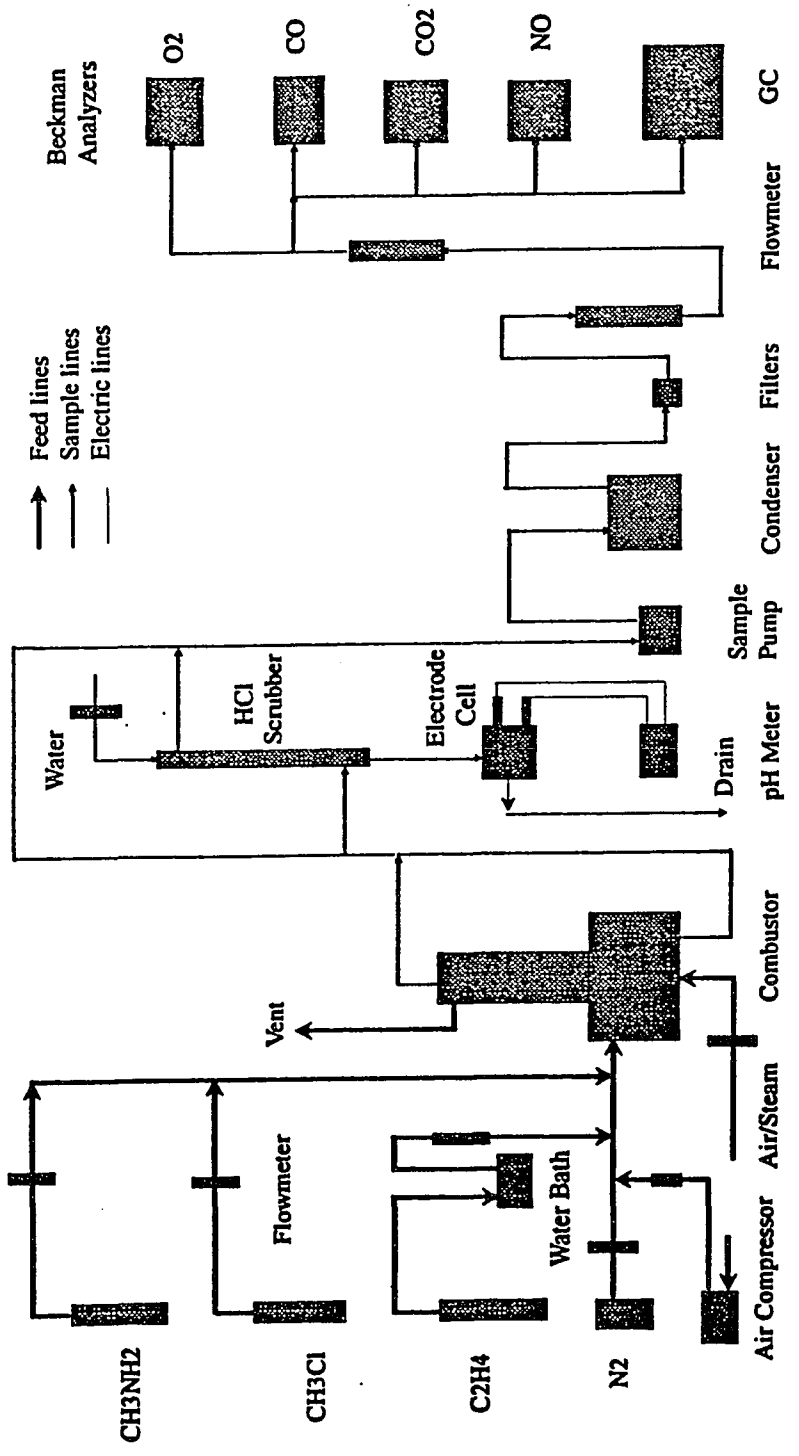

Figure 3.1 Schematic of Experimental Flowsheet

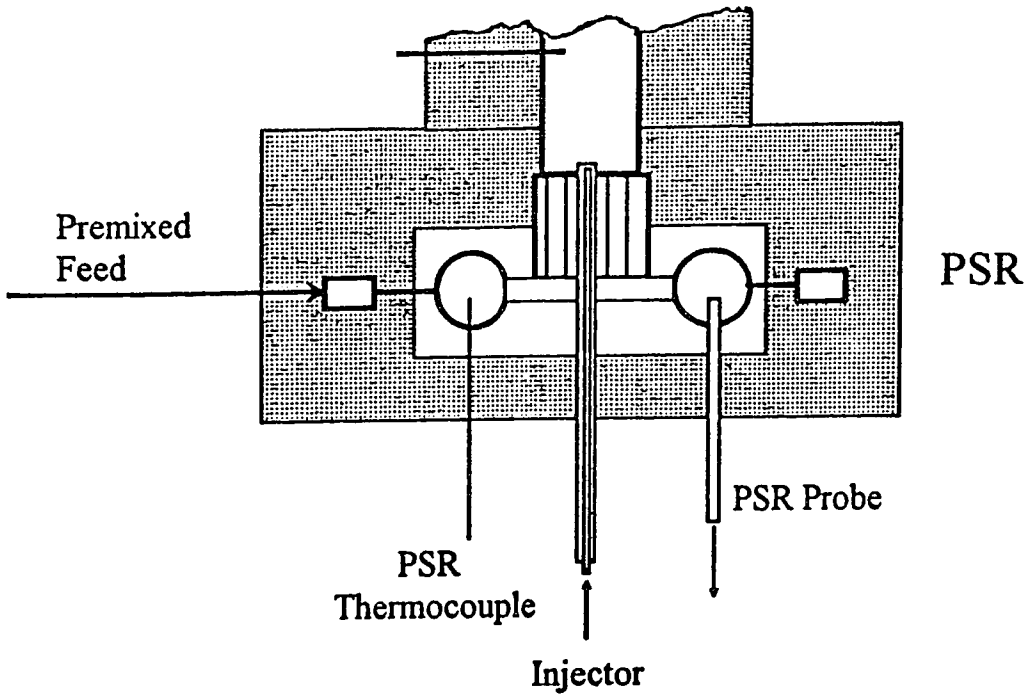

Figure 3.2 First Stage Combustor Chamber

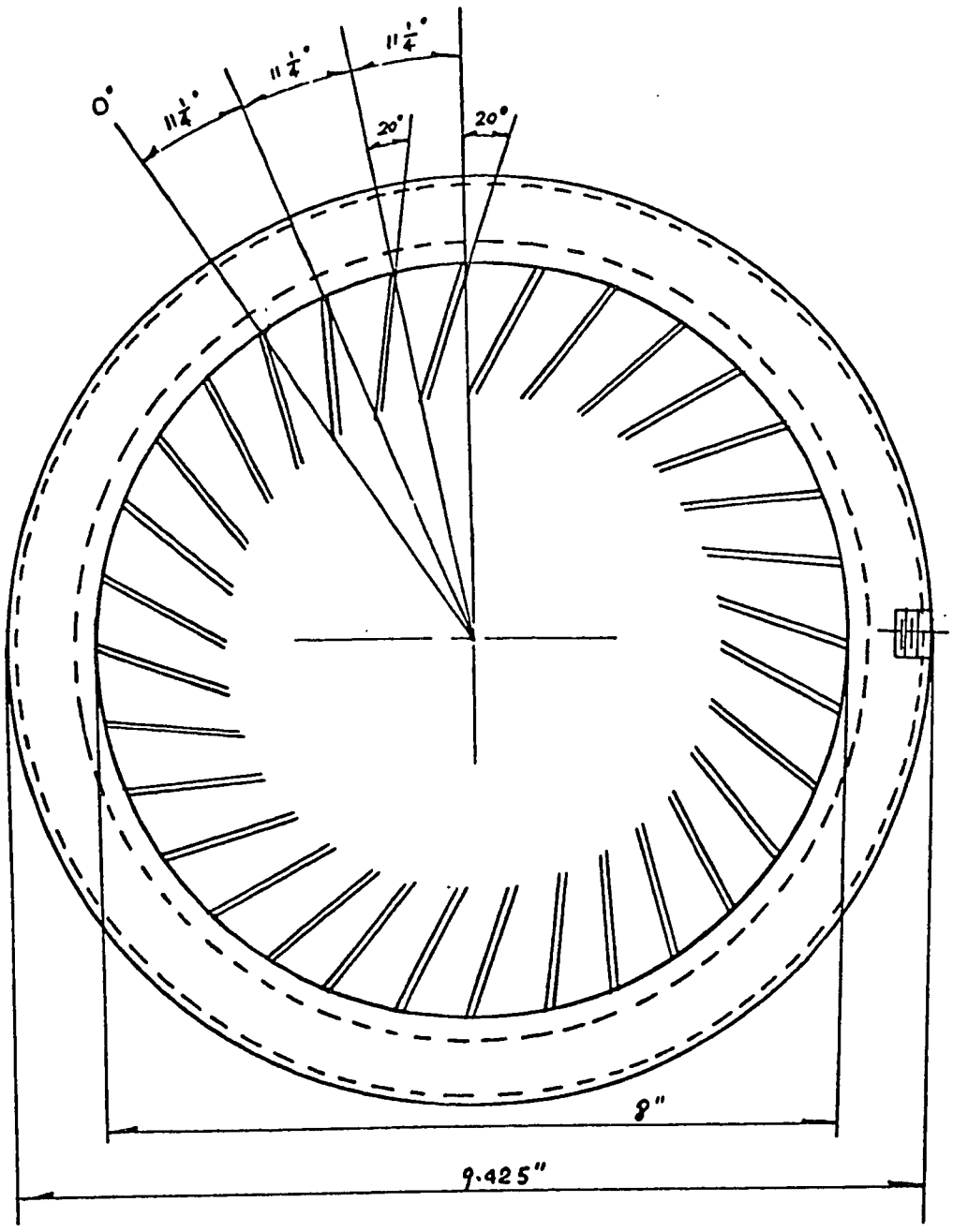

Figure 3.3 Fuel Jets and Jet Ring in the First Stage of Reactor

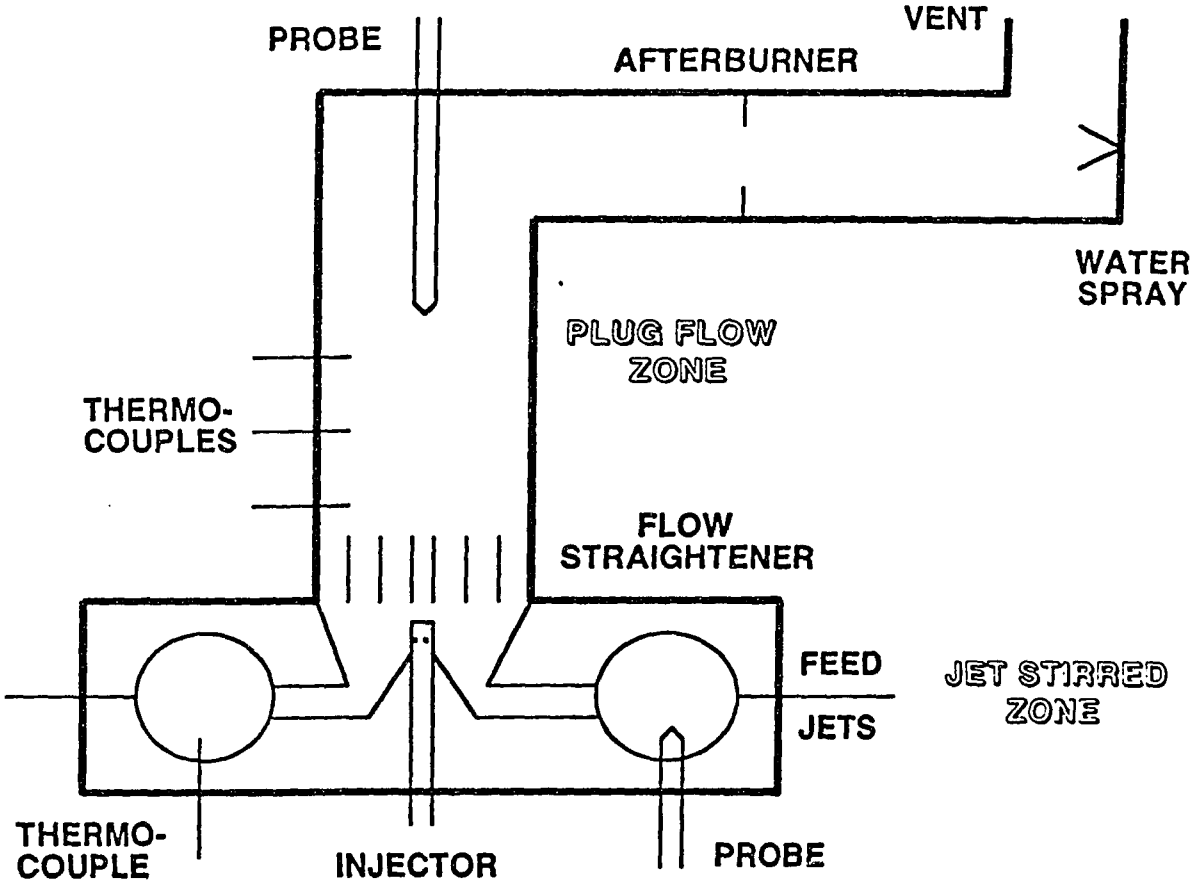

Figure 3.4 Two Stage Turbulent Flow Reactor

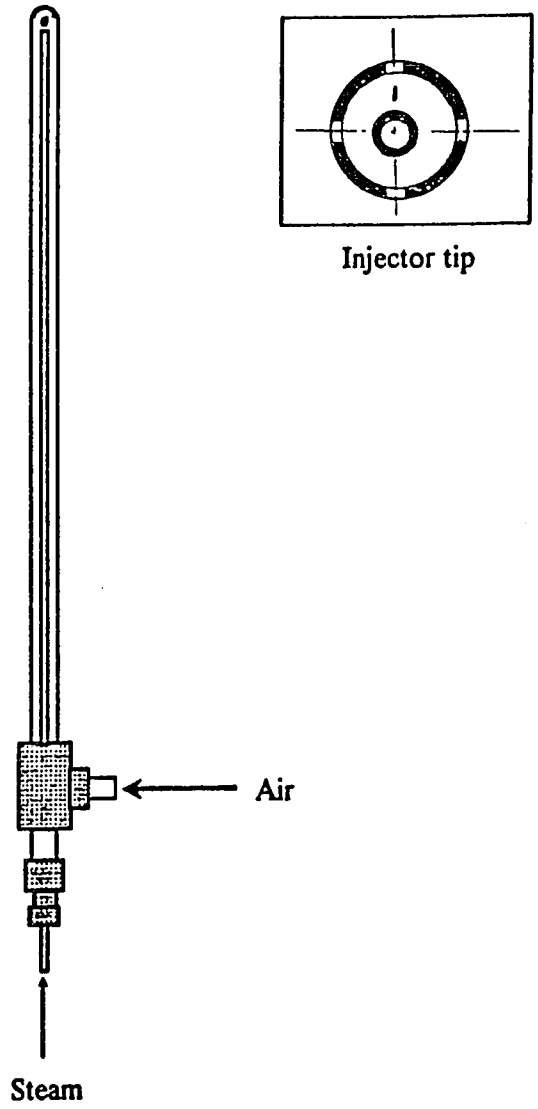

Figure 3.5 Air / Steam Injector

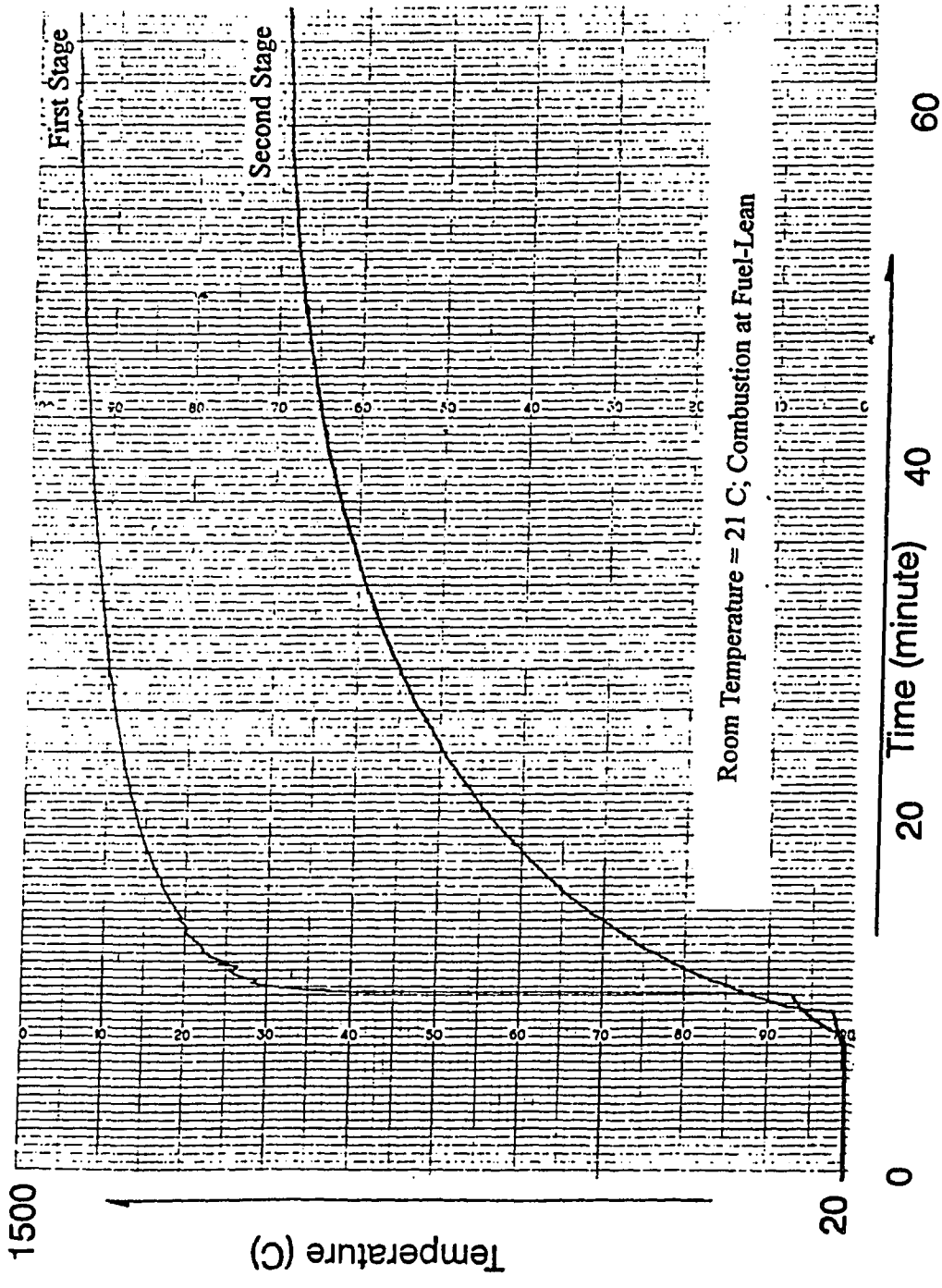

Figure 3.6 Temperature Recorder Output during Start-up (C_2H_4/Air, ϕ=0.65)

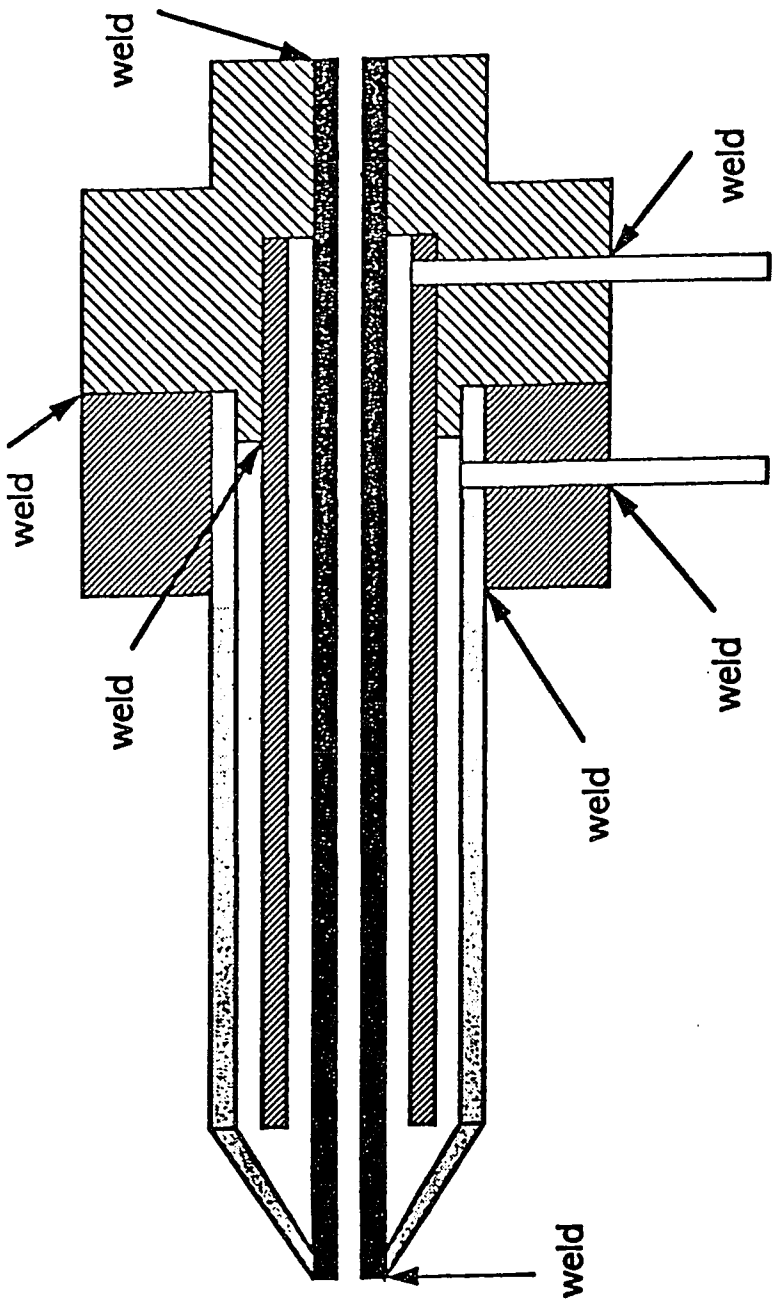

Figure 3.7 Structure of Second Stage Sample Probe (not to scale)

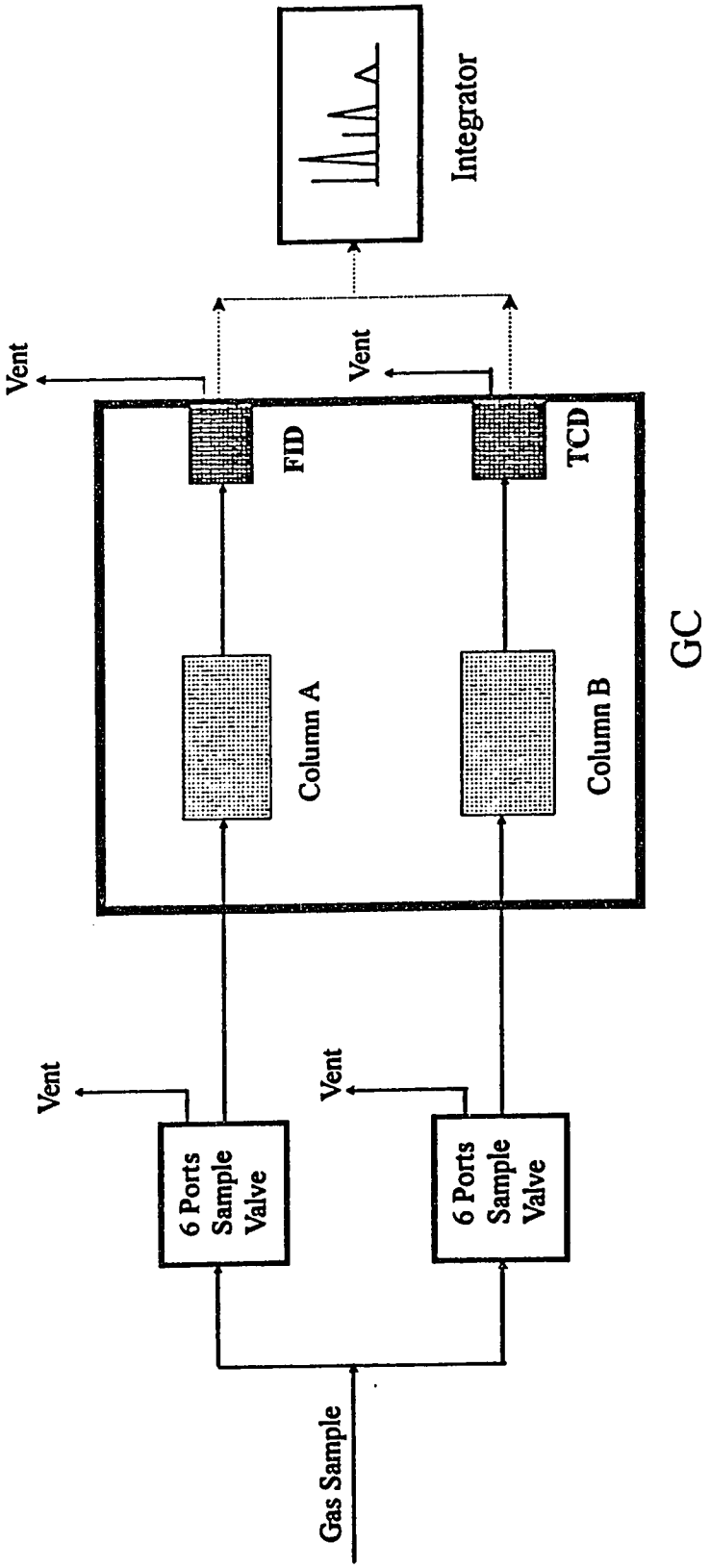

Figure 3.8 Gas Chromatograph System

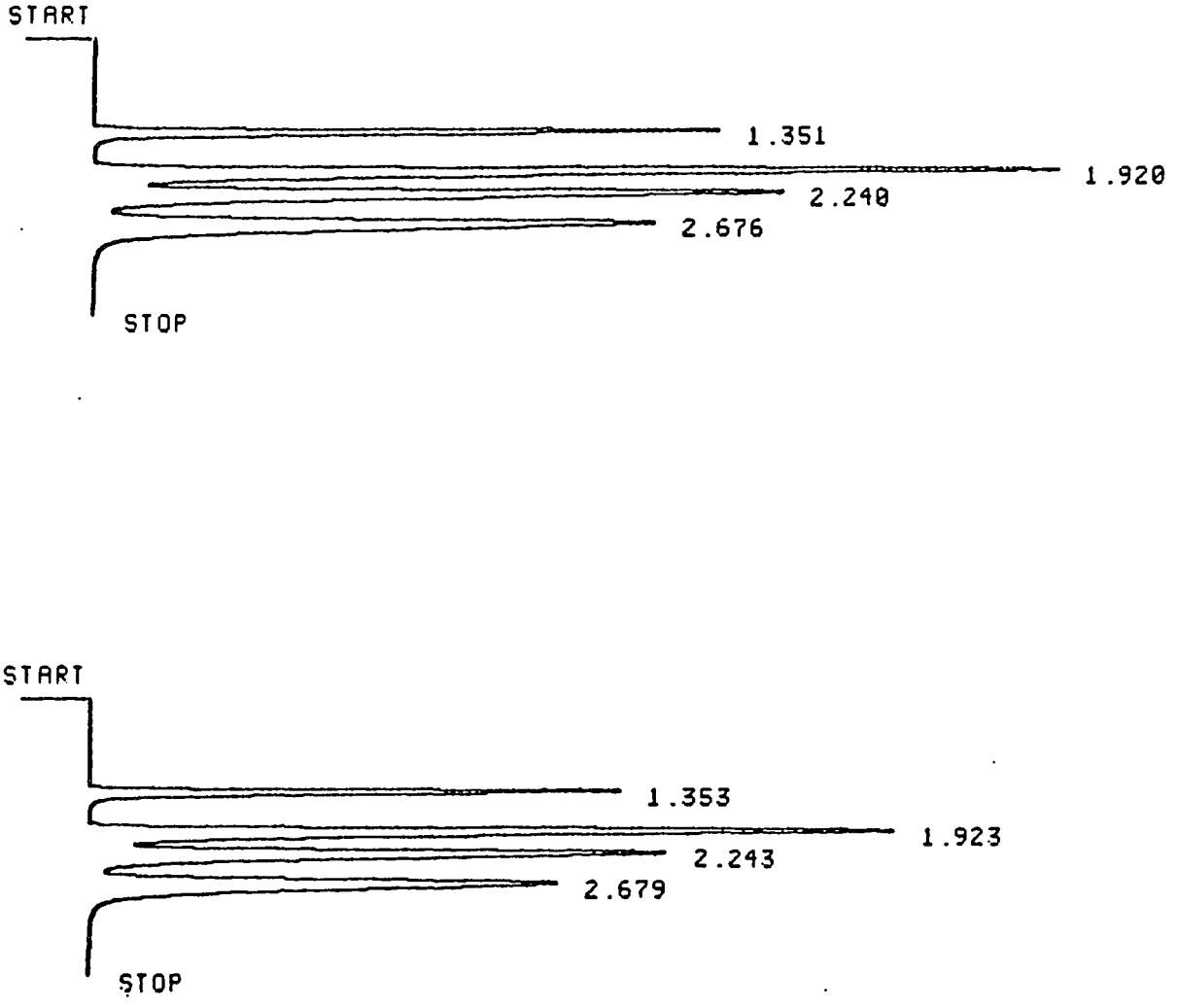

Figure 3.9 Standard Gas Sample Chromatogram (FID)

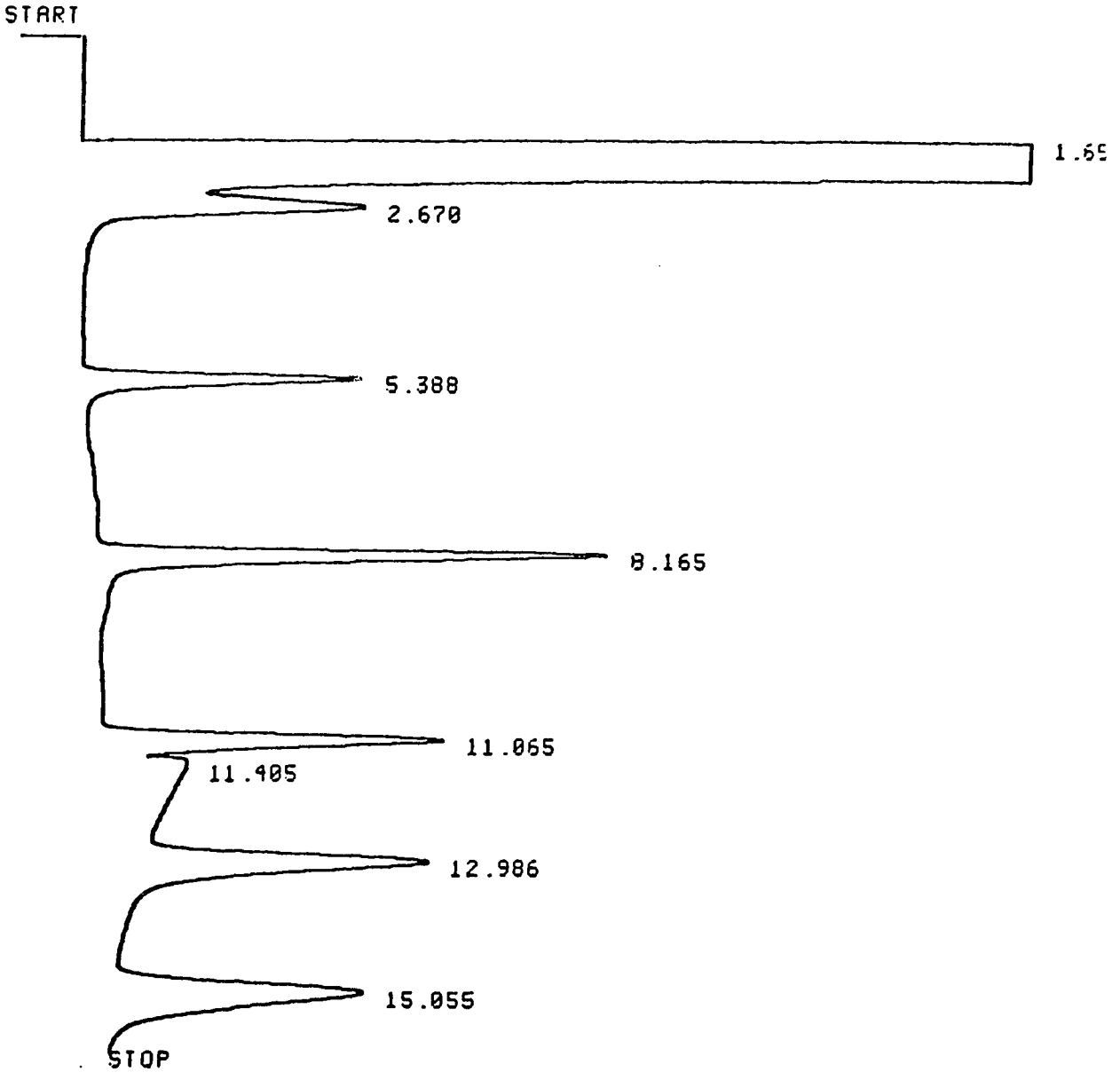

Figure 3.10 Standard Gas Sample Chromatogram (TCD)

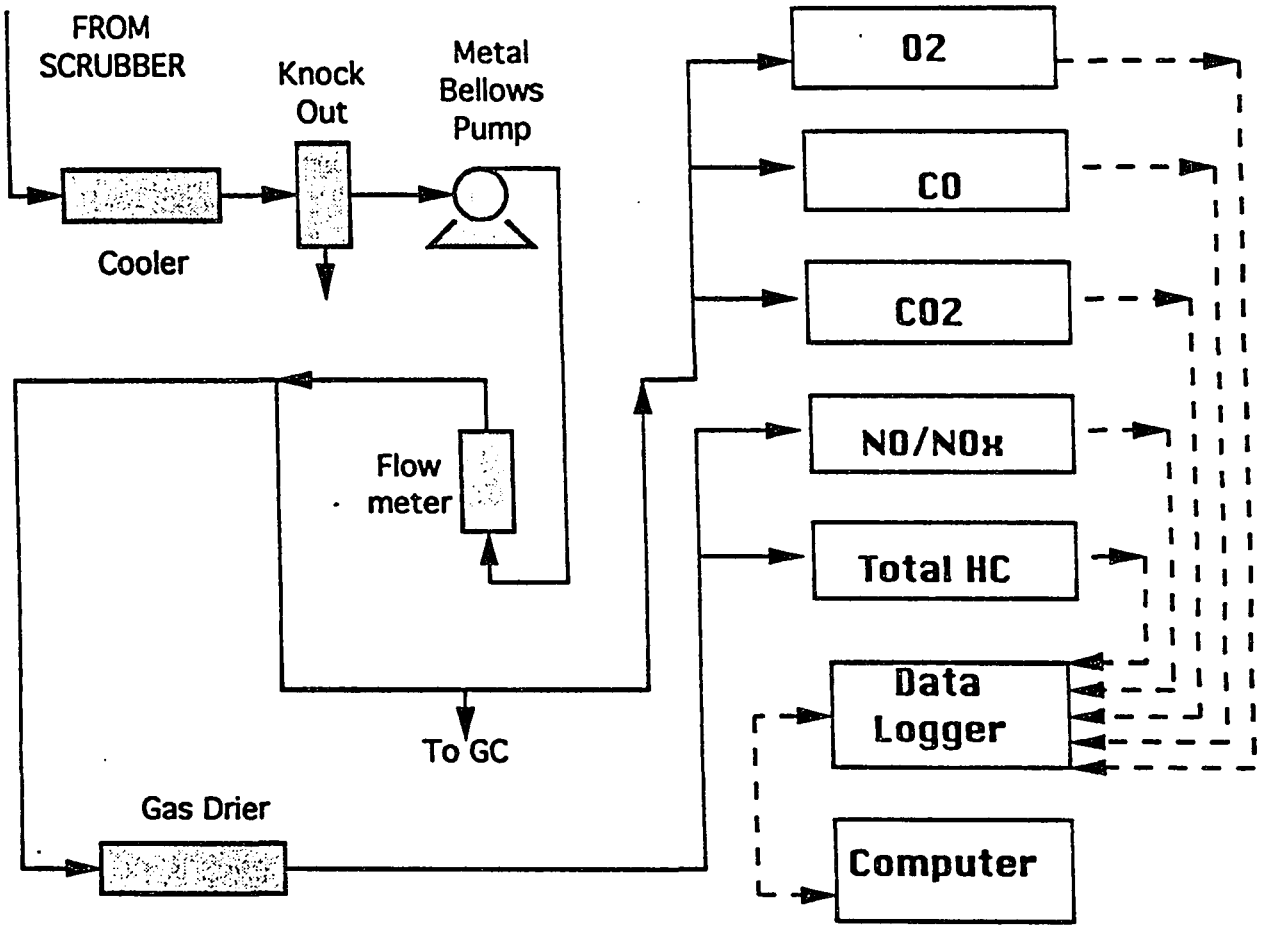

Figure 3.11 Beckman Analysis System: Analyzers, Sampling line, and Data Logger

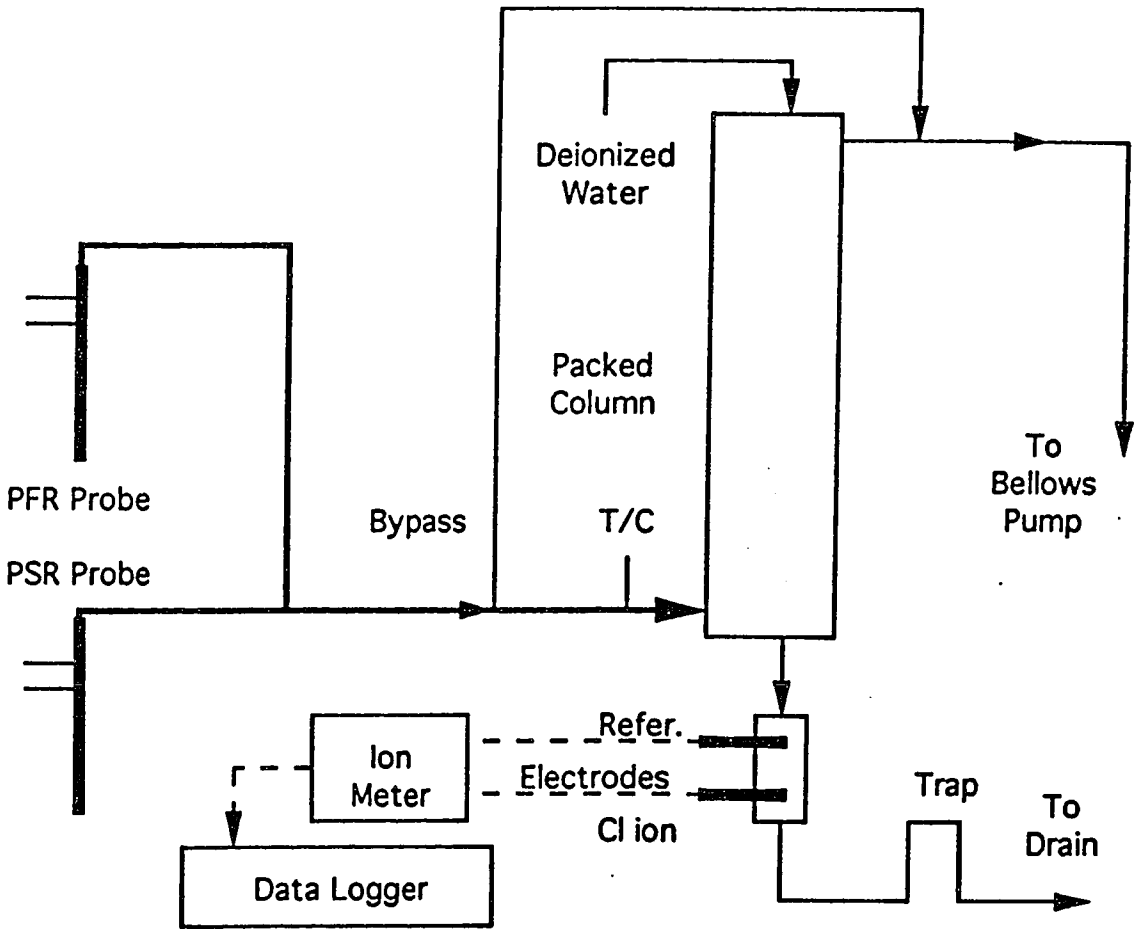

Figure 3.12 HCl Scrubber and Analysis System

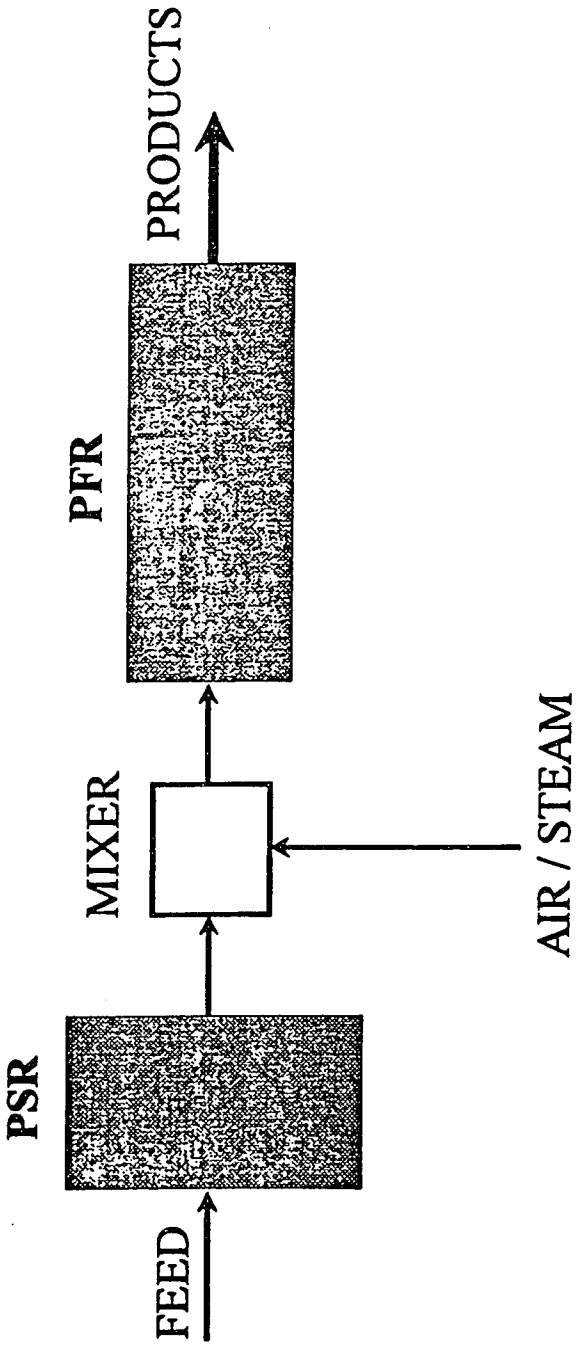

Figure 4.1 Two Stage Turbulent Flow Reactor Model

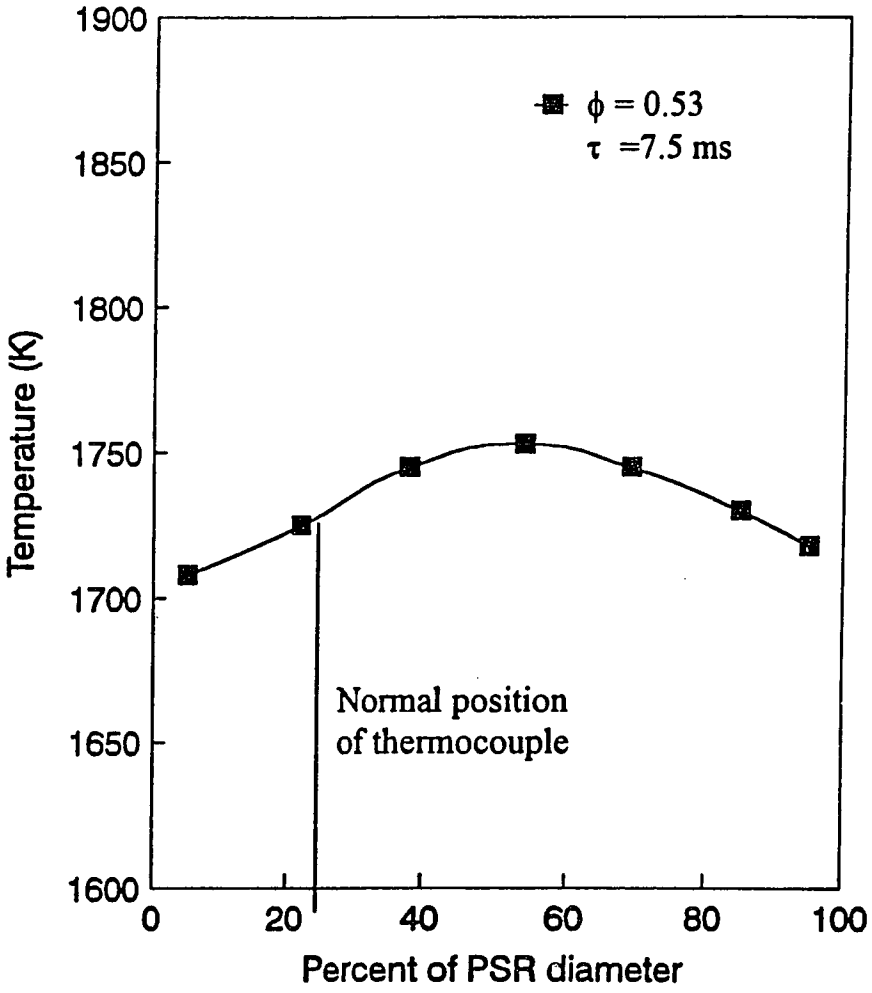

Figure 5.1 Measured Temperature Profile in PSR (C2H4 / Air)

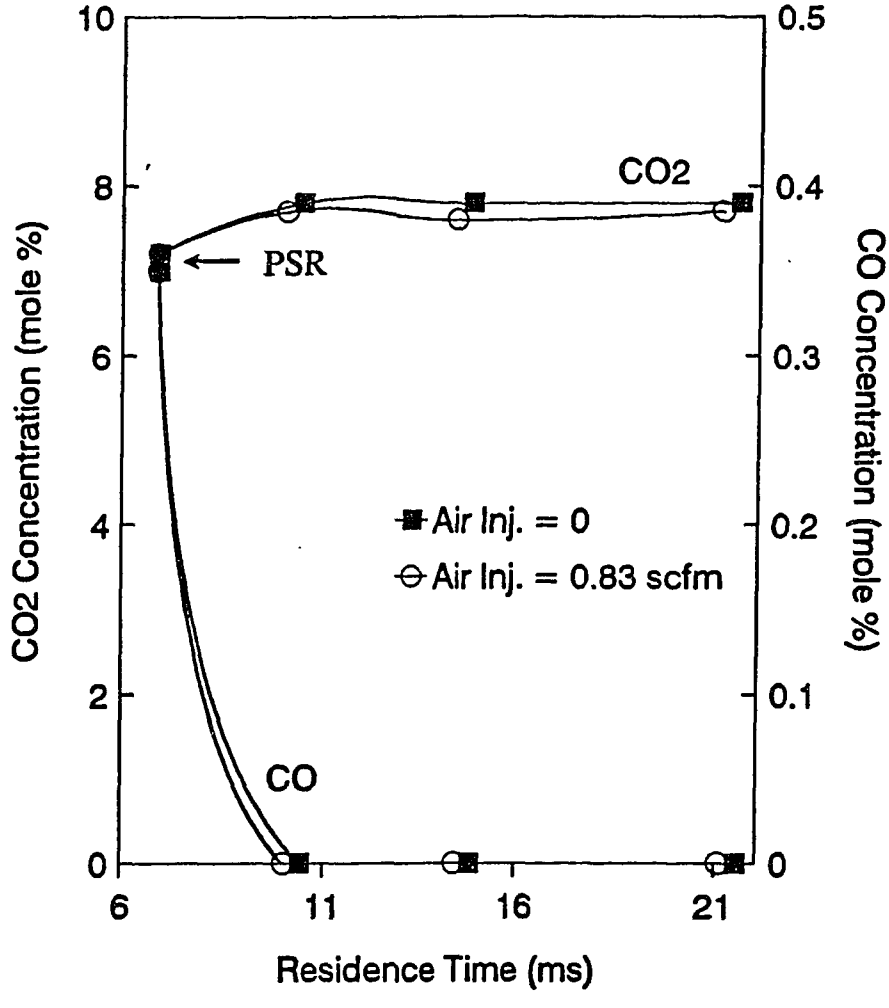

Figure 5.2 Measured CO and CO2 Concentrations at Fuel Lean (C2H4/Air, $\phi = 0.59$)

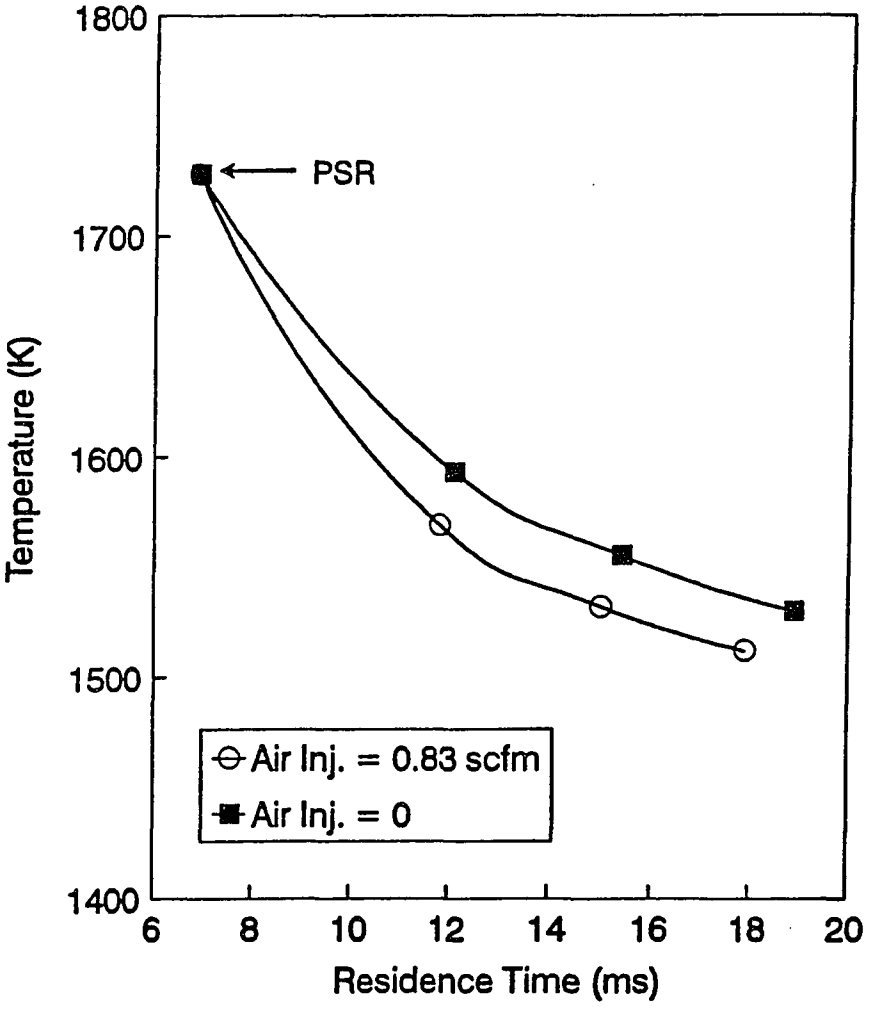

Figure 5.3 Measured Temperature Profiles at Fuel Lean (C2H4/Air, $\phi = 0.59$)

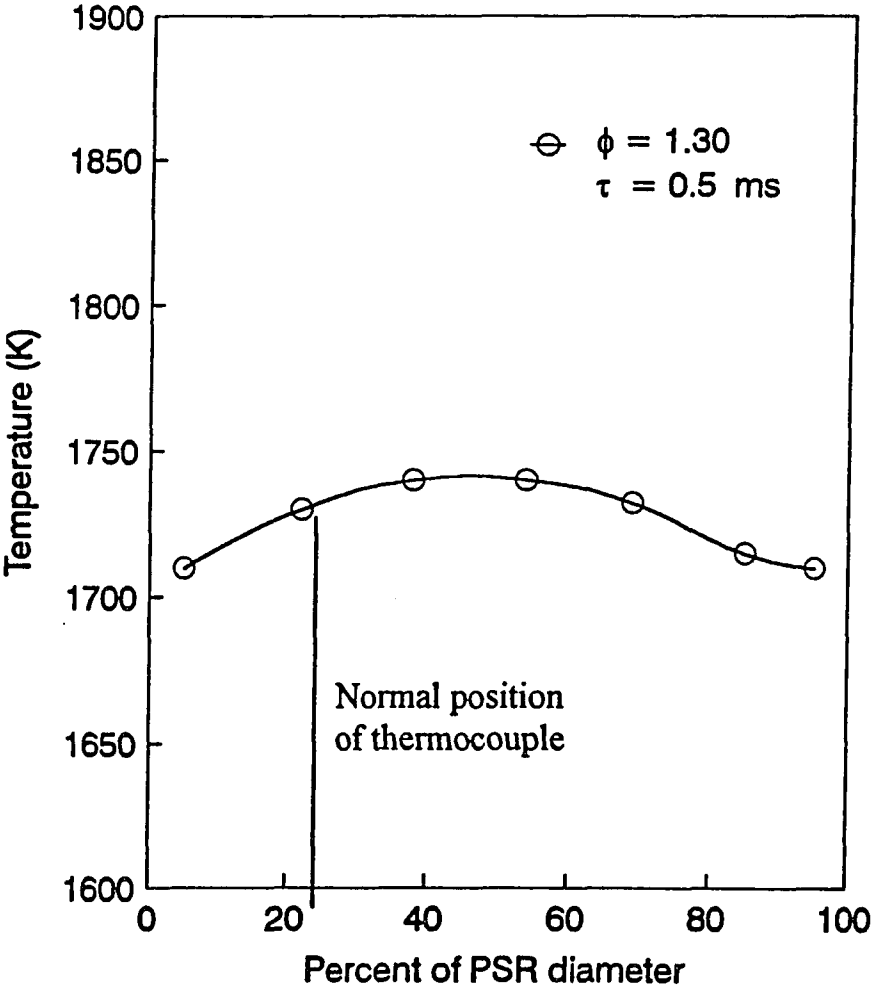

Figure 5.4 Measured Temperature Profile in PSR
(C2H4 / Air / N2)

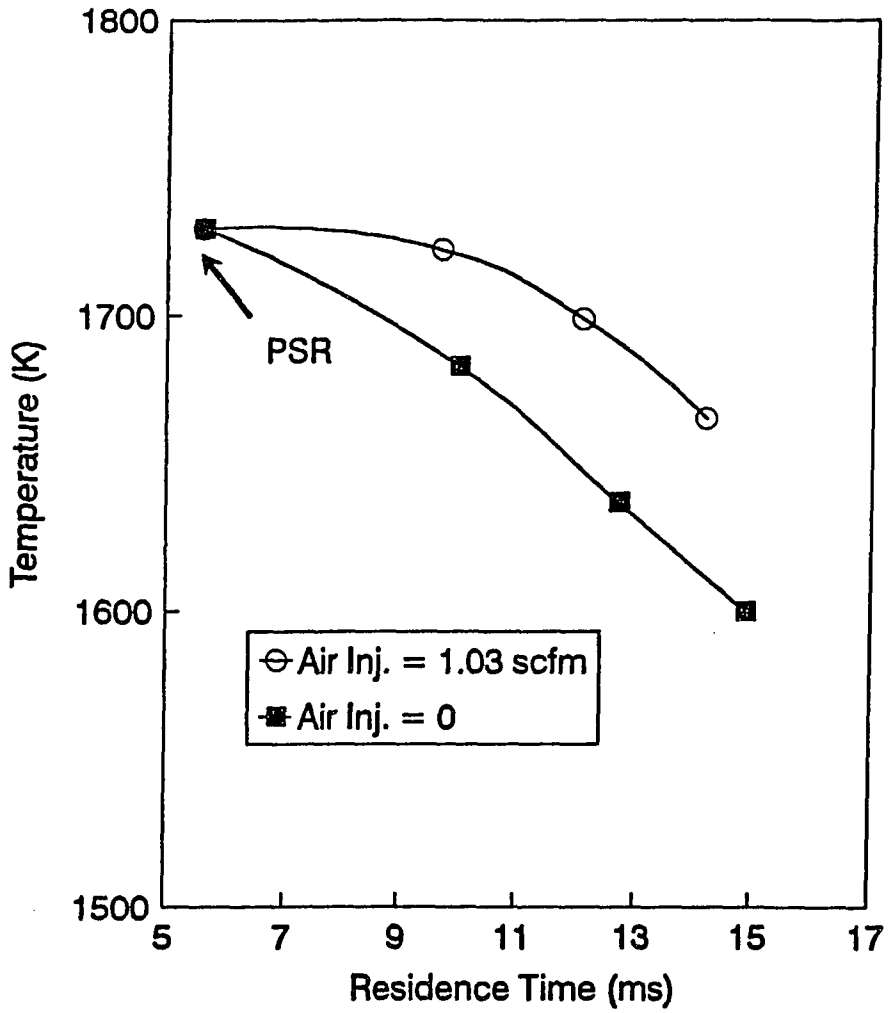

Figure 5.5 Measured Temperature Profiles at Fuel Rich

(C2H4 / Air / N2, $\phi = 1.52$)

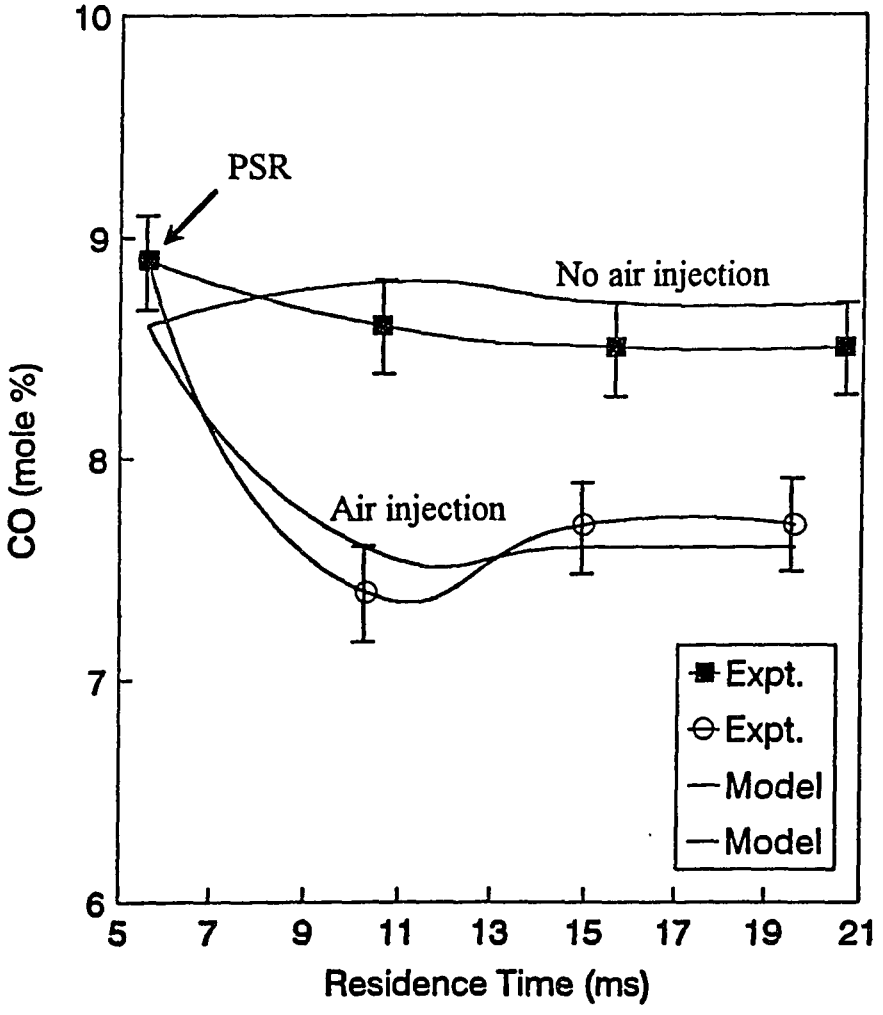

Figure 5.6 CO concentrations at Fuel Rich
(C2H4/Air/N2 ; $\phi = 1.52$, ϕ (overall) = 1.38)

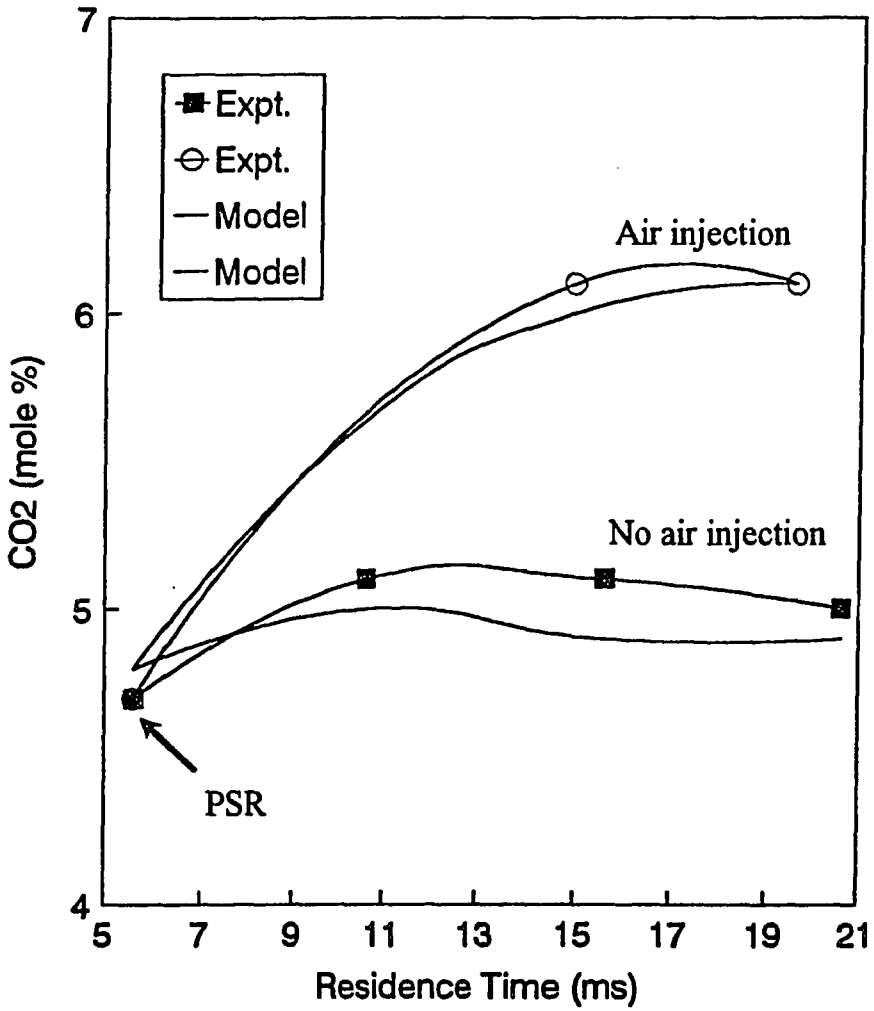

Figure 5.7 CO2 concentrations at Fuel Rich
(C2H4/Air/N2 ; $\phi = 1.52$, ϕ (overall) = 1.38)

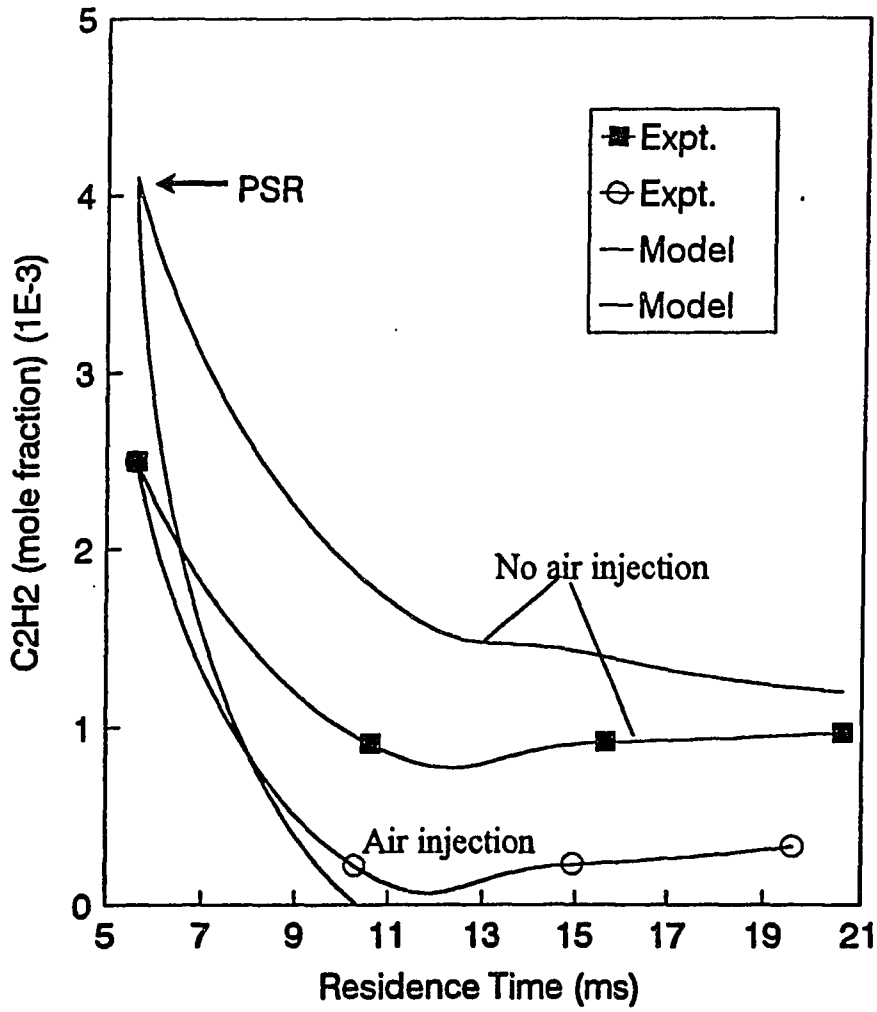

Figure 5.8 C2H2 concentrations at Fuel Rich (C2H4/Air/N2 ; $\phi = 1.52$, ϕ (overall) = 1.38)

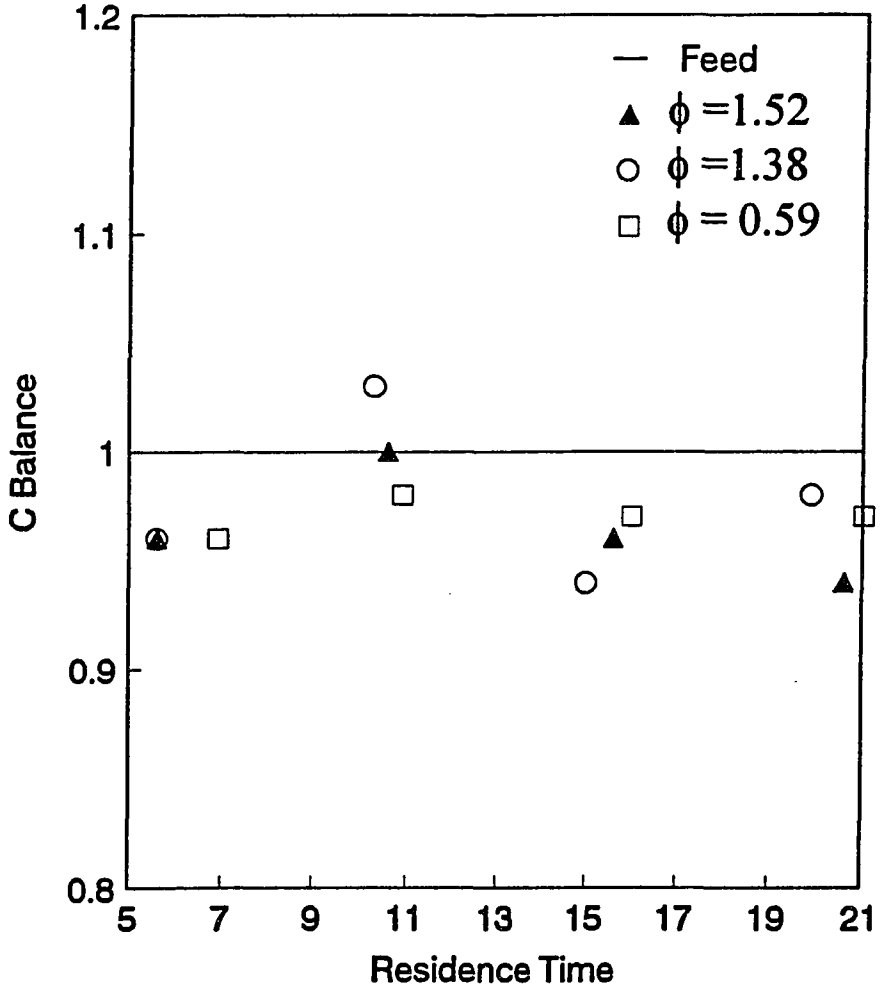

Figure 5.9 Carbon Balance for C2H4 /Air / N2 Combustions

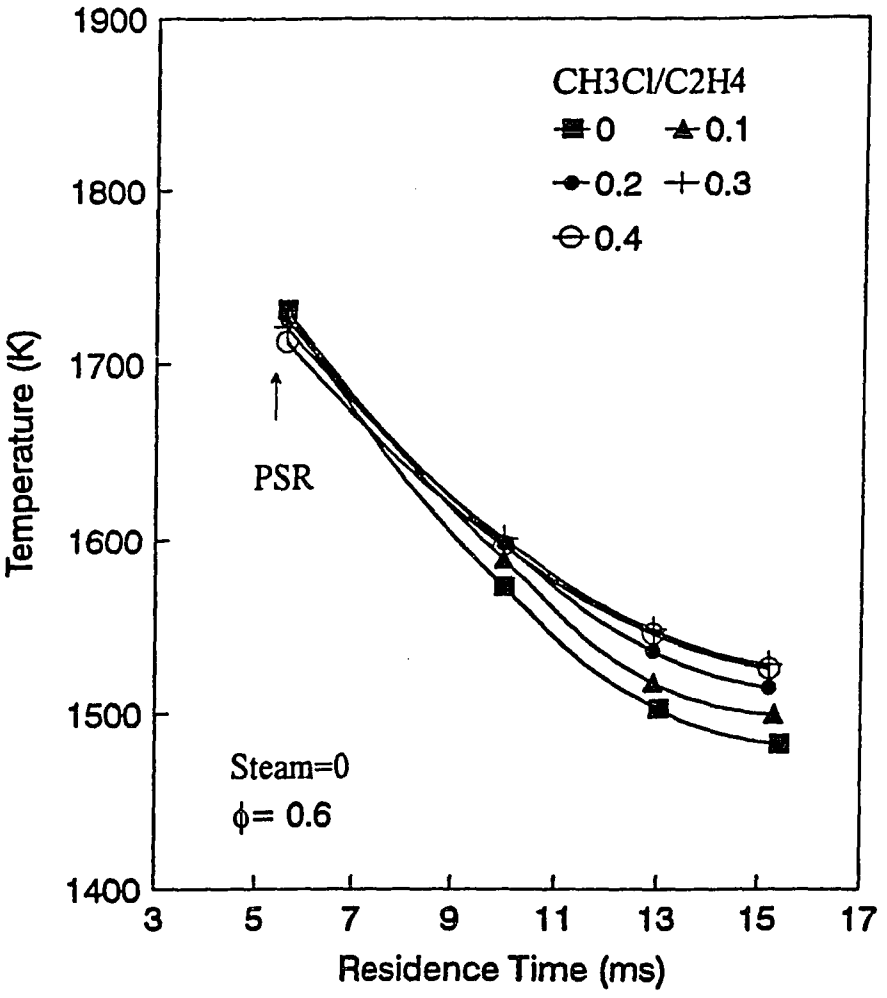

Figure 6.1 Measured Temperature Profiles at Fuel lean ($\phi = 0.6$) with Methyl Chloride Loading CH3Cl/C2H4 = 0 to 0.4

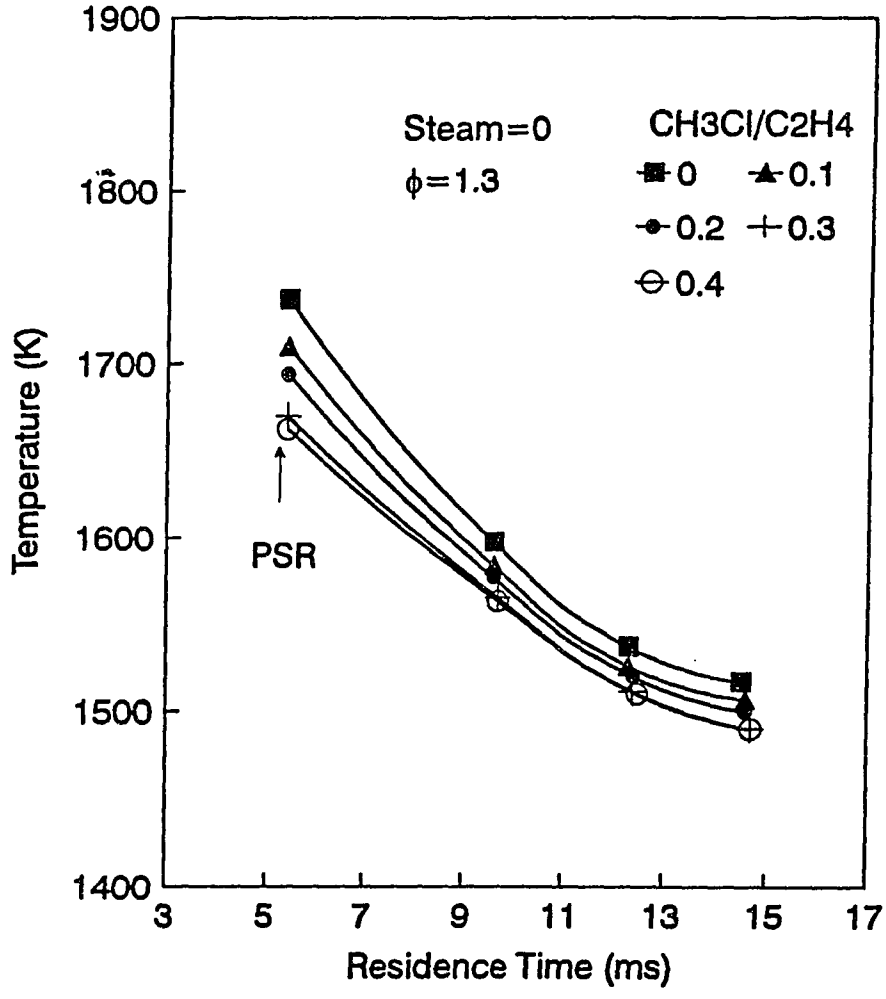

Figure 6.2 Measured Temperature Profiles at Fuel rich(ϕ =1.3) with Methyl Chloride Loading

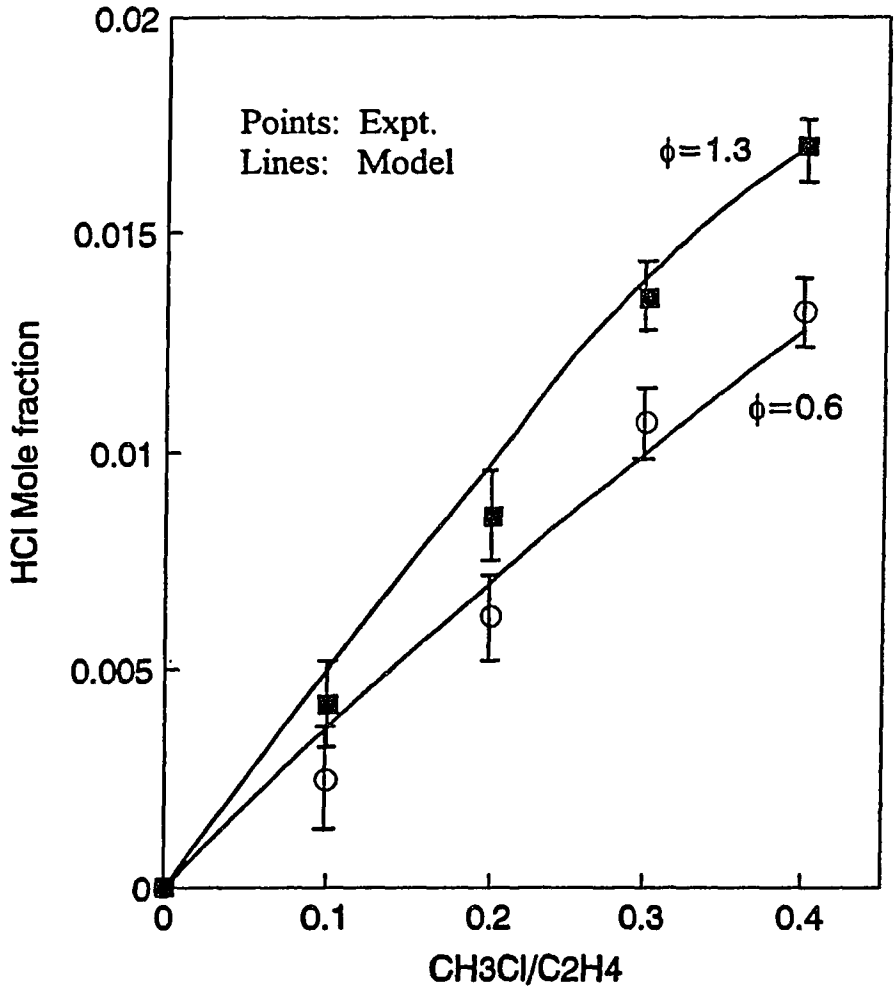

Figure 6.3 HCl Concentrations at PFR outlet

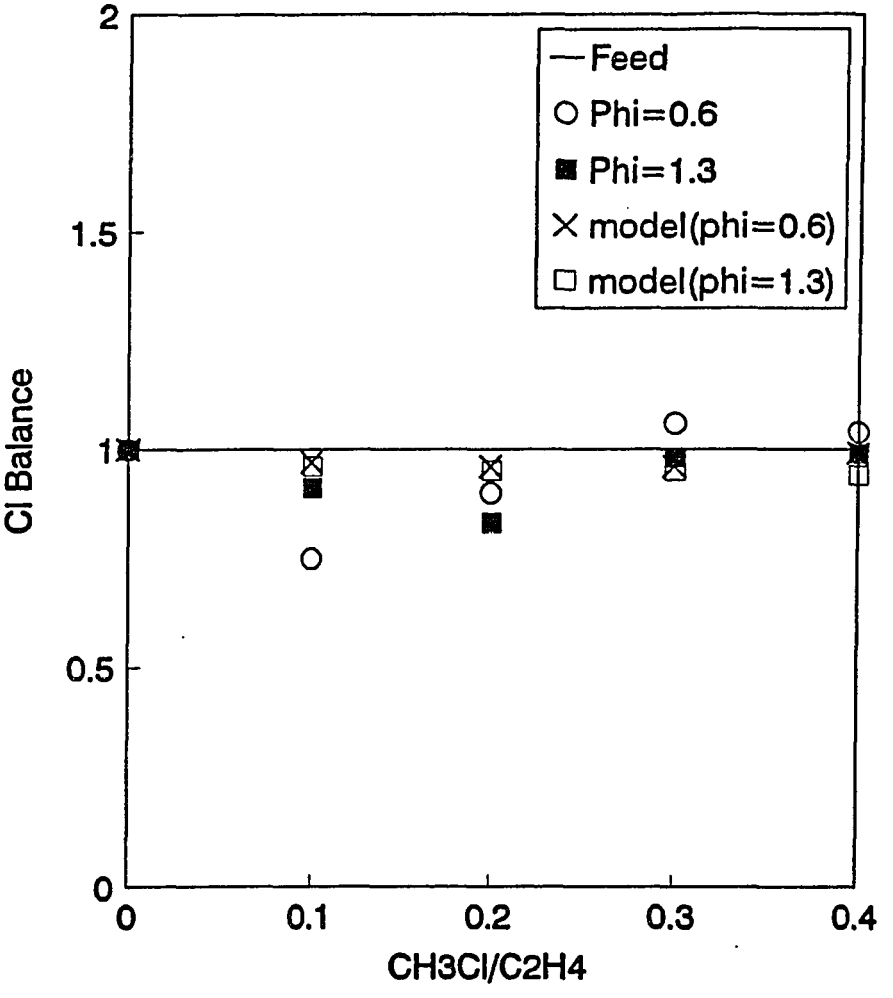

Figure 6.4 Cl Balance Made from HCl Measurement at Reactor outlet (ϕ = 0.6 and 1.3)

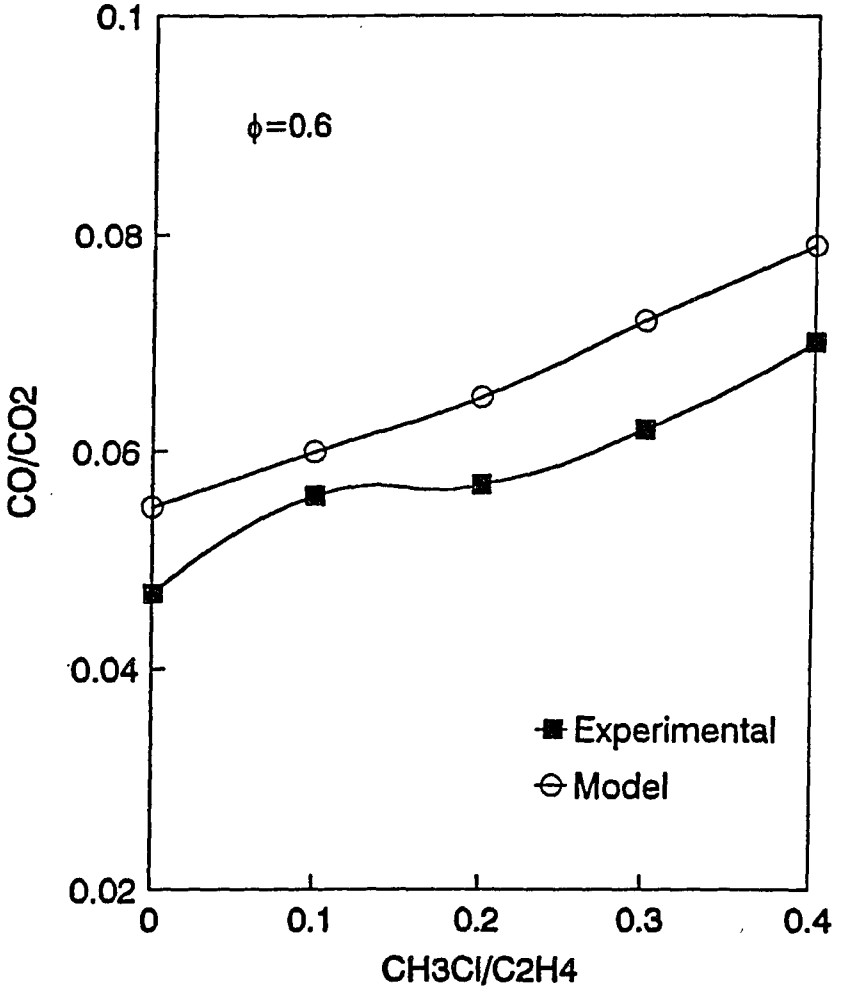

Figure 6.5 Ratio of CO/CO2 in PSR as a Function of Feed Methyl Chloride Loading

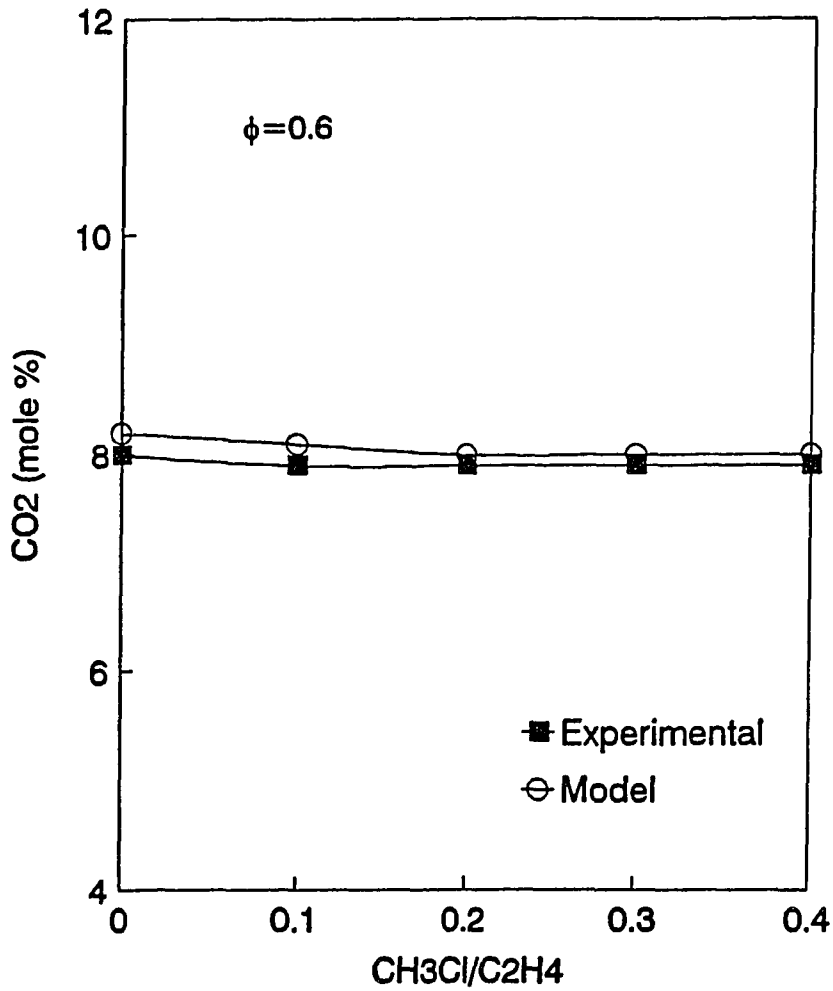

Figure 6.6 Mole Percent of CO2 at PFR outlet as a Function of Feed Methyl Chloride Loading

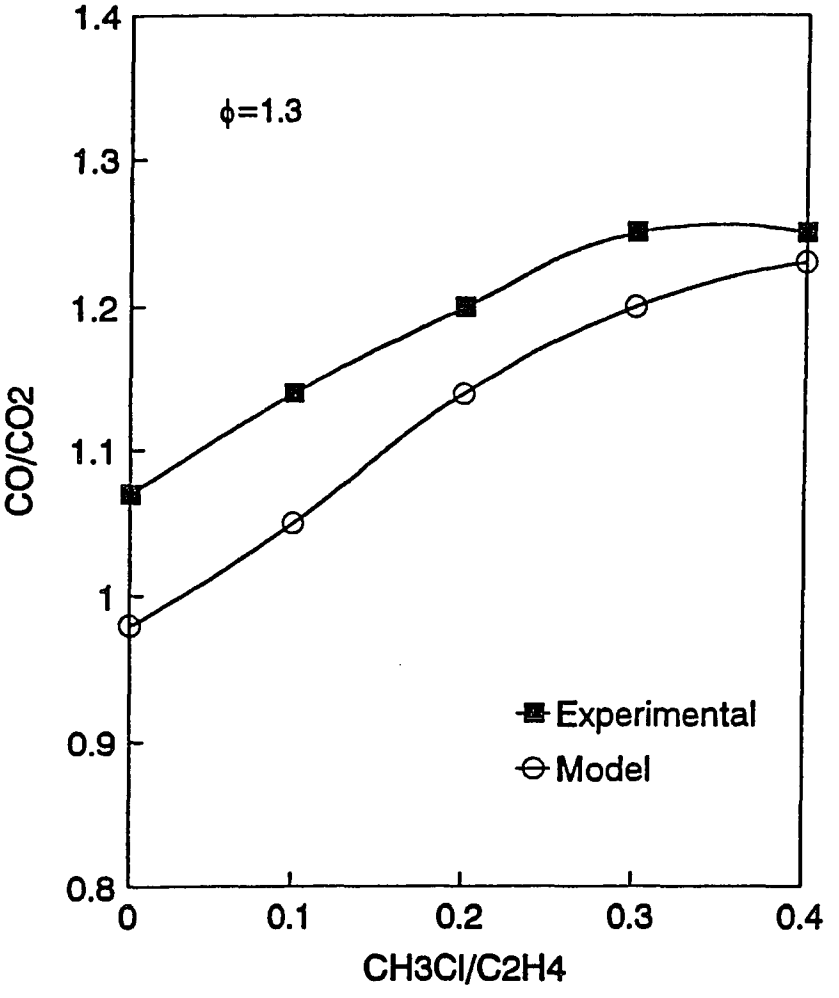

Figure 6.7 Ratio of CO/CO2 in PSR as a Function of Feed Methyl Chloride Loading ($\phi = 1.3$)

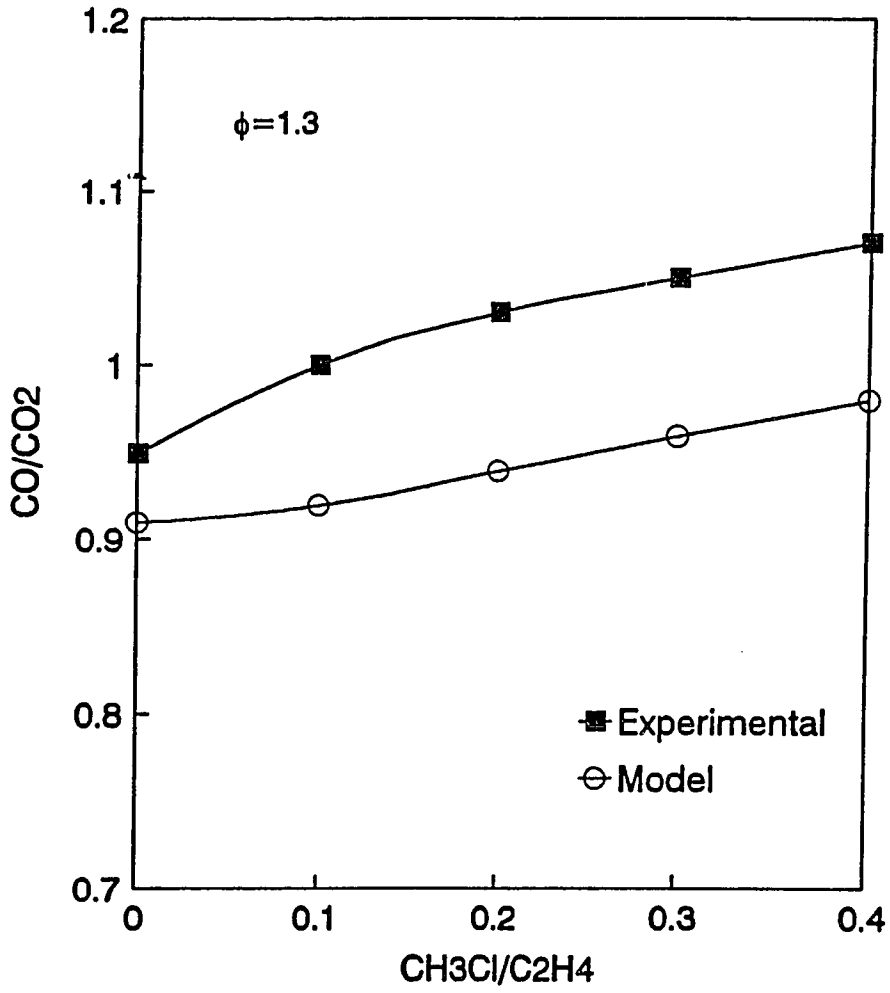

Figure 6.8 Ratio of CO/CO2 at PFR outlet as a Function of Feed Methyl Chloride Loading ($\phi = 1.3$)

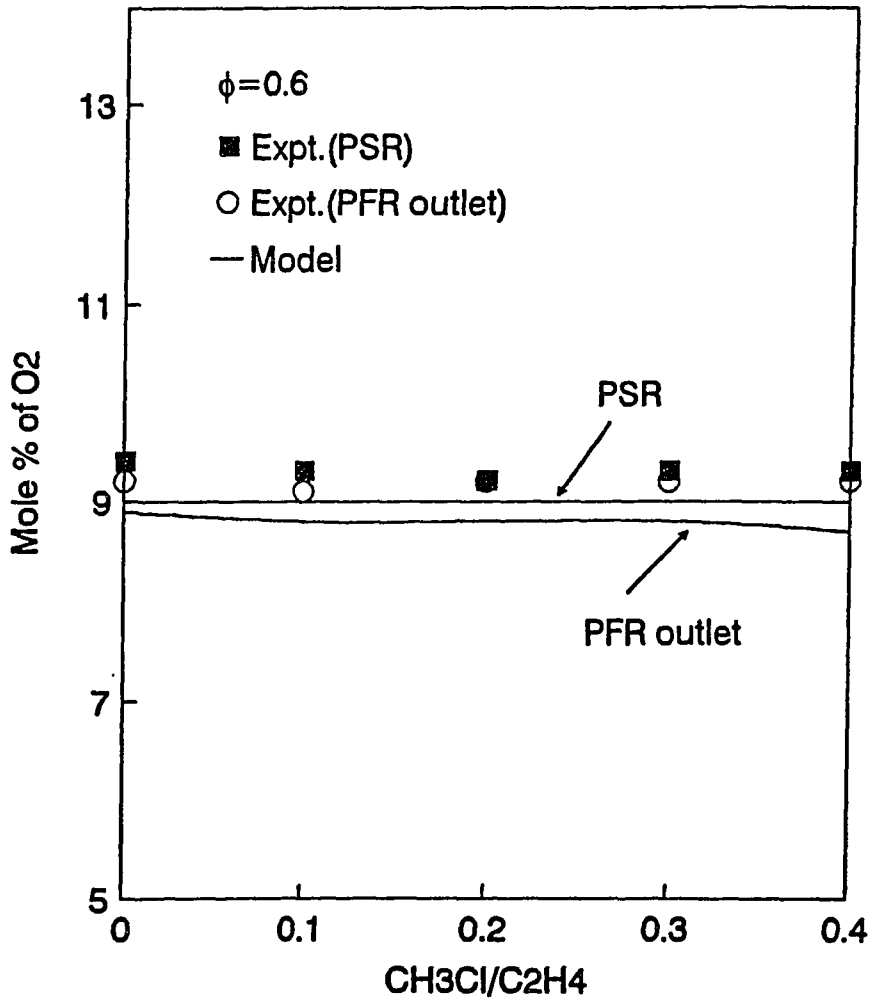

Figure 6.9 Mole Percent of O2 as a Function of Feed Methyl Chloride Loading ($\phi = 0.6$)

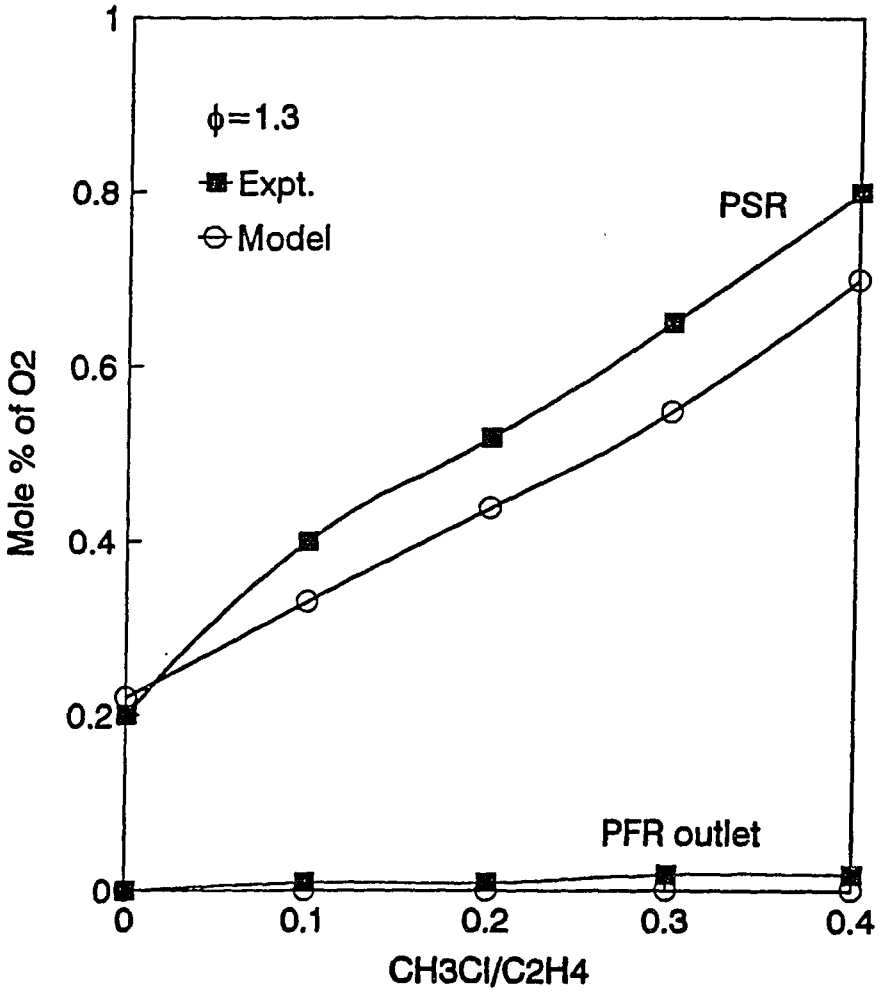

Figure 6.10 Mole Percent of O2 as a Function of Feed Methyl Chloride Loading ($\phi = 1.3$)

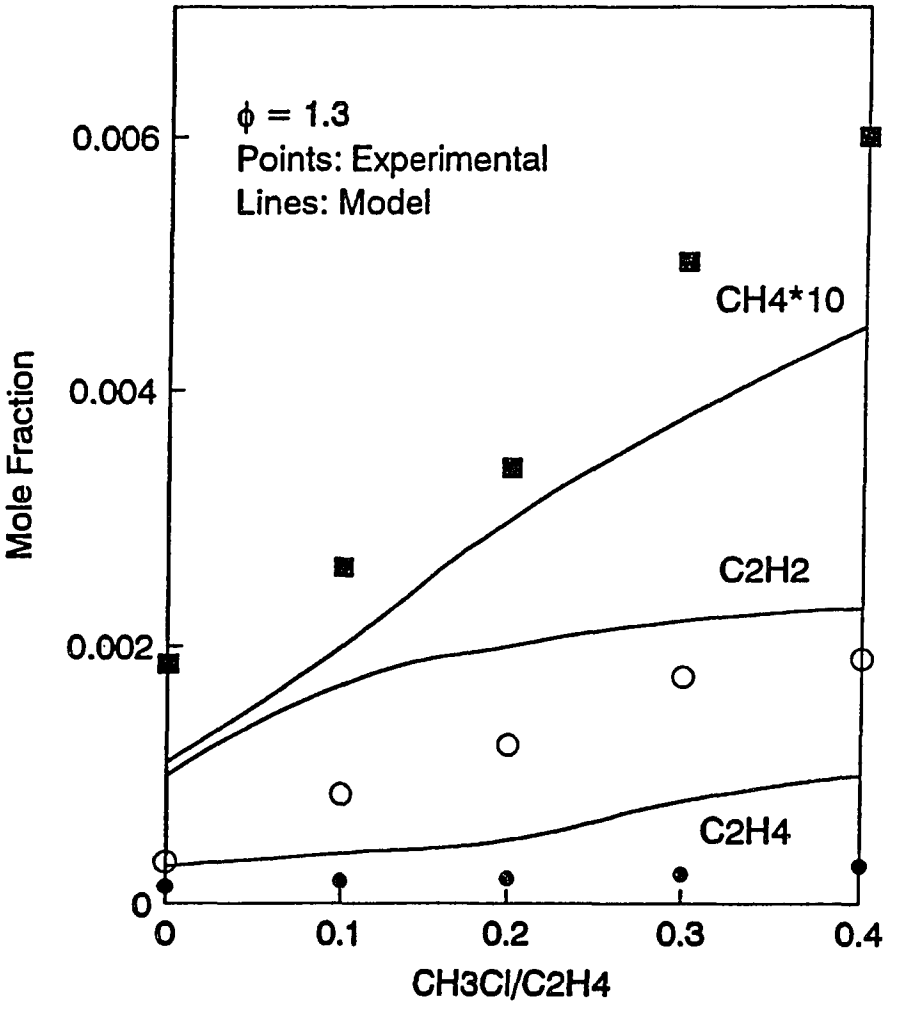

Figure 6.11 Mole fractions of unburned light hydrocarbons in PSR as functions of feed methyl chloride loading ($\phi = 1.3$)

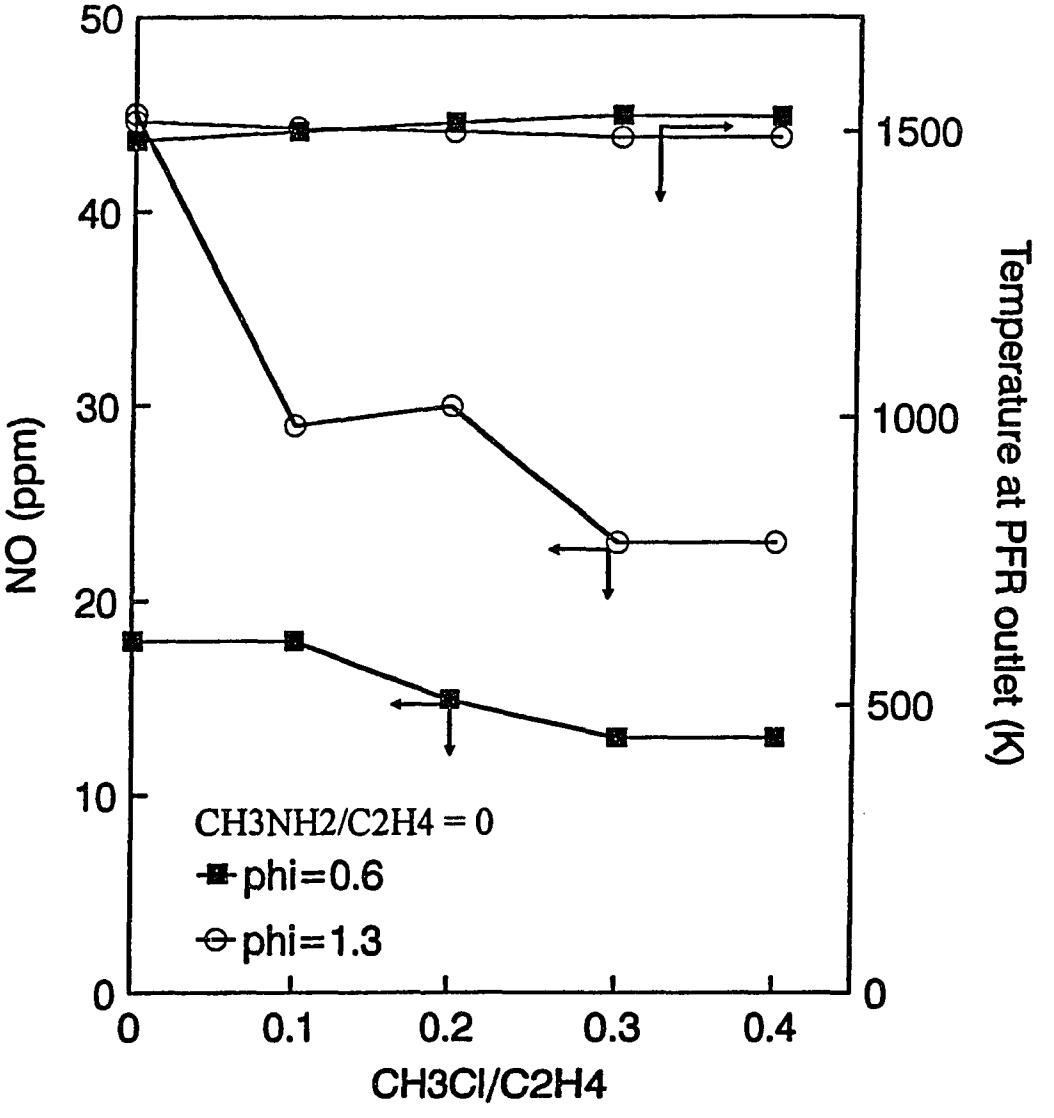

Figure 6.12 Effects of Feed Methyl Chloride Loading on NO Emission (measured at PFR outlet)

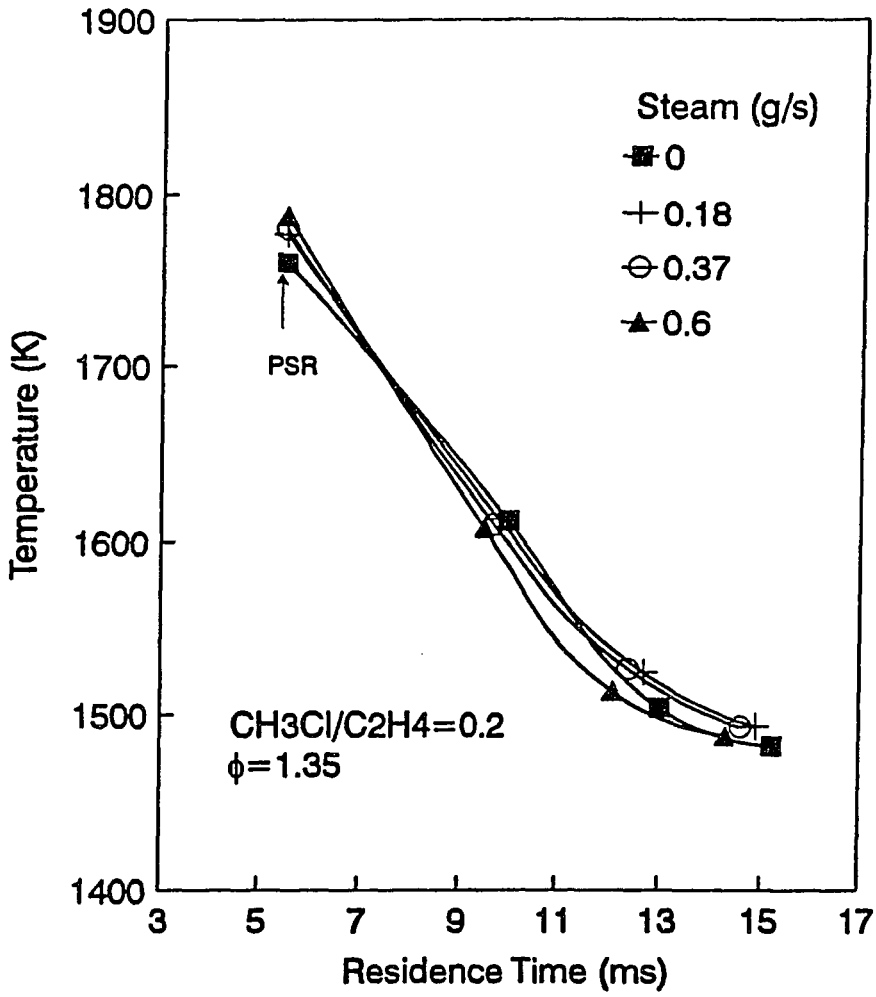

Figure 6.13 Measured Temperature Profiles under Steam Injection Conditions ($\phi = 1.35$)

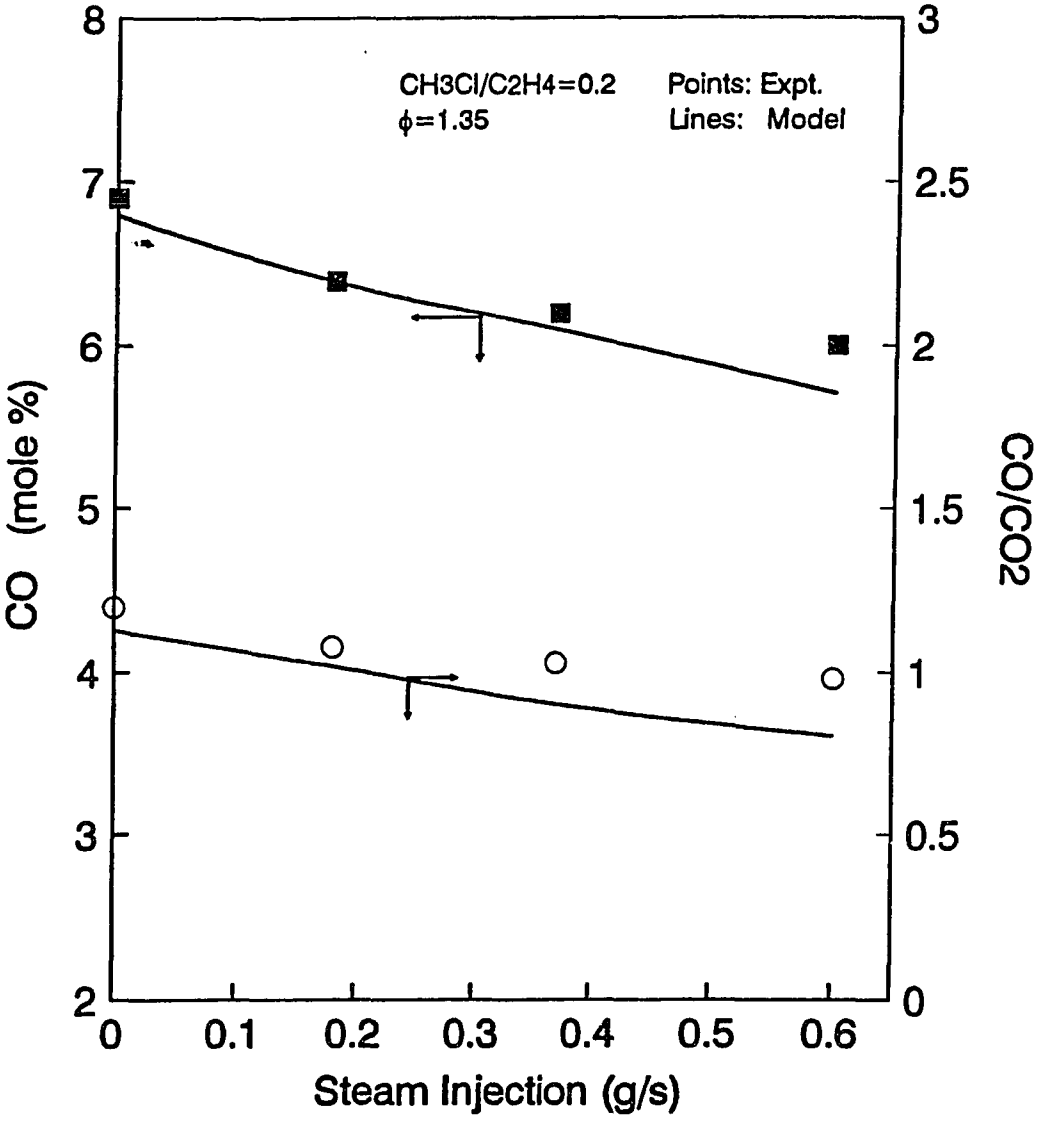

Figure 6.14 Effects of Steam Injection on CO and CO/CO2 at PFR outlet in Combustion of Methyl Chloride ($\phi = 1.35$)

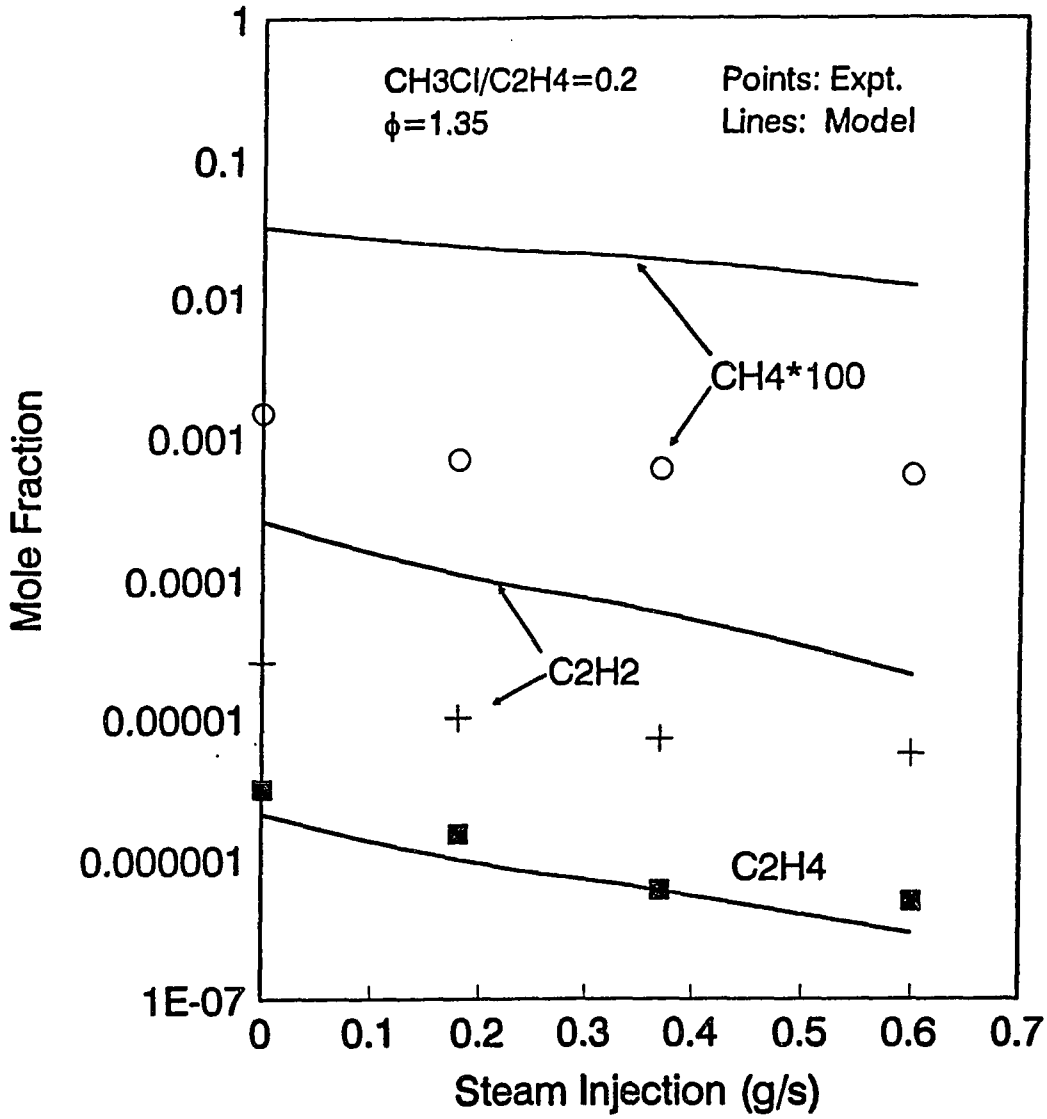

Figure 6.15 Effects of Steam Injection on unburned hydrocarbons at PFR outlet in Combustion of Methyl Chloride (ϕ =1.35)

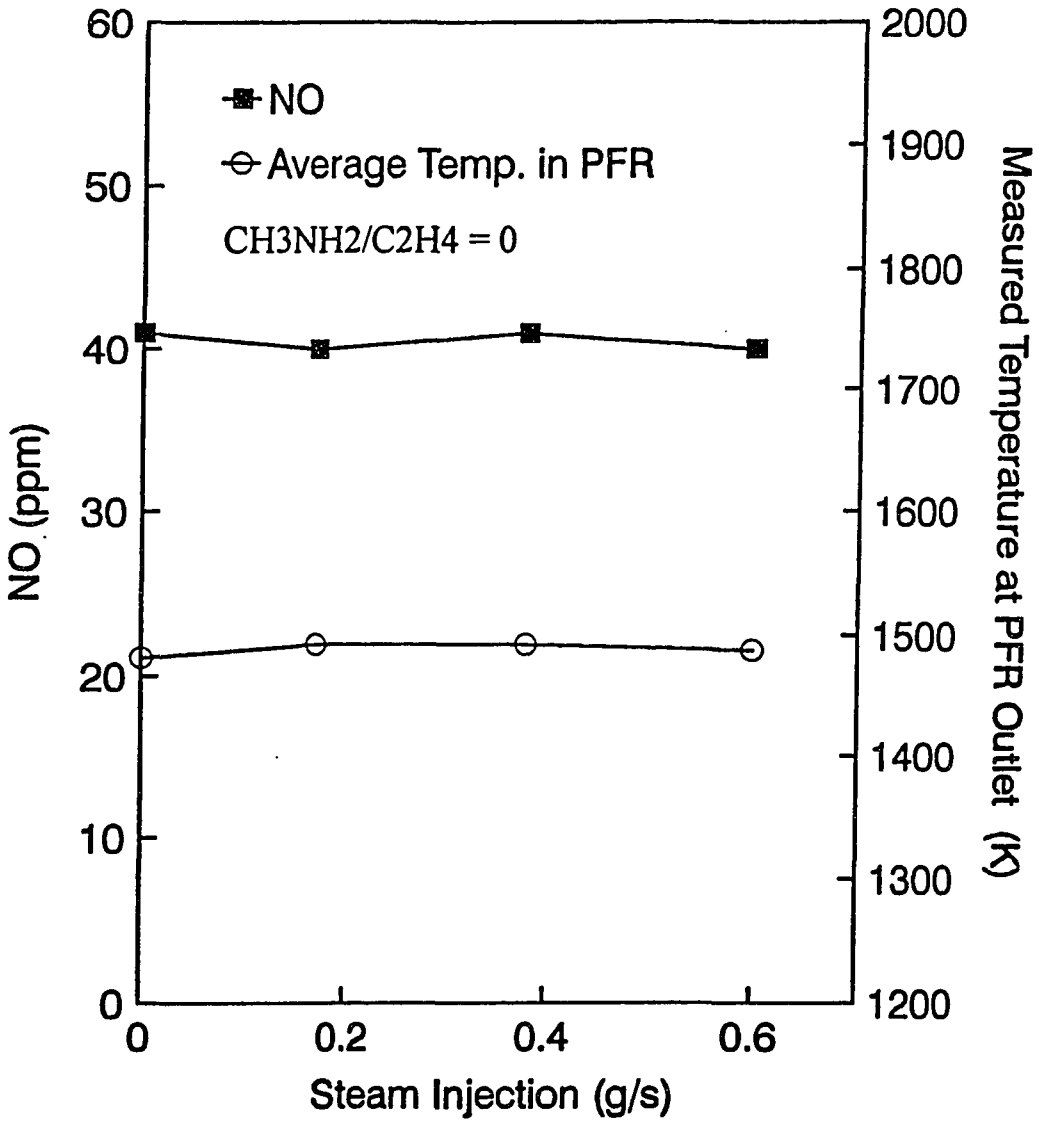

Figure 6.16 NO Emission and Measured Temperature at PFR Outlet with Steam Injection ($CH_3Cl/C_2H_4 = 0.2$; $\phi = 1.35$)

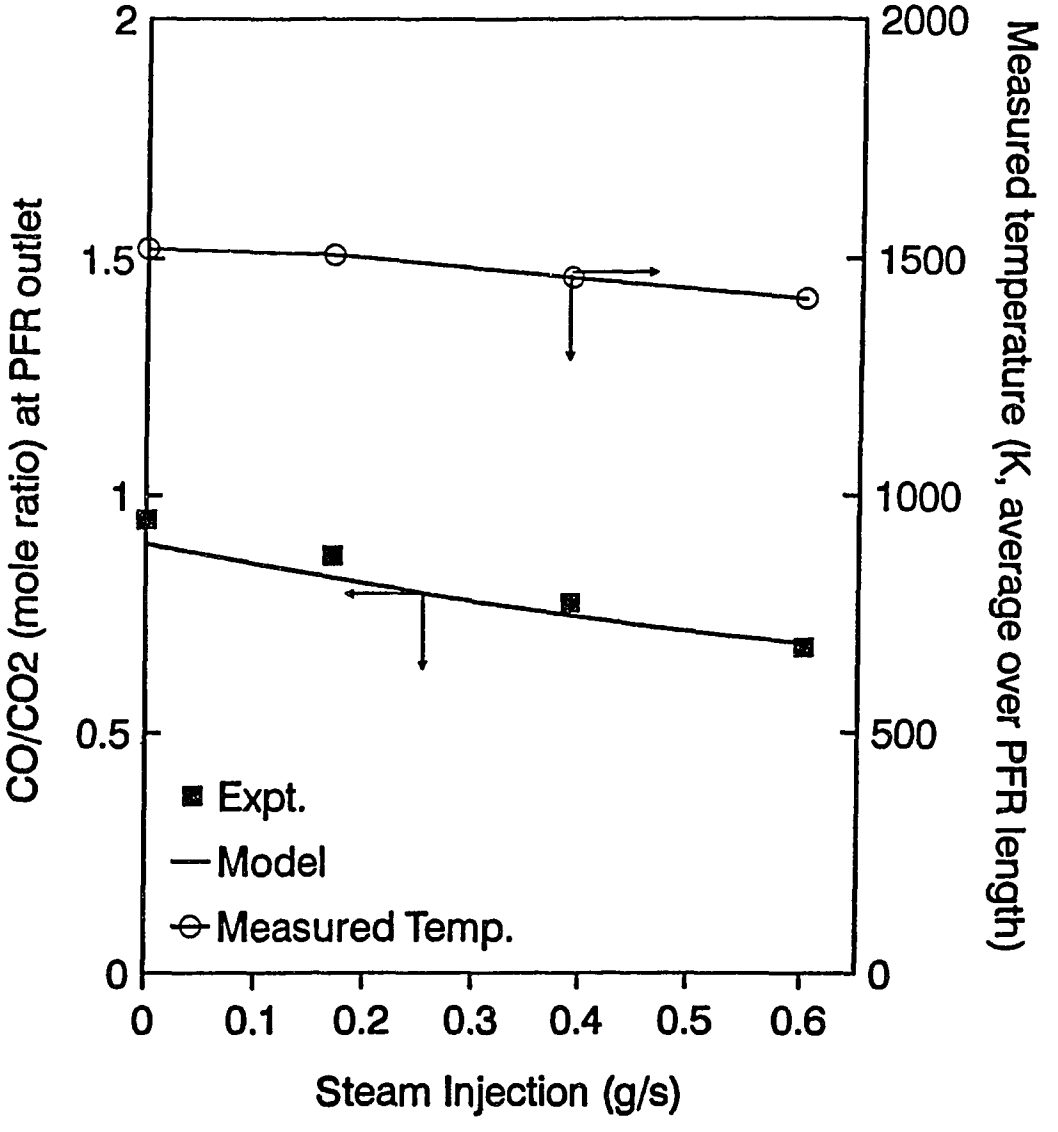

Figure 6.17 Effects of steam injection on CO/CO2 ratio at PFR outlet and on PFR temperature in combustion of C2H4/air/N2

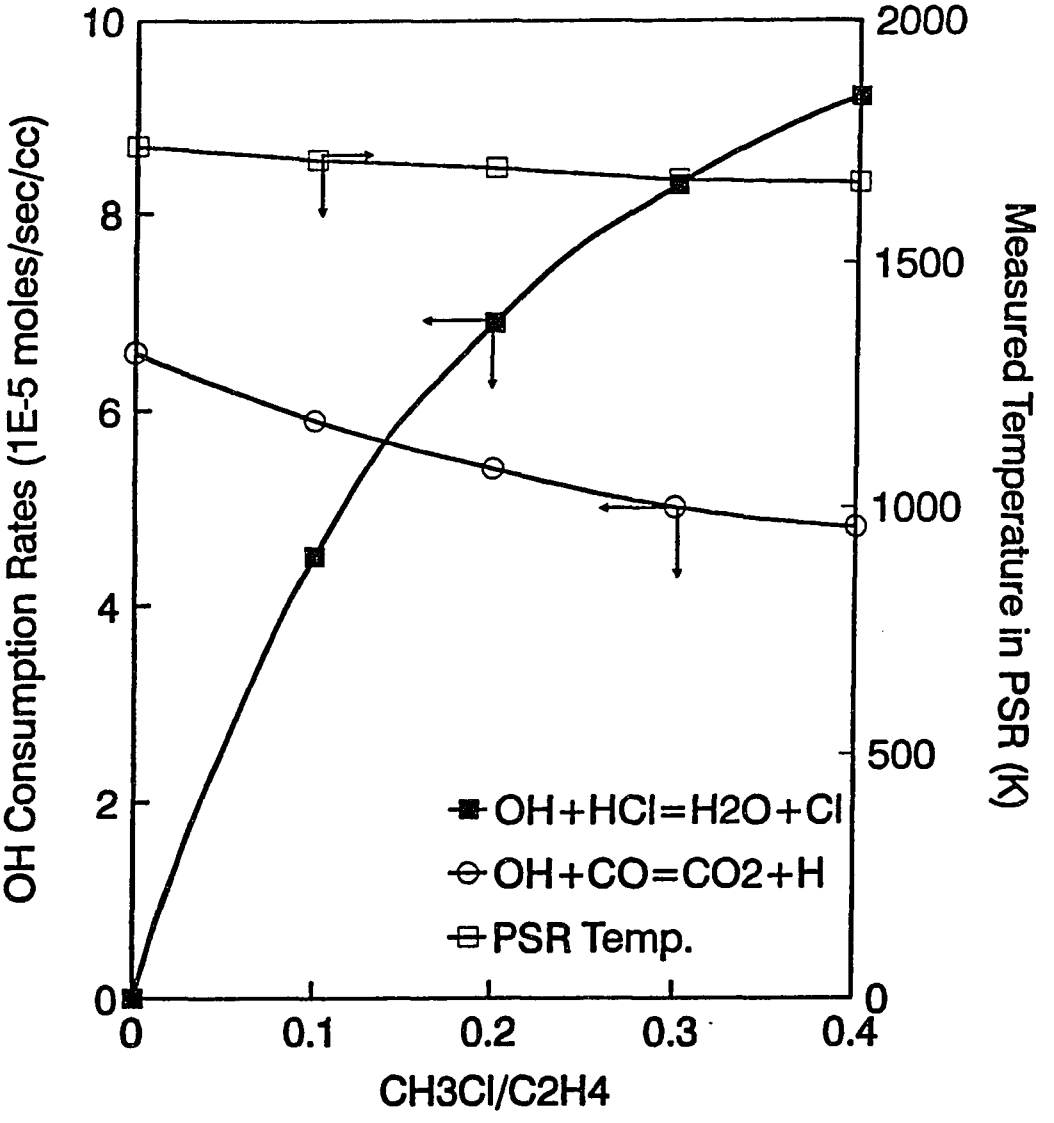

Figure 6.18 OH Consumption Rates as Functions of Feed Methyl Chloride Loading ($\phi = 1.3$)

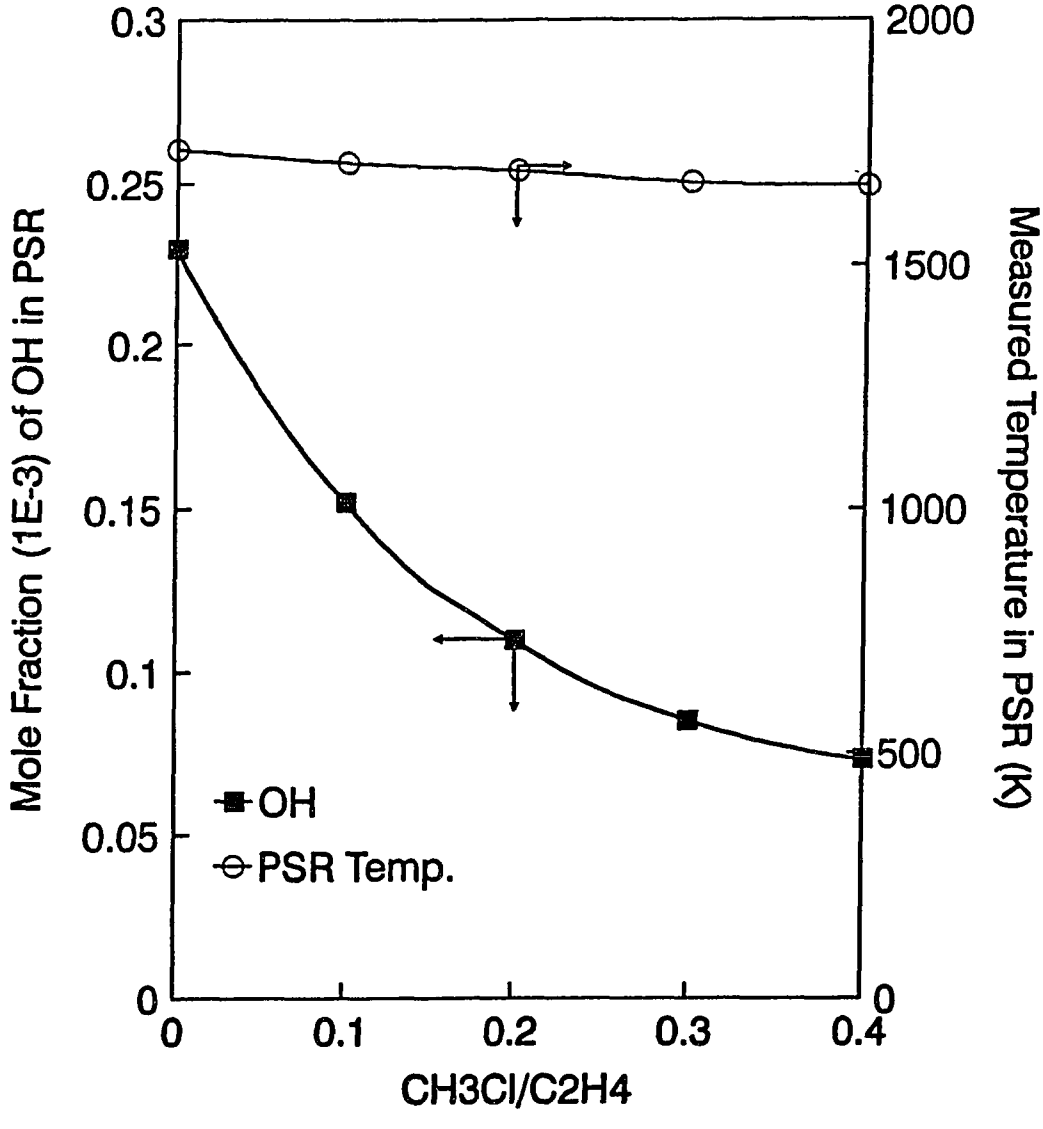

Figure 6.19 Calculated OH radical concentration and measured temperature in PSR as functions of CH3Cl loading ($\phi = 1.3$)

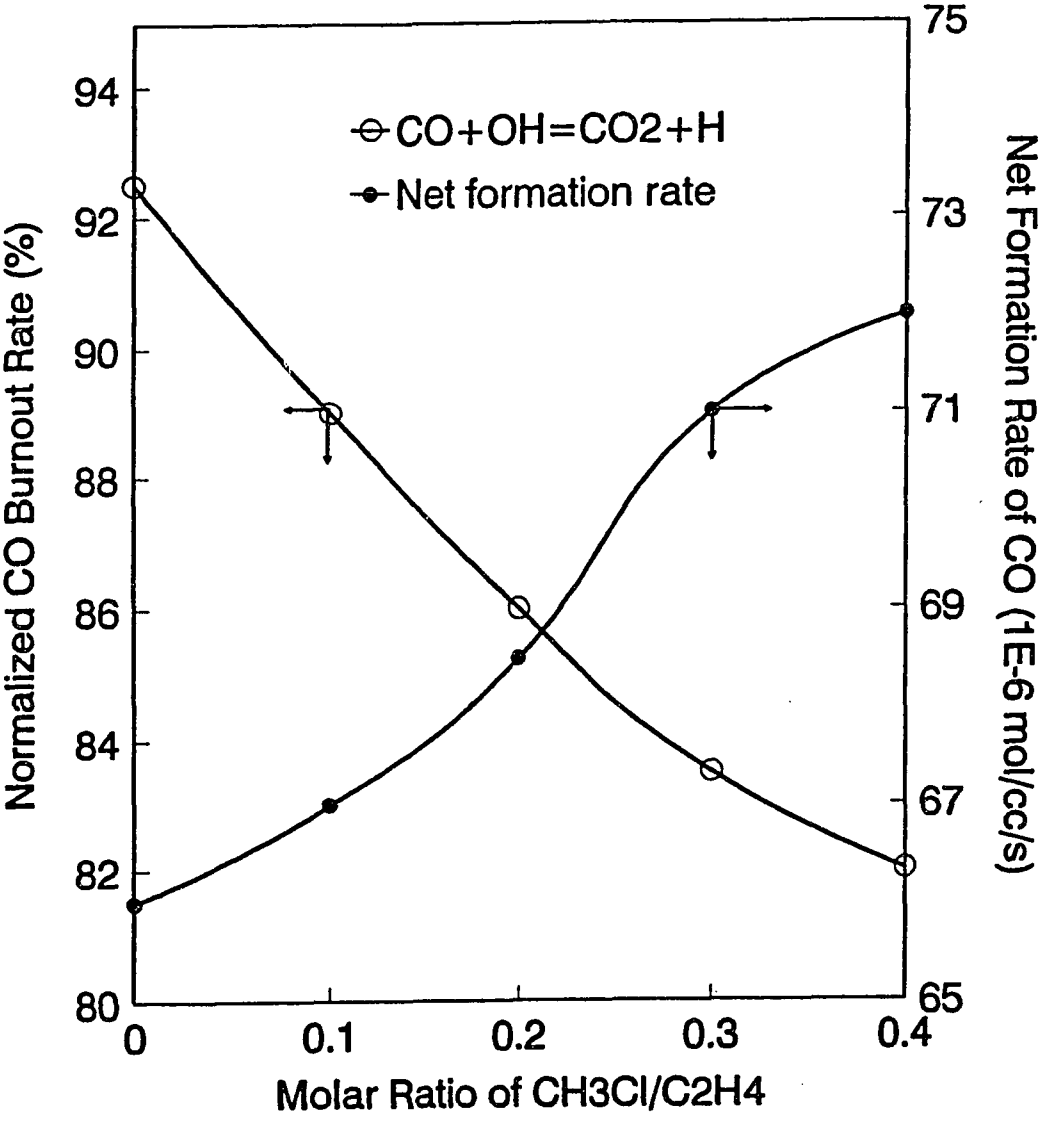

Figure 6.20 ROP Analysis of CO in PSR: Burnout and Formation Rates of CO as Functions of Feed CH3Cl Loading (ϕ = 1.3)

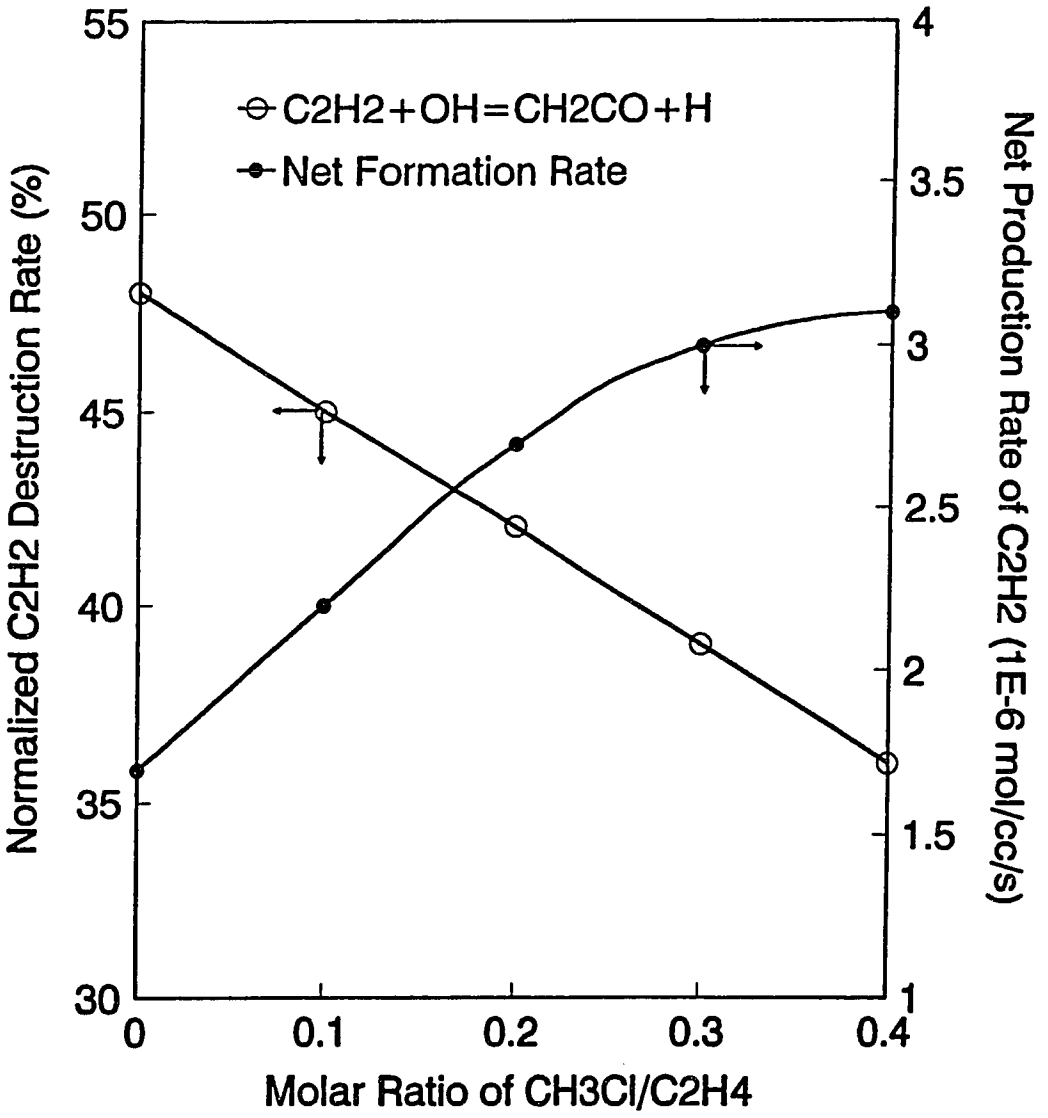

Figure 6.21 ROP Analysis of C2H2 in PSR: Destruction and Production Rates of C2H2 as Functions of Feed CH3Cl Loading (ϕ = 1.3)

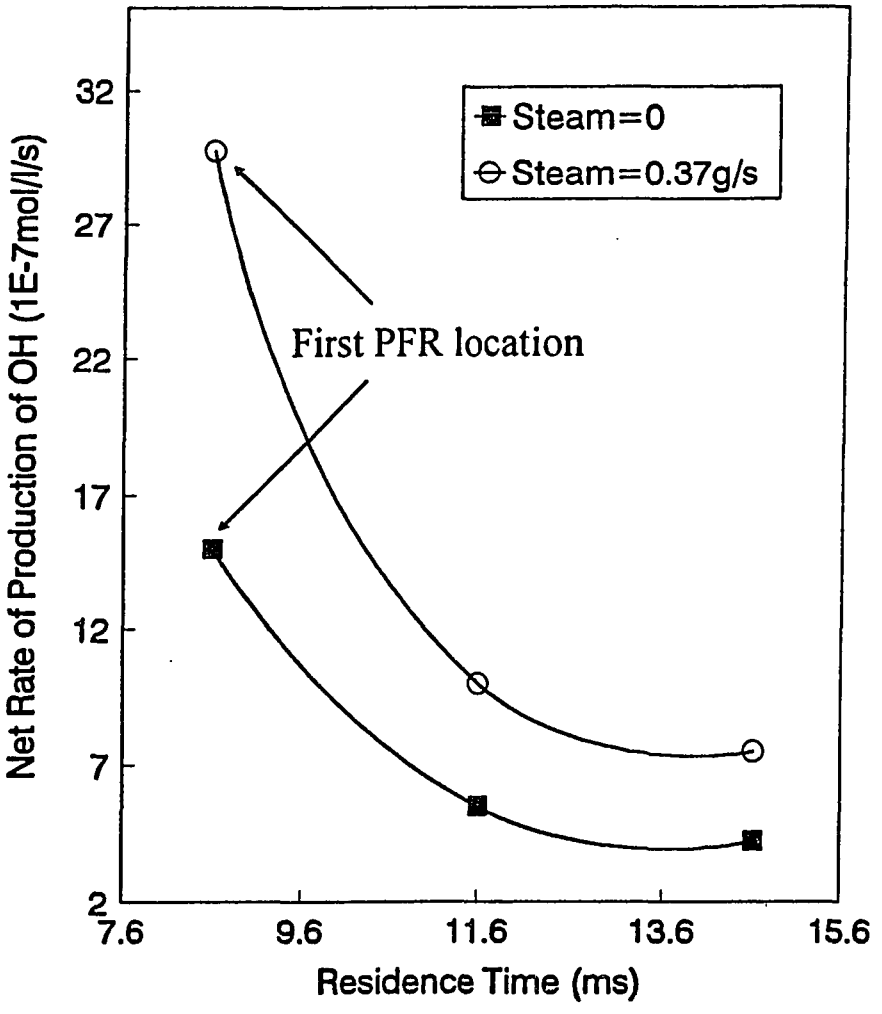

Figure 6.22 ROP Analysis of OH in PFR: Enhanced OH Production Rate by Steam Injection (ϕ = 1.35; CH3Cl/C2H4 = 0.2)

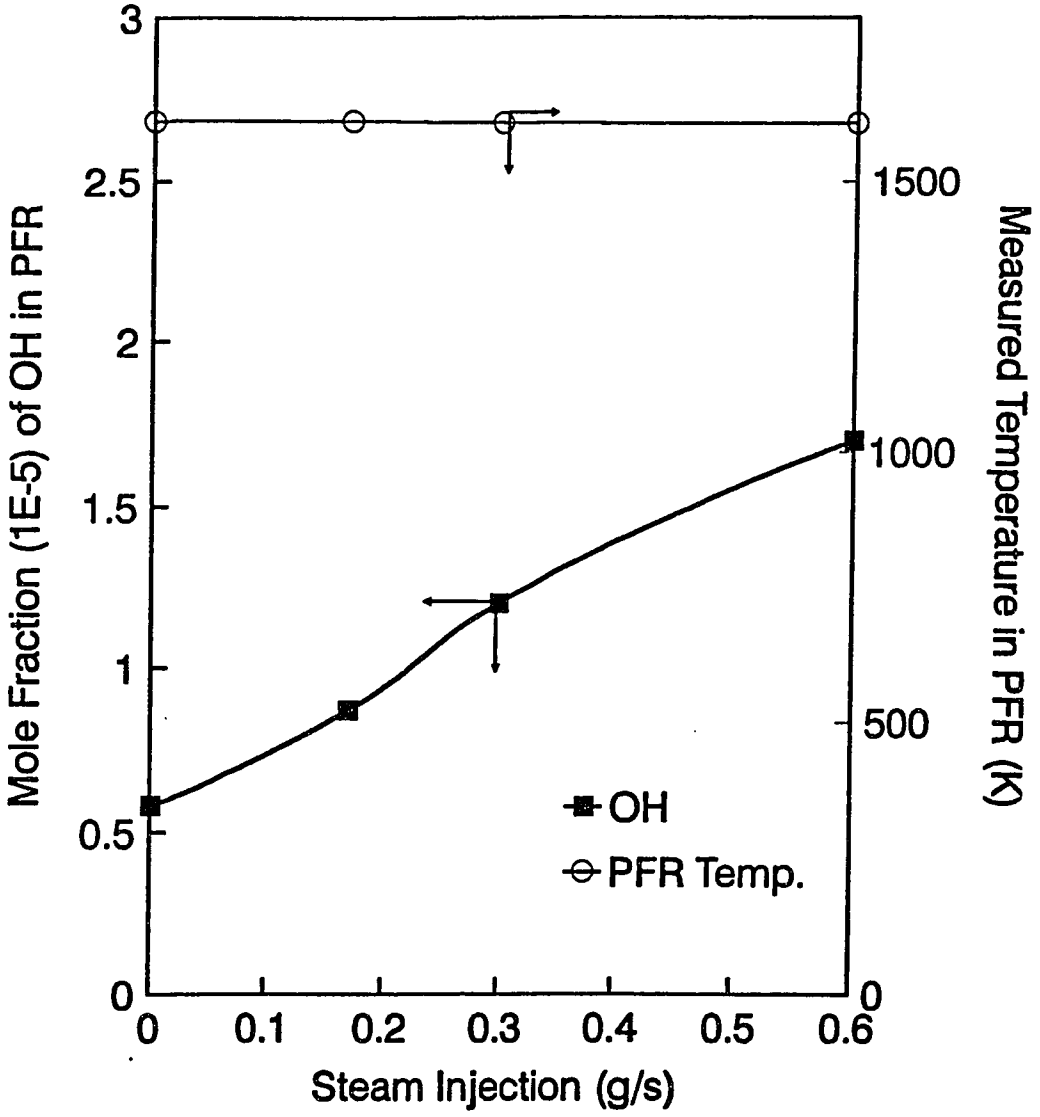

Figure 6.23 Calculated OH radical concentration and measured temperature at PFR τ = 3 ms as functions of steam injection flow rate (ϕ = 1.35, CH3Cl/C2H4=0.2)

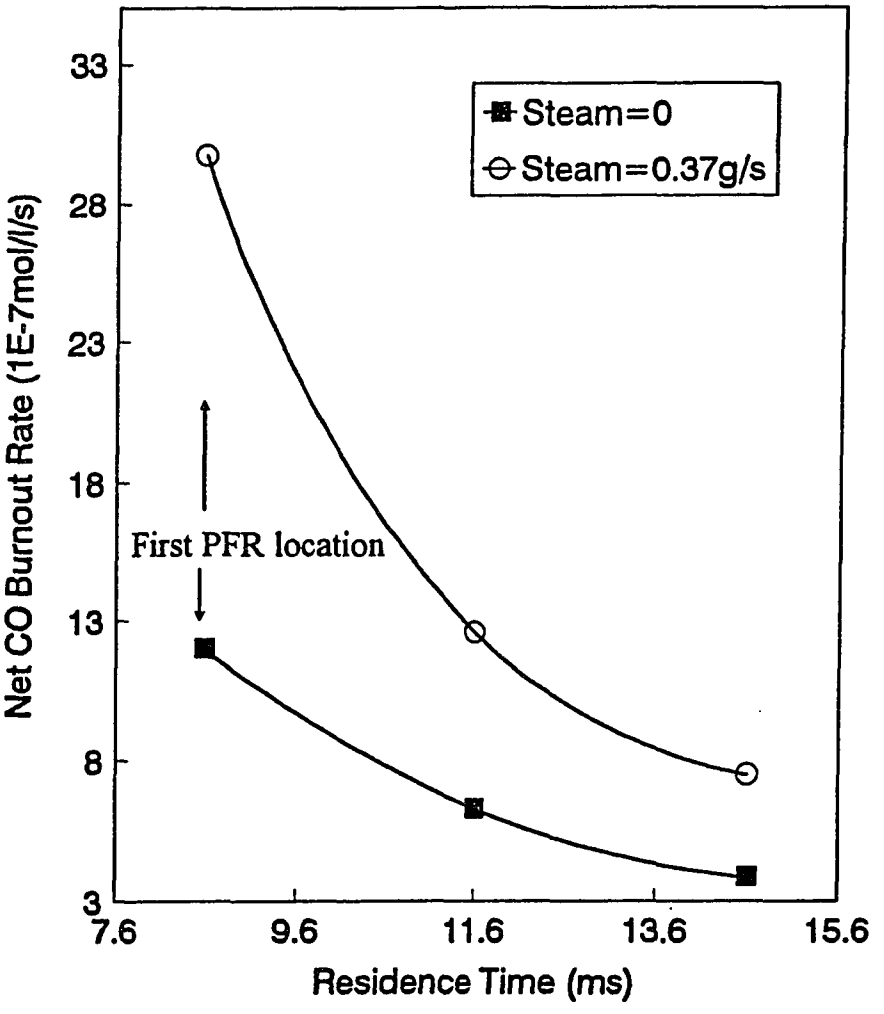

Figure 6.24 ROP Analysis of CO in PFR: Enhanced CO Burnout by Steam Injection (ϕ = 1.35; CH3Cl/C2H4 = 0.2)

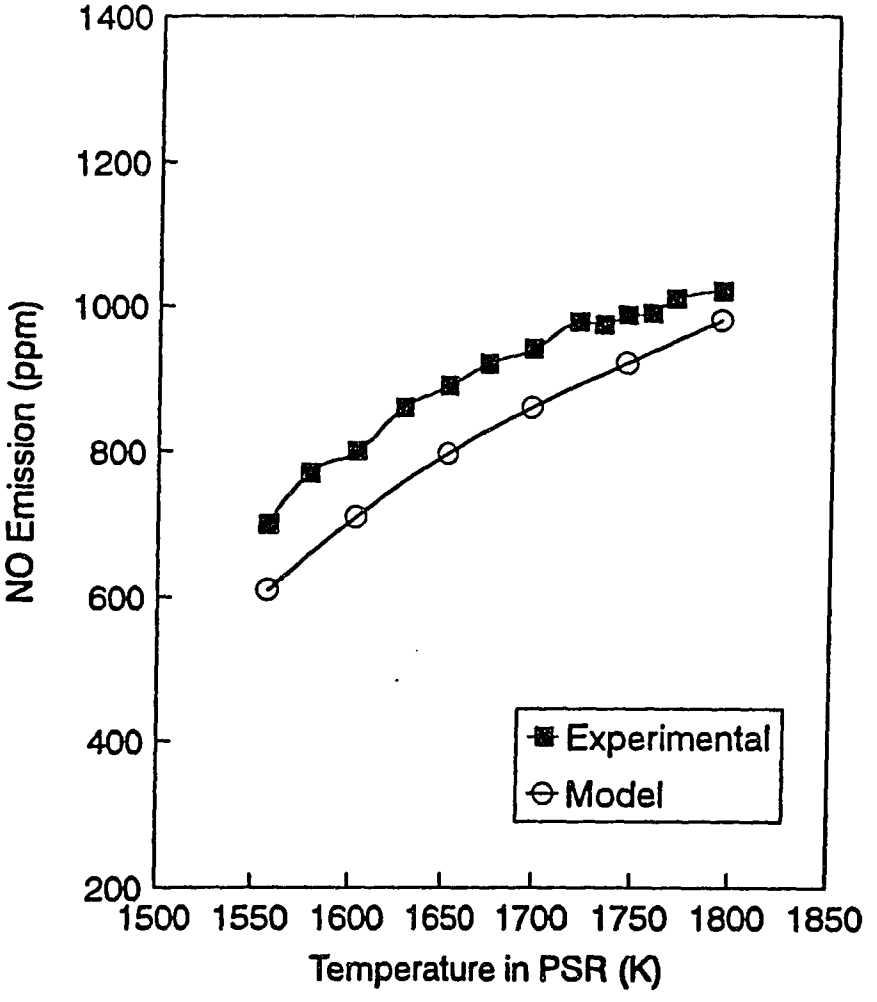

Figure 7.1 Temperature effect on Fuel NO in PSR: ϕ = 0.65, CH3NH2/C2H4=0.028

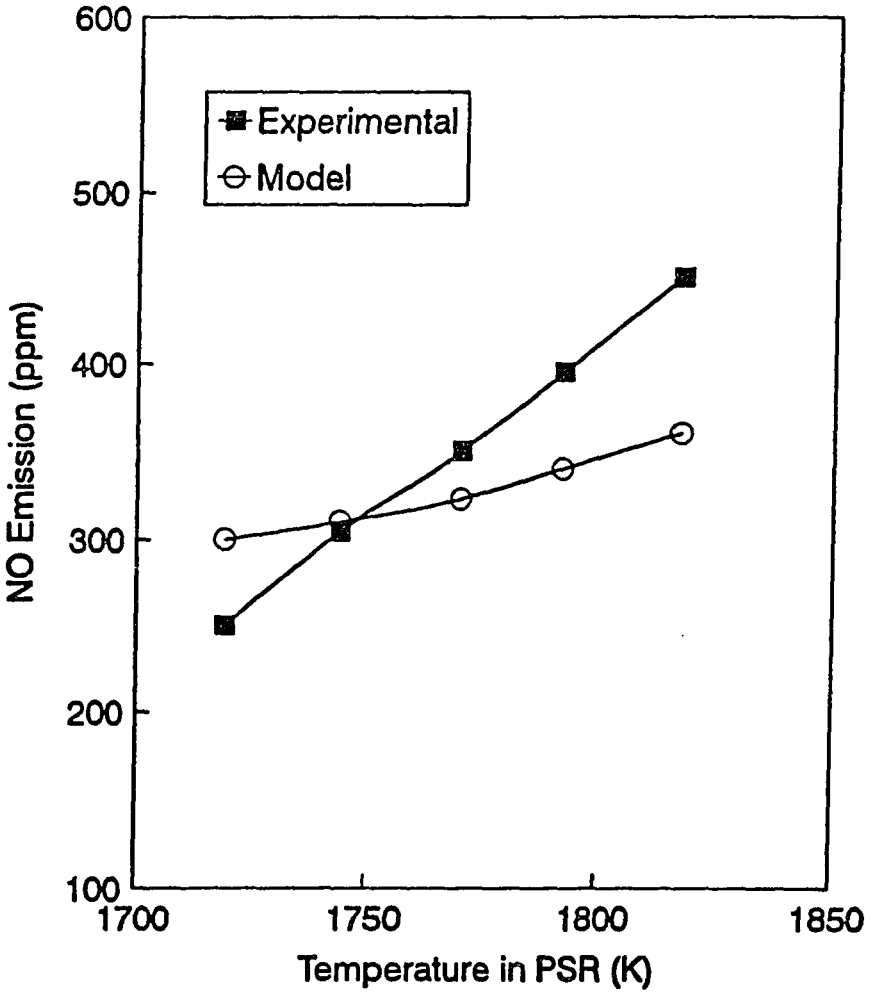

Figure 7.2 Temperature effect on fuel NO in PSR: ϕ = 1.41, CH3NH2/C2H4 = 0.058

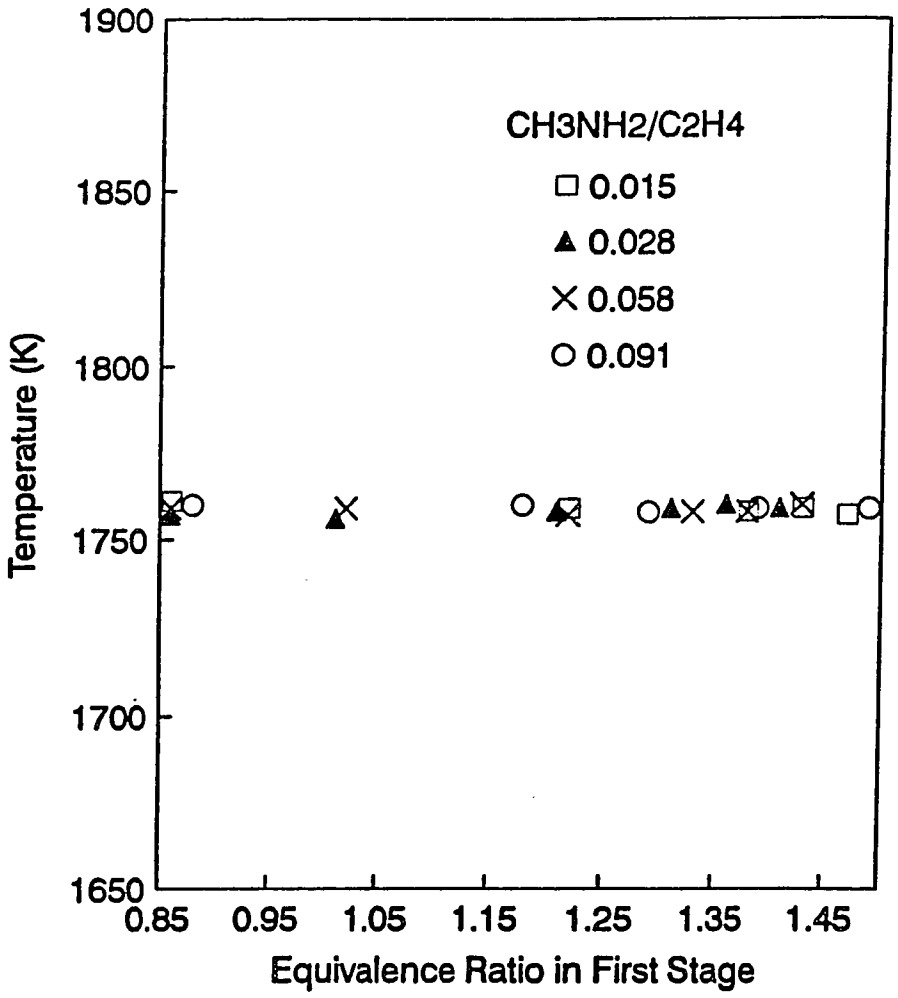

Figure 7.3 Measured temperature in PSR at each CH3NH2 loading level

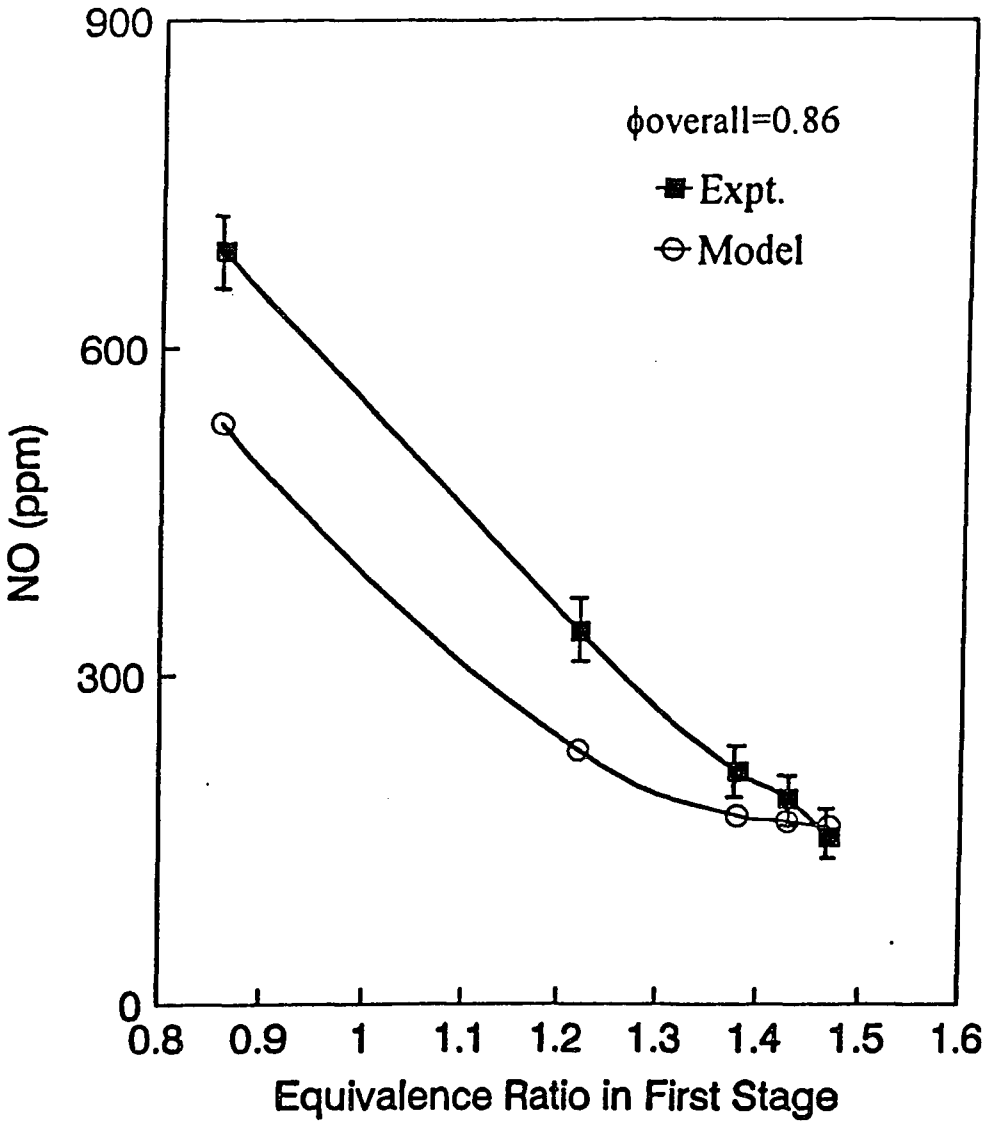

Figure 7.4 Effect of fuel equivalence ratio on NO in PSR at constant temperature of 1759 K and CH3NH2/C2H4=0.015

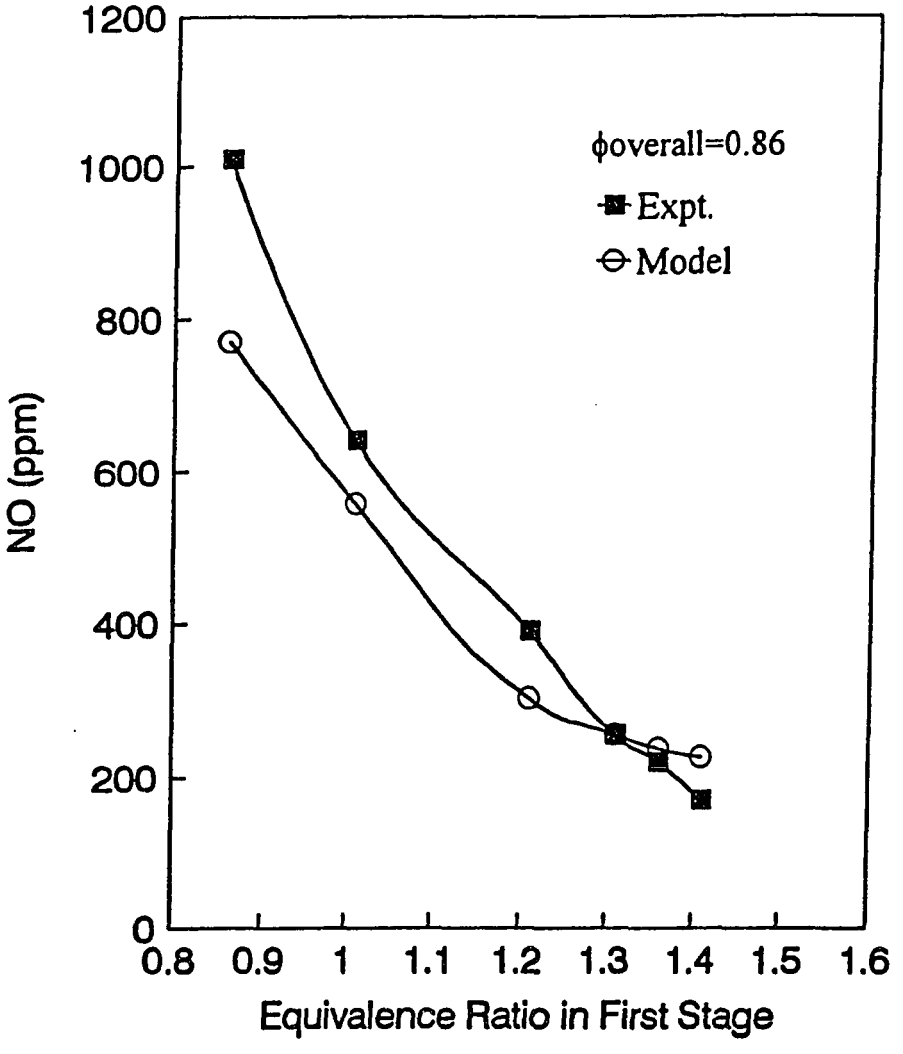

Figure 7.5 Effect of fuel equivalence ratio on NO in PSR at constant temperature of 1759 K and CH3NH2/C2H4=0.028

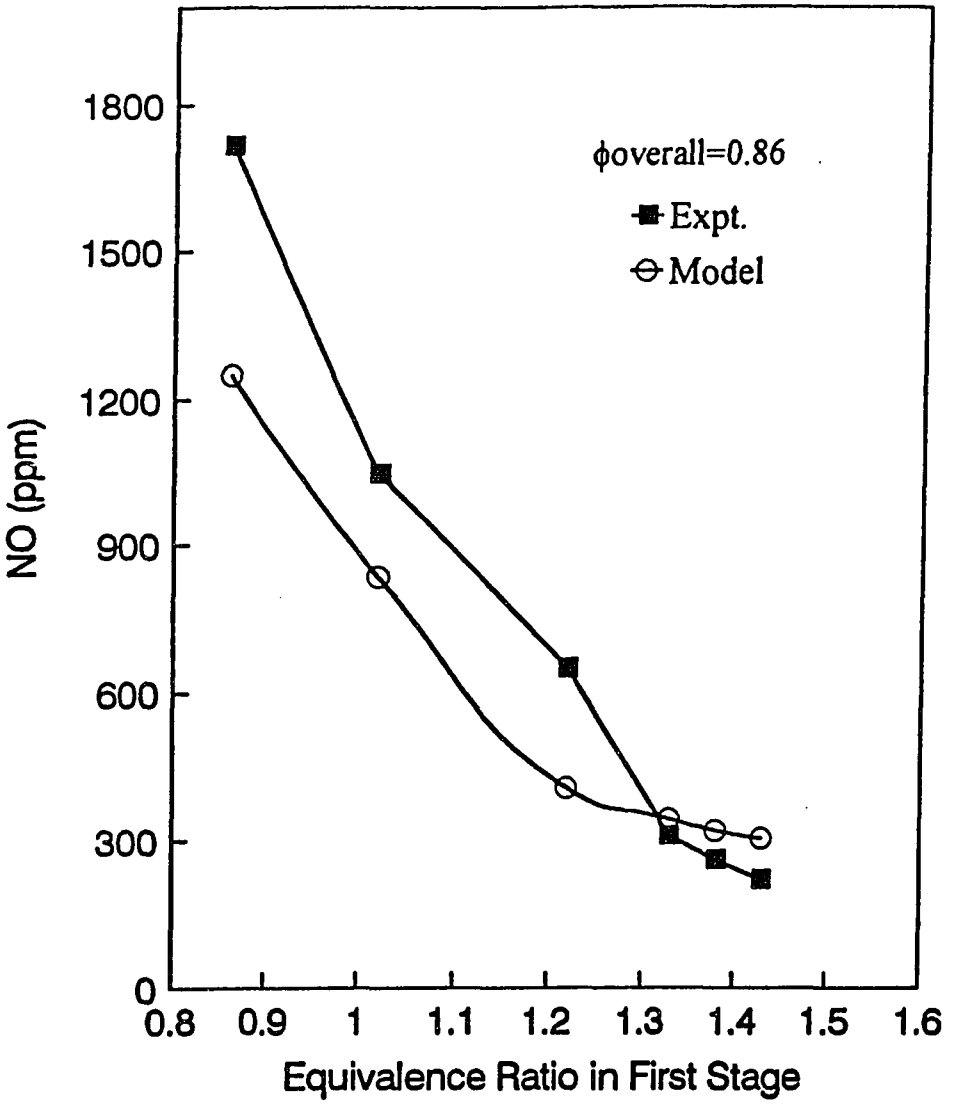

Figure 7.6 Effect of equivalence ratio on NO in PSR at constant temperature of 1759 K and CH3NH2/C2H4 = 0.058

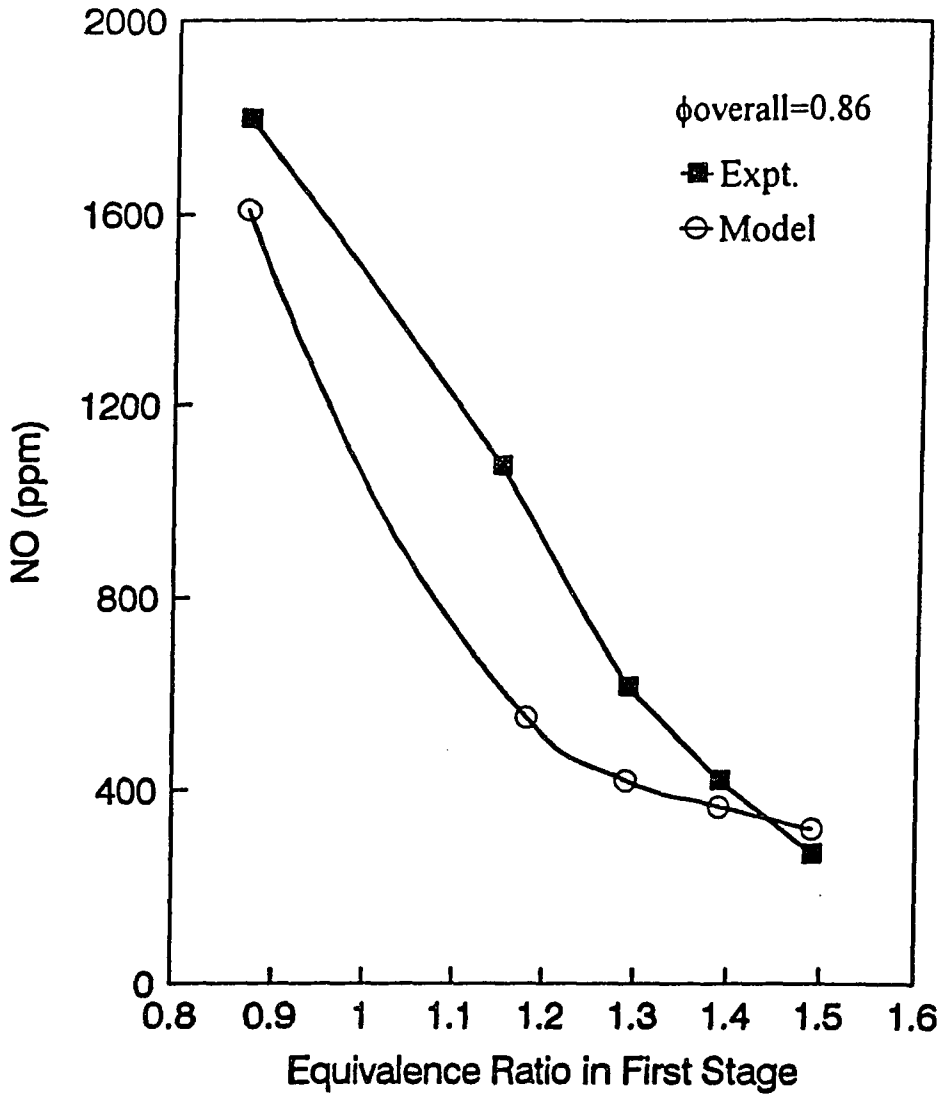

Figure 7.7 Effect of equivalence ratio on NO in PSR at constant Temperature of 1759 K and CH3NH2/C2H4=0.09

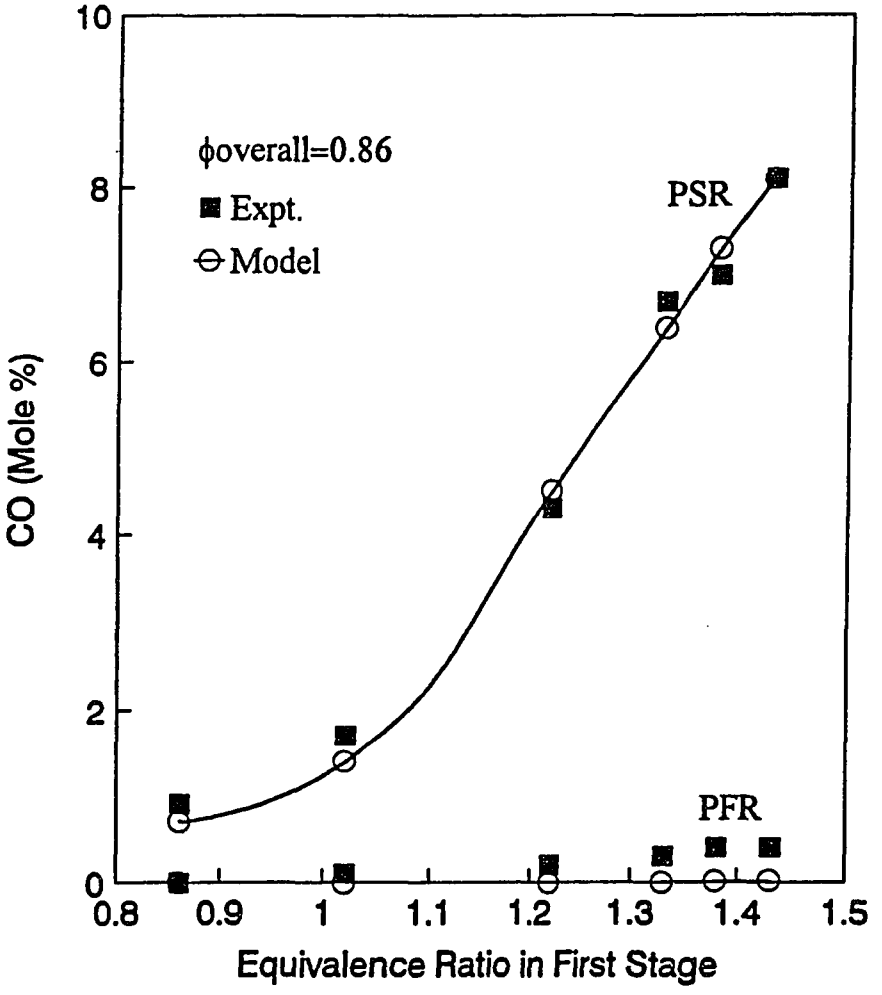

Figure 7.8 CO concentrations in PSR and at PFR outlet with air injection (CH3NH2/C2H4 = 0.058)

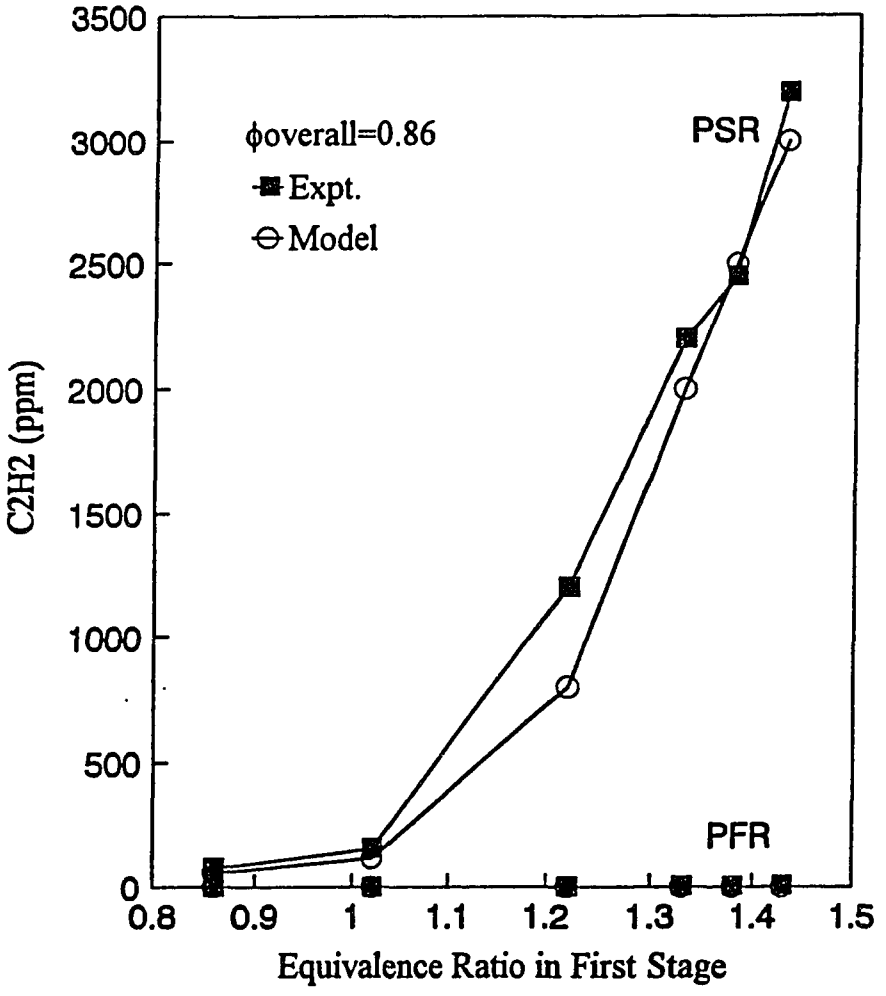

Figure 7.9 C2H2 concentrations in PSR and at PFR outlet wit air injection (CH3NH2/C2H4 = 0.058)

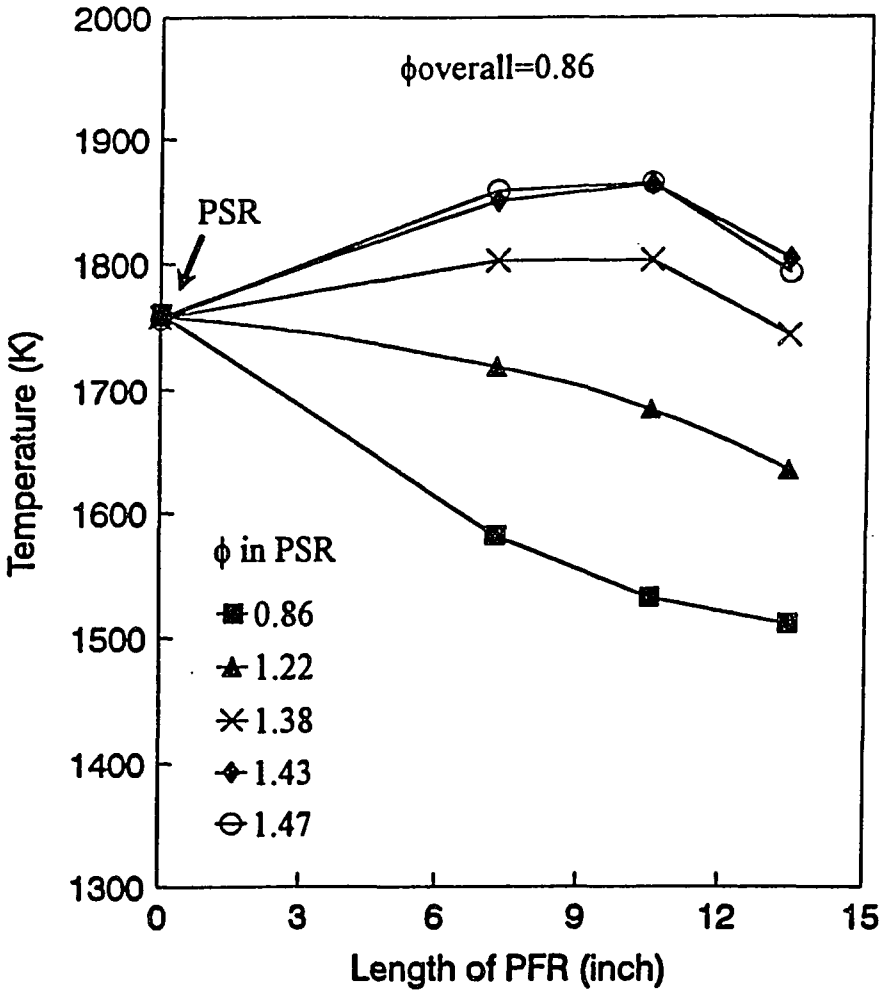

Figure 7.10 Effect of air injection on reactor temperature profiles (CH3NH2/C2H4 = 0.015)

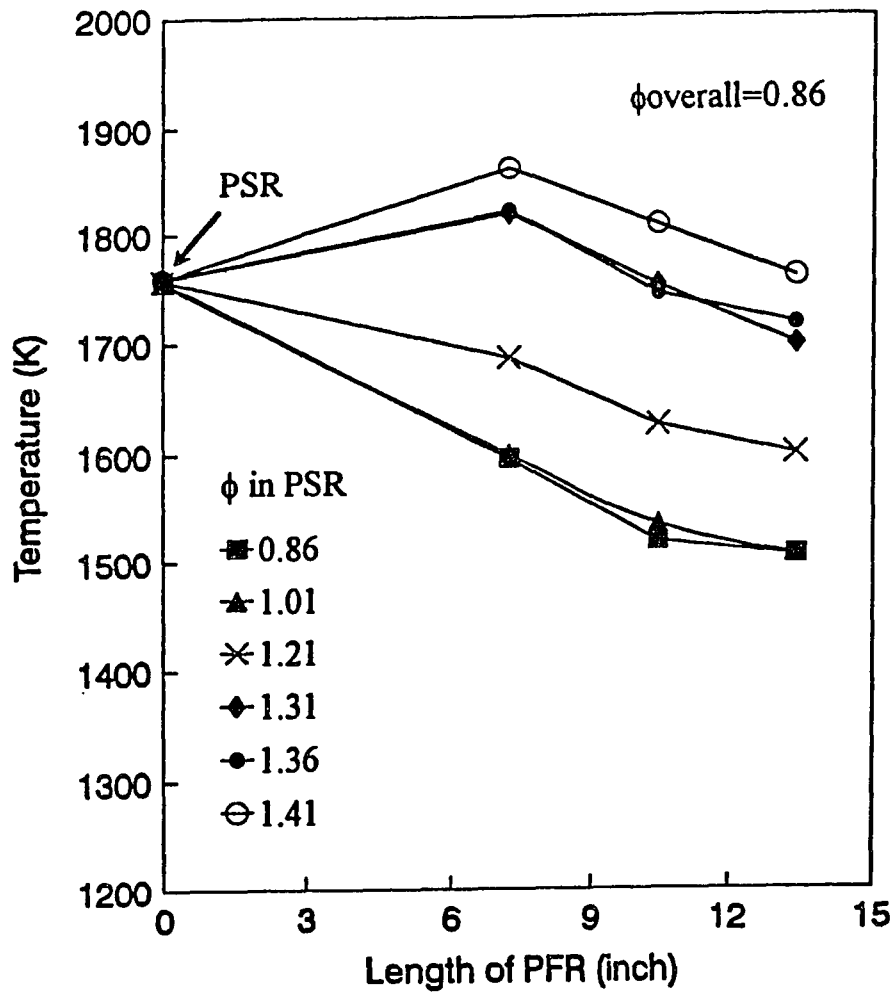

Figure 7.11 Effect of air injection on reactor temperature profiles (CH3NH2/C2H4 = 0.028)

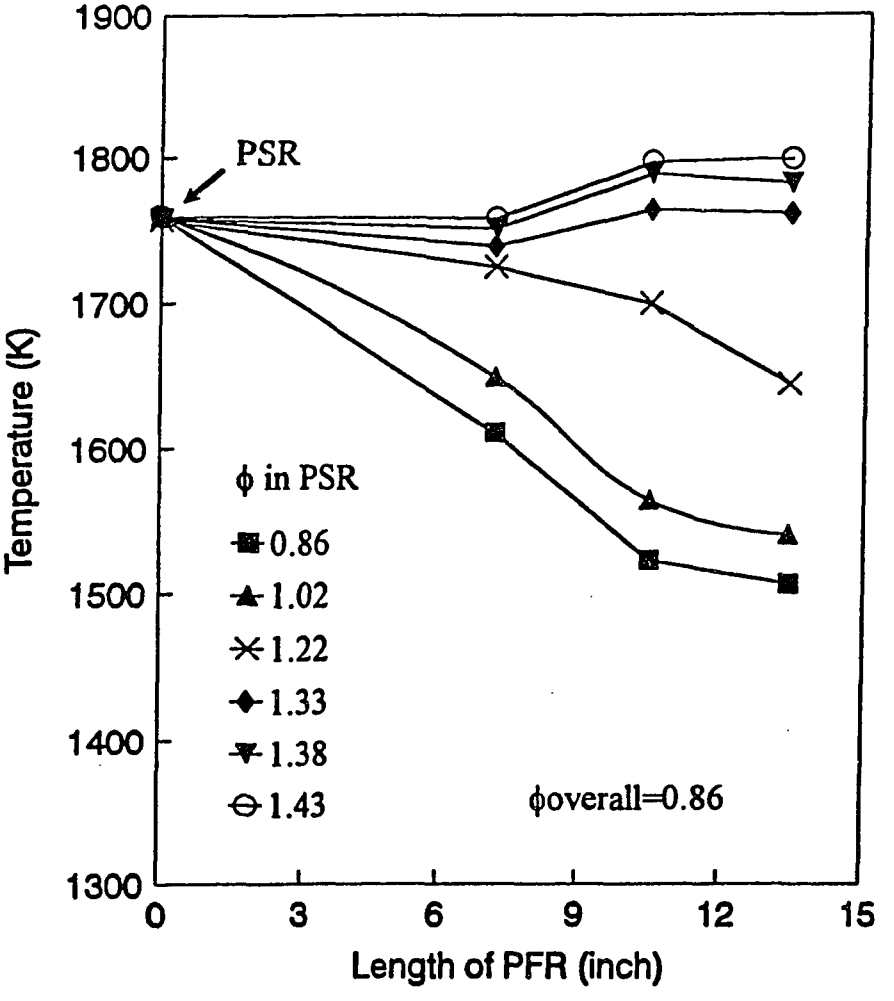

Figure 7.12 Effect of air injection on reactor temperature profiles (CH3NH2/C2H4 = 0.058)

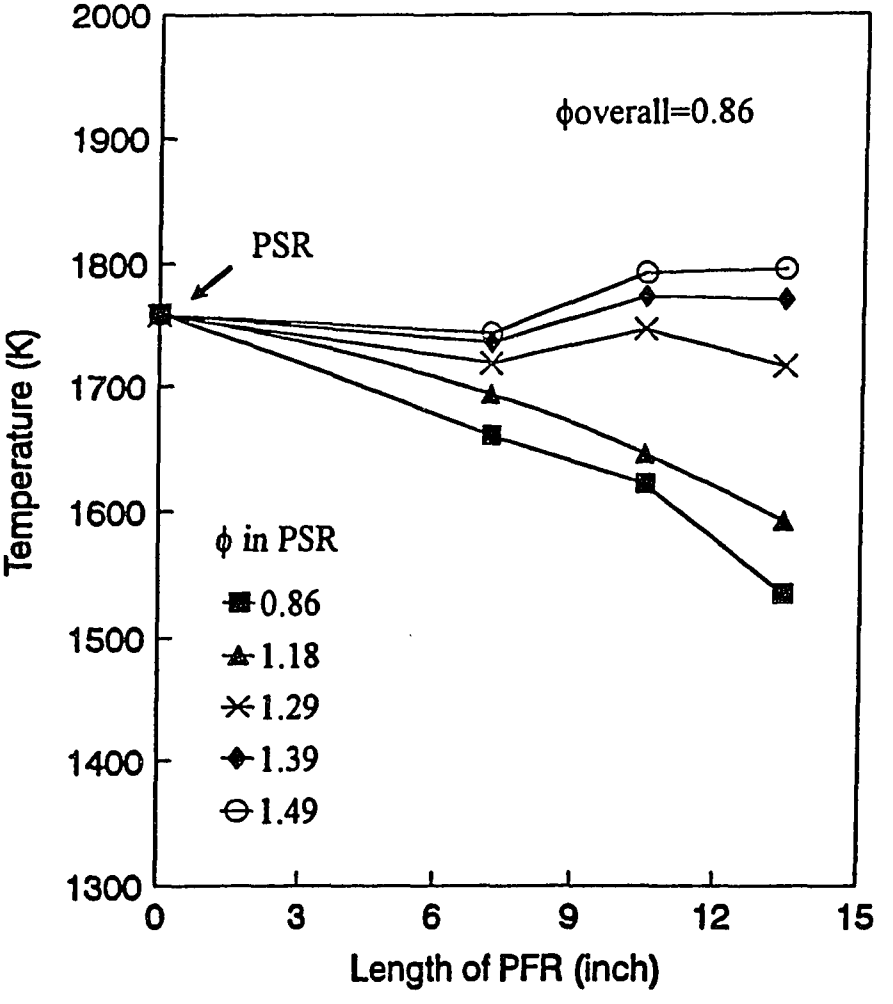

Figure 7.13 Effect of air injection on reactor temperature profiles (CH3NH2/C2H4 = 0.09)

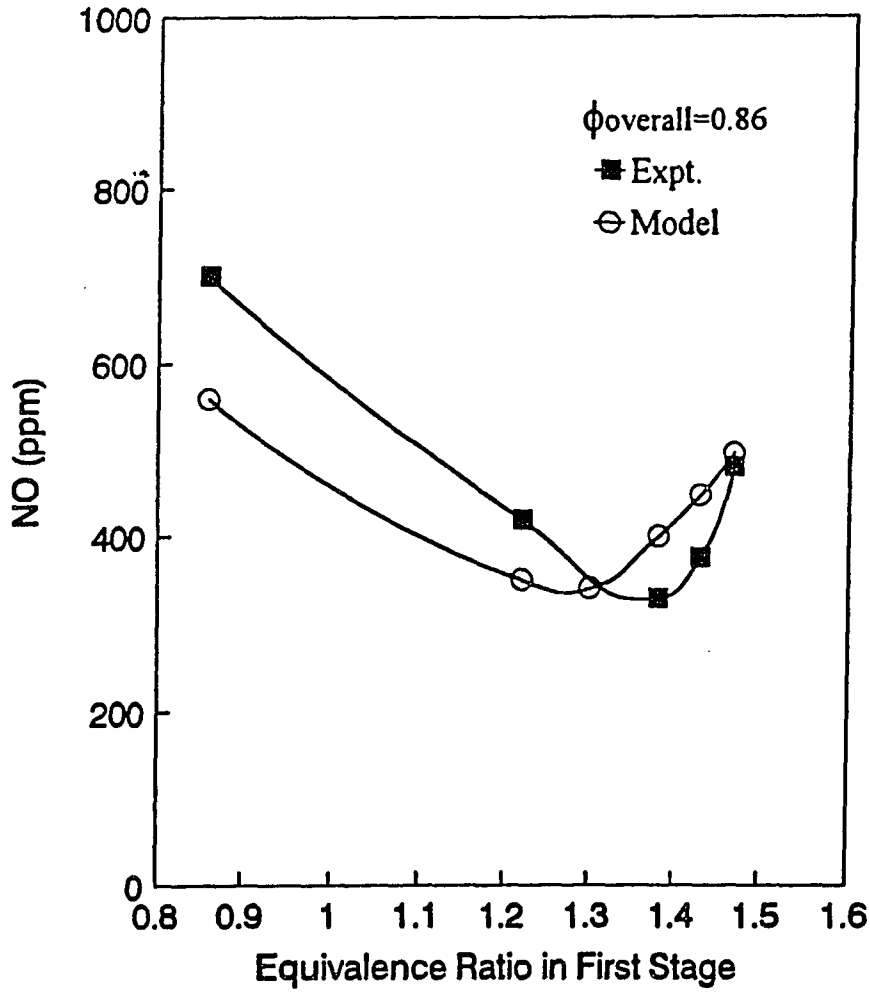

Figure 7.14 Minimum NO emission at PFR outlet from staged combustion of CH3NH2 (CH3NH2/C2H4 = 0.015)

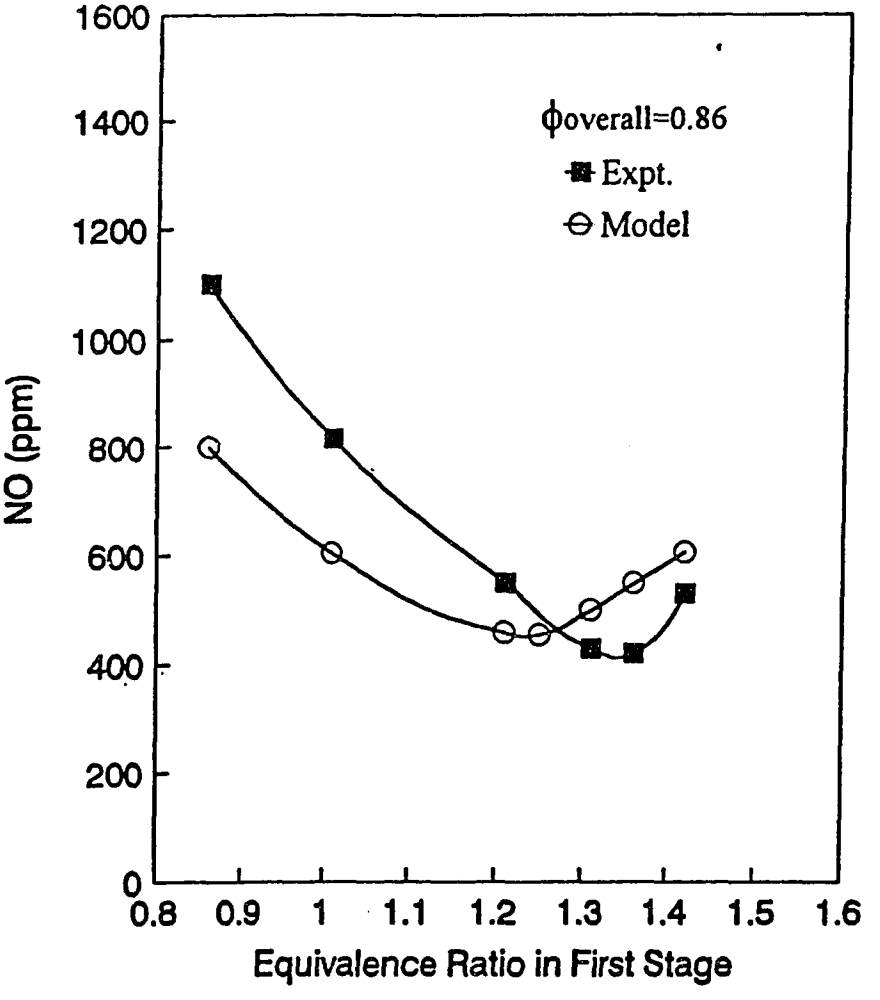

Figure 7.15 Minimum NO emission at PFR outlet from staged combustion of CH3NH2 (CH3NH2/C2H4 = 0.028)

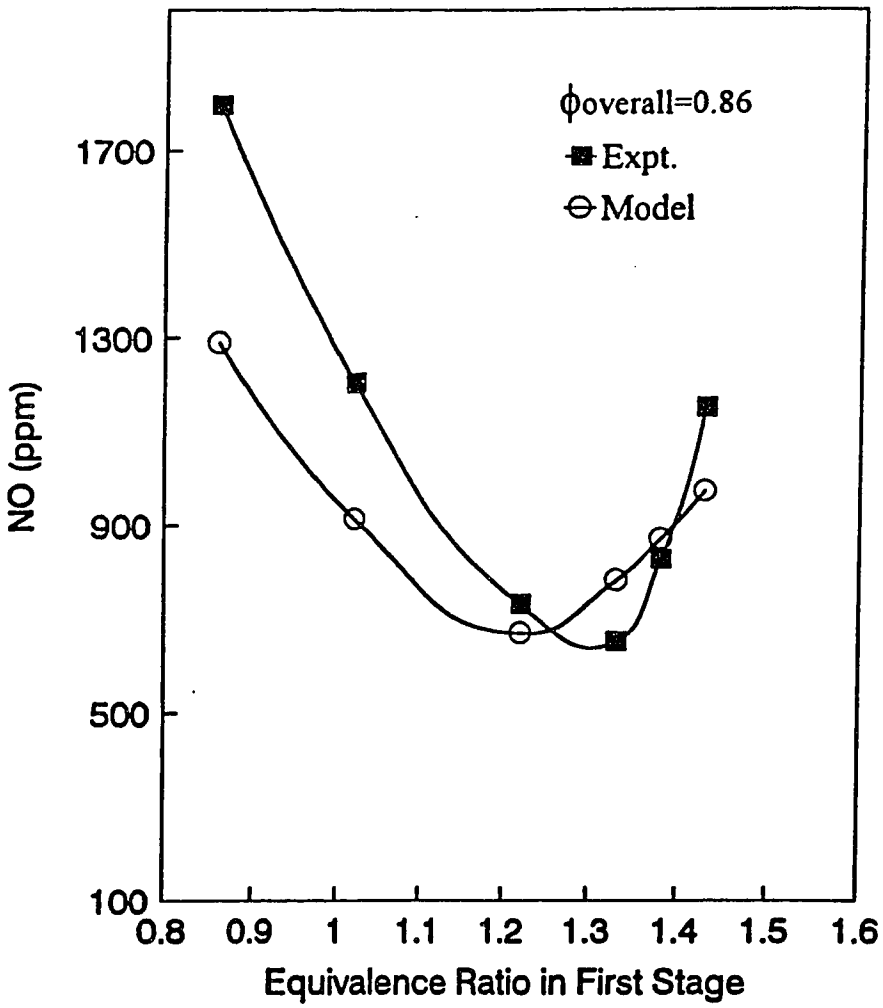

Figure 7.16 Minimum NO emission at PFR outlet from staged combustion of CH3NH2 (CH3NH2/C2H4 = 0.058)

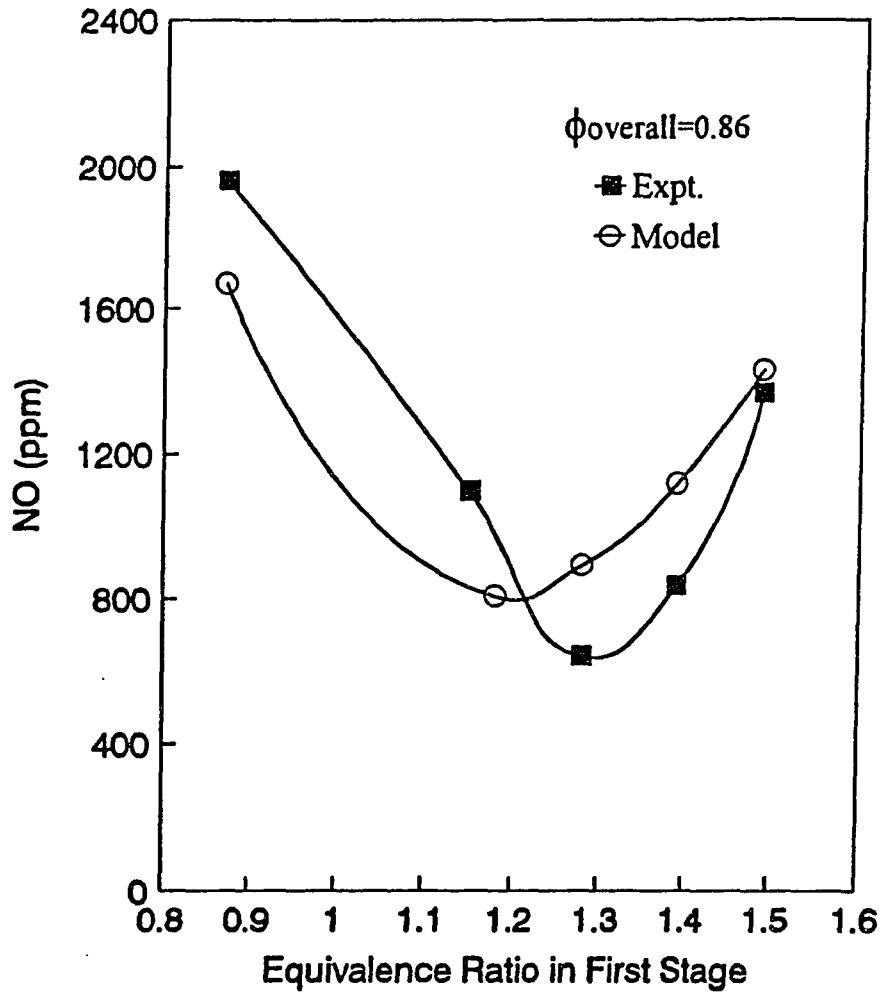

Figure 7.17 Minimum NO emission at PFR outlet from staged combustion of CH3NH2 (CH3NH2/C2H4 = 0.09)

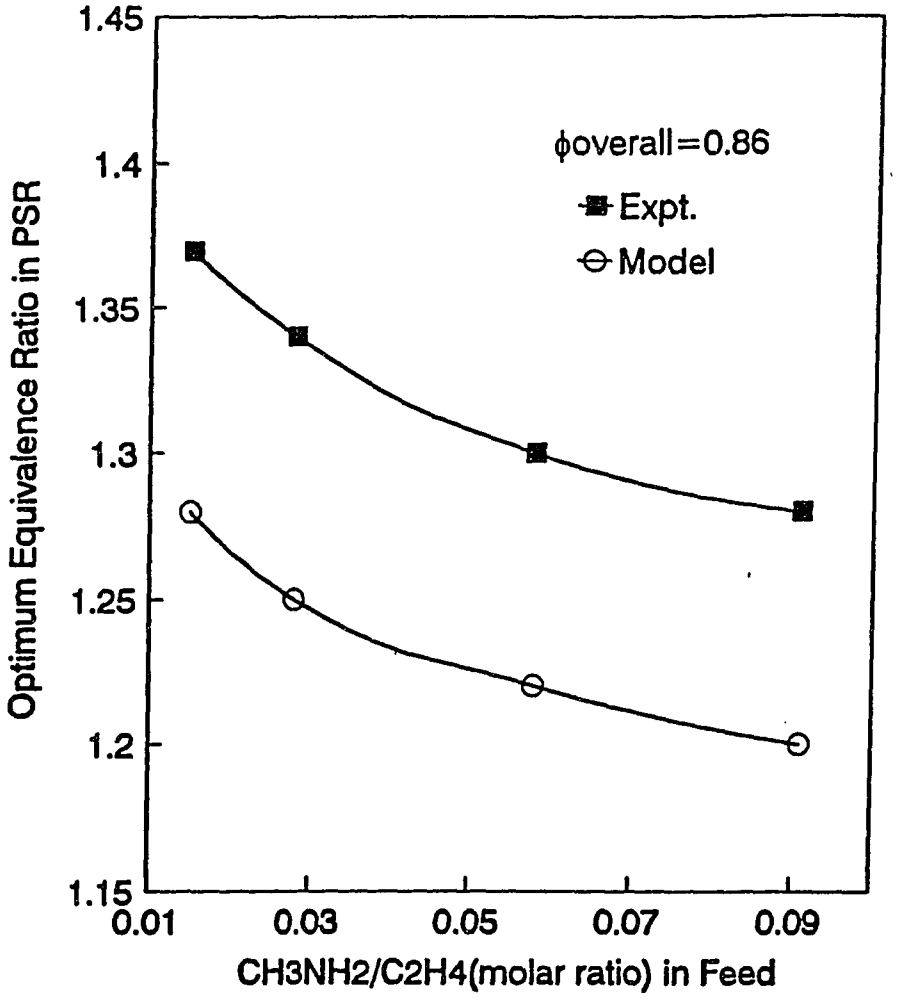

Figure 7.18 Optimal first stage ϕ as a function of feed CH3NH2 content

Common Steps:

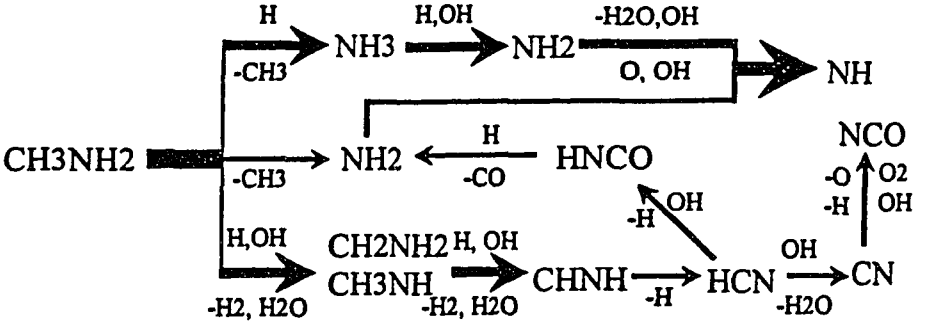

Fuel Lean (ϕ=0.86) Steps:

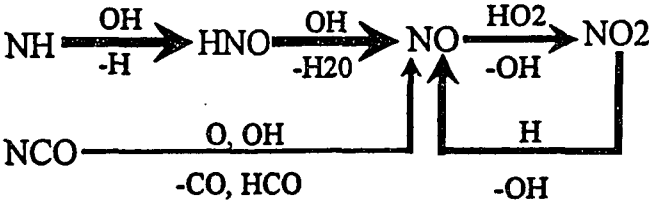

Fuel Rich (ϕ=1.34) Steps:

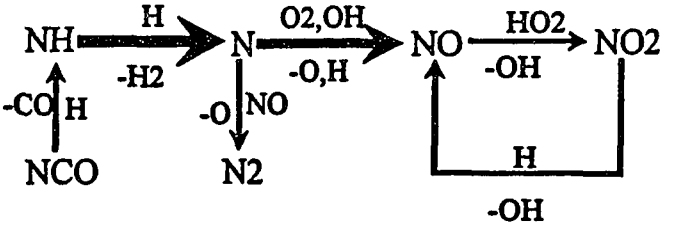

Figure 7.19 Fuel NO formation pathways in CH3NH2-doped C2H4 combustion (PSR)

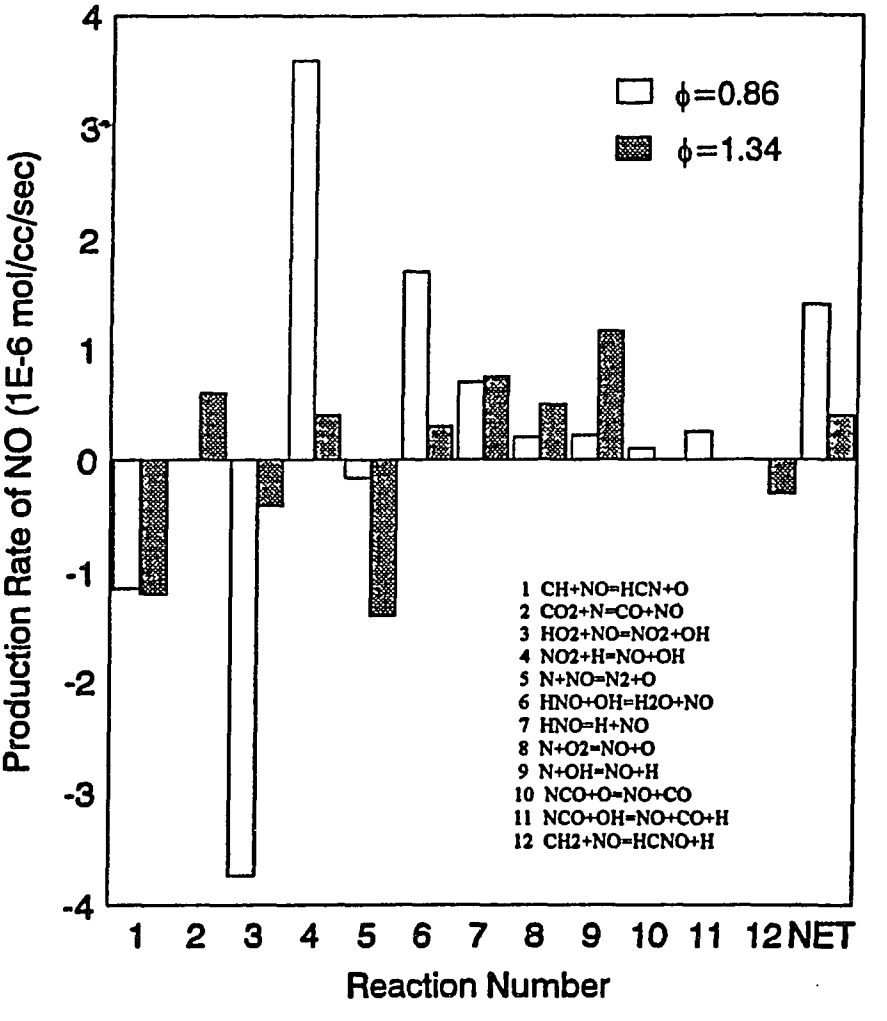

Figure 7.20 Production and consumption rates of NO under fuel-lean and rich conditions (ROP analysis in PSR)

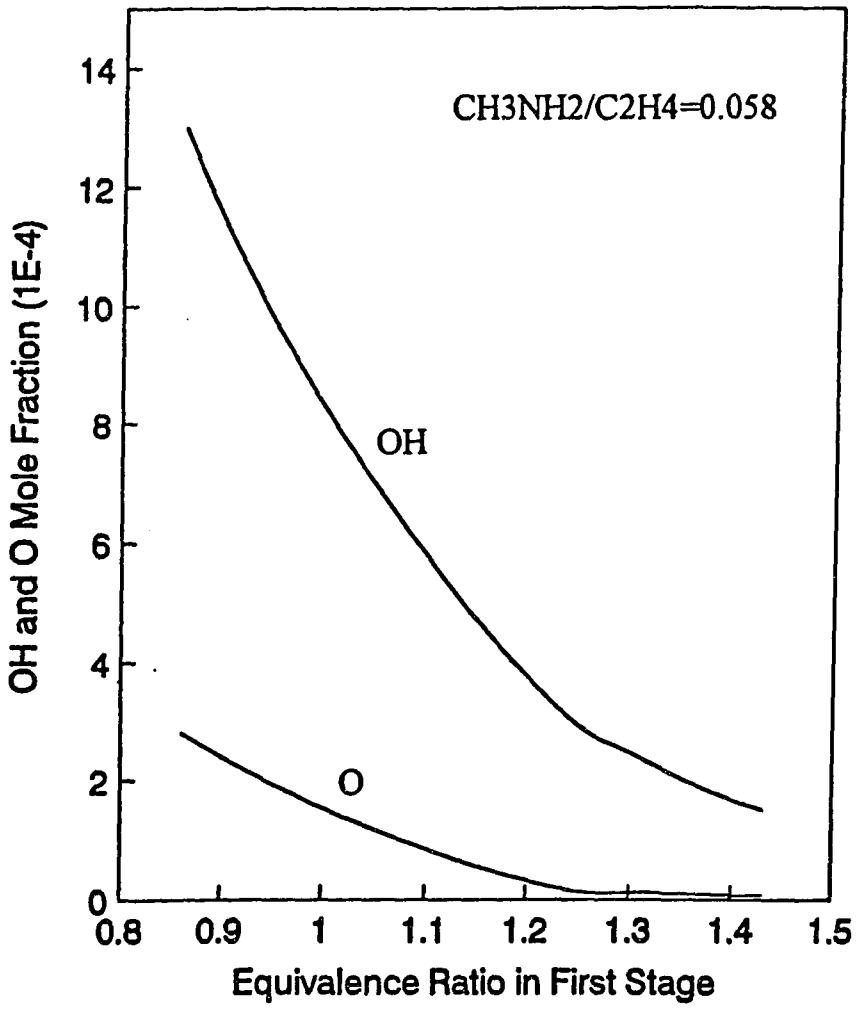

Figure 7.21 Calculated OH and O radicals concentration as functions of fuel equivalence ratio

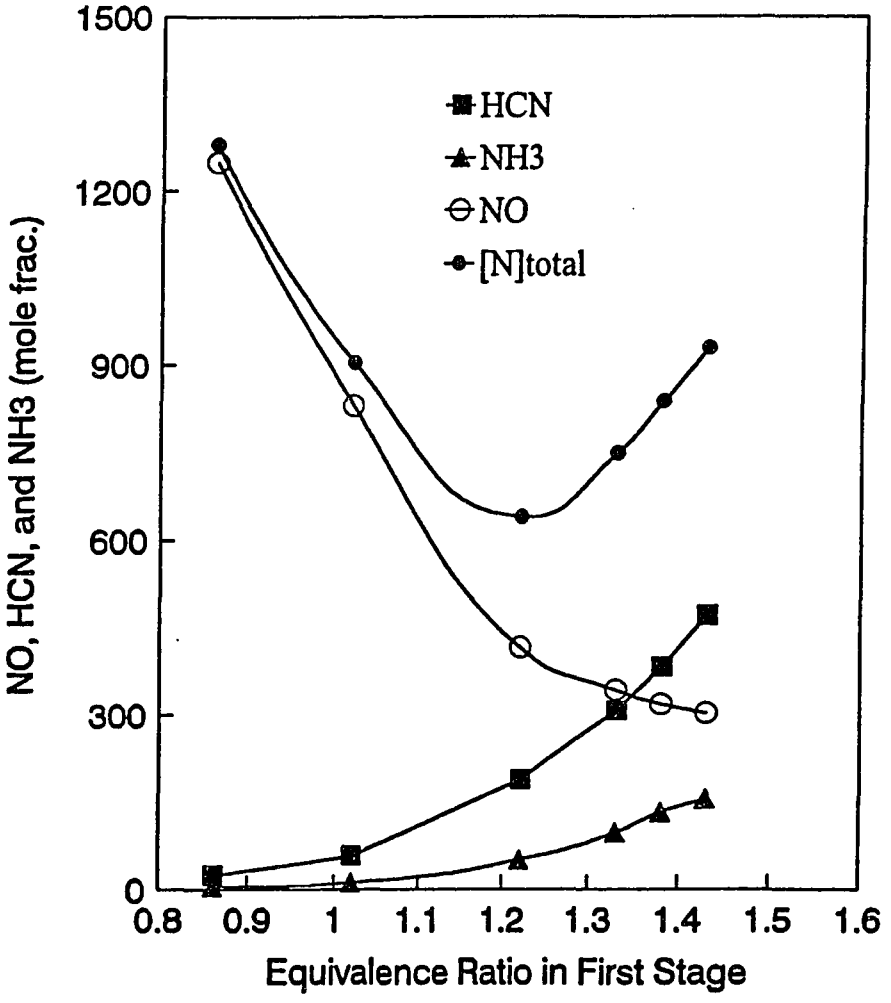

Figure 7.22 Calculated concentrations of N-containing species in PSR as functions of feed ϕ (CH3NH2/C2H4 = 0.058)

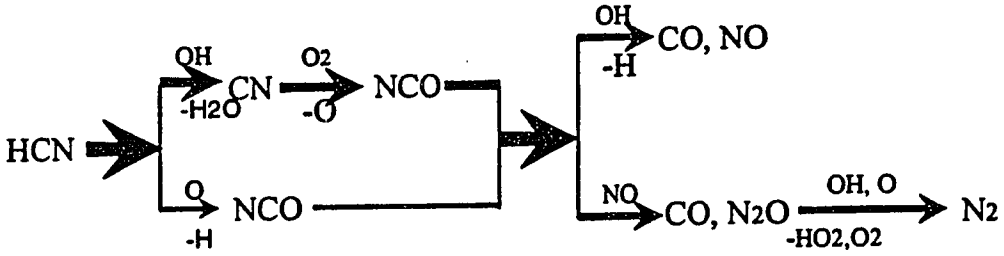

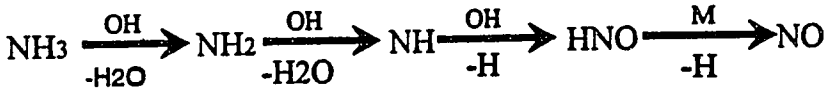

Figure 7.23 HCN and NH3 destruction pathways in CH3NH2-doped C2H4 combustion with air injection (PFR)

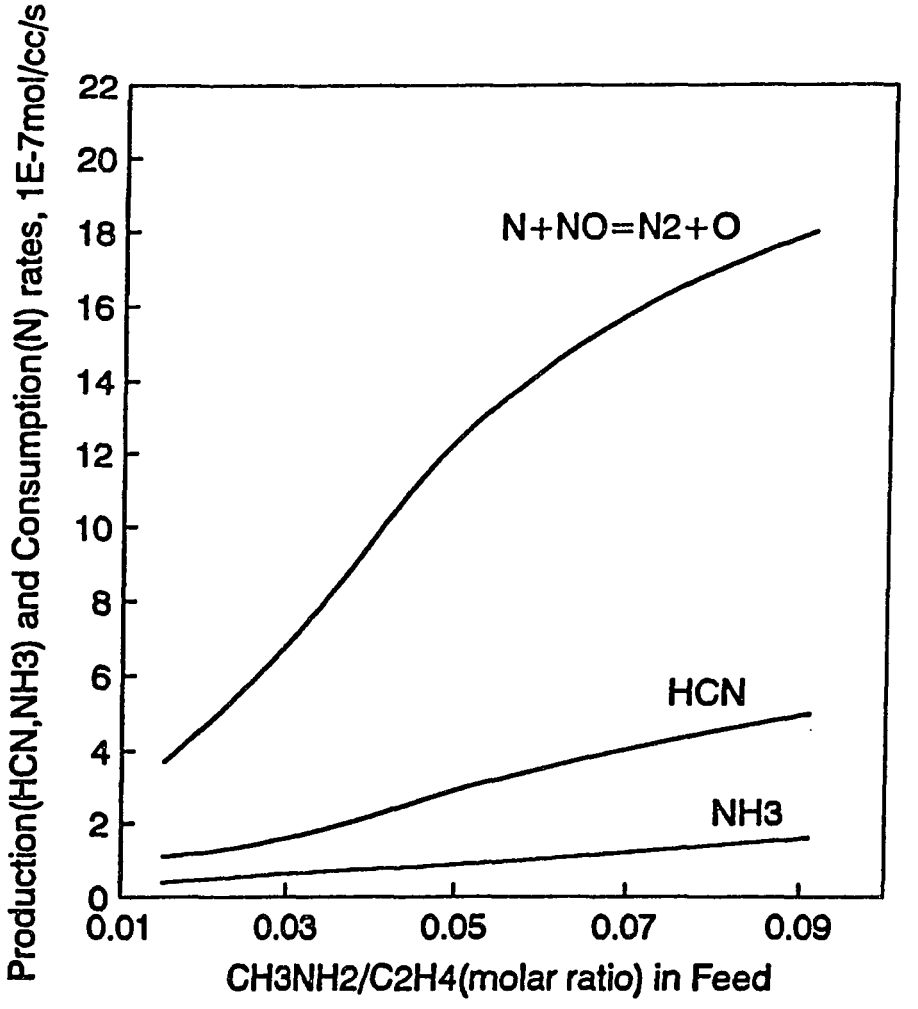

Figure 7.24 Calculated HCN and NH3 production rates and N consumption rate as functions of feed CH3NH2 content

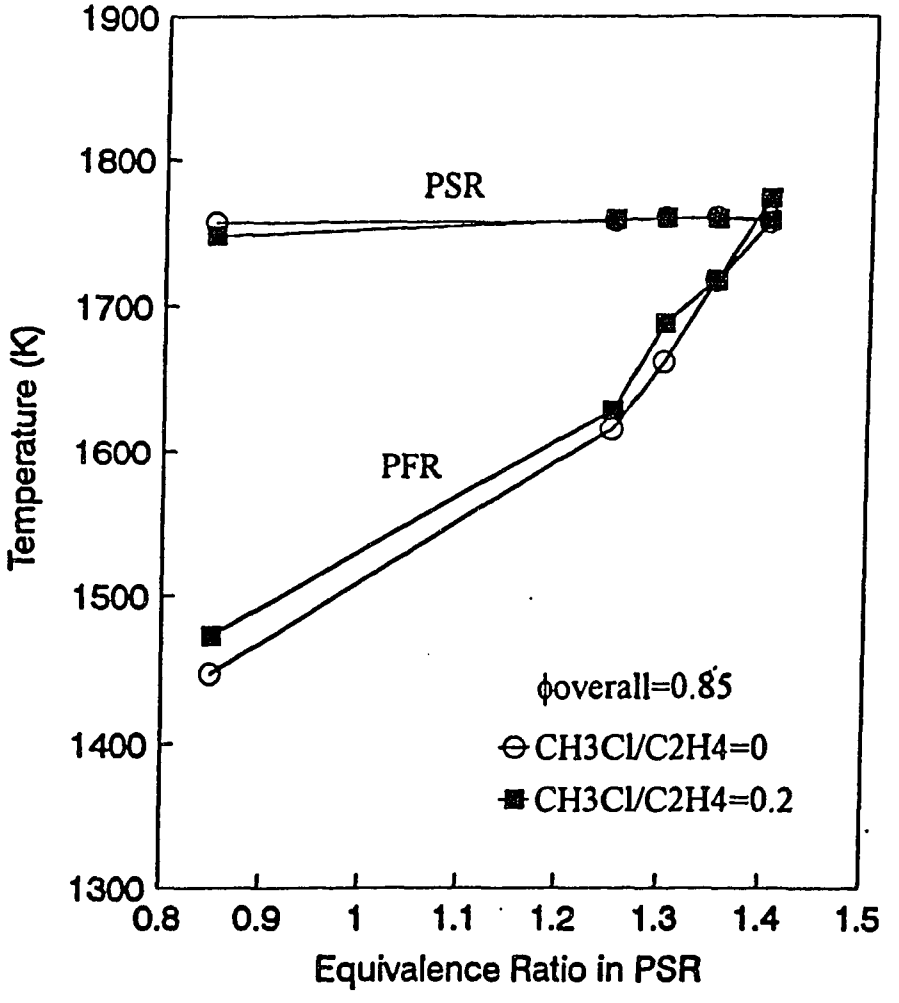

Figure 8.1 Measured temperatures in PSR and at PFR outlet (CH3NH2/C2H4 = 0.018)

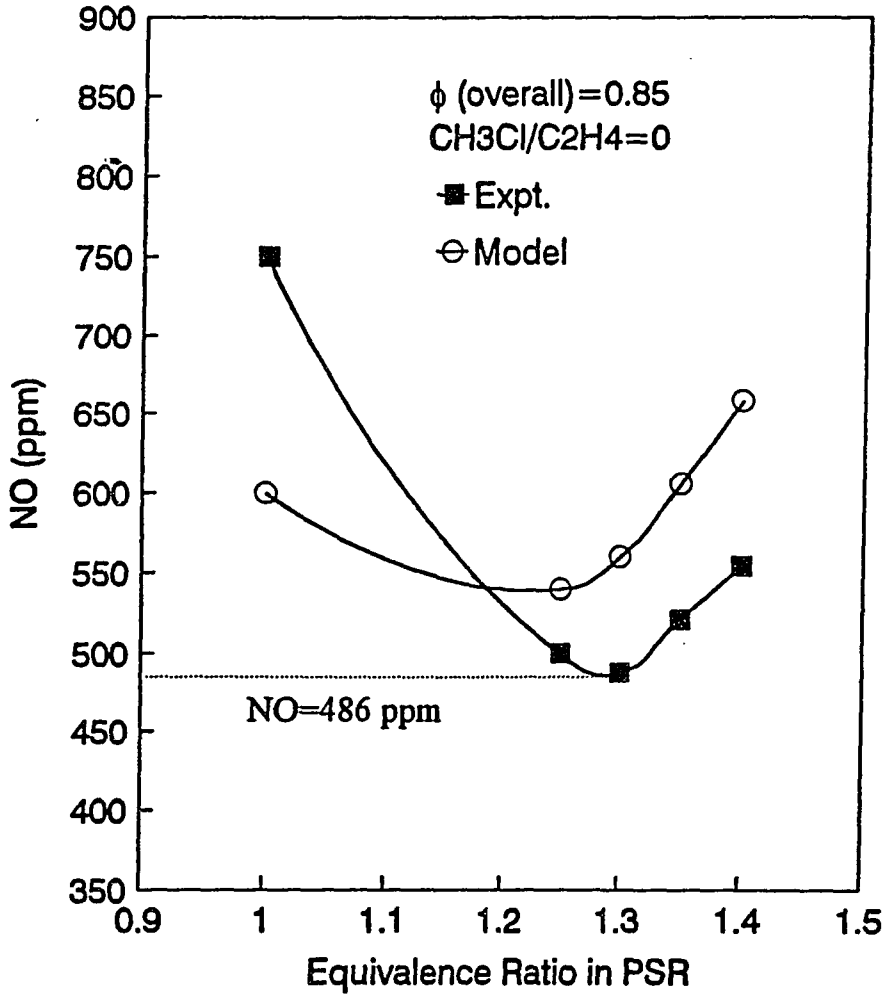

Figure 8.2 Minimum NO emission at PFR outlet with air stagi (CH3NH2/C2H4 = 0.018; CH3Cl/C2H4 = 0)

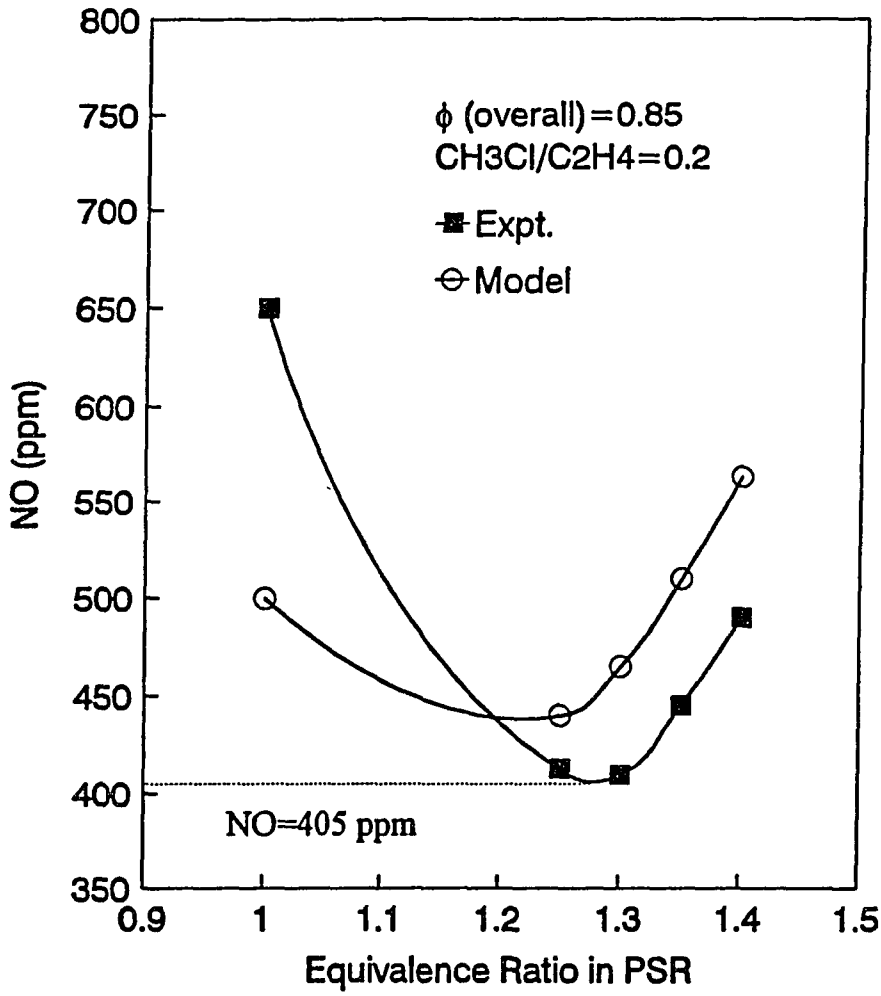

Figure 8.3 Minimum NO emission at PFR outlet with air staging (CH3NH2/C2H4 = 0.018; CH3Cl/C2H4 = 0.2)

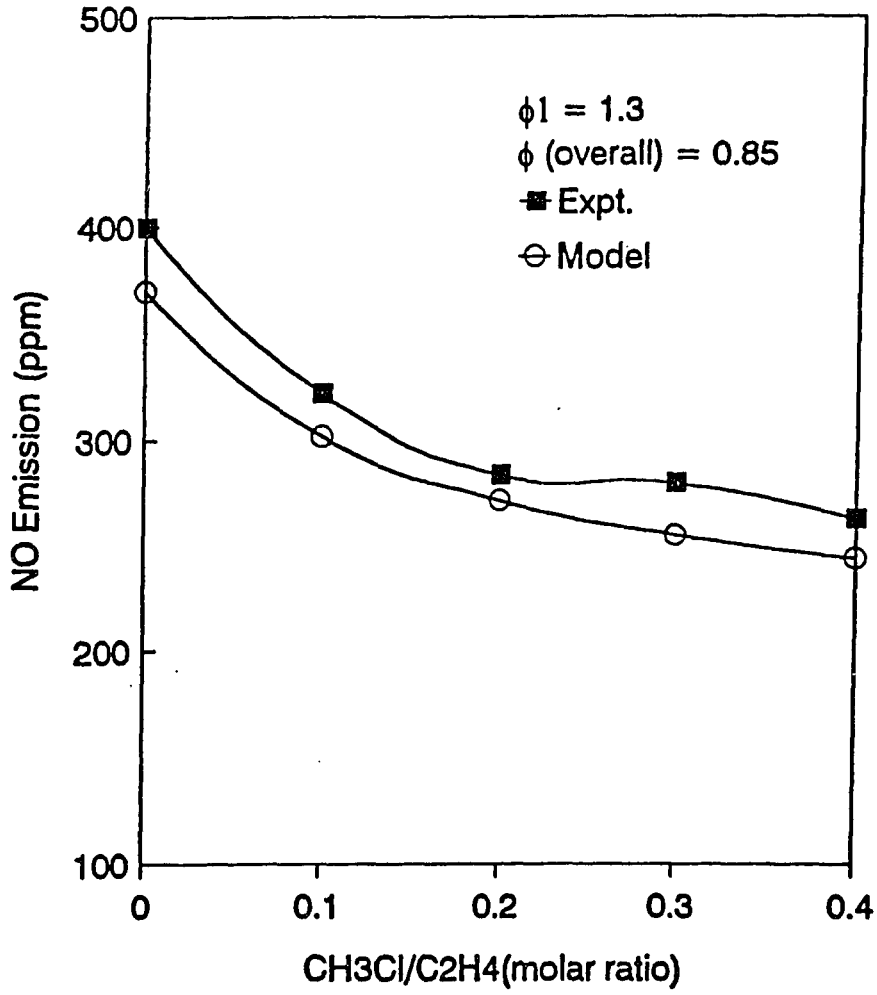

Figure 8.4 Effect of CH3Cl on NO emission from combustion of CH3NH2 with constant feed CH3NH2 concentration (PSR)

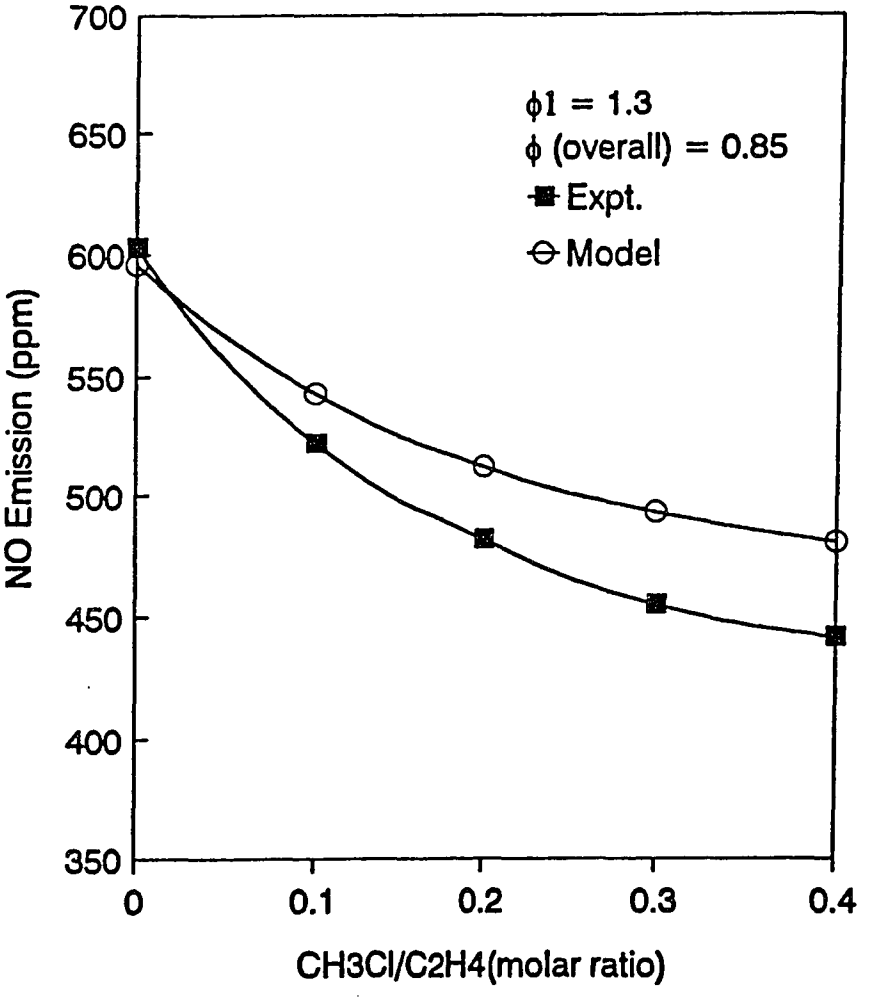

Figure 8.5 Effect of CH3Cl on NO emission from combustion of CH3NH2 with constant feed CH3NH2 concentration (PFR)

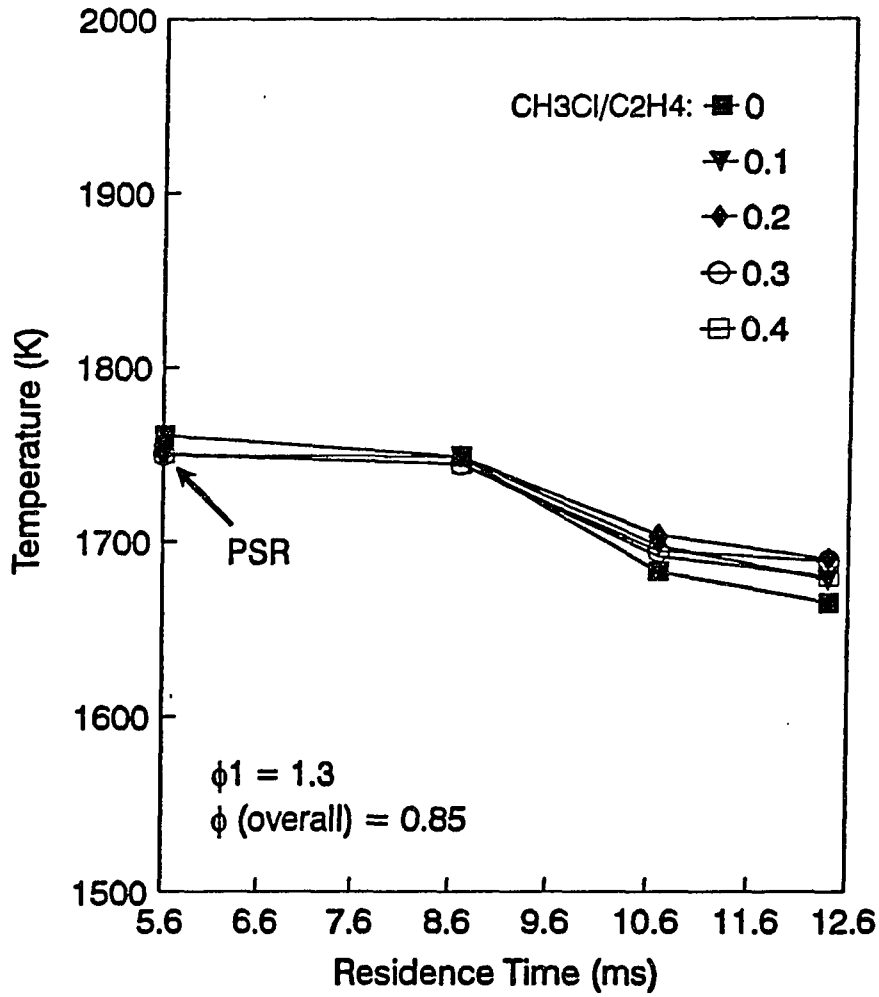

Figure 8.6 Measured reactor temperature profiles with increased CH3Cl loading level and constant feed CH3NH2 concentration

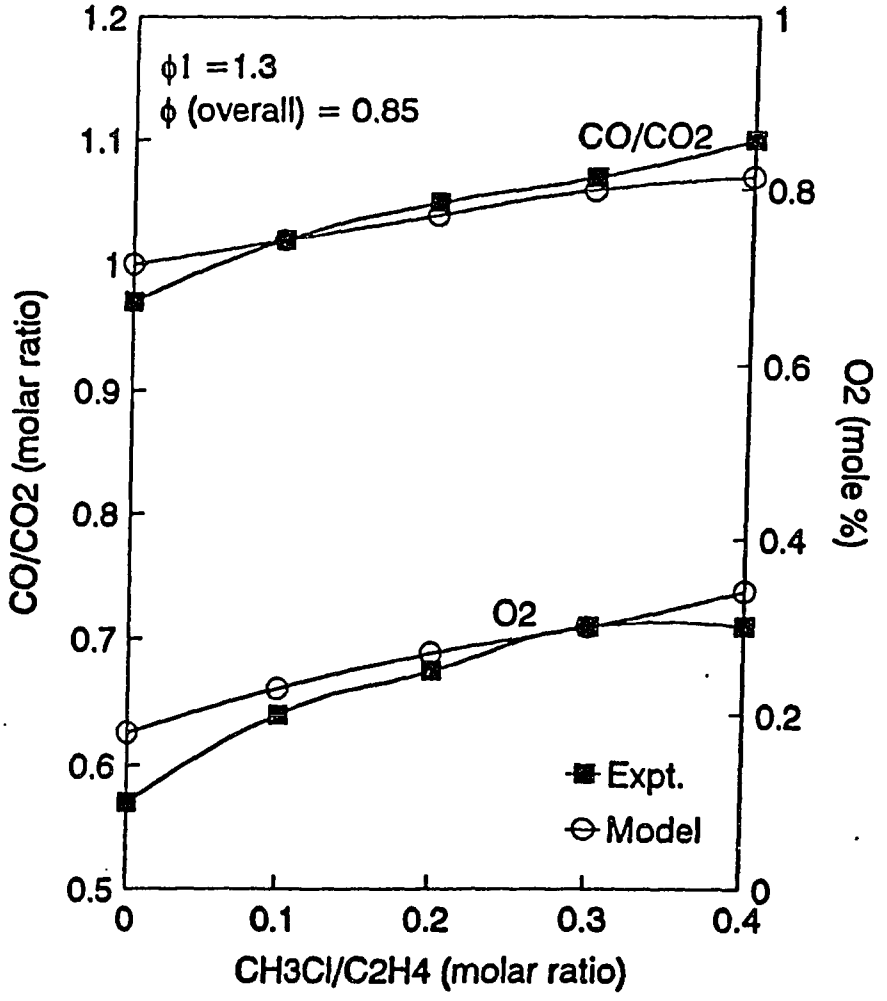

Figure 8.7 Effect of CH3Cl on CO/CO2 ratio and O2 concentration in PSR with constant feed CH3NH2 concentration

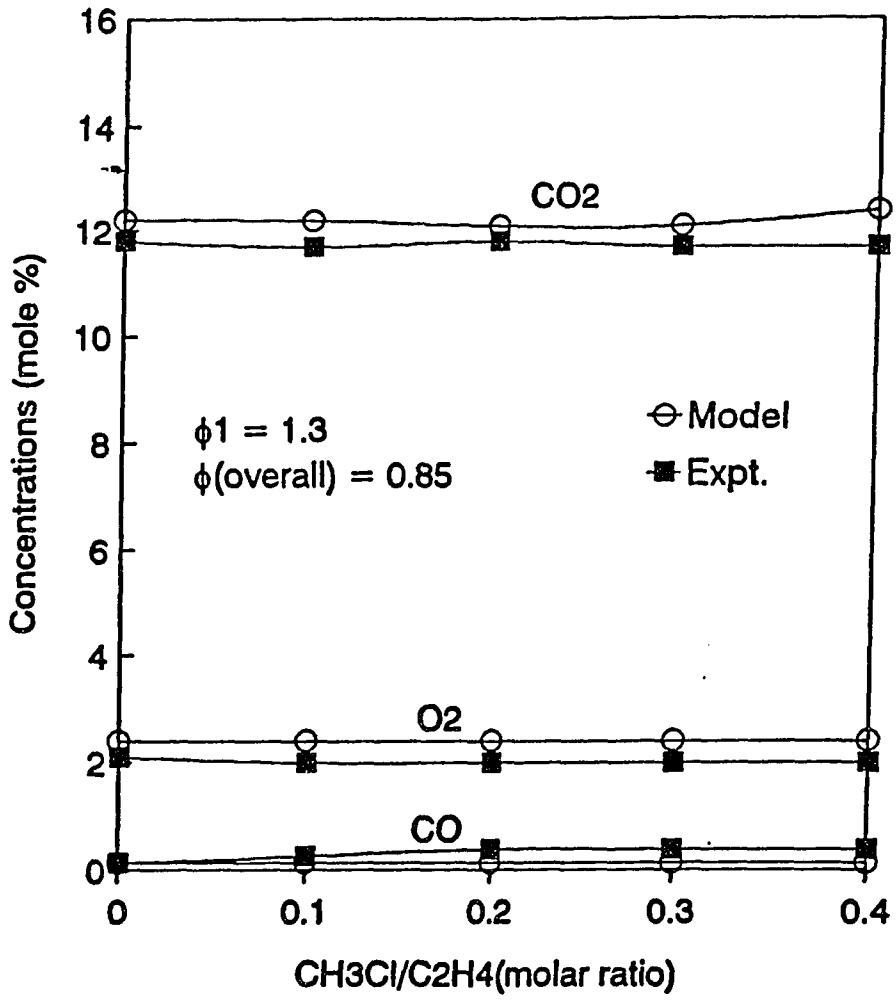

Figure 8.8 Concentrations of CO2, O2, and CO at the outlet of PFR

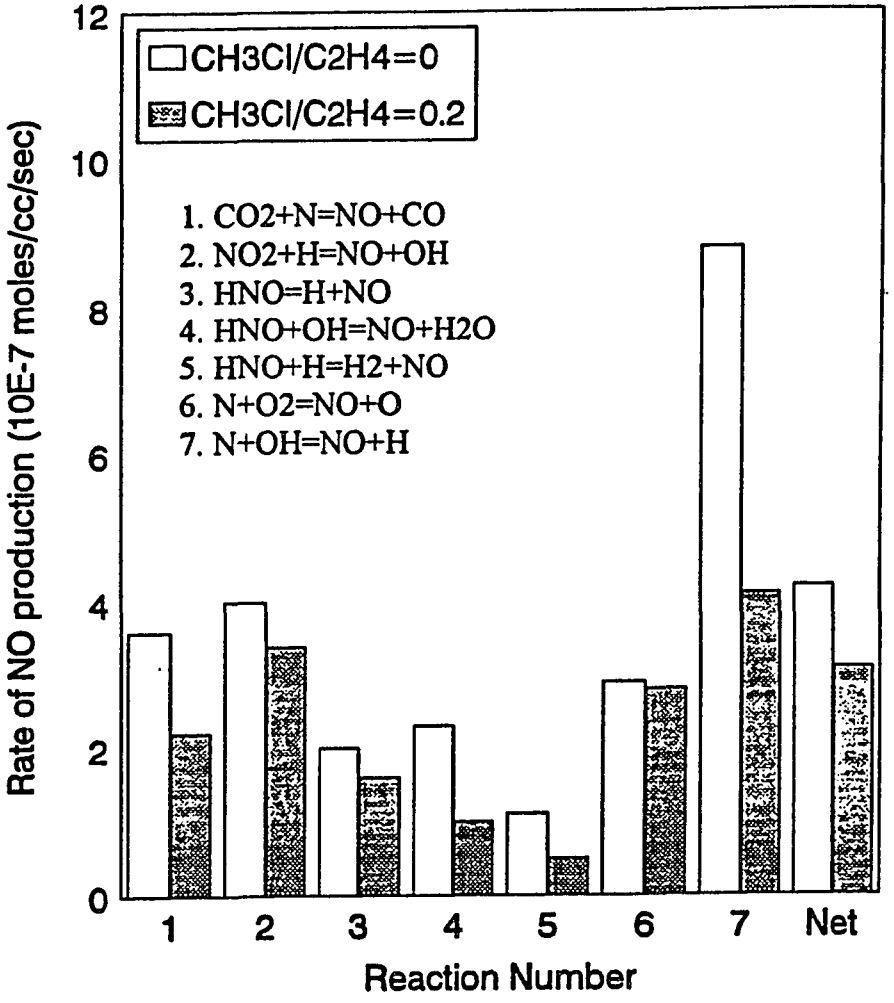

Figure 8.9 Calculated NO formation rates (PSR) in staged combustion of CH3NH2 with and without CH3Cl loading

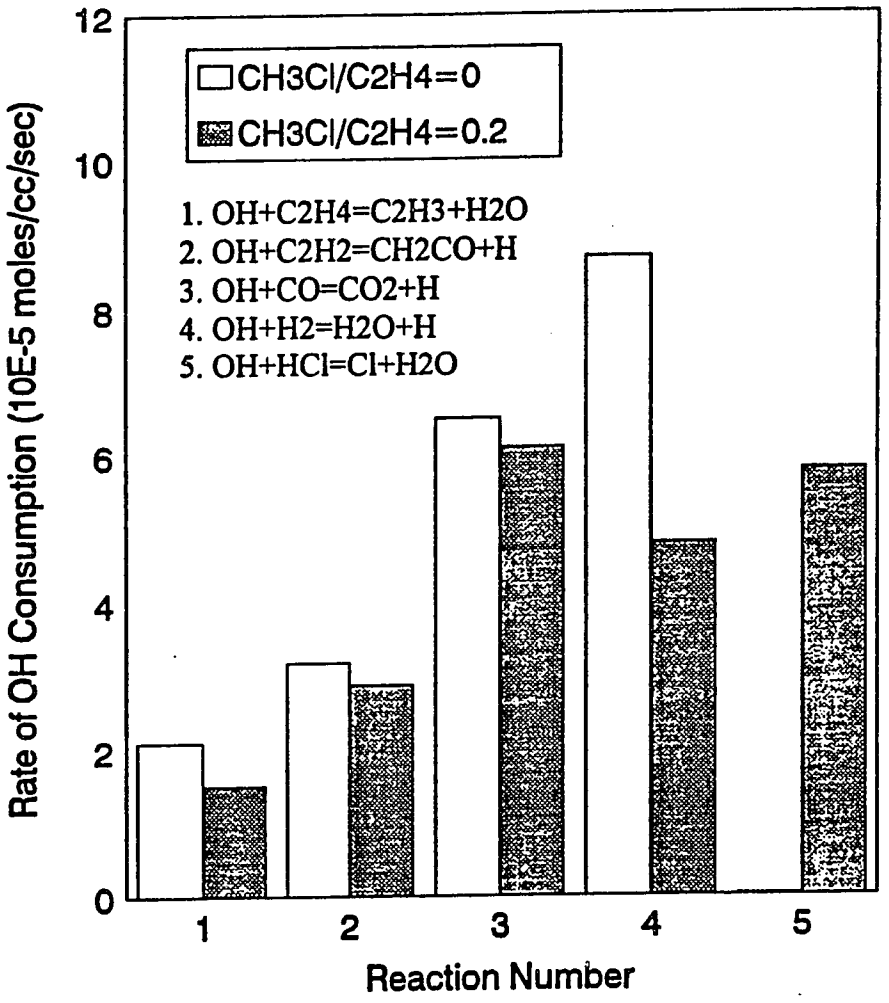

Figure 8.10 Calculated OH consumption rates (PSR) in staged combustion of CH3NH2 with and without CH3Cl loading

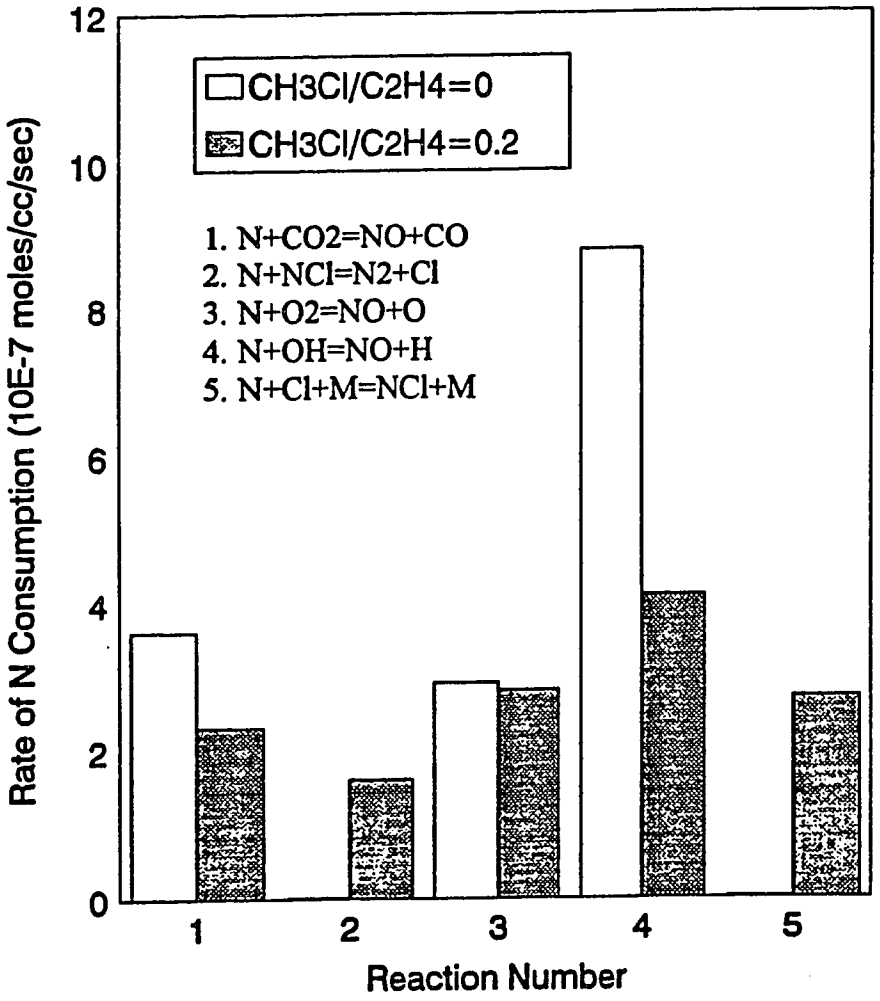

Figure 8.11 Calculated N consumption rates(PSR) in staged combustion of CH3NH2 with and without CH3Cl loading

APPENDIX B

REACTOR SIMULATION COMPUTER CODE

```
      PROGRAM BM21
C
C     PSR/PFR REACTOR MODEL BY RBB
C     ADIABATIC PSR,PFR / GIVEN PSR TEMP AND PFR TEMP FROFILE (REVISED BY F. MAO)
C     INPUT PFR RESIDENCE TIMES, GUESS PSR TEMP
C     INPUT PSR RESID. TIME OR MASS FEED RATE
C     INJECTION AFTER PSR
C
C\\\\\\\\\\\\\\\\\\\\\\\\\\\\\\\\\\\\\\\\\\\\\\\\\\\\\\\\\\\\\\\\\\\\\\\\
C  LAST REVISED:  12/20/1992,    BY F. MAO
C
C   1. PROBLEM TYPE: 0 = ENERGY BALANCE (ENRG)
C                    1 = TEMPERATURE GIVEN (TGIV)
C   2. HEAT LOSSES IN PSR (ENRG)
C   3. HEAT LOSSES IN PFR (ENRG)
C   4. PFR TEMP. PROFILE (TGIV): TEMP =A+B*TIME+C*TIME**2
C   5. PRINTOUT SPECIFICATION : 0 = PRINT ALL SPECIES
C                               1 = PRINT SPECIFIED SPECIES
C   6. WORK SPACE EXTENSION:   500 RXNS & 120 SPECIES.
C
C
C  LAST REVISED:  2/1/1993,     BY F. MAO
C
C   1. RATE OF PRODUCTION IN PSR AND PFR (ALL OR SPECIFIED SPECIES)
C   2  SENSITIVITY ANALYSIS IN PSR  (ALL OR SPECIFIED SPECIES)
C\\\\\\\\\\\\\\\\\\\\\\\\\\\\\\\\\\\\\\\\\\\\\\\\\\\\\\\\\\\\\\\\\\\\\\\\
C
C
C
      IMPLICIT REAL*8 (A-H,O-Z)
      CHARACTER*80 KEYWORD,KEYWORD2(70)
      CHARACTER*18 DUMMY
      DIMENSION X(150),Y(150),Z(150),XP(150),YP(150),XINJ(150),
     1  YINJ(150),KSYM(10,150),XINP(150),VALUE(3),XMIX(150),
     2  YMIX(150),KPRT(150),KROP(150),KSEN(150)
      DIMENSION ELWRK(12000),IELWRK(150)
      COMMON/WRK/IWORK(20000),WORK(30000)
      COMMON/PARAM/KK,P,RU,WT(150)
      COMMON/DUM/WDOT(150),H(150)
C//////////////////////
      COMMON/DTF/MFLAG, BBBB, CCCC, CPB
C//////////////////////
      DIMENSION XFEED(150),ICHAR(70),ICHAR2(70),ISYM(10),XPFR(150)
      DIMENSION TPS(3), PPS(2), TPF(3), PPF(2), XSQ(150),XFQ(150)
C
      DATA LIW/150/,LRW/12000/, NLMAX/55/, NK/4/
      DATA LENIWK/20000/, LENWK/30000/, NCHAR/70/
C
      DATA LIN/5/, LPSRINP2/10/, IFLAG/0/
      DATA LPSRBIN/15/, LFINAL/12/, LINK/25/
C
      EXTERNAL FUN
C
C       OPEN THE CHEMKIN LINK FILE
```

```
C
      OPEN(UNIT=LINK, STATUS='OLD', FORM='UNFORMATTED')
C
C       INITIALIZE CHEMKIN
C
      CALL CKINIT(LENIWK,LENWK,LINK,LFINAL,IWORK,WORK)
      CALL CKINDX(IWORK,WORK,MM,KK,II,LENEL,LENSYM,NFIT)
      CALL CKSYMS(LENSYM,IWORK,WORK,KSYM)
      CALL CKWT(IWORK,WORK,WT)
      CALL CKRP(IWORK,WORK,RU,RUC,PATM)
      CLOSE(LINK)
C//////////////////////////
C
C     INPUT A FLAG No. FOR PROBLEM TYPE  (0=ENRG, 1=TGIV)
C
      READ(LIN,7600) (ICHAR(N),N=1,NCHAR)
      CALL XNUM (ICHAR,NCHAR,1,VALUE,IERR)
      IF(IERR .EQ. 0) GO TO 15
      WRITE(LFINAL,8400)
      STOP
 15   CONTINUE
      MFLAG = VALUE(1)
C
C       READ HEAT LOSSES IN BOTH PSR AND PFR (CAL/SEC)
C
      IF(MFLAG .EQ. 0) THEN
       READ(LIN,7600) (ICHAR(N),N=1,NCHAR)
       CALL XNUM (ICHAR,NCHAR,2,VALUE,IERR)
       IF(IERR .EQ. 0) GO TO 25
       WRITE(LFINAL,8400)
       STOP
 25    CONTINUE
       QLOS1 = VALUE(1)
       QLOS2 = VALUE(2)
      ENDIF
C//////////////////////
C
C       READ PRESSURE AND FEED TEMPERATURE
C
      READ(LIN,7600) (ICHAR(N),N=1,NCHAR)
      CALL XNUM (ICHAR,NCHAR,2,VALUE,IERR)
      IF(IERR .EQ. 0) GO TO 35
      WRITE(LFINAL,8400)
      STOP
 35   CONTINUE
      PA=VALUE(1)
      TFEED = VALUE(2)
      P=PA*PATM
C
C       READ THE INITIAL NON-ZERO MOLE FRACTIONS
C
 40   CONTINUE
      READ(LIN,7600)(ICHAR(N),N=1,NCHAR)
      IF(ICHAR(1).EQ.1HE .AND. ICHAR(2).EQ.1HN .AND.
```

```
     1  ICHAR(3).EQ.1HD)GO TO 45
        CALL SYMNUM(KK,LENSYM,NCHAR,1,KSYM,ICHAR,ISYM,KSPEC,VALUE)
        IF (KSPEC .LE. 0) GO TO 40
        XFEED(KSPEC)=VALUE(1)
        GO TO 40
   45 CONTINUE
C
C       NORMALIZE THE FEED MOLE FRACTIONS
C
        XTOT=0.0E0
        DO 50 K=1,KK
        XTOT=XTOT+XFEED(K)
   50 CONTINUE
        IF (XTOT.EQ.1.0000) GOTO 51
        WRITE (LFINAL,111)
   51 CONTINUE
        DO 55 K=1,KK
        XFEED(K)=XFEED(K)/XTOT
   55 CONTINUE
C////////////////////////////////////
C
C       INPUT LSODE PRINTOUT INCREMENT, PFR TAU
C
        READ(LIN,7600) (ICHAR(N),N=1,NCHAR)
        CALL XNUM(ICHAR,NCHAR,2,VALUE,IERR)
        IF(IERR .EQ. 0) GO TO 101
        WRITE(LFINAL,8400)
        STOP
  101 CONTINUE
        DELT = VALUE(1)
        TPFR1 = VALUE(2)
C
C       INPUT PSR INITIAL-GUESS OR GIVEN TEMP.
C
        READ(LIN,7600) (ICHAR(N),N=1,NCHAR)
        CALL XNUM(ICHAR,NCHAR,1,VALUE,IERR)
        IF(IERR .EQ. 0) GO TO 102
        WRITE(LFINAL,8400)
        STOP
  102 CONTINUE
        TGUESS = VALUE(1)
C
C       INPUT PFR TEMP. PROFILE (TEMP=AAAA+BBBB*TIME+CCCC*TIME**2)
C
        IF(MFLAG .EQ. 1) THEN
          READ(LIN,7600) (ICHAR(N),N=1,NCHAR)
          CALL XNUM(ICHAR,NCHAR,3,VALUE,IERR)
          IF(IERR .EQ. 0) GO TO 103
          WRITE(LFINAL,8400)
          STOP
  103   CONTINUE
          AAAA = VALUE(1)
          BBBB = VALUE(2)
          CCCC = VALUE(3)
```

```
      ENDIF
C////////////////////////////////////
C
C       INPUT PSR TAU OR MASS FEED RATE
C          START WITH A LOGIC SWITCH
C
      READ (LIN,7600) (ICHAR(N),N=1,NCHAR)
      CALL XNUM(ICHAR,NCHAR,2,VALUE,IERR)
      IF (IERR.EQ.0) GOTO 142
      WRITE (LFINAL,8400)
      STOP
  142 CONTINUE
      ISWITCH = INT(VALUE(1))
      IF (ISWITCH.EQ.0) GOTO 492
      FEEDRATE = VALUE(2)
      GOTO 740
  492 CONTINUE
      PSRTAU = VALUE(2)
C
C       INPUT THE COMPOSITION OF INJECTION MATERIAL
C
  740 CONTINUE
      READ(LIN,7600)(ICHAR(N),N=1,NCHAR)
      IF(ICHAR(1).EQ.1HE .AND. ICHAR(2).EQ.1HN .AND.
     1  ICHAR(3).EQ.1HD)GO TO 745
      CALL SYMNUM(KK,LENSYM,NCHAR,1,KSYM,ICHAR,ISYM,KSPEC,VALUE)
      IF (KSPEC .LE. 0) GO TO 740
      XINJ(KSPEC)=VALUE(1)
      GO TO 740
  745 CONTINUE
C
C      INPUT THE MASS RATE AND TEMP. OF INJECTION
C
      READ (LIN,7600) (ICHAR(N),N=1,NCHAR)
      CALL XNUM(ICHAR,NCHAR,2,VALUE,IERR)
      IF (IERR.EQ.0) GOTO 842
      WRITE (LFINAL,8400)
      STOP
  842 CONTINUE
      RINJ = VALUE(1)
      TINJ = VALUE(2)
      IF (RINJ.EQ.0.0) GOTO 960
      IFLAG = 1
C
C      NORMALIZE THE INJECTION MOLE FRACTIONS
C
      XTOT=0.0E0
      DO 950 K=1,KK
      XTOT=XTOT+XINJ(K)
  950 CONTINUE
      IF (XTOT.EQ.1.0000) GOTO 951
      WRITE (LFINAL,111)
  951 CONTINUE
      DO 955 K=1,KK
```

```
      XINJ(K)=XINJ(K)/XTOT
  955 CONTINUE
      CALL CKXTY (XINJ,IWORK,WORK,YINJ)
  960 CONTINUE
C////////////////////////
C
C     INPUT A FLAG No. FOR PRINT OUT SPECIFICATION
C       (0=PRINT OUT ALL SPECIESS; 1=SPECIFIED SPECIES)
C
      READ(LIN,7600) (ICHAR(N),N=1,NCHAR)
      CALL XNUM (ICHAR,NCHAR,1,VALUE,IERR)
      IF(IERR .EQ. 0) GO TO 16
      WRITE(LFINAL,8400)
      STOP
   16 CONTINUE
      KFLAG = VALUE(1)
C
C       READ PRINTING SPECIES
C
      IF(KFLAG .EQ. 1) THEN
       MM = 0
   17  CONTINUE
       READ(LIN,7600)(ICHAR(N),N=1,NCHAR)
       IF(ICHAR(1).EQ.1HE .AND. ICHAR(2).EQ.1HN .AND.
     1    ICHAR(3).EQ.1HD)GO TO 18
       CALL SYMNUM(KK,LENSYM,NCHAR,1,KSYM,ICHAR,ISYM,KSPEC,VALUE)
       IF (KSPEC .LE. 0) GO TO 17
       MM = MM + 1
       KPRT(MM) = KSPEC
       GO TO 17
   18  CONTINUE
      ENDIF
C
C     INPUT A FLAG No. FOR R-O-P ANALYSIS
C       (0=NONE ; 1=ALL SPECIES ; 2=SELECTED SPECIES)
C
      READ(LIN,7600) (ICHAR(N),N=1,NCHAR)
      CALL XNUM (ICHAR,NCHAR,1,VALUE,IERR)
      IF(IERR .EQ. 0) GO TO 160
      WRITE(LFINAL,8400)
      STOP
  160 CONTINUE
      NFLAG = VALUE(1)
C
C     INPUT A THRESHOLD VALUE FOR R-O-P
C
      IF(NFLAG .NE. 0) THEN
       READ(LIN,7600) (ICHAR(N),N=1,NCHAR)
       CALL XNUM (ICHAR,NCHAR,1,VALUE,IERR)
       IF(IERR .EQ. 0) GO TO 162
       WRITE(LFINAL,8400)
       STOP
  162  CONTINUE
       THRP = VALUE(1)
```

```
      ENDIF
C
C       INPUT SELECTED SPECIES FOR R-O-P
C
      IF(NFLAG .EQ. 2) THEN
       NN = 0
  170  CONTINUE
       READ(LIN,7600)(ICHAR(N),N=1,NCHAR)
       IF(ICHAR(1).EQ.1HE .AND. ICHAR(2).EQ.1HN .AND.
     1    ICHAR(3).EQ.1HD)GO TO 180
       CALL SYMNUM(KK,LENSYM,NCHAR,1,KSYM,ICHAR,ISYM,KSPEC,VALUE)
       IF (KSPEC .LE. 0) GO TO 170
       NN = NN + 1
       KROP(NN) = KSPEC
       GO TO 170
  180  CONTINUE
      ENDIF
C
C     INPUT A FLAG No. FOR SENS. ANAL.
C       (0=NONE; 1=ALL; 2=SELECTED SPECIES; 3=TEMP.)
C
      READ(LIN,7600) (ICHAR(N),N=1,NCHAR)
      CALL XNUM (ICHAR,NCHAR,1,VALUE,IERR)
      IF(IERR .EQ. 0) GO TO 161
      WRITE(LFINAL,8400)
      STOP
  161 CONTINUE
      JFLAG = VALUE(1)
C
C     INPUT TWO THRESHOLD VALUES FOR SENS. OF SPECIES & TEMP.
C
      IF(JFLAG .NE. 0) THEN
       READ(LIN,7600) (ICHAR(N),N=1,NCHAR)
       CALL XNUM (ICHAR,NCHAR,2,VALUE,IERR)
       IF(IERR .EQ. 0) GO TO 163
       WRITE(LFINAL,8400)
       STOP
  163   CONTINUE
       THSES = VALUE(1)
       THSET = VALUE(2)
      ENDIF
C
C       INPUT SELECTED SPECIES FOR SENS.
C
      IF(JFLAG .EQ. 2) THEN
       NNS = 0
  171  CONTINUE
       READ(LIN,7600)(ICHAR(N),N=1,NCHAR)
       IF(ICHAR(1).EQ.1HE .AND. ICHAR(2).EQ.1HN .AND.
     1    ICHAR(3).EQ.1HD)GO TO 181
       CALL SYMNUM(KK,LENSYM,NCHAR,1,KSYM,ICHAR,ISYM,KSPEC,VALUE)
       IF (KSPEC .LE. 0) GO TO 171
       NNS = NNS + 1
       KSEN(NNS) = KSPEC
```

```
      GO TO 171
 181  CONTINUE
     ENDIF
C
C      INPUT 2 FLAG No. FOR PROBE QUENCH CALC. (PSR & PFR)
C       (0=NONE; 1=QUENCH CALC.)
C
     READ(LIN,7600) (ICHAR(N),N=1,NCHAR)
     CALL XNUM (ICHAR,NCHAR,2,VALUE,IERR)
     IF(IERR .EQ. 0) GO TO 191
     WRITE(LFINAL,8400)
     STOP
 191 CONTINUE
     JSPQF = VALUE(1)
     JFPQF = VALUE(2)
C
C      INPUT TEMP. , PRESS. PROFILES AND RESD. TIME IN PSR PROBE
C
     IF(JSPQF .EQ. 1)THEN
      READ(LIN,7600) (ICHAR(N),N=1,NCHAR)
      CALL XNUM (ICHAR,NCHAR,3,VALUE,IERR)
      IF(IERR .EQ. 0) GO TO 192
      WRITE(LFINAL,8400)
      STOP
 192   CONTINUE
      TPS(1) = VALUE(1)
      TPS(2) = VALUE(2)
      TPS(3) = VALUE(3)
C
      READ(LIN,7600) (ICHAR(N),N=1,NCHAR)
      CALL XNUM (ICHAR,NCHAR,3,VALUE,IERR)
      IF(IERR .EQ. 0) GO TO 193
      WRITE(LFINAL,8400)
      STOP
 193   CONTINUE
      PPS(1) = VALUE(1)
      PPS(2) = VALUE(2)
      RSTS = VALUE(3)
     ENDIF
C
C      INPUT TEMP. , PRESS. PROFILE AND RESD. TIME IN PFR PROBE
C
     IF(JFPQF .EQ. 1)THEN
      READ(LIN,7600) (ICHAR(N),N=1,NCHAR)
      CALL XNUM (ICHAR,NCHAR,3,VALUE,IERR)
      IF(IERR .EQ. 0) GO TO 194
      WRITE(LFINAL,8400)
      STOP
 194   CONTINUE
      TPF(1) = VALUE(1)
      TPF(2) = VALUE(2)
      TPF(3) = VALUE(3)
C
      READ(LIN,7600) (ICHAR(N),N=1,NCHAR)
```

```
      CALL XNUM (ICHAR,NCHAR,3,VALUE,IERR)
      IF(IERR .EQ. 0) GO TO 195
      WRITE(LFINAL,8400)
      STOP
 195  CONTINUE
      PPF(1) = VALUE(1)
      PPF(2) = VALUE(2)
      RSTF = VALUE(3)
     ENDIF
C\\\\\\\\\\\\\\\\\\\\\\\\\\\\\\\\\\\\\\
     CLOSE(LIN)
C
C       WRITE FILE FOR PSR INPUT
C
     VPSR1=250.
C////////////////////////////
     IF(MFLAG .EQ. 0 ) THEN
      WRITE (LPSRINP2,2224)
     ELSE
      WRITE (LPSRINP2,2225)
     ENDIF
C
     IF(NFLAG .EQ. 1) THEN
      WRITE (LPSRINP2,2004)
     ENDIF
     IF(NFLAG .NE. 0) THEN
       WRITE(LPSRINP2,2002) THRP
     ENDIF
     IF(NFLAG .EQ. 2) THEN
      WRITE(LPSRINP2,2005) ((KSYM(I,KROP(J)),I=1,LENSYM),J=1,NN)
     ENDIF
C
     IF(JFLAG .EQ. 1) THEN
      WRITE (LPSRINP2,2006)
     ENDIF
     IF(JFLAG .NE. 0) THEN
      WRITE (LPSRINP2,2003) THSES
      WRITE (LPSRINP2,2001) THSET
     ENDIF
     IF(JFLAG .EQ. 3) THEN
      WRITE (LPSRINP2,2007)
     ENDIF
     IF(JFLAG .EQ. 2) THEN
      WRITE(LPSRINP2,2008) ((KSYM(I,KSEN(J)),I=1,LENSYM),J=1,NNS)
     ENDIF
C//////////////////////////////
     WRITE (LPSRINP2,3003) TGUESS
     WRITE (LPSRINP2,3005) TFEED
     WRITE (LPSRINP2,2229) PA
     IF (ISWITCH.EQ.1) GOTO 3218
     WRITE (LPSRINP2,2302) PSRTAU
     GOTO 3237
3218 CONTINUE
     WRITE (LPSRINP2,2231) feedrate
```

```
3237 CONTINUE
     WRITE (LPSRINP2,2226) VPSR1
C////////////////////!////////////////
     IF(MFLAG .EQ. 0 ) THEN
      PSRHL = QLOS1
      PFRHL = QLOS2
      WRITE (LPSRINP2,2227) PSRHL
     ENDIF
C//////////////////////////////////////
     DO 3534 JK=1,KK
     WRITE (LPSRINP2,2223) (KSYM(I,JK),I=1,LENSYM),xfeed(JK)
3534 CONTINUE
     WRITE (LPSRINP2,2228)
     CLOSE (LPSRINP2,STATUS='KEEP')
     CONTINUE
     WRITE (LFINAL,3000)
3000 FORMAT(1X,'              ')
C\\\\\\\\\\\\\\\\\\\\\\\\\\\\\\\\\\\\\\\\
     WRITE(24,498)
C\\\\\\\\\\\\\\\\\\\\\\\\\\\\\\\\\\\\\\\\
C
C    ****** PSR CALCULATION ******
C
     CALL B3PSR
C
     WRITE (LFINAL,3001)
3001 FORMAT(1X,'                    ')
     OPEN (LPSRBIN,STATUS='OLD',FORM='UNFORMATTED')
     REWIND (LPSRBIN)
     READ (LPSRBIN) DUMMY
     READ (LPSRBIN) NNP
     KKP=NNP-1
     READ (LPSRBIN) EQUIVP1,PP1,TAUP1,FLRTP1,VP1,QP1
     READ (LPSRBIN) TINP1,(XINP(K),K=1,KKP)
     READ (LPSRBIN) TP,(YP(K),K=1,KKP)
     CLOSE (LPSRBIN,STATUS='DELETE')
C//////////////////////////////////////
     CLOSE (LPSRINP2,STATUS='KEEP')
C//////////////////////////////////////
     CALL CKYTX(YP,IWORK,WORK,XP)
C
C    ****** PSR PROBE QUENCH ******
C
     IF(JSPQF .EQ. 1) THEN
      CALL PQ(TPS,PPS,RSTS,XP,XSQ)
     ENDIF
C
     WRITE(LFINAL,1519)
     WRITE(LFINAL,4543) PA,TFEED
     WRITE(LFINAL,7020)
     DO IJ=1,KK
C\\\\\\\\\\\\\\\\\\\\\\\\\\
C
C    OUTPUT NON-ZERO FEED COMPOSITION
```

```
C
      IF(XFEED(IJ) .GT. 0.0) THEN
       WRITE(LFINAL,2203) (KSYM(I,IJ),I=1,LENSYM),XFEED(IJ)
      ENDIF
    END DO
    WRITE(LFINAL,1517)
    WRITE(LFINAL,1514)
C\\\\\\\\\\\\\\\\\\\\\\\\\\\\\\\\\\\\\\\\
    WRITE(24,499) TAUP1
    WRITE(LFINAL,1518) TAUP1
    WRITE(LFINAL,9752) FLRTP1
    IF(MFLAG .EQ. 0) THEN
     WRITE(LFINAL,9770) TP
    ELSE
     WRITE(LFINAL,9771) TP
    ENDIF
C\\\\\\\\\\\\\\\\\\\\\\\\\\\\\\\\\\\\\\\\
    WRITE(LFINAL,1520)
    DO IJ=1,KK
C\\\\\\\\\\\\\\\\\\\\\\\\\\\\\\\\\\\\\\\\\\\\
C
C    OUTPUT SPECIFIED SPECIES MOLE FRACTIONS OF PSR
C
     IF(KFLAG .EQ. 1) THEN
      DO JJ = 1,KK
       KP = KPRT(JJ)
       IF(IJ .EQ. KP) THEN
        IF(JSPQF .EQ. 1) THEN
        WRITE(LFINAL,2203) (KSYM(I,IJ),I=1,LENSYM),XP(IJ),XSQ(IJ)
        ELSE
        WRITE(LFINAL,2203) (KSYM(I,IJ),I=1,LENSYM),XP(IJ)
        ENDIF
       ENDIF
      END DO
      GO TO 19
     ENDIF
     IF(JSPQF .EQ. 1) THEN
      WRITE(LFINAL,2203) (KSYM(I,IJ),I=1,LENSYM),XP(IJ),XSQ(IJ)
     ELSE
      WRITE(LFINAL,2203) (KSYM(I,IJ),I=1,LENSYM),XP(IJ)
     ENDIF
 19   CONTINUE
    END DO
    WRITE(LFINAL,1517)
C
C\\\\\\\\\\\\\\\\\\\\\\\\\\\\\\\\\\\\\\\\\\\\
C
    IF (IFLAG.EQ.0) GOTO 433
C\\\\\\\\\\\\\\\\\\\\\\\\\\\\\\\\\\\\\\\\
C
C    DESCRIPTION OF INJECTION MATERIALS
C
    WRITE(LFINAL,4004)
    WRITE(LFINAL,4006)TINJ,RINJ
```

```
      DO IJ=1,KK
       IF(XINJ(IJ) .GT. 0.0) THEN
        WRITE(LFINAL,2203) (KSYM(I,IJ),I=1,LENSYM),XINJ(IJ)
       ENDIF
      END DO
      WRITE(LFINAL,1517)
C
C       MIXING THE INJECTION MATERIAL INTO THE PSR OUTLET GAS
C
      CALL MIX(KK,IWORK,WORK,FLRTP1,RINJ,XP,XINJ,
     1   TP,TINJ,YP,YINJ,TMIX,YMIX,RMIX)
      CALL CKYTX (YMIX,IWORK,WORK,XMIX)
      WRITE(LFINAL,4000)
      WRITE(LFINAL,4002) TMIX,RMIX
      DO IJ=1,KK
C\\\\\\\\\\\\\\\\\\\\\\\\\\\\\\\\\\\\\\\\
       IF(KFLAG .EQ. 1) THEN
        DO JJ = 1,KK
         KP = KPRT(JJ)
         IF(IJ .EQ. KP) THEN
          WRITE(LFINAL,2203) (KSYM(I,IJ),I=1,LENSYM),XMIX(IJ)
         ENDIF
        END DO
        GO TO 29
       ENDIF
       WRITE(LFINAL,2203) (KSYM(I,IJ),I=1,LENSYM),XMIX(IJ)
 29    CONTINUE
C\\\\\\\\\\\\\\\\\\\\\\\\\\\\\\\\\\\\\\\\
      END DO
      WRITE(LFINAL,1517)
C
C       INITIAL VALUES OF LSODE
C
C////////////////////////////
      IF(MFLAG .EQ. 1) THEN
       Z(1) = TP
       TEMPFR = TP
      ELSE
       Z(1) = TMIX
       TEMPFR = TMIX
      ENDIF
C////////////////////////////
      DO 431 J=1,KK
       Z(J+1) = YMIX(J)
       XPFR(J) = XMIX(J)
 431 CONTINUE
      GOTO 481
 433 CONTINUE
      Z(1) = TP
      TEMPFR = TP
      DO 481 J=1,KK
       Z(J+1) = YP(J)
       XPFR(J) = XP(J)
 481 CONTINUE
```

```
      P=PA*PATM
      VPFR1=0.0
C
C     SET THE INTEGRATION CONTROL PARAMETERS FOR LSODE
C
 8222 CONTINUE
      NEQ=KK+1
      TT1=0.0
      JCNT=0
      NLINES=NLMAX+1
      WRITE(LFINAL,*) '****** PFR RESULTS ******'
      WRITE(LFINAL,*) '       '
      WRITE(LFINAL,1378) DELT,TPFR1
      NTI=INT(TPFR1/DELT)
C
C       INTEGRATION LOOP FOR PFR
C
 250 CONTINUE
      MF=22
      ITOL=1
      IOPT=0
      RTOL=1.E-3
      ITASK=1
      ATOL=1.E-9
      ISTATE=1
C\\\\\\\\\\\\\\\\\\\\\\\\\\\\\\\\\\\\\\\\
C
C       PRINT THE SOLUTION
C
      WRITE(LFINAL,7100)
      IF(MFLAG .EQ. 0) THEN
       WRITE(LFINAL,7102)
      ELSE
       WRITE(LFINAL,7101)
      ENDIF
C
C     CALCULATE TEMPERATURE DROP DUE TO HEAT LOSS IN PFR
C
      IF(MFLAG .EQ. 0) THEN
       IF(TT1 .GT. 0.0) THEN
        CALL TDEC(TEMPFR, PFRHL, FLRTP1, CPB , DELT)
        Z(1) = TEMPFR
       ENDIF
      ENDIF
C
C     ****** PFR QUENCH CACULATION ******
C
      IF(JFPQF .EQ. 1) THEN
       CALL PQ(TPF,PPF,RSTF,XPFR,XFQ)
      ENDIF
C
      WRITE(LFINAL,7105)TT1,TEMPFR,VPFR1
      DO IJ=1,KK
       IF(KFLAG .EQ. 1) THEN
```

```
      DO JJ = 1,KK
       KP = KPRT(JJ)
       IF(IJ .EQ. KP) THEN
        IF(JFPQF .EQ. 1) THEN
         WRITE(LFINAL,2203) (KSYM(I,IJ),I=1,LENSYM),XPFR(IJ),XFQ(IJ)
        ELSE
         WRITE(LFINAL,2203) (KSYM(I,IJ),I=1,LENSYM),XPFR(IJ)
        ENDIF
       ENDIF
      END DO
      GO TO 39
     ENDIF
      IF(JFPQF .EQ. 1)THEN
       WRITE(LFINAL,2203) (KSYM(I,IJ),I=1,LENSYM),XPFR(IJ),XFQ(IJ)
      ELSE
       WRITE(LFINAL,2203) (KSYM(I,IJ),I=1,LENSYM),XPFR(IJ)
      ENDIF
 39   CONTINUE
     END DO
     WRITE(LFINAL,1517)
C
C    CALCULATION OF PFR R-O-P
C
     IF(NFLAG .EQ. 0) GO TO 49
     IF(NFLAG .EQ. 1) THEN
      DO JJ = 1,KK
        KROP(JJ) = JJ
      END DO
     ENDIF
      KK1 = KK + 1
      CALL PFRROP(24, 15, KK, II, KK1,
    1           LENSYM, KSYM, P, Z,
    2           KROP, THRP, TT1)
     CLOSE (LPSRBIN,STATUS='DELETE')
 49  CONTINUE
C\\\\\\\\\\\\\\\\\\\\\\\\\\\\\\\\\\\\\\\\\\\\\\\\
C
C       CALL DIFFERENTIAL EQUATION SOLVER LSODE
C
     TT2=TT1+DELT
     CALL LSODE(FUN,NEQ,Z,TT1,TT2,ITOL,RTOL,ATOL,ITASK,ISTATE,IOPT,
    1  ELWRK,LRW,IELWRK,LIW,JAC,MF)
     IF (ISTATE.EQ.2) GOTO 67
     WRITE(LFINAL,1212) ISTATE
     STOP
 67  TEMPFR=Z(1)
     WRITE(*,*) TEMPFR
     DO 400 K=1,KK
      Y(K)=Z(K+1)
 400 CONTINUE
     JCNT=JCNT+1
     CALL CKRHOY(P,TEMPFR,Y,IWORK,WORK,RHOINC)
     VOLINC=DELT*FLRTP1/RHOINC
     VPFR1=VPFR1+VOLINC
```

```
C
      CALL CKYTX(Y,IWORK,WORK,XPFR)
C
      IF (JCNT.GT.NTI) GOTO 999
      GOTO 250
C
  999 CONTINUE
      CLOSE(LFINAL)
C
C       FORMATS
C
   111 FORMAT(1X,//)
   115 FORMAT(1X,'ELAPSED PFR TIME:',E10.3,5X,'CUM. PFR VOL:',F5.1)
   702 FORMAT(1x,'MOLE FRACTIONS')
   888 FORMAT(1x,'Temp:',F8.1)
   498 FORMAT(/////,23X,'RATE-OF-PRODUCTION OF PSR')
   499 FORMAT(//,20X,'RESIDENT TIME OF PSR = ',E10.3,'  SEC.')
  1212 FORMAT('ISTATE=',I4)
  1378 FORMAT(1X,'DELT (sec):',E10.2,5X,'TPFR1 (sec):',E10.2)
  1514 FORMAT(1X,'****** PSR RESULTS ******',/)
  1517 FORMAT(1X,'    ')
  1518 FORMAT(1X,'PSRTAU (sec):',E10.2)
  1519 FORMAT(1X,'****** FEED CONDITIONS ******',/)
  1520 FORMAT(1X,'CALC. PSR MOLE FRACTIONS         PSR+PQ')
  2203 FORMAT(1X,10A1,1X,E11.4,9X,E11.4)
  2223 FORMAT('REAC',1X,10A1,1X,E11.4)
  2002 FORMAT('EPSR',F6.3)
  2003 FORMAT('EPSS',F7.4)
  2001 FORMAT('EPST',F7.4)
  2004 FORMAT('AROP')
  2005 FORMAT(('ROP ',6(1X,10A1)))
  2006 FORMAT('ASEN')
  2007 FORMAT('SENT')
  2008 FORMAT(('SEN ',6(1X,10A1)))
  2224 FORMAT('ENRG')
  2225 FORMAT('TGIV')
  2226 FORMAT('VOL ',1X,E11.4)
  2227 FORMAT('QLOS',1X,E11.4)
  2228 FORMAT('END')
  2229 FORMAT('PRES',1X,E11.4)
  2231 FORMAT('FLRT',1X,E11.4)
  2302 FORMAT('TAU',1X,E11.4)
  3003 FORMAT('TEMP',1X,E11.4)
  3005 FORMAT('TINL',1X,E11.4)
  4000 FORMAT(1X,'****** RESULTS OF MIXING - INTO PFR ******',/)
  4002 FORMAT(1X,'TEMP (K): ',F6.1,1X,'MASS RATE (g/s): ',F5.1)
  4004 FORMAT(1X,'****** DESCRIPTION OF INJ. MATERIAL ******',/)
  4006 FORMAT(1X,'TEMP (K): ',F6.1,1X,'MASS RATE (g/s): ',F5.1)
  4543 FORMAT(1X,'PRES (atm):',F5.1,5X,'TFEED (K):',F7.1)
  7003 FORMAT(1H1)
  7020 FORMAT(2X,'INPUT MOLE FRACTIONS')
  7100 FORMAT(3X,6HT(SEC),5X,6HTMP(K),3X,7HVOL(CC),'    PFR+PQ')
  7101 FORMAT(3X,6H     ,5X,6H(TGIV),3X,7H      )
  7102 FORMAT(3X,6H     ,5X,6H(CALC),3X,7H      )
```

```
 7105 FORMAT(E10.2,3X,F6.1,3X,F6.1,3X,4E11.3)
 7110 FORMAT(34X,4(1X,10A1))
 7115 FORMAT(31X,10E11.3)
 7600 FORMAT(80A1)
 8400 FORMAT(1X,'ERROR IN INPUT FILE')
 9752 FORMAT(1X,'MASS RATE (g/s):',F7.2)
 9770 FORMAT(1X,'CALC. PSR TEMP (K):',F7.1)
 9771 FORMAT(1X,'GIVEN PSR TEMP (K):',F7.1)
    END
C
C
    SUBROUTINE FUN(N,TIME,Z,ZP)
    IMPLICIT REAL*8(A-H,O-Z)
    DIMENSION Z(N),ZP(N)
    COMMON/WRK/IWORK(20000),WORK(30000)
    COMMON/PARAM/KK,P,RU,WT(150)
    COMMON/DUM/WDOT(150),H(150)
C////////////////////////////////////
    COMMON/DTF/MFLAG, BBBB, CCCC, CPB
C////////////////////////////////////
C
C     VARIABLES IN Z ARE
C       Z(1)=T
C       Z(K+1)=Y(K)
C
C      CALL CHEMKIN SUBROUTINES
C
    CALL CKWYP(P,Z(1),Z(2),IWORK,WORK,WDOT)
    CALL CKHMS(Z(1),IWORK,WORK,H)
    CALL CKRHOY(P,Z(1),Z(2),IWORK,WORK,RHO)
    CALL CKCPBS(Z(1),Z(2),IWORK,WORK,CPB)
C
C      FORM GOVERNING EQUATIONS
C
C////////////////////////////////////
    IF(MFLAG .EQ. 0) THEN
     SUM=0.
     DO 100 K=1,KK
      SUM=SUM+H(K)*WDOT(K)*WT(K)
100   CONTINUE
     ZP(1)=-1.0*SUM/(RHO*CPB)
     DO 202 K=1,KK
      ZP(K+1)=WDOT(K)*WT(K)/RHO
202   CONTINUE
   ELSE
     ZP(1)= BBBB + 2.0 * CCCC * TIME
     DO 203 K=1,KK
      ZP(K+1)=WDOT(K)*WT(K)/RHO
203   CONTINUE
   ENDIF
C////////////////////////////////////////
   RETURN
   END
C
```

```
      SUBROUTINE B3PSR
      IMPLICIT REAL*8 (A-H,O-Z)
      PARAMETER (LENLWK=400, LENIWK=20000, LENRWK=30000)
      DIMENSION LWORK(LENLWK), IWORK(LENIWK), RWORK(LENRWK)
      DATA LIN/10/, LOUT/6/, LRSTRT/14/, LSAVE/15/, LRECOV/16/,
     1    LINKCK/25/
      OPEN(UNIT=LIN, STATUS='OLD', FORM='FORMATTED')
      OPEN(UNIT=LOUT, STATUS='NEW', FORM='FORMATTED')
      OPEN(UNIT=LRSTRT, STATUS='OLD',
     1 FORM='UNFORMATTED',READONLY)
      OPEN(UNIT=LSAVE, STATUS='NEW', FORM='UNFORMATTED')
      OPEN(UNIT=LRECOV, STATUS='NEW', FORM='UNFORMATTED')
      OPEN(UNIT=LINKCK, STATUS='OLD', FORM='UNFORMATTED',
     1 READONLY)
      CALL PSR (LIN,LOUT,LINKCK,LRSTRT,LSAVE,LRECOV,LENLWK,LWORK,
     1        LENIWK,IWORK,LENRWK,RWORK)
      WRITE (LOUT,9821)
 9821 FORMAT(2X,'RETURNING TO MAIN PROGRAM')
      RETURN
      END
C
      SUBROUTINE MIX(KK,IWORK,WORK,SMDOT1,SMDOT2,X1,X2,T1,T2,
     1           Y1,Y2, TI,YTOL,SMDOTTOL)
C
C     THIS SUBROUTINE CALCULATES THE MIX TEMPERATURE OF TWO
C     STREAMS
C
      IMPLICIT REAL*8 (A-H,O-Z)
      DIMENSION X1(150),X2(150),HMS1(150),WORK(30000),IWORK(20000),
     1        HMS2(150),HMLTOL(150),Y1(150),Y2(150),YTOL(150),
     2        XTOL(150)
      CALL CKHMS(T1,IWORK,WORK,HMS1)
      CALL CKHMS(T2,IWORK,WORK,HMS2)
      CALL CKCPBS(T1,Y1,IWORK,WORK,CPAV1)
      CALL CKCPBS(T2,Y2,IWORK,WORK,CPAV2)
      DATA LFINAL/12/
      SMDOTTOL=SMDOT1+SMDOT2
      HTOL=0.
      DO I=1,KK
       YTOL(I)=0.
      END DO
C
C         CALCULATE TOTAL ENTHALPY AND MASS FRACTIONS
C
      DO 100 I=1,KK
       HTOL=HTOL+Y1(I)*HMS1(I)*SMDOT1+Y2(I)*HMS2(I)*SMDOT2
       YTOL(I)=(Y1(I)*SMDOT1+Y2(I)*SMDOT2)/(SMDOT1+SMDOT2)
  100 CONTINUE
C
C       CALCULATE FIRST GUESS FOR MIX TEMPERATURE
C
      TI=(SMDOT1*CPAV1*T1+SMDOT2*CPAV2*T2)/(SMDOT1*
     1 CPAV1+SMDOT2*CPAV2)
      write(*,*)'TI1=',ti
```

```
      CALL CKCPBS(TI,Y1,IWORK,WORK,CPAV1I)
      CALL CKCPBS(TI,Y2,IWORK,WORK,CPAV2I)
      CPAV1=(CPAV1+CPAV1I)/2.
      CPAV2=(CPAV2+CPAV2I)/2.
      TI=(SMDOT1*CPAV1*T1+SMDOT2*CPAV2*T2)/(SMDOT1*
     1  CPAV1+SMDOT2*CPAV2)
      RETURN
      END
```

APPENDIX C

SIMULATION INPUT CARDS

1			1 = Temp. given; 0 = Adiabatic reactor
1.0	400.0		Reactor pressure (atm) and temp. (K)
C2H4	0.06142		Feed mole fractions
O2	0.13475		
N2	0.80291		
CH3CL	0.00		
CH3NH2	0.00091		
END			
3.0E-03	9.0E-03		PFR printout step and residence time (s)
1758			PSR temp. (K)
1758.0	19484	-1325194	PFR temp. interpolation coefficients
1	8.571		Input flag: 1 = flow rate (g/s); 0 = PSR τ (s)
N2	0.79		Injection mole fractions
O2	0.21		
H2O	0.0		
END			
3.12	400.0		Injection flow rate (g/s) and Temp. (K)
1			Input flag: 1 = print out specified species
CO	1		0 = print out all species
C2H2	1		Specified species
END			
2			Input flag: 2 = ROP of specified species
			1 = ROP of all species
			0 = no ROP
0.01			ROP threshold

CO	1	Specified species
NO	1	
NH3	1	
END		
2		Input flag: 0 = no SENS. analysis 1 = SENS. for all species 2 = SENS. for specified species 3 = SENS. for Temp.
0.1	0.1	Thresholds of species and Temp. SENS
HCN	1	Specified species
NO	1	
END		

APPENDIX D

REACTION MECHANISM

(used for $C_2H_4/CH_3Cl/CH_3NH_2/air/N_2$ combustion)

ELEMENTS
H O C CL N

SPECIES
CH3NH2 CH2NH2 CH3NH CH2NH CHNH
NH2CL NOCL NO2CL NHCL NCL CNCL
OH CH NO NH CN O CH3 C2H6 CH4 CH3O CH2OH
CH2 CH2S C2H4 C2H CH2O C2H5 C2H2 CH2CO
C C4H2 C3H3 C3H2 C4H3 O2 H HO2 H2 H2O CO2 CO HCO HCCO HCCOH
H2O2 N H2CN HCN HCNO HOCN HNCO NCO C2N2 NO2 NH2 N2O
NNH NH3 HNO N2H2 C2H3 N2
CH3CL HCL C2H3CL CH2CL2 CL2 CCLO COCL2
CLO HOCL CL C2H5CL CHCLO CH2CCL2 CHCLCHCL
CHCL3 C2HCL3 C2H3CL3 CHCL2 CH2CL CH2CLCCL2 CH2CLCHCL
CH3CCL3 CH3CCL2 CCL3CH2 CH3CHCL2 CH3CHCL
CCL CCL2 CCL3 CCL4 CH2CCL CHCL2CH2 CH2CLCH2 CH2CLOO C2HCL CHCL
C2H2CL3 C2CL2 C2H2CL4 C2H4CL2 CH2CLO

REACTIONS	A	n	E_a	Source
CH3NH2 + CL = CH2NH2 + HCL	5.4E13	0	1000	a
CH3NH2 + CL = CH3NH + HCL	5.0E13	0	3000	a
CL + NH3 = NH2 + HCL	5.8E12	0	6000	a
CL + NH2 = NH2CL (QRRK)	2.9E22	-3.7	1850	a
CL + NH2 = NH + HCL (QRRK)	3.3E14	-0.12	101	a
CL + NH2 = NHCL + H (QRRK)	3.7E16	-0.73	40830	a
CL + NH = NHCL (QRRK)	4.3E13	-1.86	370	a
CL + NH = N + HCL (QRRK)	1.6E14	-0.01	10	a
CL + NH = NCL + H (QRRK)	4.2E09	0.6	4090	a
NH2CL + OH = H2O + NHCL	2.1E13	0	2500	a
NHCL + OH = H2O + NCL	1.5E13	0	1200	a
NHCL + H = H2 + NCL	2.0E13	0	1500	a
NHCL + N = N2 + HCL	3.0E13	0	0	a
NH2CL + CL = HCL + NHCL	2.5E13	0	2700	a
NH2CL + H = H2 + NHCL	3.9E12	0	5000	a
N + CL + M = NCL + M H2O/3.0/N2/5.0/HCL/5.0/	8.5E17	0	0	a

N + CL2 = NCL + CL		3.5E12	0	5800	a
CN + CL + M = CNCL + M		4.0E16	0	0	a
H2O/3.0/N2/5.0/HCL/5.0/					
NCL + NCL = N2 + CL2	(NIST)	5.8E13	0	0	a
NCL + N = N2 + CL	(NIST)	7.6E14	0	0	a
HCN + CL = HCL + CN	(NIST)	1.0E14	0	19000	a
CN + CL2 = CNCL + CL	(NIST)	3.6E12	0	0	a
CNCL + N = N2 + CCL	(NIST)	1.0E13	0	0	a
CL + NO + M = NOCL + M	(NIST)	1.7E17	-1.39	340	a
NOCL + H = NO + HCL	(NIST)	4.6E13	0	910	a
NOCL + CL = NO + CL2	(NIST)	4.0E13	0	-350	a
CH3 + NH2 = CH3NH2	(QRRK)	2.7E54	-12.1	22700	a
CH3 + NH2 = CH2NH2 + H	(QRRK)	3.8E15	-0.64	14530	a
CH3 + NH2 = CH3NH + H	(QRRK)	4.4E13	-0.31	16637	a
CH3 + NH2 = CH2NH + H2	(QRRK)	6.2E27	-4.73	13000	a
CH3NH2 + CH3 = CH2NH2 + CH4		5.0E13	0.0	19400	a
CH3NH2 + NH2 = CH2NH2 + NH3		1.1E12	0.0	9900	a
CH3NH2 + H = CH2NH2 + H2		7.2E08	1.0	4908	b
CH3NH2 + H = CH3 + NH3		3.9E14	0.0	11428	c
CH2NH2 = CH2NH + H		1.2E12	0.0	41000	a
CH2NH = CHNH + H	(QRRK)	2.4E15	-0.53	3500	a
CHNH + H = HCN + H2	(QRRK)	5.5E27	-4.43	6970	a
CH2NH + H = CHNH + H2		1.5E14	0.0	10169	a
CHNH = HCN + H		6.9E12	0.0	21000	a
CH3NH2 + O2 = CH2NH2 + HO2		4.0E12	0.0	42000	c
CH3NH2 + O = CH2NH2 + OH		5.4E12	0.0	1643	c
CH3NH2 + OH = CH2NH2 + H2O		1.9E12	0.0	1790	a
CH3NH2 + HO2 = CH2NH2 + H2O2		1.6E12	0.0	6400	c
CH2NH2 + O2 = CH2NH + HO2		9.1E13	0.0	9800	c
CH2NH2 + O = CH2NH + OH		5.0E13	0.0	0.0	c
CH2NH2 + OH = CH2NH + H2O		2.4E13	0.0	0.0	a
CH2NH + O = CHNH + OH		4.0E14	0.0	19000	a
CH2NH + OH = CHNH + H2O		3.0E13	0.0	3000	a
CHNH + O = HCN + OH		3.0E13	0.0	0.0	c
H2CNH + O = CH2O + NH		1.7E06	2.1	0.0	b
CH3NH = CH2NH + H		1.3E42	-9.2	41337	b
CH3 + CH3 = C2H6	(QRRK)	4.00E57	-13.00	24800	a
CH3 + CH3 = C2H5 + H	(QRRK)	4.03E18	-1.620	16080	a
CH3 + CH3 = C2H4 + H2	(QRRK)	5.60E35	-7.080	20050	a
CH3+H+M=CH4+M		6.00E16	-1.000	0.	d
H2/2.0/CO/2.0/CO2/3.0/H2O/5.0/					
CH2OH + H = CH3 + OH		1.00E14	0.000	0	d
CH2OH + H = CH2O + H2		2.00E13	0.000	0.	d
CH2OH + OH = CH2O + H2O		1.00E13	0.000	0.	d
CH2OH + O = CH2O + OH		1.00E13	0.000	0.	d

CH2OH + O2 = CH2O + HO2		1.48E+13	0.000	1500.	d
CH2 + H = CH + H2		5.00E+13	0.000	0.	d
CH2 + OH = CH + H2O		1.13E+07	2.000	3000.	d
CH2 + OH = CH2O + H		2.50E+13	0.000	0.	d
CH + O2 = HCO + O		3.30E+13	0.000	0.	d
CH + O = CO + H		5.70E+13	0.000	0.	d
CH + OH = HCO + H		3.00E+13	0.000	0.	d
CH + CO2 = HCO + CO		3.40E+12	0.000	690.	d
CH + H2O = CH3O		5.71E+12	0.00	-750.	d
CH + H = C + H2		1.50E+14	0.0	0.0	d
CH + CH2O = CH2CO + H		9.46E+13	0.000	-515.	d
CH + C2H2 = C3H2 + H		1.00E+14	0.000	0.	d
CH + CH2 = C2H2 + H		4.00E+13	0.000	0.	d
CH + CH3 = C2H3 + H		3.00E+13	0.000	0.	d
CH + CH4 = C2H4 + H		6.00E+13	0.000	0.	d
C + O2 =CO + O		2.0E+13	0.00	0.	d
C + OH = CO + H		5.0E+13	0.0	0.0	d
C + CH3 = C2H2 +H		5.00E+13	0.0	0.0	d
C + CH2 = C2H + H		5.00E+13	0.0	0.0	d
CH2 + CO2 = CH2O + CO		1.10E+11	0.000	1000.	d
CH2 + O = CO + 2H		5.00E+13	0.000	0.	d
CH2 + O = CO + H2		3.00E+13	0.000	0.	d
CH2 + O2 = CO2 + 2H		1.60E+12	0.000	1000.	d
CH2 + O2 = CH2O + O		5.00E+13	0.000	9000.	d
CH2 + O2 = CO2+ H2		6.90E+11	0.000	500.	d
CH2 + O2 = CO+ H2O		1.90E+10	0.000	-1000.	d
CH2 + O2 = CO+ OH + H		8.60E+10	0.000	-500.	d
CH2 + O2 = HCO + OH		4.30E+10	0.000	-500.	d
C2H4 + O = CH3 + HCO		1.60E+09	1.200	746.	d
CH2 + CH3 = C2H4 + H		3.00E+13	0.000	0.	d
H + C2H4 = C2H5	(QRRK)	3.20E+47	-10.10	20070	d
H + C2H2 + M = C2H3 + M		5.54E+12	0.00	2410.	d
H2/2.0/CO/2.0/CO2/3.0/H2O/5.0/					
C2H3 + O = CH2CO + H		3.00E+13	0.000	0.	d
C2H3 + OH = C2H2 + H2O		5.00E+12	0.000	0.	d
C2H3 + CH2 = C2H2 + CH3		3.00E+13	0.000	0.	d
C2H3 + C2H = 2C2H2		3.00E+13	0.000	0.	d
C2H3 + CH = CH2 + C2H2		5.00E+13	0.000	0.	d
OH + C2H2 = HCCOH + H		5.04E+05	2.300	13500.	d
HCCOH + H = CH2CO + H		1.00E+13	0.00	0.	d
C2H + O2 = 2CO + H		5.00E+13	0.000	1500.	d
C2H + C2H2 = C4H2 + H		3.00E+13	0.000	0.	d
H + HCCO = CH2 + CO		1.00E+14	0.000	0.	d
O + HCCO = H + 2CO		1.00E+14	0.000	0.	d
O2 + HCCO = OH+ 2CO		1.60E+12	0.000	854.	d

CH + HCCO = C2H2 + CO	5.00E+13	0.000	0.	d
CH2S + C2H6 = CH3 + C2H5	1.2E+14	0.0	0.0	d
CH2S + O2 = CO + OH + H	3.0E+13	0.0	0.0	d
CH2S + H = CH2 + H	2.0E+14	0.0	0.0	d
2HCCO = C2H2 + 2CO	1.00E+13	0.000	0.	d
C2H + O = CH + CO	5.00E+13	0.000	0.	d
C2H + OH = HCCO + H	2.00E+13	0.000	0.	d
2CH2 = C2H2 + H2	4.00E+13	0.000	0.	d
CH2 + HCCO = C2H3 + CO	3.00E+13	0.000	0.	d
CH2 + C2H2 = C3H3+ H	1.20E+13	0.000	6600.	d
C4H2 + OH = C3H2 + HCO	6.66E+12	0.000	-410.	d
C3H2 + O2 = HCO + HCCO	1.00E+13	0.000	0.	d
C3H3 + O2 = CH2CO + HCO	3.00E+10	0.000	2868.	d
C3H3 + O = CH2O + C2H	2.00E+13	0.000	0.	d
C3H3 + OH = C3H2 + H2O	2.00E+13	0.000	0.	d
2C2H2 = C4H3 + H	2.00E+12	0.000	45900.	d
C4H3 + M = C4H2 + H + M	1.00E+16	0.000	59700.	d
CH2S + C2H2 = C3H3 + H	3.0E+13	0.0	0.0	d
C4H2 + O = C3H2 + CO	1.20E+12	0.000	0.	d
C2H2 + O2 = HCCO + OH	2.00E+08	1.500	30100.	d
C2H2 + M = C2H + H + M	4.20E+16	0.000	107000.	d
C2H4+ M = C2H2 + H2 + M	1.50E+15	0.000	55800.	d
C2H4 + M = C2H3 + H + M	1.40E+15	0.000	82360.	d
H2 + O2 = 2OH	1.70E+13	0.000	47780.	d
2H + M = H2 + M	1.00E+18	-1.000	0.	d
H2/0.0/H2O/0.0/CO2/0.0/				
2H + H2 = 2H2	9.20E+16	-0.600	0.	d
2H + H2O = H2 + H2O	6.00E+19	-1.250	0.	d
2H + CO2 = H2 + CO2	5.49E+20	-2.000	0.	d
CH + N2 = HCN + N	1.00E+12	0.000	19200.	e
CN + N = C + N2	1.04E+15	-0.5	0.0	d
CH2 + N2 = HCN + NH	1.00E+13	0.000	74000.	d
H2CN + N = N2 + CH2	2.00E+13	0.000	0.	d
H2CN + M = HCN + H + M	3.00E+14	0.000	22000.	d
CH + NO = HCN + O	5.30E+13	0.000	0.	b
CH2 + NO = HCNO + H	1.39E+12	0.000	-1100.	d
CH3 + NO = HCN + H2O	1.00E+11	0.000	15000.	d
CH3 + NO = H2CN + OH	1.00E+11	0.000	15000.	d
HCCO + NO = HCNO + CO	2.00E+11	0.000	0.	d
CH2S + NO = HCN + OH	2.00E+13	0.000	0.	d
HCNO + H = HCN + OH	1.00E+14	0.000	1200.	d
CH2 + N = HCN + H	5.00E+13	0.000	0.	d
CH+N=H+CN	1.30E+13	0.000	0.	d
CO2 + N = NO + CO	1.90E+11	0.000	3400.	d
HCCO + N = HCN + CO	5.00E+13	0.000	0.	d

CH3 + N = H2CN + H	3.00E+13	0.000	0.	d
C2H3 + N = HCN + CH2	2.00E+13	0.000	0.	d
C3H3 + N = HCN + C2H2	1.00E+13	0.000	0.	d
HCN+OH=CN+H2O	1.45E+13	0.000	10929.	d
HCN + OH = HOCN + H	5.85E+04	2.400	12500.	d
HCN + OH = HNCO + H	9.20E+11	0.000	0.0	d
HCN + OH = NH2 + CO	6.50E+10	0.000	11000.	d
HOCN + H = HNCO + H	1.00E+13	0.000	0.	d
HCN + O = NCO + H	1.38E+04	2.640	4980.	d
HCN + O = NH + CO	3.45E+03	2.640	4980.	d
HCN+O=CN+OH	2.70E+09	1.580	29200.	d
CN+H2= HCN + H	2.95E+05	2.450	2237.	d
CN +O= CO + N	1.80E+13	0.000	0.	d
CN + O2 = NCO + O	5.60E+12	0.000	0.	d
CN + OH = NCO + H	6.00E+13	0.000	0.	d
CN + HCN = C2N2 + H	2.00E+13	0.000	0.	d
CN + NO2 = NCO + NO	3.00E+13	0.000	0.	d
CN + N2O = NCO + N2	1.00E+13	0.000	0.	d
C2N2 + O = NCO + CN	4.57E+12	0.000	8880.	d
C2N2 + OH = HOCN + CN	1.86E+11	0.000	2900.	d
HO2 + NO = NO2 + OH	2.11E+12	0.000	-479.	d
NO2 + H = NO + OH	3.50E+14	0.000	1500.	d
NO2 + O = NO + O2	1.00E+13	0.000	600.	d
NO2 + M = NO + O + M	1.10E+16	0.000	66000.	d
NCO + H = NH + CO	5.00E+13	0.000	0.	d
NCO + O = NO + CO	2.00E+13	0.000	0.	d
NCO + N = N2 + CO	2.00E+13	0.000	0.	d
NCO + OH = NO + CO + H	1.00E+13	0.000	0.	d
NCO + M = N + CO + M	3.10E+16	-0.500	48000.	d
NCO + NO = N2O + CO	1.00E+13	0.000	-390.	d
NCO + H2 = HNCO + H	8.58E+12	0.000	9000.	d
HNCO + H = NH2 + CO	2.00E+13	0.000	3000.	d
NH + O2 = HNO + O	1.00E+13	0.000	12000.	d
NH + O2 = NO + OH	7.60E+10	0.000	1530.	d
NH + NO = N2O + H	2.40E+15	-0.800	0.	d
N2O + OH = N2 + HO2	2.00E+12	0.000	10000.	d
N2O + H = N2 + OH	7.60E+13	0.000	15200.	d
N2O + M = N2 + O + M	1.60E+14	0.000	51600.	d
N2O + O = N2 + O2	1.00E+14	0.000	28200.	d
N2O + O = 2NO	1.00E+14	0.000	28200.	d
NH + OH = HNO + H	2.00E+13	0.200	0.	d
NH + OH = N + H2O	5.00E+11	0.500	2000.	d
NH + N = N2 + H	3.00E+13	0.000	0.	d
NH + H = N + H2	1.00E+14	0.000	0.	d
NH2 + O = HNO + H	6.63E+14	-0.500	0.	d

NH2 + O = NH + OH		6.75E+12	0.000	0.	d
NH2 + OH = NH + H2O		4.00E+06	2.000	994.	b
NH2 + H = NH + H2		6.92E+13	0.000	3650.	d
NH2 + NO = NNH + OH		6.40E+15	-1.250	0.	d
NH2 + NO = N2 + H2O		6.20E+15	-1.250	0.	d
NH3 + OH = NH2 + H2O		5.0E+07	1.60	954.	b
NH3 + H = NH2 + H2		6.36E+05	2.390	10171.	d
NH3 + O = NH2 + OH		2.10E+13	0.000	9000.	d
NNH = N2 + H		1.00E+04	0.000	0.	d
NNH + NO = N2 + HNO		5.00E+13	0.000	0.	d
NNH + H = N2 + H2		1.00E+14	0.000	0.	d
NNH + OH = N2 + H2O		5.00E+13	0.000	0.	d
NNH + NH2 = N2 + NH3		5.00E+13	0.000	0.	d
NNH + NH = N2 + NH2		5.00E+13	0.000	0.	d
NNH + O = N2O + H		1.00E+14	0.000	0.	d
HNO + M = H + NO + M		1.50E+16	0.000	48680.	d
H2O/10.0/O2/2.0/N2/2.0/H2/2.0/					
HNO + OH = NO + H2O		3.60E+13	0.000	0.	d
HNO + H = H2 + NO		5.00E+12	0.000	0.	d
HNO + NH2 = NH3 + NO		2.00E+13	0.000	1000.	d
N + NO = N2 + O		3.27E+12	0.100	0.	d
N + O2 = NO + O		6.40E+09	1.000	6280.	d
N + OH = NO + H		3.80E+13	0.000	0.	d
NNH+O=N2+OH		1.0E14	0.0	0.0	d
2HNO=H2O+N2O		3.95E12	0.0	5000.	d
HNO+NO=N2O+OH		2.0E12	0.0	26000.	d
NH2 + NH = N2H2+H		5.0E13	0.0	0.0	d
2NH=N2+2H		2.54E13	0.0	0.0	d
NH2+N=N2+2H		7.2E13	0.0	0.	d
N2H2+M=NNH+H + M		5.0E16	0.0	50000.	d
H2O/15./O2/2.0/N2/2.0/H2/2.0/					
N2H2 + H = NNH + H2		5.0E13	0.0	1000.	d
N2H2+O=NNH+OH		2.0E13	0.0	1000.	d
N2H2+O=NH2+NO		1.0E13	0.0	0.0	d
N2H2+OH=NNH+H2O		1.0E13	0.0	1000.	d
N2H2+NO=N2O+NH2		3.0E12	0.0	0.0	d
N2H2+NH=NNH+NH2		1.0E13	0.0	1000.	d
N2H2+NH2=NH3+NNH		1.0E13	0.0	1000.	d
2NH2=N2H2+H2		5.0E11	0.0	0.0	d
NH2+O2=HNO+OH		4.5E12	0.0	25000.	d
C2H6+CH3=C2H5+CH4		2.7E-01	4.0	8280.	f
CH3+C2H5=CH4+C2H4		5.5E+11	0.	0.	f
CH2CL2 = CHCL + HCL		8.73E37	-7.68	86730.	f
CH2CL2 = CH2CL + CL		7.40E40	-7.87	84990.	f
CH2CL + H = CH3 + CL	(QRRK)	5.21E14	-0.42	830.	a

CH2CL + H = CH3Cl	(QRRK)	8.80E29	-5.7	6070.	a
CH2CL + H = CH2S + HCL	(QRRK)	1.40E12	0.0	35050.	a
CH2CL2 + H = CH2CL + HCL		7.00E13	0.00	7100.	f
CHCL2 + H2 = CH2CL2 + H		4.63E12	0.00	15295.	f
CH2CL + H2 = CH3CL + H		3.90E12	0.00	14059.	f
CH2CL2 + CL = CHCL2 + HCL		2.79E13	0.00	2940.	f
CH3CL + H = CH3 + HCL		6.64E13	0.00	7620.	f
CH4 = CH3 + H		1.03E33	-5.58	111810.	f
CH4 + H = CH3 + H2		1.55E14	0.00	11000.	f
CH4 + CL = CH3 + HCL		3.09E13	0.00	3600.	f
CH3CL + CL = CH2CL + HCL		3.16E13	0.00	3300.	f
CH2CL2 + CH3 = CH4 + CHCL2		6.76E10	0.00	7200.	f
CH2CL2 + CH3 = CH3CL + CH2CL		1.40E11	0.00	4900.	f
CH3CL + CH3 = CH4 + CH2CL		3.30E11	0.00	9400.	f
CHCL2 + CHCL2 = C2H2CL4		9.08E45	-10.56	13170.	f
CHCL2 + CHCL2 = C2H2CL3 + CL		1.36E30	-5.23	14180.	f
CHCL2 + CHCL2 = C2HCL3 + HCL		6.72E35	-7.11	13210.	f
CH2CL + CH2CL = C2H4CL2		7.84E45	-10.21	13150.	f
CH2CL + CH2CL = CH2CLCH2 + CL		9.34E29	-4.94	14070.	f
CH2CL + CH2CL = C2H3CL + HCL		3.75E35	-6.73	13160.	f
CH2CL + CHCL2 = C2H3CL3		6.41E33	-10.22	12910.	f
CH2CL + CHCL2 = CH2CCL2 + HCL		3.75E36	-7.22	13620.	f
CH2CL + CHCL2 = CHCLCHCL + HCL		1.22E37	-7.20	13640.	f
CH2CL + CH3 = C2H5CL		3.27E40	-8.49	10590.	f
CH2CL + CH3 = C2H4 + HCL		1.48E21	-2.19	5207.	f
CH2CL + CH3 = C2H5 + CL		9.27E19	-2.07	10130.	f
CHCL2 + CH3 = CH3CHCL2		2.28E41	-8.68	11620.	f
CHCL2 + CH3 = C2H3CL + HCL		1.35E30	-4.96	11550.	f
CHCL2 + CH3 = CH3CHCL + CL		2.74E25	-3.45	12810.	f
CHCL2 + H = CH2CL2		4.81E26	-4.82	3810.	f
CHCL2 + H = CH2CL + CL		1.25E14	-0.03	570.	f
C2H3CL + H = CH2CLCH2		5.01E23	-4.21	8470.	f
C2H3CL + H = C2H4 + CL		1.55E13	-0.02	5840.	f
C2H3CL + H = C2H3 + HCL		1.20E12	0.00	15000.	f
C2HCL3 + H = CH2CLCCL2		1.51E23	-4.18	7520.	f
C2HCL3 + H = C2H2CL3		2.87E22	-4.09	10890.	f
C2HCL3 + H = CH2CCL2 + CL		1.45E13	-0.01	5830.	f
C2HCL3 + H = CHCLCHCL + CL		7.37E12	-0.01	9220.	f
C2H3CL3 = CHCLCHCL + HCL		1.39E20	-2.03	60450.	f
C2H3CL3 = CH2CCL2 + HCL		3.13E19	-2.02	60330.	f
CH3CHCL2 = C2H3CL + HCL		2.94E21	-2.37	59460.	f
CH3CHCL2 = CH3CHCL + CL		3.17E42	-8.10	92670.	f
C2H2CL4 = C2HCL3 + HCL		8.62E21	-2.57	51870.	f
C2H4CL2 = C2H3CL + HCL		6.76E19	-1.93	58710.	f
C2H5CL = C2H4 + HCL		7.81E19	-2.00	60660.	f

C2H5CL = C2H5 + CL	2.35E43	-8.50	96980.	f
C2H5CL + CL = HCL + CH3CHCL	3.55E13	0.00	1500.	f
C2H5CL + CL = HCL + CH2CLCH2	1.12E13	0.00	1500.	f
C2H5CL + H = HCL + C2H5	1.00E14	0.00	7900.	f
C2H3CL = C2H2 + HCL	1.62E28	-4.29	75780.	f
C2H3CL = C2H3 + CL	1.71E38	-7.13	96370.	f
C2H4 = C2H2 + H2	8.52E43	-8.32	121240.	f
C2H4 = C2H3 + H	8.53E30	-5.87	118240.	f
CH2CCL2 + H = C2H3CL+ CL	7.21E12	0.00	7510.	f
CHCLCHCL + H = C2H3CL + CL	3.44E13	-0.03	5890.	f
C2H6 + H = C2H5 + H2	5.4E2	3.6	5210.	f
C2H6 + CL = C2H5 + HCL	4.6E13	0.00	179.	f
C2H6 + O = C2H5 + OH	2.51E13	0.00	6400.	f
C2H6 + OH = C2H5 + H2O	6.3E06	2.0	645.0	f
C2H5 + O = CH2O + CH3	1.00E13	0.00	0.0	f
C2H5 + O2 = C2H4 + HO2	2.00E12	0.00	4992.	f
C2H5 + HO2 = C2H4 + H2O2	3.01E11	0.00	0.0	f
C2H4 + OH = C2H3 + H2O	3.5E13	0.0	3012.	f
C2H4 + CH3 = CH4 + C2H3	4.20E11	0.00	11113.	f
C2H4 + O2 = C2H3 + HO2	4.22E13	0.00	57623.	f
C2H4 + H = C2H3 + H2	6.92E14	0.00	14500.	f
C2H4 + CL = C2H3 + HCL	1.0E14	0.00	7000.	f
C2H3 = C2H2 + H	9.3E22	-3.7	37255.0	f
C2H3 + O2 = C2H2 + HO2	1.6E13	0.00	10400.0	f
C2H3 + O2 = HCO + CH2O	3.97E12	0.00	-250.	f
C2H3 + H = C2H2 + H2	1.0E13	0.0	0.0	f
C2H3 + CL = C2H2 + HCL	1.0E13	0.0	0.0	f
C2H2 + CL = C2H + HCL	1.58E14	0.00	16900.	f
C2H2 + O2 = C2H + HO2	1.21E13	0.00	74520.	f
C2H2 + O = CO + CH2	4.10E08	1.50	1697.	f
C2H2 + O = HCCO + H	4.0E14	0.00	10660.	f
C2H2 + OH = C2H + H2O	1.45E04	2.68	12040.	f
C2H2 + OH = CH2CO + H	3.00E12	0.00	1100.	f
C2H + O2 = CO + HCO	2.41E12	0.00	0.0	f
C2H + H2 = C2H2 + H	1.15E13	0.00	2880.	f
C2H + CH4 = C2H2 + CH3	1.81E12	0.00	500.	f
C2H + OH = CH2 + CO	1.81E13	0.00	0.0	f
C2H + OH = C2H2 + O	1.81E13	0.00	0.0	f
HCCO + H = CH2S + CO	3.00E13	0.00	0.0	f
CH2CO + O = CH2 + CO2	1.74E12	0.00	1350.	f
CH2CO + H = HCCO + H2	5.00E13	0.00	8000.	f
CH2CO + O = HCCO + OH	1.00E13	0.00	8000.	f
CH2CO + OH = HCCO + H2O	7.50E12	0.00	2000.	f
CH2CO + M = CH2 + CO + M	3.00E15	0.00	75980.	f
CH2CO + OH = HCO + CH2O	2.80E13	0.00	0.0	f

CH2CO + H = CH3 + CO	1.50E04	2.83	672.8	f
CH2S + M = CH2 + M	1.00E13	0.00	0.0	f
CH2S + O2 = CO + H2O	2.41E11	0.00	0.0	f
CH2S + CH4 = C2H5 + H	9.43E12	-0.13	6620.	f
CH2S + CH4 = CH3 + CH3	3.45E22	-2.48	7460.	f
CH2S + CH4 = C2H6	5.78E46	-10.31	12830.	f
CH2S + CH3CL = C2H5CL	7.85E31	-6.15	5830.	f
CH2S + CH3CL = C2H4 + HCL	1.60E18	-1.47	2710.	f
CH2S + CH3CL = C2H5 + CL	3.09E07	1.70	520.	f
CH2S + H2 = CH4	3.82E25	-4.47	3770.	f
CH2S + H2 = CH3 + H	1.27E14	-0.08	130.	f
CH2 + CH4 = CH3 + CH3	1.82E05	0.00	0.0	f
CH2 + CH3CL = CH3 + CH2CL	9.10E04	0.00	0.0	f
CH2 + H2 = CH3 + H	3.01E09	0.00	0.0	f
CH2 + H2O = CH3 + OH	9.64E07	0.00	0.0	f
CH4 + O2 = CH3 + HO2	4.04E13	0.00	56910.	f
CH4 + O = CH3 + OH	1.02E09	1.5	8600.	f
CH4 + OH = CH3 + H2O	1.93E05	2.4	2110.	f
CH4 + HO2 = CH3 + H2O2	2.00E13	0.00	18000.	f
CH3 + O2 = CH2O + OH	3.59E09	-0.14	10150.	f
CH3 + O2 = CH3O + O	2.88E15	-1.15	30850.	f
CH3 + O = CH2O + H	7.00E13	0.00	0.0	f
CH3 + OH = CH3O + H	3.87E12	-0.19	13741.	f
CH3 + HO2= CH3O + OH	2.00E13	0.0	0.0	f
CH3O + O2 = CH2O + HO2	6.62E10	0.00	2600.	f
CH3O + M = CH2O + H + M	1.00E14	0.00	25100.	f
CH3O + CO = CO2 + CH3	1.57E13	0.00	11800.	f
CH3O + HO2 = CH2O + H2O2	3.01E11	0.00	0.0	f
CH3O + CH3 = CH4 + CH2O	2.41E13	0.00	0.0	f
CH3O + O = OH + CH2O	6.03E12	0.00	0.0	f
CH3O + OH = H2O + CH2O	1.81E13	0.00	0.0	f
CH3O + H = CH2O + H2	1.99E13	0.0	0.0	f
CH3O + CH2 = CH3 + CH2O	1.81E13	0.0	0.0	f
CH3O + C2H5 = C2H6 + CH2O	2.41E13	0.0	0.0	f
CH3O + CLO = HOCL + CH2O	2.41E13	0.0	0.0	f
CH3O + CL = HCL + CH2O	4.0E14	0.0	0.0	f
CH2O + CLO = HCO + HOCL	5.50E03	2.81	5860.	f
CH2O + C2H5 = HCO + C2H6	5.50E03	2.81	5860.	f
CH2O + CH3 = CH4 + HCO	1.00E11	0.00	6090.	f
CH2O + H = HCO + H2	2.50E13	0.00	3990.	f
CH2O + O = HCO + OH	3.50E13	0.00	3510.	f
CH2O + OH= HCO + H2O	3.00E13	0.00	1190.	f
CH2O + HO2= HCO + H2O2	1.00E12	0.00	8000.	f
CH2O + CL = HCO + HCL	5.00E13	0.00	500.	
CH2O + M = HCO + H + M	5.00E16	0.00	76200.	f

CH2O + O2 = HCO + HO2	2.05E13	0.00	38945.	f
HCO + M = H + CO + M	7.10E14	0.00	16802.	f
HCO + H = CO + H2	2.00E14	0.00	0.0	f
HCO + O2 = CO + HO2	3.0E12	0.00	0.0	f
HCO + O = CO + OH	3.01E13	0.00	0.0	f
HCO + O = H + CO2	3.01E13	0.00	0.0	f
HCO + OH = CO + H2O	3.01E13	0.00	0.0	f
CO + OH = CO2 + H	4.40E06	1.50	-740.	f
CO + HO2=CO2+OH	1.50E14	0.00	23573.	f
CO + O2 = CO2 +O	2.50E12	0.00	47800.	f
CO + O + M = CO2 + M	6.17E14	0.00	3000.	f
H + O2 = O + OH	1.2E17	-0.910	16504.	f
H+O2 = HO2	7.00E17	-0.80	0.0	f
O + H2O = OH + OH	1.5E10	1.14	17244.	f
H + OH + M =H2O + M	7.5E23	-2.6	0.0	f
O2 + M = O + O + M	1.20E14	0.00	107552.	f
H + O + M = OH + M	2.29E14	0.00	3900.	f
H + HO2=OH + OH	1.69E14	0.00	870.	f
H + HO2 = H2 + O2	6.62E13	0.00	2130.	f
O + HO2 = OH + O2	2.00E13	0.00	0.0	f
OH + HO2 = H2O + O2	2.00E13	0.00	0.0	f
OH + H2O2 = HO2 + H2O	1.75E12	0.0	320.	f
O + H2O2 = HO2 + OH	9.63E06	2.0	3970.	f
H + H2O2 = H2 + HO2	4.82E13	0.0	7950.	f
H + H2O2 = OH + H2O	2.41E13	0.0	3970.	f
O2 + H2O2 = HO2 + HO2	5.42E13	0.0	39740.	f
H2O2 + M = OH + OH + M	1.29E33	-4.86	53250.	f
O + HCL = OH + CL	5.24E12	0.00	6400.	f
OH + HCL = CL + H2O	1.58E13	0.00	1000.	f
H2 + OH = H2O + H	1.0E8	1.6	3296.	f
H2 + O = H + OH	1.5E7	2.0	7547.	f
CL + CL + M = CL2 + M	2.34E14	0.00	-1800.	f
H + CL + M = HCL + M	1.00E17	0.00	0.0	f
H + O2 + M = HO2 + M	7.0E17	-0.8	0.0	f
H + HCL = H2 + CL	7.90E12	0.00	3400.	f
CL + HO2= HCL + O2	1.08E13	0.00	-338.	f
CL + HO2 = CLO + OH	2.47E13	0.00	894.	f
CLO + CO = CL + CO2	6.03E11	0.00	17400.	f
CHCLO + H = HCO + HCL	8.33E13	0.00	7400.	f
CHCLO + H = CH2O + CL	6.99E14	-0.58	6360.	f
CH3 + CLO = CH3O + CL	3.33E11	0.46	30.	f
CH3 + CLO = CH2O + HCL	3.47E18	-1.80	2070.	f
CH2CL2 + O2 = CHCL2 + HO2	1.35E13	0.00	51800.	f
CH2CL2 + HO2 = CHCL2 + H2O2	6.67E12	0.00	18270.	f
CH2CL2 + OH = CHCL2 + H2O	2.83E12	0.00	2090.	f

CH2CL2 + O = CHCL2 + OH		6.00E12	0.00	5760.	f
CH2CL + O2 = CH2CLOO		2.73E33	-7.50	4440	f
CH2CL + O2 = CH2O + CLO		1.91E14	-1.27	3810.	f
CH2CL + O2 = CHCLO +OH		4.00E13	0.00	34000.	f
CH2CL + O = CH2CLO		1.29E15	-1.98	1100.	f
CH2CL + O = CH2O + CL		5.59E13	-0.13	710.	f
CH2CL + OH = CH2O + HCL	(QRRK)	3.41E18	-1.54	3370.	a
CH2CL + OH = CH3O + CL	(QRRK)	2.10E10	0.82	5980.	a
CH2CL + HO2 = CH2CLO + OH		1.00E13	0.00	0.0	f
CH2CLO = CHCLO + H		1.83E27	-5.13	21170.	f
CH2CLO = CH2O + CL		4.53E31	-6.41	22560.	f
CHCLO = HCO + CL		8.86E29	-5.15	92920.	f
CHCLO = CO + HCL		1.10E30	-5.19	92960.	f
CH2CL + CLO = CH2CLO + CL		4.15E12	0.07	1110.	f
CH2CL + CLO = CHCLO + HCL		4.13E19	-2.22	2360.	f
CH2CL + CH2O = CH3CL + HCO		2.00E11	0.00	6000.	f
CH3CL + O2 = CH2CL + HO2		2.02E13	0.00	54000.	f
CH3CL + O = CH2CL + OH		1.70E13	0.00	7300.	f
CH3CL + OH = CH2CL + H2O		2.45E12	0.00	2700.	f
CH3CL + HO2 = CH2CL + H2O2		1.00E13	0.00	21660.	f
H2O2 + CL = HCL + HO2		6.62E12	0.00	1950.	f
CLO + CH4 = CH3 + HOCL		6.03E11	0.00	15000.	f
CLO + CH3CL = CH2CL + HOCL		3.03E11	0.00	10700.	f
CLO + H2 = HOCL + H		6.03E11	0.00	14100.	f
OH + HOCL = H2O + CLO		1.81E12	0.00	990.	f
H + HOCL = HCL + OH		9.55E13	0.00	7620.	f
CL + HOCL = CL2 + OH		1.81E12	0.00	260.	f
CL + HOCL = HCL + CLO		7.28E12	0.00	100.	f
O + HOCL = OH + CLO		6.03E12	0.00	4370.	f
HOCL = CL + OH		1.76E20	-3.01	56720.	f
HOCL = H + CLO		8.12E14	-2.09	93690.	f
O + CL2 = CL + CLO		2.51E12	0.00	2720.	f
H + CL2 = HCL + CL		8.59E13	0.00	1170.	f
C2H3 + CL2 = C2H3CL + CL		5.25E12	0.00	-480.	f
CHCLO + OH = CCLO + H2O		7.5E12	0.00	1200.	f
CHCLO + O = CCLO + OH		8.8E12	0.00	3500.	f
CHCLO + O2 = CCLO + HO2		4.5E12	0.00	41800.	f
CHCLO + CL = CCLO + HCL		1.25E13	0.00	500.	f
CHCLO + CH3 = CCLO + CH4		2.5E13	0.00	6000.	f
CHCLO + CH3 = HCO + CH3CL		1.5E13	0.00	8800.	f
CHCLO + CLO = CCLO + HOCL		1.1E13	0.00	500.	f
CCLO + OH = CO + HOCL		3.3E12	0.00	0.0	f
CCLO + O2 = CO2 + CLO		1.0E13	0.0	0.0	f
CCLO + CL = CO + CL2		4.0E14	0.00	800.	f
COCL2 + M = CCLO + CL + M		1.2E16	0.00	75500.	f

COCL2 + OH = CCLO + HOCL	1.0E13	0.00	23300.	f
COCL2 + O = CCLO + CLO	2.0E13	0.00	17000.	f
COCL2 + H = CCLO + HCL	5.0E13	0.00	6300.	f
COCL2 + CL = CCLO + CL2	3.2E14	0.00	23500.	f
COCL2 + CH3 = CCLO + CH3CL	1.9E13	0.00	12900.	f
CHCL3 = CHCL2 + CL	5.7E12	0.00	67700.	f
CHCL3 = CCL2 + HCL	5.2E12	0.00	51500.	f
CHCL3 + OH = H2O + CCL3	3.3E12	0.00	2300.	f
CHCL3 + O2 = HO2 + CCL3	1.0E13	0.00	47200.	f
CHCL3 + HO2 = H2O2 + CCL3	4.5E10	0.00	14200.	f
CHCL3 + H = HCL + CHCL2	3.6E12	0.00	6200.	f
CHCL3 + O = OH + CCL3	3.00E12	0.00	4900.	f
CHCL3 + CH3 = CH3CL + CHCL2	2.4E13	0.00	12000.	f
CHCL3 + CL = HCL + CCL3	1.6E13	0.00	3300.	f
CCL3 + H2 = CHCL3 + H	5.01E12	0.00	14300.	f
CCL3 + CH4 = CHCL3 + CH3	5.00E12	0.00	14900.	f
CCL2 + O2 = COCL2 + O	5.78E10	0.00	4100.	f
CHCLCHCL = C2HCL + HCL	7.26E13	0.00	69090.	f
CH2CCL2 = C2HCL + HCL	1.45E14	0.00	69220.	f
C2HCL3 = C2CL2 + HCL	7.26E13	0.00	74440.	f
C2HCL + H = HCL + C2H	1.00E13	0.00	17030.	f
C2HCL + H = C2H2 + CL	2.00E13	0.00	2100.	f
CCL3 + CH3 = C2H3CL3	9.54E46	-10.66	11740.	f
CCL3 + CH3 = CH2CCL2 + HCL	1.62E30	-5.33	8640.	f
CCL3 + CH3 = CH3CCL2 + CL	3.98E22	-2.63	7090.	f
CCL3 + CH2CL = C2H2CL4	4.01E45	-10.15	10670.	f
CCL3 + CH2CL = C2HCL3 + HCL	4.74E30	-5.08	8810.	f
CCL3 + CH2CL = C2H2CL3 + CL	5.90E23	-2.84	8960.	f
CHCL + CHCL = CHCLCHCL	4.00E12	0.0	0.0	f
CHCL + O2 = CHCLO + O	1.50E13	0.0	2860.	f
CHCL + O = CHCLO	1.00E13	0.0	0.0	f
CHCL + O2 = CO + HOCL	1.20E11	0.0	0.0	f

a. Developed in this work.
b. Taken from Bozzelli and Dean (1994)
c. Taken from Hwang et al. (1990)
d. Taken from Miller and Bowman (1989)
e. Taken from Roth et al. (1984)
f. Taken from Ho et al. (1992) and Ho (1993)

Reaction Rate Constant: $k = A\ T^n \exp(-E_a / R / T)$; Units: K, second, cm^3 , cal / mole.

APPENDIX E

THERMODYNAMIC DATA

(Cl- and N-containing species)

UNITS:KCAL

SPECIES	HF(298)	S(298)	CP300	CP400	CP500	CP600	CP800	CP1000
			CP1500	CP2000	CP2500	CP3000	CP3500	CP4000	CP5000
N2	.00	45.77	6.85	6.99	7.14	7.28	7.54	7.79	8.28
			8.61	8.83	8.96	9.03	9.07	9.11	
N	112.98	36.61	4.97	4.97	4.97	4.97	4.97	4.97	4.97
			4.97	4.97	4.97	4.97	4.97	4.97	
N2H2	50.90	52.21	8.77	9.90	10.93	11.88	13.52	14.82	16.88
			17.99	18.63	18.98	19.17	19.30	19.54	
N2H3	36.79	54.64	10.58	12.35	13.92	15.30	17.56	19.25	21.81
			23.22	24.06	24.54	24.82	25.01	25.34	
N2H4	22.79	57.05	12.28	14.73	16.79	18.50	21.16	23.10	26.33
			28.22	29.36	30.02	30.41	30.68	31.11	
N2O	19.61	52.55	9.42	10.33	11.05	11.62	12.42	12.89	13.41
			13.63	13.74	13.79	13.81	13.82	13.87	
N2O+	318.78	55.89	10.22	11.02	11.68	12.22	13.03	13.57	14.34
			14.72	14.93	15.04	15.10	15.16	15.30	
N2O4	2.17	72.76	18.57	21.15	23.23	24.87	27.17	28.55	30.17
			30.87	31.23	31.39	31.46	31.51	31.65	
N3	99.03	54.11	9.67	10.72	11.52	12.10	12.82	13.18	13.57
			13.72	13.80	13.83	13.84	13.85	13.88	
NCO	38.10	55.50	9.57	10.47	11.22	11.83	12.74	13.34	14.09
			14.43	14.61	14.69	14.73	14.76	14.83	
NF	59.52	51.43	7.31	7.64	7.90	8.12	8.44	8.66	8.96
			9.11	9.18	9.22	9.24	9.26	9.31	
NFO	-15.70	59.30	9.92	10.63	11.20	11.67	12.35	12.79	13.33
			13.57	13.70	13.76	13.79	13.81	13.86	
NFO2	-26.00	62.21	12.02	13.65	14.94	15.95	17.33	18.13	19.01
			19.39	19.58	19.66	19.70	19.72	19.80	
NH	85.23	43.30	6.90	6.95	7.02	7.10	7.28	7.49	7.99
			8.37	8.62	8.77	8.85	8.89	8.93	
NH2	45.50	46.51	8.03	8.24	8.50	8.81	9.49	10.16	11.50

12.33 12.83 13.13 13.30 13.42 13.61

NH3 -10.97 46.04 8.53 9.30 10.08 10.84 12.30 13.59 15.94
17.32 18.15 18.62 18.90 19.09 19.40

NNH 58.59 53.63 8.47 8.95 9.43 9.91 10.78 11.52 12.62
13.14 13.43 13.56 13.61 13.66 13.79

NO 21.58 50.35 7.00 7.20 7.38 7.54 7.84 8.08 8.53
8.81 8.99 9.10 9.16 9.20 9.24

NO+ 236.72 47.35 7.41 7.41 7.41 7.41 7.41 7.41 7.41
7.41 7.41 7.41 7.41 7.41 7.41

NO2 7.91 57.36 8.89 9.70 10.38 10.95 11.83 12.41 13.13
13.46 13.63 13.71 13.75 13.77 13.84

NO2- -48.45 56.54 9.74 10.00 10.38 10.85 11.97 13.21 16.11
18.02 19.05 19.53 19.71 19.76 19.85

NO3 17.00 60.39 11.47 13.40 14.89 16.01 17.48 18.26 19.10
19.45 19.62 19.69 19.72 19.74 19.81

NH2OH -9.00 60.17 10.88 12.11 13.42 14.69 16.80 18.12 20.75
39.01 .00 .00 .00 .00 .00

NH2O 15.90 56.62 8.49 9.51 10.53 11.52 13.35 14.87 17.07
17.68 .00 .00 .00 .00 .00

NH2NO 17.90 61.22 12.12 14.36 16.23 17.81 20.31 22.19 24.02
16.10 .00 .00 .00 .00 .00

CH2N 59.03 53.60 8.53 9.55 10.54 11.50 13.24 14.69 16.96 S
18.09 18.73 19.03 19.19 19.30 19.57

CL 28.90 39.50 5.30 5.30 5.30 5.30 5.30 5.30 5.30
5.30 5.30 5.30 5.30 5.30 5.30

HCL -22.00 44.60 6.78 6.87 6.97 7.07 7.28 7.50 8.01
8.37 8.61 8.76 8.84 8.88 8.91

CL2 .00 53.30 8.19 8.36 8.49 8.61 8.80 8.94 9.15
9.26 9.33 9.37 9.39 9.40 9.42

CHCL 71.03 56.13 8.73 9.50 10.15 10.75 11.98 13.31 14.68
1.21 .00 .00 .00 .00 .00

CH2CL 26.10 59.63 9.25 10.18 11.12 12.07 14.01 15.88 18.28
10.75 .00 .00 .00 .00 .00

CCL2 52.10 49.00 10.98 11.91 12.52 12.93 13.50 14.07 15.39
8.76 .00 .00 .00 .00 .00

CHCL2 23.50 67.43 13.02 13.99 14.72 15.34 16.59 18.07 19.77

		.73	.00	.00	.00	.00	.00		
CCL3	19.00	71.03	15.13	16.61	17.52	18.07	18.68	19.21	19.48
		2.81	.00	.00	.00	.00	.00		
CCL4	-22.90	74.23	19.81	21.80	23.01	23.71	24.43	25.06	25.47
		3.40	.00	.00	.00	.00	.00		
CH3CL	-19.50	56.03	9.72	11.49	13.14	14.63	17.06	18.75	21.81
		32.45	.00	.00	.00	.00	.00		
CH2CL2	-22.80	64.53	12.22	14.16	15.81	17.20	19.32	20.78	22.90
		24.83	.00	.00	.00	.00	.00		
CHCL3	-24.20	70.63	15.66	17.77	19.29	20.39	21.84	22.86	24.19
		14.69	.00	.00	.00	.00	.00		
C2HCL	46.90	58.13	13.08	14.24	15.11	15.78	16.76	17.54	18.79
		14.42	.00	.00	.00	.00	.00		
C2CL2	50.10	65.03	15.66	16.74	17.47	17.97	18.69	19.39	19.98
		6.53	.00	.00	.00	.00	.00		
C2H3CL	8.40	63.03	12.39	15.17	17.61	19.68	22.58	24.04	26.83
		49.26	.00	.00	.00	.00	.00		
CH2CCL2	.60	69.23	15.83	18.36	20.48	22.21	24.66	26.05	28.21
		37.39	.00	.00	.00	.00	.00		
CHCLCHCL	.70	69.23	15.83	18.36	20.48	22.21	24.66	26.05	28.21
		37.39	.00	.00	.00	.00	.00		
CH2CCL	60.43	64.43	11.29	14.02	16.30	18.21	21.16	23.33	26.79
		26.56	.00	.00	.00	.00	.00		
C2H2CL	60.43	64.43	11.29	14.02	16.30	18.21	21.16	23.33	26.79
		26.56	.00	.00	.00	.00	.00		
CCL2CH	58.23	68.83	17.43	20.19	22.18	23.62	25.57	27.02	28.57
		12.18	.00	.00	.00	.00	.00		
C2HCL2	58.23	68.83	17.43	20.19	22.18	23.62	25.57	27.02	28.57
		12.18	.00	.00	.00	.00	.00		
C2HCL3	-1.40	77.63	19.21	21.78	23.71	25.11	26.80	27.60	28.90
		30.92	.00	.00	.00	.00	.00		
CH2CLCH2	20.70	68.53	14.06	17.23	20.00	22.37	25.95	28.27	33.42
		53.58	.00	.00	.00	.00	.00		
CH2CH2CL	20.70	68.53	14.06	17.23	20.00	22.37	25.95	28.27	33.42
		53.58	.00	.00	.00	.00	.00		
C2H4CL	17.50	67.33	14.19	16.98	19.61	21.97	25.59	27.74	32.53

		62.86	.00	.00	.00	.00	.00		
CH3CHCL	17.50	67.33	14.19	16.98	19.61	21.97	25.59	27.74	32.53
		62.86	.00	.00	.00	.00	.00		
CH3CCL2	10.50	73.63	17.30	20.15	22.73	24.96	28.21	29.92	33.03
		57.72	.00	.00	.00	.00	.00		
CHCL2CH2	16.40	74.33	17.39	20.19	22.76	25.00	28.29	30.03	33.03
		57.72	.00	.00	.00	.00	.00		
CH2CLCHCL	11.40	75.83	16.87	19.82	22.42	24.62	27.79	29.55	33.23
		55.61	.00	.00	.00	.00	.00		
C2H3CL2	11.40	74.33	17.30	20.15	22.73	24.96	28.21	29.92	33.03
		57.72	.00	.00	.00	.00	.00		
CH2CLCCL2	7.00	83.23	20.21	23.20	25.60	27.50	30.12	31.68	34.50
		41.52	.00	.00	.00	.00	.00		
CCL3CH2	11.90	82.93	20.21	23.20	25.60	27.50	30.12	31.68	34.50
		41.52	.00	.00	.00	.00	.00		
C2H2CL3	8.50	83.13	20.21	23.20	25.60	27.50	30.12	31.68	34.50
		41.52	.00	.00	.00	.00	.00		
C2H5CL	-26.80	66.03	15.26	18.24	21.40	24.39	28.89	30.98	36.28
		99.79	.00	.00	.00	.00	.00		
CH3CHCL2	-30.60	72.83	18.36	21.59	24.63	27.31	31.18	33.09	37.86
		82.00	.00	.00	.00	.00	.00		
C2H4CL2	-31.00	73.73	19.02	21.93	24.61	26.97	30.56	32.78	38.74
		71.30	.00	.00	.00	.00	.00		
CH2CLCH2CL	-31.00	73.73	19.02	21.93	24.61	26.97	30.56	32.78	38.74
		71.30	.00	.00	.00	.00	.00		
CH3CCL3	-30.90	78.63	22.60	25.58	28.28	30.60	33.90	35.53	38.93
		68.91	.00	.00	.00	.00	.00		
C2H3CL3	-30.90	78.63	22.60	25.58	28.28	30.60	33.90	35.53	38.93
		68.91	.00	.00	.00	.00	.00		
C2H2CL4	-37.20	86.03	25.26	28.54	31.22	33.35	36.12	37.39	39.82
		57.37	.00	.00	.00	.00	.00		
C2HCL4	5.80	87.93	23.46	26.54	28.77	30.37	32.39	33.69	35.68
		27.37	.00	.00	.00	.00	.00		
C2HCL5	-34.00	91.03	28.42	31.78	34.37	36.32	38.65	39.56	40.51
		48.02	.00	.00	.00	.00	.00		
C2CL6	-33.80	95.13	32.51	35.92	38.16	39.58	41.08	41.98	42.47

		19.55	.00	.00	.00	.00	.00		
C2CL5	7.50	92.23	27.42	30.31	32.26	33.56	35.13	36.24	36.77
		13.37	.00	.00	.00	.00	.00		
C2CL3	56.53	79.03	20.93	23.36	25.18	26.51	28.07	28.74	29.71
		32.66	.00	.00	.00	.00	.00		
C2CL4	-3.40	81.43	22.62	25.01	26.67	27.81	29.20	30.10	30.48
		14.80	.00	.00	.00	.00	.00		
CH2CLCHCL2	-35.40	81.53	21.12	24.53	27.51	29.99	33.41	35.10	38.94
		68.78	.00	.00	.00	.00	.00		
CLO	24.20	54.10	7.66	7.92	8.13	8.31	8.58	8.78	9.06
		9.20	9.28	9.32	9.35	9.36	9.40		
CL2O	21.00	64.03	11.35	12.26	12.77	13.04	13.29	13.59	13.78
		.66	.00	.00	.00	.00	.00		
CLO2	25.00	61.53	9.85	10.98	11.71	12.19	12.81	13.38	13.79
		.61	.00	.00	.00	.00	.00		
HOCL	-17.80	56.53	8.86	9.55	10.06	10.44	11.03	11.57	12.39
		6.96	.00	.00	.00	.00	.00		
COCL2	-52.60	67.83	13.74	15.26	16.27	16.94	17.79	18.50	19.18
		4.90	.00	.00	.00	.00	.00		
CHCLO	-39.30	61.83	11.05	12.47	13.54	14.37	15.60	16.59	18.08
		11.97	.00	.00	.00	.00	.00		
CLO	24.20	54.10	7.66	7.92	8.13	8.31	8.58	8.78	9.06
		9.20	9.28	9.32	9.35	9.36	9.40		
CL2O	21.00	64.03	11.35	12.26	12.77	13.04	13.29	13.59	13.78
		.66	.00	.00	.00	.00	.00		
OCLO	25.00	61.53	9.85	10.98	11.71	12.19	12.81	13.38	13.79
		.61	.00	.00	.00	.00	.00		
HOCL	-17.80	56.53	8.86	9.55	10.06	10.44	11.03	11.57	12.39
		6.96	.00	.00	.00	.00	.00		
COCL2	-52.60	67.83	13.74	15.26	16.27	16.94	17.79	18.50	19.18
		4.90	.00	.00	.00	.00	.00		
CHCLO	-39.30	61.83	11.05	12.47	13.54	14.37	15.60	16.59	18.08
		11.97	.00	.00	.00	.00	.00		
CCL	103.23	53.60	7.75	8.01	8.21	8.37	8.60	8.74	8.93
		9.01	9.04	9.05	9.06	9.06	9.09		
C2CL	125.93	59.33	11.42	12.02	12.44	12.76	13.37	14.12	14.98

		3.06	.00	.00	.00	.00	.00		
C2HCL2	58.63	70.63	17.43	20.19	22.18	23.62	25.57	27.02	28.57
		12.18	.00	.00	.00	.00	.00		
C2H2CL2	1.10	69.23	15.83	18.36	20.48	22.21	24.66	26.05	28.21
		37.39	.00	.00	.00	.00	.00		
PHCL2	7.10	81.43	28.47	33.50	39.38	44.96	52.34	53.08	56.32
		234.18	.00	.00	.00	.00	.00		
CC6H5CL	12.30	74.73	23.28	30.31	36.39	41.36	48.11	52.23	82.73
		253.24	.00	.00	.00	.00	.00		
PHPHCL	38.30	113.83	41.25	50.50	61.82	72.67	86.87	89.38	140.59
		731.33	.00	.00	.00	.00	.00		
PHCLPHCL	38.80	121.13	45.54	54.40	65.52	76.18	89.74	91.18	145.32
		781.36	.00	.00	.00	.00	.00		
CH2CLO	2.10	63.23	11.21	13.21	14.95	16.44	18.71	20.19	22.40
		28.44	.00	.00	.00	.00	.00		
CH2CLOO	3.50	73.13	15.77	16.71	18.10	19.68	22.65	24.66	27.03
		47.63	.00	.00	.00	.00	.00		
CH2OOCL	10.00	78.63	17.29	20.15	22.28	23.95	26.64	29.11	31.56
		2.71	.00	.00	.00	.00	.00		
CCLO	-4.00	63.53	10.75	11.27	11.65	11.94	12.42	12.88	13.38
		7.54	.00	.00	.00	.00	.00		
CH3NH2	-5.50	57.93	11.34	14.44	17.03	19.19	22.48	24.79	28.20
		29.97	31.06	31.86	32.64	33.54	35.57		
CH2NH2	36.20	57.93	13.01	15.00	16.74	18.25	20.74	22.66	25.81
		27.59	28.65	29.24	29.58	29.81	30.21		
CH2NH	21.80	55.93	9.03	10.86	12.51	13.99	16.47	18.37	21.27
		22.91	23.87	24.41	24.72	24.93	25.29		
CHNH	66.13	55.93	9.15	10.37	11.47	12.45	14.09	15.34	17.24
		18.24	18.80	19.10	19.26	19.38	19.59		
CH3NH	43.26	59.70	11.09	13.21	15.06	16.69	19.37	21.46	25.00
		27.16	28.58	29.50	30.13	30.60	31.32		
NH2CL	6.30	59.62	9.20	10.20	11.24	12.28	14.19	15.72	17.69
		18.60	19.08	19.30	19.41	19.49	19.67		
NOCL	12.35	62.52	10.64	11.28	11.79	12.20	12.76	13.10	13.50
		13.68	13.77	13.81	13.83	13.84	13.87		
NO2CL	2.90	65.03	12.75	14.25	15.40	16.26	17.38	18.01	18.84

		19.25	19.47	19.58	19.64	19.68	19.77		
NHCL	57.00	56.22	8.25	9.57	10.64	11.49	12.69	13.39	14.01
		14.15	14.19	14.17	14.15	14.14	14.17		
NCL	65.02	54.10	7.53	7.88	8.15	8.36	8.62	8.76	8.92
		9.01	9.08	9.12	9.12	9.09	9.00		
CNCL	33.00	56.52	10.85	11.61	12.22	12.71	13.38	13.80	14.34
		14.58	14.70	14.76	14.79	14.81	14.85		

APPENDIX F

QRRK CALCULATIONS

Input Parameters for QRRK Calculation of Reactions

$$NH + Cl \underset{k_{-1}}{\overset{k_1}{<==>}} [NHCl]^* \xrightarrow{k_2} N + HCl$$
$$\downarrow k_3$$
$$H + NCl$$

k		A (cm^3/mol/s)	E_a (cal/mol)
k_1		2.0E14	0
k_{-1}		8.2E14	53420
k_2		6.0E15	30300
k_3		6.4E13	58400
υ	1588 cm^{-1}		
σ	4.16 Å		
ε / κ	225 K		

k_1: A_1 from $CH_3 + Cl = CH_3Cl$; $E_a = 0$ for radical/radical combination reaction

k_{-1}: A_{-1} from A_1 and thermodynamics (NJIT Therm. code); $E_a = \Delta H_{rxn} - RT_m$

k_2: A_2 from A_{-2} and thermodynamics (NJIT Therm. code), A_{-2} from $N + N = N_2$; $E_a = \Delta H_{rxn} - RT_m$

k_3: A_3 from A_{-3} and thermodynamics (NJIT Therm. code), A_{-3} from $H + NH_2 = NH_3$; $E_a = \Delta H_{rxn} - RT_m$

υ, σ, and ε / κ taken from CHCl

Calculated Apparent Forward Reaction Rate Constants*

(P=760 torr; Bath gas: N_2)

Reaction	A (cm^3/mol/s)	n	E_a (cal/mol)
NH + Cl = NHCl	4.3E13	-1.90	370.0
NH + Cl = N + HCl	1.6E14	-0.01	10.0
NH + Cl = H + NCl	4.2E09	0.60	4090
NHCl = NH + Cl	1.2E08	1.25	960.0

* $k = A\ T^n \exp(-E_a/R/T)$

Input Parameters for QRRK Calculation of Reactions

$$NH_2 + Cl \underset{k_{-1}}{\overset{k_1}{<==>}} [NH_2Cl]^* \xrightarrow{k_2} NH + HCl$$
$$\downarrow k_3$$
$$H + NHCl$$

k		A (cm^3/mol/s)	E_a (cal/mol)
k_1		2.0E14	0
k_{-1}		9.0E14	64000
k_2		1.8E15	61100
k_3		1.4E15	102000
υ	1565 cm^{-1}		
σ	4.18 Å		
ε / κ	350 K		

k_1: A_1 from $CH_3 + Cl = CH_3Cl$; $E_a = 0$ for radical/radical combination reaction

k_{-1}: A_{-1} from A_1 and thermodynamics (NJIT Therm. code); $E_a = \Delta H_{rxn} - RT_m$

k_2: A_2 from A_{-2} and thermodynamics (NJIT Therm. code), A_{-2} from $CH_2 + HCl = CH_3Cl$; $E_a = \Delta H_{rxn} - RT_m$

k_3: A_3 from A_{-3} and thermodynamics (NJIT Therm. code), A_{-3} from $H + CH_3 = CH_4$; $E_a = \Delta H_{rxn} - RT_m$

υ, σ, and ε / κ taken from CH_3Cl

Calculated Apparent Forward Reaction Rate Constants*

(P=760 torr; Bath gas: N_2)

Reaction	A (cm^3/mol/s)	n	E_a (cal/mol)
$NH_2 + Cl = NH_2Cl$	2.9E22	-3.70	1850.0
$NH_2 + Cl = NH + HCl$	3.3E14	-0.12	101.0
$NH_2 + Cl = H + NHCl$	3.7E16	-0.73	40830
$NH_2Cl = NH_2 + Cl$	1.2E08	0.82	5800.0

* $k = A\ T^n \exp(-E_a/R/T)$

Input Parameters for QRRK Calculation of Reactions

$$NH_2 + CH_3 \underset{k_{-1}}{\overset{k_1}{\Longleftrightarrow}} [CH_3NH_2]^* \xrightarrow{k_2} CH_2NH_2 + H$$
$$\downarrow k_3$$
$$CH_2NH + H_2$$

k		A (cm^3/mol/s)	E_a (cal/mol)
k_1		2.4E13	0
k_{-1}		1.6E16	83400
k_2		1.3E16	95500
k_3		5.1E12	74000
υ	1509 cm^{-1}		
σ	4.3 Å		
ε / κ	252 K		

k_1: A_1 from $CH_3 + CH_3 = C_2H_6$, Baulch, D. L., et. al., *Comb. and Flame*, 37, p313(1980); $E_a = 0$ for radical/radical combination reaction

k_{-1}: A_{-1} from A_1 and thermodynamics (NJIT Therm. code); $E_a = \Delta H_{rxn} - RT_m$

k_2: A_2 from $C_2H_6 = C_2H_5 + H$, Dean, A. M., *J. Phys. Chem*, 89, p4600(1985). $E_a = \Delta H_{rxn} - RT_m$

k_3: $A_3 = (ekT_m / h) \exp(\Delta S^* / R)$ (transition state theory) × degeneracy, $\Delta S^* =$ -7.5, $E_a = \Delta H_{rxn} + 45$ (kcal / mol)

υ, σ, and ε / κ taken from C_2H_6

Calculated Apparent Forward Reaction Rate Constants*

(P=760 torr; Bath gas: N_2)

Reaction	A (cm^3/mol/s)	n	E_a (cal/mol)
$NH_2 + CH_3 = CH_3NH_2$	2.7E54	-12.1	22700
$NH_2 + CH_3 = CH_2NH_2 + H$	3.8E15	0.64	14500
$NH_2 + CH_3 = CH_2NH + H_2$	6.2E27	-4.73	13000
$CH_3NH_2 = NH_2 + CH_3$	4.0E22	-2.46	10220

* $k = A\ T^n \exp(-E_a/R/T)$

Input Parameters for QRRK Calculation of Reactions

$$CHNH + H \underset{k_{-1}}{\overset{k_1}{<==>}} [CH_2NH]^* \xrightarrow{k_2} HCN + H_2$$

k		A (cm^3/mol/s)	E_a (cal/mol)
k_1		2.0E13	0
k_{-1}		2.9E16	96100
k_2		5.0E12	58200
υ	1580 cm^{-1}		
σ	4.0 Å		
ε / κ	281 K		

k_1: A_1 from $C_2H_3 + H = C_2H_4$; $E_a = 0$ for radical/radical combination reaction

k_{-1}: A_{-1} from A_1 and thermodynamics (NJIT Therm. code); $E_a = \Delta H_{rxn} - RT_m$

k_2: $A_2 = (ekT_m / h) \exp(\Delta S^* / R)$ (transition state theory) × degeneracy, $\Delta S^* =$ -7.5, $E_a = \Delta H_{rxn} + 45$ (kcal / mol)

υ, σ, and ε / κ taken from C_2H_4

Calculated Apparent Forward Reaction Rate Constants*

(P=760 torr; Bath gas: N_2)

Reaction	A (cm^3/mol/s)	n	E_a (cal/mol)
CHNH + H = CH_2NH	2.4E35	-7.20	9160
CHNH + H = HCN + H_2	5.5E27	-4.43	6970
CH_2NH = CHNH + H	2.4E15	-0.53	3500

* $k = A\ T^n \exp(-E_a/R/T)$

Input Parameters for QRRK Calculation of Reactions

$$CH_3 + CH_3 \underset{k_{-1}}{\overset{k_1}{\Longleftrightarrow}} [C_2H_6]^* \overset{k_2}{\rightarrow} C_2H_5 + H$$
$$\downarrow k_3$$
$$H_2 + C_2H_4$$

k		A (cm^3/mol/s)	E_a (cal/mol)
k_1		1.0E13	0
k_{-1}		2.4E16	89800
k_2		1.3E16	101000
k_3		3.0E12	78000
υ	1509 cm^{-1}		
σ	4.34 Å		
ε / κ	247 K		

k_1: A_1 from A_{-1} and thermodynamics (NJIT Therm code); $E_a = 0$ for radical/radical combination reaction

k_{-1}: A_{-1} from Warnatz, J., *Combustion Chemistry* (ed. W. C. Gardiner, Jr.) Speringer-verlag, NY 1984; $E_a = \Delta H_{rxn} - RT_m$

k_2: A_2 from Dean, A. M., *J. Phys. Chem.* 89, p4600 (1985); $E_a = \Delta H_{rxn} - RT_m$

k_3: $A_3 = (ekT_m / h) \exp(\Delta S^* / R)$ (transition state theory) × degeneracy, $\Delta S^* =$ -7.5, $E_a = \Delta H_{rxn} + 45$ (kcal / mol)

υ, σ, and ε / κ taken from C_2H_6

Calculated Apparent Forward Reaction Rate Constants*

(P=760 torr; Bath gas: N_2)

Reaction	A (cm^3/mol/s)	n	E_a (cal/mol)
$CH_3 + CH_3 = C_2H_6$	4.4E57	-13.0	24840
$CH_3 + CH_3 = C_2H_5 + H$	4.0E18	-1.62	16080
$CH_3 + CH_3 = C_2H_4 + H_2$	5.6E35	-7.08	20050
$C_2H_6 = CH_3 + CH_3$	1.2E29	-4.19	16590

* $k = A\ T^n \exp(-E_a/R/T)$

Input Parameters for QRRK Calculation of Reactions

$$H + C_2H_4 \underset{k_{-1}}{\overset{k_1}{<==>}} [C_2H_5]^*$$

k		A (cm^3/mol/s)	E_a (cal/mol)
k_1		4.0E13	2600
k_{-1}		1.2E13	38900
υ	1526 cm^{-1}		
σ	4.34 Å		
ε / κ	247 K		

k_1: A_1 and E_a from Dean, A. M. *J. Phys. Chem.* 89, p4600 (1985)

k_{-1}: A_{-1} from A_1 and thermodynamics (NJIT Therm. code); E_a from Warnatz, J., *Combustion Chemistry* (ed. W. C. Gardiner, Jr.) Speringer-verlag, NY 1984;

υ, σ, and ε / κ taken from C_2H_5

Calculated Apparent Forward Reaction Rate Constants*

(P=760 torr; Bath gas: N_2)

Reaction	A (cm^3/mol/s)	n	E_a (cal/mol)
$H + C_2H_4 = C_2H_5$	3.2E47	-10.1	20070
$C_2H_5 = H + C_2H_4$	1.4E23	-2.55	13040

* $k = A\ T^n \exp(-E_a/R/T)$

Input Parameters for QRRK Calculation of Reactions

$$CH_2Cl + OH \underset{k_{-1}}{\overset{k_1}{<=>}} [CH_2ClOH]^* \xrightarrow{k_2} CH_2OH + Cl$$
$$\downarrow k_3$$
$$CH_2O + HCl$$

k		A (cm^3/mol/s)	E_a (cal/mol)
k_1		5.1E13	0
k_{-1}		2.4E16	91000
k_2		5.5E15	81200
k_3		7.6E13	42000
υ	1200 cm^{-1}		
σ	4.61 Å		
ε / κ	535 K		

k_1: A_1 from $CH_2Cl + CH_3 = C_2H_5Cl$, Wissman, M. and Benson, S. W, *Int. J. Chem. Kinet.*, 1984, 16, 307; $E_a = 0$ for radical/radical combination reaction

k_{-1}: A_{-1} from A_1 and thermodynamics (NJIT Therm. code); $E_a = \Delta H_{rxn} - RT_m$

k_2: A_2 from A_{-2} and thermodynamics (NJIT Therm. code), A_{-2} from Ho and Bozzelli, Ref. (22); $E_a = \Delta H_{rxn} - RT_m$

k_3: $A_3 = (ekT_m / h) \exp(\Delta S^* / R)$ (transition state theory) × degeneracy, $\Delta S^* =$ -4.0; $E_a = \Delta H_{rxn} + 37.5$ (kcal / mol)

υ, σ, and ε / κ taken from CH_2ClOH

Calculated Apparent Forward Reaction Rate Constants*

(P=760 torr; Bath gas: N_2)

Reaction	A (cm^3/mol/s)	n	E_a (cal/mol)
$CH_2Cl + OH = CH_2ClOH$	1.3E26	-4.82	5000
$CH_2Cl + OH = CH_2OH+Cl$	2.1E10	0.82	5980
$CH_2Cl + OH = CH_2O+HCl$	3.4E18	-1.54	3370
$CH_2ClOH = CH_2Cl + OH$	8.6E09	1.02	9890

* $k = A\ T^n \exp(-E_a/R/T)$

Input Parameters for QRRK Calculation of Reactions

$$CH_2Cl + H \underset{k_{-1}}{\overset{k_1}{<==>}} [CH_3Cl]^* \overset{k_2}{\rightarrow} CH_3 + Cl$$
$$\downarrow k_3$$
$$CH_2 + HCl$$

k		A (cm^3/mol/s)	E_a (cal/mol)
k_1		2.0E13	0
k_{-1}		1.8E15	94000
k_2		1.0E15	80230
k_3		2.9E14	127500
υ	1575 cm^{-1}		
σ	4.18 Å		
ε / κ	350 K		

k_1: A_1 from $C_3H_7 + H = C_3H_8$, Warnatz, J., *Combustion Chemistry* (ed. W. C. Gardiner, Jr.) Speringer-verlag, NY 1984; $E_a = 0$ for radical/radical combination reaction

k_{-1}: A_{-1} from A_1 and thermodynamics (NJIT Therm. code); $E_a = \Delta H_{rxn} - RT_m$

k_2: A_2 from Ho and Bozzelli, Ref. (22); $E_a = \Delta H_{rxn} - RT_m$

k_3: $A_3 = (ekT_m / h) \exp(\Delta S^* / R)$ (transition state theory) × degeneracy, $\Delta S^* = 0$; $E_a = \Delta H_{rxn} + 37.5$ (kcal / mol)

υ, σ, and ε / κ taken from CH_3Cl

Calculated Apparent Forward Reaction Rate Constants*

(P=760 torr; Bath gas: N_2)

Reaction	A (cm^3/mol/s)	n	E_a (cal/mol)
$CH_2Cl + H = CH_3Cl$	8.8E29	-5.70	6070
$CH_2Cl + H = CH_3 + Cl$	5.2E14	-0.42	830
$CH_2Cl + H = CH_2 + HCl$	1.4E12	0.0	35050
$CH_3Cl = CH_2Cl + H$	7.4E08	1.15	2140

* $k = A\ T^n \exp(-E_a/R/T)$

APPENDIX G

EXPERIMENTAL PROCEDURE

Operation of Two Stage Combustor

(1) Switch on the heater in water bath for warm up ethylene gas and set temperature at 90 °C.

(2) Turn on sample probe coolant and set flow for upper probe at 35 psig and 25 psig for lower probe. Activate coolant flow switch/alarm system.

(3) Turn on jet ring cool water and afterburner spray waters. Set flow rates separately at 20, 30, and 25 psig.

(4) Turn on afterburner blow air and check exhaust system vacuum pressure.

(5) Activate digital temperature readout and analog recorder.

(6) Set main air flowmeter to 25 at 80 psig.

(7) Set ignition air flowmeter to 50 at 55 psig

(8) Set ignition hydrogen flowmeter to 30 at 55 psig

(9) Ignite the combustor by press spark button and looking for first stage temperature jump from room temperature to about 100 °C.

(10) Flow fuel ethylene slowly to 27 at 80 psig and increase main air to 42 at 80 psig (fuel equivalence ratio = 0.7); looking for large temperature jump over 1000 °C.

(11) Turn off ignition hydrogen. Keeping flow ignition air for 2 minutes to flushing the ignition pipe, then turn the air off.

(12) Keep combustion at fuel-lean ($\phi = 0.7$) for 60 to 90 minutes

(13) Check temperature increasing curves on the analog recorder and looking for straight line to see combustor attending steady state.

(14) Take data or change feed conditions.

(15) To shut down the combustor, cut fuel first and allow coolant and main air flow through the reactor for about one hour after fuel cutting. Turn off all electric instruments.

Operation of GC, Beckman Analyzer, and HCl Scrubber

(1) Turn on carrier gases for GC FID and TCD and set nitrogen flow rate at 70 psig and helium flow rate at 30 psig.

(2) Turn on GC and set temperature programs.

(3) Turn on air and hydrogen gas for FID and reference helium gas for TCD.

(4) Ignite FID and looking for stable signal outputs.

(5) Turn on Beckman analyzer and warm up for one hour; Set sample coolant bath at 5 °C.

(6) Calibrate each analyzer using standard gases and zero gas (N_2).

(7) Turn on de-ion water and set flow rate in range of 15 to 18 (required when burning fuel with methyl chloride).

(8) Turn on sample pump and adjust outlet valve to keep water level in the HCl scrubber above the electrode cell.

(9) Flush sample lines for 30 minutes by drowning sample gas from the reactor, then inject samples and take data.

REFERENCES

Barat, R. B., 1990, *Characterization of The Mixing/Chemistry Interaction in The Toroidal Jet Stirred Combustor*, Ph. D. Dissertation, Massachusetts Institute of Technology.

Barat, R. B., 1992, *Combustion Science and Technology*, Vol. 84, p.187.

Barton, D. H. R. and K. E. Howlett, 1951, *J. Chem. Soc.*, Vol. 73, p.2033.

Baulch, D. L., D. D. Drysdale, and D. G. Horne, 1969, *Report No. 5*, Dept. of Physical Chemistry, The University of Leeds.

Baulch, D. L., D. D. Drysdale, J. Duxbury, and S. Grant, 1976, *Evaluate Kinetic Data for High Temperature Reactions*, Vol. 3, Butter-worths, London-Boston.

Benson, S. W., 1976, *Thermochemical Kinetics*, John Wiley, New York.

Bian J., J. Vandooren, and P. J. Van Tiggelen, 1986, *21th Symposium (International) on Combustion*, The Combustion Institute, p.953.

Blauwens, J., B. Smets, and J. Peeters, 1977, *16th Symposium (International) on Combustion*, The Combustion Institute, p.1055.

Blevins, L. G. and R. J. Roby, 1992, *Effect of High Level of Steam Addition on NO_x Reduction in Laminar Opposed Flow Diffusion Flames*, Research Report, Dept. of Chemical Engineering, Virginia Polytechnic Institute.

Bloomer, J. J. and D. L. Miller, 1992, *24th Symposium (International) on Combustion*, The Combustion Institute, p.1101.

Bose D. and S. M. Senkan, *Combustion Science and Technology*, Vol. 35 (1990) p.187

Bowman, C. T., 1992, *24th Symposium (International) on Combustion*, The Combustion Institute, p.859.

Bozzelli, J. W. and A. M. Dean, 1994, *Combustion Chemistry of Nitrogen Compounds: A Comprehensive Review and Analysis of Selected Reactions*, Chapter for the 2nd edition of *Combustion Chemistry*, edited by W. C. Gardiner, Jr. (in press).

Breen, P. B., 1977, *16th Symposium (International) on Combustion*, The Combustion Institution, Pittsburgh, p.19.

Brouwer, J., J. P. Longwell, and A. F. Sarofim, 1992 *Combustion Science and Technology*, Vol. 85, p.87.

REFERENCES
(Continued)

Chang, W. D. and S. M. Senkan, 1985, *Combustion Science and Technology,* Vol. 43, p.49.

Chelliah, H. K., G. Yu, T. O. Hahn, and C. K. Law, 1992, *24th Symposium (International) on Combustion*, The combustion Institute, p.1083.

Clyne, M. A. A. and B. A. Thrush, 1961, *Proc. Royal Soc. A*, 261, p. 2596.

Chuang S. C. and J. W. Bozzelli, 1986, *Ind. Eng. Chem. Process Des. Dev*, Vol. 25, p.317.

Dean, A. M., 1985, *Journal of Physical Chemistry*, Vol. 89, p4600.

Dean, A. J., D. F. Davidson, R. K. Hanson, and C. T. Bowman, 1988, *Western State Section / Comb. Inst. Meet,* p.88.

Drake, M. C., 1985, *Kinetics of Nitric Oxide Formation in Laminar and Turbulent Methane Combustion*, Gas Reasearch Institute Report GIR-85/0271.

Duff, R. E. and E. Davidson, 1959, *Journal of Physical Chemistry*, 31, p1018.

Fenimore C. P., 1971, *13th Symposium (International) on Combustion*, The Combustion Institute, p.373.

Fenimore, C. P., 1972, *Combustion and Flame*, Vol. 19, p289.

Fisher, E. M., Koshland, C. P., M. J. Hall, R. F. Sawyer, and D. Lucas, 1990, *23th Symposium (International) on Combustion*, The Combustion Institute, p.895.

Garg, A., 1994, *Chemical Eginerring Progress,* No.1, p46.

Garner, F. H., R. Long, A. J. Graham, and A. Badakshan, 1957, *6th Symposium (International) on Combustion*, Reinhold, New York, p.802.

Gerhold, B. W., C. P. Fenimore, and P. K. Dederick, 1978, *17th Symposium (International) on Combustion,* The Combustion Institution, Pittsburgh, p.703.

Glarborg, P., R. J. Kee, J. F. Grcar, J. A. Miller, 1986, *Sandia National Laboratories Report,* SAND86-8209, Livermore, CA.

Gibbs, B. M., F. G. Pereira, and J. M. Beer, 1977, *16th Symposium (International) on Combustion,* The Combustion Institution, Pittsburgh, p.461.

REFERENCES
(Continued)

Glick, H. S., J. J. Klein, and W. Squire, 1957, *Journal of Physical Chemistry,* 27, p.850.

Goodal, A. M. and K. E. Howlett, 1954, *J. Chem. Soc,* Vol. 76, p.2599.

Hanson, R. K. and S. Salimian, 1984, *Survey of Rate Constant in the N/H/O System, Combustion Chemistry,* Springer, New York.

Higashihara, T., W. C. Gardiner Jr, and S. M. Hwang , 1987, *The Journal of Physical Chemistry,* Vol.91, p1900.

Hindmarsh, A. C., 1983, *Scientfic Computing,* Vol. 1, North Holland, Amsterdam.

Ho. W, 1993, *Pyrolysis and Oxidation of Chloromethanes, Experiments and Modeling,* Ph.D. Dissertation, New Jersey Institute of Technology.

Ho. W, R. B. Barat, and J. W. Bozzelli, 1992, *Combustion and Flame*, 88, p265.

Hoare, M. R., R. G. W. Norrish, and G. Whittingham, 1959, *Proc. Roy Soc.*, London, A250, p.197.

Hwang, S. M., T. Higashihara, K. S. Shin, and W. C. Gardiner Jr., 1990, *The Journal of Physical Chemistry,* Vol.94, No.7, p2883.

Intergovernmental Panel on Climate Change, 1993, The supplementary Report to the IPCC Assessment, *Climate Change 1992,* Cambridge University Press, p.38.

Jeoung, S. C., K. Y. Choo, and S. W. Benson, 1991, *Journal of Physical Chemistry* Vol. 95, No. 19, p.7282.

Karra, S. B., D. Gutman, and S. M. Senkan, 1988, *Combustion Science and Technology,* Vol. 45, p.45.

Karra, S. B. and S. M. Senkan, 1987, *Combustion Science and Technology*, Vol. 54, p.333.

Kee, R. J., and J. A. Miller, 1986, *Sandia National Laboratories Report,* SAND86-8841, Livermore, CA.

Kolb, T., P. Jansohn, and W. Leuckel, 1988, *22th Symposium (International) on Combustion*, The Combustion Institute, p.1193.

REFERENCES
(Continued)

Koshland, C. P., E. M. Fisher, and D. Lucas, 1992, *Combustion Science and Technology,* Vol. 82, p.49.

Lam, F. W., 1988, *The Formation of Polycyclic Aromatic Hyfrocarbons and Soot in A Jet-Stirred/Plug-Flow Reactor,* Ph.D. Dissertation, Massachusetts Institute of Technology.

Linak, W. P., J. A., 1991, Mulholland, et al., *Hazardous Waste and Harzardous Materials,* Vol. 8, No 1, p1.

Lyon, R. K., 1990, *23th Symposium (International) on Combustion,* The Combustion Institute, p.903.

Martin, F. J. and P. K. Dederick, 1977, *16th Symposium (International) on Combustion,* The Combustion Institution, Pittsburgh, p.191.

Matsui, Y. and A. Yuuki, 1985, *Jap. Journal of Applied Physics,* 24, p.598.

Matsui, Y. and T. Nomaguchi, 1978, *Combustion and Flame,* 32, p.205.

Miller, J. A., M. C. Branch, W. J. McLean, D. W. Chandler, M. D. Smooke, and R. J. Kee, 1985, *20th Symposium (International) on Combustion,* The Combustion Institution, Pittsburgh, p.673.

Miller, J. A. and C. T. Bowman, 1989, *Prog. Energy Combust. Sci.* Vol. 15, p.287.

Miyauchi, T., Y. Mori, and T. Yamaguchi, 1981, *18th Symposium (International) on Combustion,* The Combustion Institute, p.43.

Morly, C., 1976, *Combustion and Flame,* 27, p.189.

Nenniger, J. E., 1983, *Polycyclic Aromatic Hydrcarbon Production in A Jet-Stirred Combustor,* Ph.D. Dissertation, Massachusetts Institute of Technology.

NIST, 1992, Standard Reference Database 17, Version 4.0.

Peck, R. E, P. Glarborg, and J. E. Johnsson, 1991, *Combustion Science and Technology,* Vol. 76, p81.

Ritter E. R. and J. W. Bozzelli, 1990, *Combustion Science and Technology,* Vol. 7, p.117

Ritter, E. R and J. W. Bozzelli, 1991, *Int. J. Chem. Kinetics,* 23, p767.

REFERENCES
(Continued)

Ritter, E. R, 1991, *J. Chem. Info. Sci*, 31, p400.

Roth, P. and M. Ibreighith, 1984, *Combustion and Flame*, 55, p729.

Salimian, S., R. K. Hanson, and C. H. Kruger, 1987, *Combustion and Flame*, 56, p83.

Sarofim, A. F. and R. C. Flagen, 1976, *Prog. in Energy and Combustion Science*, 2, p.1.

Senkan, S. M., 1986, Environmental Science and Technology, Vol. 20, No. 12, p.1243.

Senser, D. W., V. A. Cundy, and J. S. Morse, 1987, *Combustion Science and Technology*, Vol. 51, p.209.

Sun, W. H., J. P. Longwell, and A. F. Sarofim, 1987, Paper presented at the symposium on the Formation and Control of NO_X Emission from Combustion Source, ACS Award Symposium on the Chemistry of Contemporary Technological Problems, *193th ACS National Meeting.*

Song, Y. H., W. D. Blair, V. J. Siminski, and W. Bartok, 1981, *18th Symposium (International) on Combustion*, The Combustion Institution, p.53.

Szekely, A., R. K. Hanson, and C. T. Bowman, 1985, *20th Symposium (International) on Combustion*, The Combustion Institute, p.647.

Toshimi, T., T. Toshharo, and O. Mitsunibo., 1979, Combustion and Flame, Vol. 37, p.17.

Tseregounis, S. I. and O. I. Smith, 1983, *Combustion Science and Technology*, Vol. 30, p.231.

U. S. Environmental Protection Agency, 1993, Estimation of Greenhouse Gas Emissions and Sinks for the United States 1990, *Review Draft*, Washington, DC, June 21, p.25.

U.S. Environmental Protection Agency, 1980, *Research Summary*: Controlling Nitrogen Oxides, EPA-600/8-80-004.

Vaughn, C. B., W. H. Sun, J. B. Howard, and J. P. Longwell, 1991, *Combustion and Flame*, Vol. 84, p.38.

Wang. L, P. J. Jalvy, and R. B. Barat, 1993, "The Effect of CH_3Cl Addition on A Atmospheric Pressure Fuel Lean CH_4/Air Premixed Laminar Flat Flame", Submitted to *Combustion Science and Technology.*

REFERENCES
(Continued)

Weissman, M. and S. W. Benson, 1984, *Int. J. of Chem Kine*. Vol. 16, p.307.

Wendt, J. O. L. and J. M. Ekmann, 1975, *Combustion and Flame,* 25, p.355.

Westbrook, C. K., 1982, *19th Symposium (International) on Combustion,* The Combustion Institute, p.127.

Westenberg, A. A., 1971, *Combustion Science and Technology,* 4, p.59.

Wilson, W. E., J. T. O'Donovan, and R. M. Fristrom, 1969, *12th Symposium (International) on Combustion*, The Combustion Institute, p.929.

Wood, S. C., 1994, *Chemical Engineering Progress*, No.1, p.32.

Wuebbles, D. and J. A. Edmonds, 1991, *Primer on Greenhouse gases,* Chelsea, MI: Lewis Publisher, Inc., p.15.

Zeldovich, Ya. B., 1946, *Acta Physiochem,* U.R.S.S., Vol. 21, p.577.